LEABHARLANN CHOLÁISTE NA TRÍONÓIDE, BAILE ÁTHA CLIATH | TRINITY COLLEGE LIBRARY DUBLIN
Ollscoil Átha Cliath | The University of Dublin

Terms and Conditions of Use of Digitised Theses from Trinity College Library Dublin

Copyright statement

All material supplied by Trinity College Library is protected by copyright (under the Copyright and Related Rights Act, 2000 as amended) and other relevant Intellectual Property Rights. By accessing and using a Digitised Thesis from Trinity College Library you acknowledge that all Intellectual Property Rights in any Works supplied are the sole and exclusive property of the copyright and/or other IPR holder. Specific copyright holders may not be explicitly identified. Use of materials from other sources within a thesis should not be construed as a claim over them.

A non-exclusive, non-transferable licence is hereby granted to those using or reproducing, in whole or in part, the material for valid purposes, providing the copyright owners are acknowledged using the normal conventions. Where specific permission to use material is required, this is identified and such permission must be sought from the copyright holder or agency cited.

Liability statement

By using a Digitised Thesis, I accept that Trinity College Dublin bears no legal responsibility for the accuracy, legality or comprehensiveness of materials contained within the thesis, and that Trinity College Dublin accepts no liability for indirect, consequential, or incidental, damages or losses arising from use of the thesis for whatever reason. Information located in a thesis may be subject to specific use constraints, details of which may not be explicitly described. It is the responsibility of potential and actual users to be aware of such constraints and to abide by them. By making use of material from a digitised thesis, you accept these copyright and disclaimer provisions. Where it is brought to the attention of Trinity College Library that there may be a breach of copyright or other restraint, it is the policy to withdraw or take down access to a thesis while the issue is being resolved.

Access Agreement

By using a Digitised Thesis from Trinity College Library you are bound by the following Terms & Conditions. Please read them carefully.

I have read and I understand the following statement: All material supplied via a Digitised Thesis from Trinity College Library is protected by copyright and other intellectual property rights, and duplication or sale of all or part of any of a thesis is not permitted, except that material may be duplicated by you for your research use or for educational purposes in electronic or print form providing the copyright owners are acknowledged using the normal conventions. You must obtain permission for any other use. Electronic or print copies may not be offered, whether for sale or otherwise to anyone. This copy has been supplied on the understanding that it is copyright material and that no quotation from the thesis may be published without proper acknowledgement.

An investigation into the role of TMED1 in the IL-33/ST2L signalling pathway

Thesis submitted to the

University of Dublin

for the

Degree of Doctor of Philosophy

By

Dympna Connolly

School of Biochemistry and Immunology

Trinity College

Dublin

Ireland

October 2012

Declaration

This thesis is submitted by the undersigned to the University of Dublin for the examination of Doctorate in Philosophy. The work herein is entirely my own. This work has not been submitted as exercise for a degree to any other university. The library at Trinity College, Dublin, has my full permission to lend or copy this thesis upon request.

Thesis 9997

First and foremost I would like to thank my supervisors Luke O'Neill and Anne McGettrick, without whom this thesis would not have been possible. I thank you both for your guidance, advice and support. A huge thank you also goes out to all the members of the O'Neill lab, both past and present. Thank you all for making the lab such a great place to work and for always being willing to lend a helping hand, not to mention the friendship, the cups of tea and of course, the nights out.

I thank my parents. You've always been encouraging and supportive, and I wouldn't be where I am today without you. Also I would like to thank my favourite brother and sister, for providing a welcome distraction from work and pretending to listen, at least some of the time. Also thank you to Nana, for your support, encouragement and visits. To you, I dedicate this work.

Thanks to everyone in Ashtown, particularly those that have put up with me while I've been writing up and making sure that I had a constant supply of Jammie Dodgers! A special thanks to Jen, it's been great to have someone around that has been through it all. Finally, thanks to all my friends, for showing an interest and listening whether or not you knew what I was talking about, and for the help in making some great memories over the four years.

Table of contents

Table of contents ii

List of figures vi

List of tables ix

Abbreviations xi

Abstract xiv

Chapter One **1**

1.1 The immune system 2

1.2 Innate immune system 2

1.3 IL-1 receptor (IL-1R)/Toll-like receptor (TLR) superfamily 4

1.4 Toll-like receptors 7

1.5 IL-1R-like receptors 7

1.6 IL-1R/TLR signalling pathways 10

1.7 The isoforms of ST2 11

1.8 ST2L expression 14

1.9 ST2L ligand identification 16

1.10 The IL-33/ST2L signalling pathway 20

1.11 IL-33 and ST2L in host defence and disease 21

1.13 Localisation and trafficking of the TLR and IL-1R superfamily members 28

1.14 Trafficking of the ST2L receptor 30

1.15 The p24 protein family 31

1.15.1 p24 Family Members 31

1.15.2 The properties of TMED proteins 35

1.15.3 Functions of TMED proteins 37

1.16 Functions of TMED proteins in immune pathways 39

1.17 TMED1 (T1/ST2 receptor binding protein / p24γ_1 / tp24) 39

1.18 Project aims and objectives 42

Chapter Two **43**

2.1 Materials 44

2.2 Bacterial transformation and plasmid purification 48

2.3 Cell culture 48

2.4 Transient transfection of HEK-293 cells with expression vectors 50

2.5 Transient transfection of HEK-293 cells with siRNA and HMC 1.1 cells with expression vectors 50

2.6 Transient transfection of THP-1 cells with siRNA 51

2.7 Protease protection assay 52

2.8 Co-immunoprecipitation assay 52

2.9 Site Directed Mutagenesis of TMED1 and ST2L constructs 54

2.10 SDS-PAGE (sodium dodecyl sulphate-polyacrylamide gel electrophoresis) 56

2.11 Western blotting 58

2.11.1 Transfer method 58

2.11.2 Blocking the membrane 59

2.11.3 Incubation with antibody 59

2.11.4 Stripping and re-probing 59

2.12 Cytotoxicity Assay 60

2.13 Reverse Transcriptase Polymerase Chain Reaction 61

2.14 Quantitative PCR 62

2.15 Luciferase Assays 63

2.15.1 Luciferase Assays with TMED1 overexpression 63

2.15.2 Luciferase Assays following endogenous TMED1 knockdown 64

2.16 Enzyme-Linked ImmunoSorbent Assay (ELISA) 64

2.16.1 Cell preparation and stimulation 64

2.16.2 ELISA procedure 64

2.17 Labelling IL-33 65

2.18 Confocal 66

2.19 Dynasore treatment 67

Chapter Three **68**

TMED1 interacts with the ST2L receptor via the association of their GOLD and TIR domains respectively. The localisation of the GOLD domain of TMED1 in the cytosol facilitates this association.

3.1 Introduction 69

3.2 Results 71

3.2.1 TMED1 localisation in resting cells 71

3.2.2 Transmembrane domains of TMED1 83

3.2.3 Localisation of the GOLD domain of TMED1 88

3.2.4 TMED1 interacts with ST2L 92

3.2.5 TMED1 does not co-immunoprecipitate with MyD88 97

3.2.6 TMED1 and ST2L interact endogenously 99

3.2.7 Defining the domains in TMED1 responsible for the TMED1-ST2L interaction 103

3.2.8 Defining the domains in ST2L responsible for the TMED1-ST2L interaction 108

3.2.9 TMED1 and ST2L co-localise 112

3.2.10 Localisation of the TMED1 and ST2L interaction 114

3.3 Discussion 119

Chapter Four **130**

TMED1 is required for optimal IL-33-induced responses. TMED1 may carry out this positive regulatory role at the early endosome.

4.1 Introduction 131

4.2 Results 133

4.2.1 The effect of IL-33 stimulation on the TMED1-ST2L interaction 133

4.2.2 TMED1-GFP dose dependent overexpression in HEK-293T cells 137

4.2.3 TMED1 does not affect basal NF-κB, AP-1 or ISRE activity 139

4.2.4 Effect of TMED1 on induced luciferase activity 141

4.2.5 The effect of TMED1 on p65-induced luciferase activity 144

4.2.6 The effect of TMED1 overexpression on IL-33-induced IL-8 production 146

4.2.7 Luciferase assays following knockdown of TMED1 148

4.2.8 TMED1 knockdown impairs IL-33-induced responses 152

4.2.9 IL-33 is internalised in a time dependent manner 157

4.2.10 IL-33 is internalised into compartments surrounded by TMED1 160

4.2.11 Enhanced localisation of TMED1 at endosomes after IL-33 stimulation 163

4.2.12 IL-33 signalling requires endocytosis 168

4.3 Discussion 171

Chapter Five **179**

5.1 Final discussion and future perspectives 180

References **187**

Appendices **208**

Record of publications 209

List of figures

Chapter One

1.1 IL-1 receptor (IL-1R)/Toll-like receptor (TLR) superfamily 6

1.2 Variants of ST2 13

1.3 ST2L positive and IL-33 response cell types 15

1.4 Structure of IL-33 and the extracellular domain of ST2L 19

1.5 The IL-33/ST2L signalling pathway 26

1.6 The early secretory pathway 34

1.7 Amino acid sequence and domain structure of TMED1 41

Chapter Three

3.1 Localisation of TMED1 in HMC 1.1 cells 73

3.2 TMED1 is not localised to the plasma membrane or nucleus in HEK-293T cells 74

3.3 TMED1 co-expression with ER-CFP 75

3.4 TMED1 co-expression with Golgi-CFP 77

3.5 TMED1 co-expression with EEA1-CFP 79

3.6 TMED1 co-expression with Rab11a-CFP 81

3.7 Localisation of TMED1 mutant constructs 86

3.8 The GOLD domain of TMED1 projects into the cytosol 90

3.9 The C-terminus of TMED1 is located in the lumen 91

3.10 TMED1 co-immunoprecipitates with ST2L-HA in HEK-293T cells 94

3.11 TMED1 co-immunoprecipitates with stably overexpressed ST2L in HEK-293-hST2L cells 95

3.12 TMED2, TMED3 or TMED7 do not co-immunoprecipitate with stably overexpressed ST2L in HEK-293-hST2L cells 96

3.13 TMED1 does not co-immunoprecipitate with MyD88 98

3.14 Detection of endogenous TMED1 in the HMC 1.1 cell line 101

3.15 Endogenous TMED1 co-immunoprecipitates with endogenous ST2L 102

3.16 Sequence alignment and domain structure of wild type and mutant TMED1 constucts 105

3.17 Mutations in TMED1 affect its ability to interact with ST2L: immunoprecipitation with GFP Trap® beads 106

3.18 Mutations in TMED1 affect its ability to interact with ST2L: immunoprecipitation with antibody coupled A/G-plus beads 107

3.19 Wild type and mutant ST2L constucts 109

3.20 Mutations in ST2L affect its ability to interact with TMED1 111

3.21TMED1-GFP and ST2L-HA can co-localise in HEK-293T 113

3.22 Localisation of ST2L in HEK-293T cells 115

3.23 Localisation of endogenous ST2L in HMC 1.1 cells 116

3.24 Co-localisation of TMED1 and ST2L at the ER 117

3.25 Co-localisation of TMED1 and ST2L at the Golgi 118

3.26 Orientation of TMED1 and TMED7 125

Chapter Four

4.1 The TMED1-ST2L interaction is evident after stimulation with IL-33 135

4.2 The endogenous TMED1-ST2L interaction is evident after stimulation with IL-33 136

4.3 TMED1 dose dependent expression in HEK-293T cells can be detected

by Western blot analysis and is not cytotoxic to cells 138

4.4 TMED1 overexpression does not affect basal NF-κB, AP-1 or ISRE activity 140

4.5 TMED1 overexpression inhibits IL-33 and IL-1-induced NF-κB luciferase 142

4.6 TMED1 overexpression inhibits LPS, PolyI:C and TNF-α-induced NF-κB luciferase as well as LPS and Poly I:C-induced ISRE luciferase 143

4.7 The observed inhibition of TMED1 in luciferase experiments is not a result of the GFP tag 145

4.8 TMED1 overexpression does not affect IL-8 production in response to IL-33 in HEK-293-hST2L cells 147

4.9 TMED1 mRNA can be detected in HEK-293T and HEK-293-hST2L cell lines 149

4.10 Optimisation of TMED1 knockdown in HEK-293-hST2L cells 150

4.11 TMED1 knockdown does not affect IL-33-induced NF-κB luciferase 151

4.12 TMED1 is needed for optimal IL-33-induced responses 154

4.13 TMED1 is required for optimal IL-33-induced IL-8 production 155

4.14 TMED1 knockdown in THP-1 cells 156

4.15 HEK-293-hST2L cells bind labelled IL-33 and the response to labelled IL-33 is comparable to unlabelled IL-33 158

4.16 IL-33 gets internalised in a time dependent manner 159

4.17 IL-33 gets internalised in a time dependent manner to compartments surrounded by TMED1 161

4.18 Enhanced co-localisation of TMED1 and EEA1 after IL-33 stimulation 165

4.19 Enhanced co-immunoprecipitation of TMED1 with EEA1 after IL-33 stimulation 167

4.20 IL-33 signalling requires endocytosis 170

4.21 Schemeatic for the involvement of TMED1 in IL-33/ST2L signalling 178

List of tables

Chapter One

1.1 IL-1R family member complexes with known ligands, potential proteases for the ligands and known antagonists of the receptors 9

1.2 Examples of diseases in which IL-33 have been associated 23

1.3 Nomenclature of the vertebrate, *Drosophila* and yeast TMED proteins 33

Chapter Two

2.1 Materials and reagents used for tissue culture 44

2.2 Cell lines 44

2.3 Ligands used for cell stimulation 44

2.4 Reagents used for cell transfection 45

2.5 Expression vectors 45

2.6 Reagents used for DNA and RNA purification and amplification 46

2.7 Reagents used for protein isolation, protease protection assays and western blotting 46

2.8 Antibodies used for Western Blotting, co-immunoprecipitation and confocal analysis 47

2.9 Reagents used for co-immunoprecipitation assays 47

2.10 Reagents used for confocal analysis 47

2.11 Reagents used for Enzyme-Linked ImmunoSorbent Assay 47

2.12 GeneJuice® quantities for transfection 50

2.13 Primers used for mutagenesis of TMED1 55

2.14 Primers used for tag attachment and mutagenesis of ST2L 55

2.15 Resolving gel 57

2.16 Stacking gel 57

2.17 Primers for PCR 61

2.18 Primers used for quantitative PCR 62

Chapter Three

3.1 Transmembrane domains of TMED1 85

Abbreviations

AP-1	Activator protein 1
BCAP	B-cell adaptor for phosphoinositide 3-kinase
BSA	Bovine serum albumin
CFP	Cyan fluorescent protein
Co-IP	Co-immunoprecipitation
COP	Coat protein complex
DAMP	Damage or danger associated molecular pattern
DIGIRR	Double Ig IL-1R related molecule
DMEM	Dulbecco's modified eagle medium
DMSO	Dimethyl sulfoxide
DNA	Deoxyribonucleic acid
DTT	Dithiothreitol
ECL	Enhanced chemiluminesence
EDTA	Ethylenediaminetetracetic acid
EEA1	Early endosome antigen 1
ELISA	Enzyme-linked immunosorbant assay
ER	Endoplasmic reticulum
ERGIC	Endoplasmic reticulum Golgi intermediate compartment
ERK	Extracellular signal-regulated kinase
EV	Empty vector
FACS	Fluorescence-activated cell sorting
FCS	Fetal calf serum
GFP	Green fluorescent protein
GLCC	GOLD, linker and coiled-coiled
GOLD	Golgi dynamics
GPCR	G-protein coupled receptor
HA	Haemagglutinin
HEK	Human embryonic kidney
HMC	Human mast cell
HRP	Horse radish peroxidase
Ig	Immunoglobulin

IKK	IκB kinase
IL	Interleukin
IL-1RAPL	IL-1 receptor accessory protein like
IMDM	Iscove's Modified Dulbecco's Medium
IRAK	Interleukin receptor associated kinase
IRF3	Interferon regulatory factor 3
ISRE	Interferon stimulated response element
JAK	Janus kinase
JNK	c-Jun N-terminal kinase
kDa	kilodalton
LB	Luria-Bertani broth
LLR	Leucine rich repeat
LPS	Lipopolysaccharide
Mal	MyD88 adaptor like
MAPK	Mitogen activated protein kinase
MHC	Major histocompatibility complex
MyD88	Myeloid differentiation factor 88
NF-κB	Nuclear factor kappa B
NK	Natural killer
NLS	Nuclear localisation sequence
PAGE	Polyacrylamide gel electrophoresis
PAMP	Pathogen-associated molecular pattern
PBMC	Peripheral blood mononuclear cells
PBS	Phosphate buffered saline
PCR	Polymerase chain reaction
PMSF	Phenylmethlsuphonylflouride
Poly I:C	Polyriboinosinic polyribocytidylic acid
PRR	Pattern recognition receptor
PVDF	Polyvinylidene difluoride
RNA	Ribonucleic acid
RPMI	Roswell Park Memorial Institute
RTK	Receptor tyrosine kinase
SARM	Sterile α-motifs and β-catenin/armadillo repeat motif

SD	Standard deviation
SDS	Sodium dodecyl sulphate
SEM	Standard error of the mean
SIGIRR	Single immunoglobulin IL-1 receptor-related
siRNA	Small interfering RNA
SNP	Single nucleotide polymorphism
SP	Signal peptide
TAG	TRAM adaptor molecule with GOLD domain
TEMED	N,N,N,N-tetramethylethylenediamine
TGN	Trans-golgi network
Th	T helper cell
TIGIRR	Three immunoglobulin IL-1 receptor-related
TIR	Toll-IL1 receptor
TLR	Toll-like receptor
TM	Transmembrane
TMED	Transmembrane emp24 domain-containing protein
TNF-α	Tumour necrosis factor alpha
Tollip	Toll/IL-1R interacting protein
TRAF	TNF receptor associated factor
Treg	Regulatory T cell
TRIF	TIR domain containing adaptor inducing IFN-beta
v/v	Volume per volume
WCL	Whole cell lysate
w/v	Weight per volume

Abstract

This thesis set out to characterise the GOLD domain containing protein, TMED1 which had been shown to associate with ST2L, the receptor for the cytokine IL-33 and to investigate its relationship with ST2L.

Co-immunoprecipitation assays and confocal microscopy confirmed an association between TMED1 and ST2L. Confocal microscopy also revealed that this association occurred at least in part, at the ER and Golgi. Experiments involving mutation and deletional constructs of both TMED1 and ST2L demonstrated that the integrity of the GOLD domain was particularly important for this association and that the interaction is mediated primarily by the GOLD domain of TMED1 and the TIR domain of ST2L. Further characterisation of TMED1 revealed that its GOLD domain projected into the cytosol, thereby facilitating the GOLD-TIR association. ST2L did not associate with other TMED family members, and TMED1 did not associate with other TIR domain containing proteins, demonstrating the specificity of the association between TMED1 and ST2L.

A role for TMED1 in IL-33-induced signalling pathways was demonstrated using siRNA mediated knockdown of TMED1. These experiments revealed that knockdown of TMED1 impaired IL-33-induced responses. In particular IL-33-induced p38 and pERK activation was impaired in the absence of TMED1. Interestingly, IL-33-induced MAPK activation was also reduced when endocytosis was inhibited, while receptor internalisation was less important for NF-κB activation. This suggests that receptor internalisation is particularly important for IL-33-induced MAPK activation.

An analysis of the localisation of TMED1 revealed that it localised to early endosomes and following IL-33 stimulation, TMED1 localisation at the early endosome

was enhanced. Given that endocytosis is required for IL-33-induced MAPK activation, and that IL-33 increases the levels of TMED1 at the early endosome, this suggests that the early endosome may be the compartment at which TMED1 performs its positive regulatory function in the IL-33/ST2L signalling pathway.

This study, therefore, reveals a role for TMED1 in the IL-33 signalling pathway and further supports the emerging evidence for an important role for TMED members in immunoregulation.

Chapter One

Introduction

Chapter 1

1.1 The immune system

The immune system functions to defend against infections and disease, and is composed of a complex network of specialised cells, organs and humoral factors. Collectively, they aim to protect the host from harmful agents. In the event that the host experiences an incident which results in its damage, the immune system initiates a response to defend the host and endeavours to return it to a more homeostatic state. The immune system has numerous ways in which it can defend the host. Some of these mechanisms are always in place, ready to provide a first line of defence and act early on in an infection. These mechanisms form what is known as the innate immune system. Other mechanisms have evolved to provide a more versatile means of defence and as such these are known as the adaptive immune system. Both systems work together for the benefit and protection of the host (Janeway, 1993, 2001).

1.2 Innate immune system

The innate immune system is a universal and ancient form of host defence against infection. During evolution, the innate immune system appeared before the adaptive system and aspects of innate immunity are found in all multi-cellular organisms, including plants and insects (Medzhitov and Janeway, 2000).

A critical feature of the innate immune system is the ability to discriminate between infectious non-self and non-infectious self (Janeway, 1992). Epithelial surfaces such as the skin, and the lining and mucosa of the respiratory and gastrointestinal tract provide the first line of defence to prevent the entry of foreign pathogens (Janeway and Medzhitov, 2002). These physical barriers are in place at all times.

Activation of the host innate immune response, following exposure to infectious non-self, is dependent on the recognition of highly conserved, essential microbial components, known as pathogen-associated molecular patterns (PAMPs) (Janeway, 1989). These PAMPs are recognised by germ-line encoded receptors known as pattern recognition receptors (PRRs) which do not require the gene rearrangement essential to adaptive immune recognition. The innate immune system uses a variety of pattern recognition receptors that can be expressed on the cell surface, in intracellular compartments, in the cytosol or secreted into the bloodstream and tissue fluids. PRRs are critical for the initial detection of PAMPs. The functions of PRRs include opsonization, activation of complement cascades, phagocytosis, activation of proinflammatory signalling pathways, and induction of apoptosis (Janeway and Medzhitov, 2002). The activation of several of these signalling cascades leads to the activation of the adaptive immune response.

The host immune response can also be activated by damage or danger associated molecular patterns (DAMPs) or alarmins. These are endogenous, host derived molecules or their derivatives which are not normally exposed, but are revealed during, after, or because of injury in the absence of pathogenic infection (Seong and Matzinger, 2004). Like PAMPs, DAMPs trigger PRRs, resulting in the recruitment and activation of receptor expressing cells of the innate immune system in a similar manner to PAMPs, which aims to restore homeostasis by promoting reconstruction of the damaged tissue (Bianchi, 2007). Mediators such as cytokines produced as a result of the activation of PAMPs and DAMPs are detected by additional receptors and can relay information to other immune cells. The recognition of endogenous DAMPs and exogenous PAMPs both convey messages and elicit responses, working together in the complex, coordinated effort of host protection.

1.3 IL-1 receptor (IL-1R)/Toll-like receptor (TLR) superfamily

The IL-1R/TLR superfamily consists of a group of germ-line encoded proteins that are considered part of the innate immune system. The first member of this superfamily identified was IL-1R1 (Sims et al., 1988). A number of years later it was noted that the cytoplasmic domain of the IL-1R1 is related to that of the *Drosophila* Toll (Gay and Keith, 1991). Toll was originally shown to have a role in the establishment of dorso-ventral polarity in *Drosophila melanogaster* embryos but it is now known to also be involved in host defence in the adult fly (Lemaitre et al., 1996). Following the observation of the similarity between Toll and the IL-1R1, a human homolog to *Drosophila* Toll was discovered (Medzhitov et al., 1997). The discovery of other homologs has led to the definition of the IL-1R/TLR superfamily based on their homologous cytosolic domain. This domain is now known as the Toll/IL-1R (TIR) domain (Bowie and O'Neill, 2000) and is essential for downstream signalling from these receptors.

The IL-1R/TLR superfamily contains many members and can be sub-divided into groups (Figure 1.1). The family can be divided into groups based on whether or not they possess transmembrane and extracellular regions. Those which do contain extracellular and membrane spanning regions can be further divided into two groups based on their homology to either the *Drosophila* Toll receptor or the IL-1R1. These two subgroups are the leucine rich repeat containing receptors, such as the TLRs, or the immunoglobulin (Ig) domain containing receptors, such as the IL-1 receptors (Kawai and Akira, 2010; O'Neill, 2008).

The family members that do not possess extracellular or transmembrane regions form another sub-group. These include Myeloid differentiation factor 88 (MyD88), MyD88 adaptor like (Mal), TIR domain containing adaptor inducing interferon-β (TRIF),

TRIF-related adaptor molecule (TRAM), and sterile α-motifs and β-catenin/armadillo repeat motif (SARM) which are all cytoplasmic and do not have any extracellular region. Another TIR domain containing adaptor known as B-cell adaptor for Phosphoinositide 3-kinase (BCAP) (Troutman et al., 2012) which has recently been shown to be involved in TLR signalling could also be included in this group of cytoplasmic TIR domain containing adaptor proteins.

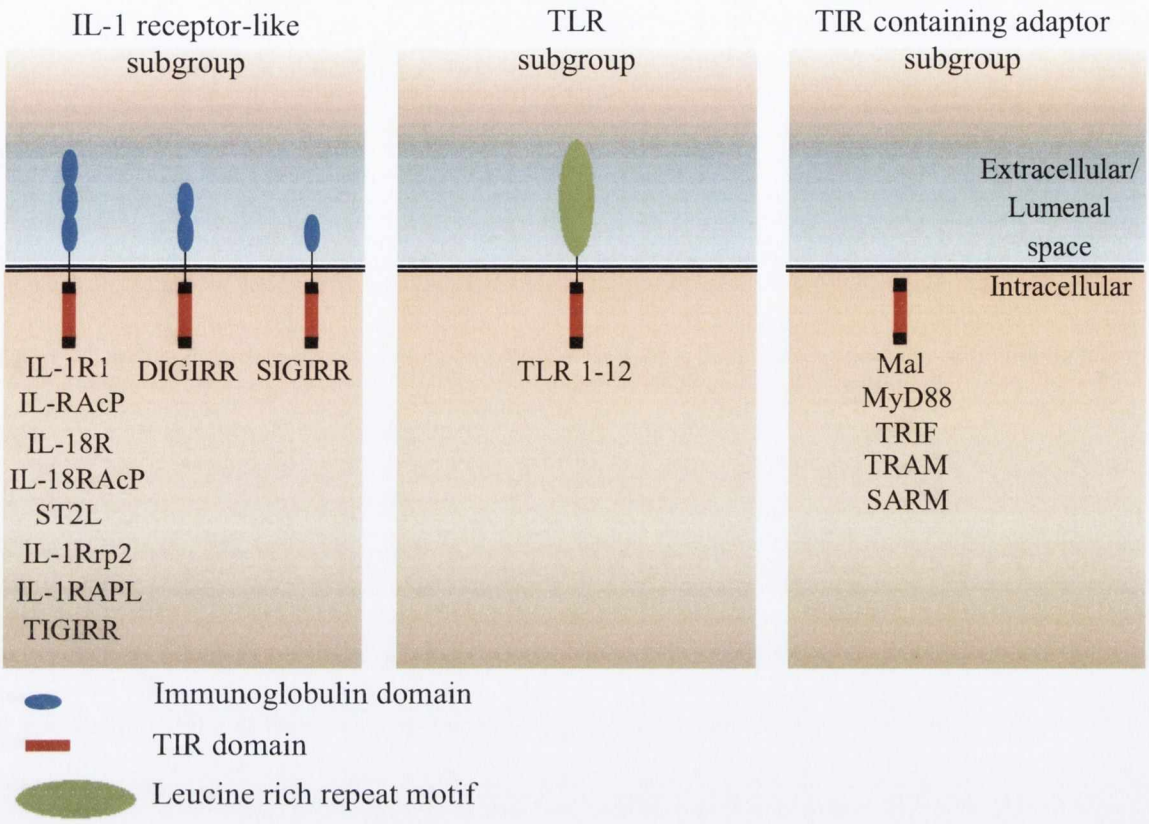


Figure 1.1 IL-1 receptor (IL-1R)/Toll-like receptor (TLR) superfamily

The IL-1R/TLR superfamily members all possess a Toll/Interleukin-1 receptor (TIR) domain. This TIR domain mediates the interaction between members of the superfamily, specifically receptor-receptor, adaptor-adaptor and receptor-adaptor protein dimerisation. The superfamily can be divided into three groups. The first group contains members which possess extracellular immunoglobulin domains, the second group contains members which have extracellular leucine rich repeats and the third group contains members which are cytoplasmic proteins. The members of the IL-1 receptor-like subgroup of the IL-1R/TLR superfamily can possess different numbers of immunoglobulin domains. IL-1RAPL, TIGIRR, and SIGIRR remain as orphans, as their ligands are unknown, while the ligands that bind other the members of this subgroup are known.

1.4 Toll-like receptors

The TLRs are type-1 transmembrane proteins which contain 16-28 copies of a LxxLxLxxNxL motif known as leucine rich repeat (LLR) at their N-terminus and a TIR domain at their C-terminus (Matsushima et al., 2007). To date, ten functional TLRs have been identified in humans while twelve have been identified in mice. TLR1-TLR9 are conserved in both species. TLR10 is functional in humans, but there is no mouse TLR10 homologue (Hasan et al., 2005). TLR11, TLR12 and TLR13 have been lost from the human genome (Kawai and Akira, 2010). Many of the ligands recognised by TLRs have been identified. They consist of various molecular patterns on pathogens known as PAMPs (Janeway, 1992). For example, tri- or diacylated lipopeptides are recognised by TLR2 in complex with TLR1 or TLR6 respectively (Morr et al., 2002; Ozinsky et al., 2000). While TLR4 detects the bacterial wall component Lipopolysaccharide (LPS) and TLR3 recognises the dsRNA synthetic analog Polyinosine-polycytidylic acid (poly (I:C)) (Alexopoulou et al., 2001; Poltorak et al., 1998).

1.5 IL-1R-like receptors

The members of the IL-1R-like subgroup each contain Ig domains in their extracellular regions. These Ig domains are involved in the recognition of members of the IL-1 family (Table 1.1). As mentioned above, IL-1R1 was the first member to be identified, and is now known to recognise IL-1α or IL-1β in concert with IL-1RAcP (Greenfeder et al., 1995). As their names suggest, IL-18R and IL-18RAcP recognise IL-18 (Cheung et al., 2005). IL-18R has also been shown to bind the IL-37b isoform (Kumar et al., 2002), while binding of IL-1Rrp2 has been reported for each of the three IL-36 isoforms (Towne et al., 2011). IL-33 binds to the receptor ST2L (Schmitz et al., 2005). This receptor is of particular interest here and will be discussed in more detail

later in the chapter. IL-1 receptor accessory protein like (IL-1RAPL), three immunoglobulin IL-1 receptor-related (TIGIRR) and single immunoglobulin IL-1 receptor-related (SIGIRR) are also in this family, although they remain as orphan receptors (Born et al., 2000; Carrie et al., 1999; Thomassen et al., 1999). Functions for IL-1RAPL and TIGIRR are presently unknown, although IL-1RAPL has been shown to activate c-Jun N-terminal kinase (JNK) but not the extracellular signal-regulated kinase (ERK) or the p38 mitogen-activated protein (MAP) kinases (Khan et al., 2004). SIGIRR does not activate these factors, probably because it does not contain two highly conserved amino acids in the TIR domain (Ser 447 and Tyr 536), that have been shown to be essential for signalling (Thomassen et al., 1999). Instead SIGIRR has been shown to negatively regulate IL-1, IL-18, IL-33, LPS, flagellin and CpG DNA-induced signalling (Bulek et al., 2009; Qin et al., 2005; Wald et al., 2003; Zhang et al., 2011). SIGIRR exerts its inhibitory effects via ligand induced association with receptors which inhibits receptor dimerisation and the recruitment of receptor proximal signalling components. While each of the IL-1R family members has been identified in mammals, another family member known as double Ig IL-1R related molecule (DIGIRR) has recently been identified in fish (Gu et al., 2011). Unlike previously identified IL-1R family members, DIGIRR possess two extracellular Ig domains, and has a subcellular distribution within the Golgi. Like SIGIRR, DIGIRR has been shown to act as a negative regulator, inhibiting LPS and IL-1β-induced NF-κB activation. Over the years, many names for the ligands of the IL-1R family members have been used interchangeably (Sims et al., 2001). Now that functions have been identified for an increased number of the ligands the nomenclature outlined in Table 1.1 has been proposed (Dinarello et al., 2010).

Ligand name	Cleaved by	Receptor complex	Antagonist	Reference
IL-1α (IL-1F1)	Calpain, elastase, granzyme-B, chymase	IL-1R1 and IL-1RAcP	IL-1Ra (IL-1F3)	(Afonina et al., 2011; Eisenberg et al., 1991; Kavita and Mizel, 1995)
IL-1β (IL-1F2)	Caspase 1, Cathepsin G, elastase, proteinase-3, granzyme-A and mast cell chymase	IL-1R1 and IL-1RAcP	IL-1Ra (IL-1F3)	(Eisenberg et al., 1991; Irmler et al., 1995; Mizutani et al., 1991; Netea et al., 2010; Thornberry et al., 1992)
IL-18 (IL-1F4, IFNγ inducing factor, IL-1γ)	Caspase 1 and Caspase 3	IL-18R and IL-18RAcP	IL-18BP	(Akita et al., 1997; Novick et al., 1999)
IL-37(b) (IL-1F7, IL-1H4, IL-1ζ, IL-1RP1/IL-1H)	Caspase 1	IL-18R	Unknown	(Kumar et al., 2002)
IL-36α (IL-1F6, FIL-1ε) **IL-36β** (IL-1F8, FIL1η, IL-1H2) **IL-36γ** (IL-1F9, IL-1ε, IL-1H1, IL-1RP2)	Unknown	IL-1Rrp2 and IL-1RAcP	IL-36Ra (IL-1F5,IL-1Hy1, FIL1δ,IL-1H3, IL-1RP3, IL-1L1, IL-1δ)	(Towne et al., 2011)
IL-33 (IL-1F11, NFHEV)	Caspase 1 Caspase 3 and Caspase 7 Calpain Elastase, cathepsin G and proteinase-3	ST2L and IL-1RAcP	sST2	(Luthi et al., 2009; Schmitz et al., 2005) (Hayakawa et al., 2009; Lefrancais et al., 2012)

Table 1.1 IL-1R family member complexes with known ligands, potential proteases for the ligands and known antagonists of the receptors

1.6 IL-1R/TLR signalling pathways

The IL-1-induced signalling pathway is initiated following the formation of a ligand-induced receptor complex consisting of IL-1R and IL-1RAcP. The adaptor protein MyD88 is recruited to the receptor complex following stimulation via its TIR domain (Burns et al., 1998). Interleukin-1 receptor-associated kinase (IRAK) proteins are then recruited to the complex. These proteins interact with MyD88 via their death domains (Neumann et al., 2008). IRAK4 phosphorylates IRAK1 which induces its autophosphorylation activity (Li et al., 2002). Hyperphosphorylated IRAK1 is then released from the receptor complex (Kollewe et al., 2004). The association of IRAK1 with TNF-α receptor associated factor 6 (TRAF6) activates TRAF6 and leads to the recruitment of a TGF-β activated kinase-1 (TAK1)/TAK binding protein-2/3 (TAB2/3) complex and TAK1 activation by phosphorylation (Wang et al., 2001). Activated TAK1 phosphorylates the IkappaB kinase (IKK) complex, which in turn phosphorylates inhibitor of kappa B alpha (IκBα). IκBα is subsequently degraded allowing the p65/p50 subunits of the NF-κB complex to enter the nucleus and induce gene expression. TAK1 is also an upstream activator of MAPKs and induces the activation of the transcription factor AP-1(Ninomiya-Tsuji et al., 1999).

As mentioned above, IL-1 signalling requires the use of the TIR domain containing adaptor MyD88. While this signalling pathway only requires one adaptor, other signalling pathways use more than one. For example, LPS-induced TLR4 signalling utilises the adaptors Mal, MyD88, TRIF and TRAM. TLR4 activates two separate signalling pathways, the MyD88-dependent and MyD88-independent pathways. The adaptors Mal and MyD88 facilitate the activation of the MyD88-dependent pathway at the plasma membrane, resulting in the activation of NF-κB. TRIF and TRAM facilitate the MyD88-independent pathway which leads to interferon regulatory factor 3 (IRF3)

activation. TLR4 and TRAM have been shown to traffic to early endosomes following receptor stimulation and MyD88-independent signalling is mediated from this compartment (Kagan et al., 2008).

1.7 The isoforms of ST2

ST2 was initially discovered in 1989 by two independent laboratories working with growth stimulated mouse 3T3 fibroblasts (Klemenz et al., 1989; Tominaga, 1989; Werenskiold et al., 1989). These groups described a 2.7 kb transcript encoding an approximately 37 kDa unglycosylated secreted protein corresponding to a 60 - 70 kDa glycosylated product. This secreted and soluble form is now known as sST2. A longer form has since been identified which is known as ST2L (alternative names include T1/ST2, Fit-1 or DER-4) (Yanagisawa et al., 1993). Both ST2L and sST2 are encoded by the IL-1RL1 (ST2) gene on chromosome 2 and are generated by alternative promoter usage and 3' processing (Iwahana et al., 1999). ST2L is a transmembrane receptor, which consists of three extracellular Ig domains for ligand binding, followed by a transmembrane region and an intracellular TIR domain, for signal transduction. The three extracellular Ig domains contain three disulfide bonds (between amino acids 36-87, 133-181 and 235-303) and at least eight glycosylation sites (Yanagisawa et al., 1993). sST2 contains the three Ig domains of ST2L, but lacks the transmembrane and cytoplasmic domains and includes a unique nine amino acid C terminal sequence (Gachter et al., 1996). Two other isoforms also exist as a result of alternative splicing, namely ST2V and ST2LV. Insertion of a new exon which leads to a change in the C-terminal portion of ST2 causes it to gain a hydrophobic tail instead of the third immunoglobulin domain. This variant is called ST2V (Tominaga et al., 1999) while ST2LV, which was identified in chicken, lacks the transmembrane domain and therefore is secreted (Iwahana et al.,

2004). ST2LV mRNA or protein has not yet been detected in humans or mice, posing the possibility that ST2LV is absent in mammals. The known variants of ST2 are shown in Figure 1.2.

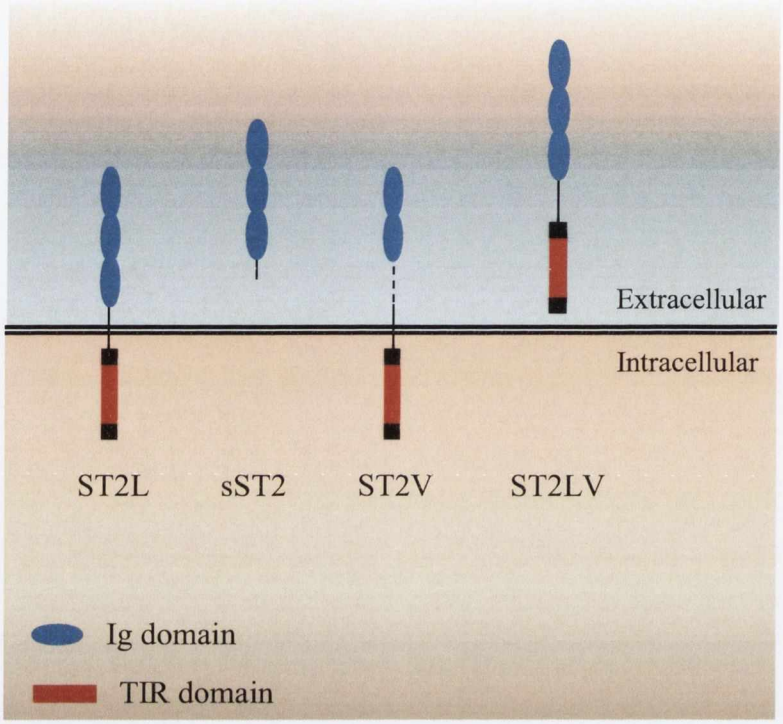


Figure 1.2 Variants of ST2

Four ST2 variants have been identified to date: ST2L, sST2, ST2V and ST2LV. ST2L contains three extracellular Ig domains, followed by a transmembrane region and an intracellular TIR domain. The secreted and soluble form, sST2 contains three Ig domains, but lacks the transmembrane and cytoplasmic domains and includes a unique nine amino acid C terminal sequence. ST2V lacks the third Ig domain of ST2L while ST2LV lacks the transmembrane domain and therefore is secreted.

1.8 ST2L expression

As mentioned previously ST2L is a transmembrane receptor with three extracellular Ig domains and an intracellular TIR domain. This receptor is highly expressed by T helper type 2 (Th2) cells and mast cells (Allakhverdi et al., 2007; Xu et al., 1998). Although it is expressed on Th2 cells, ST2L is not found on naive T cells, T helper type 1 (Th1) cells, T helper type 17 (Th17) cells or regulatory T (Treg) cells (Lecart et al., 2002; Nakae et al., 2007). Expression of ST2 mRNA has been detected in basophils, eosinophils and neutrophils, although at much lower levels than in mast cells (Suzukawa et al., 2008a; Suzukawa et al., 2008b). Fluorescence-activated cell sorting (FACS) analysis revealed the presence of extremely low levels of surface expressed ST2L in basophils (Suzukawa et al., 2008a) and eosinophils (Suzukawa et al., 2008b). However, ST2L is more apparent following intracellular staining in these cell types, suggesting that there is an additional intracellular pool of ST2L. This is also the case for dendritic cells (Rank et al., 2009). Low levels of surface expressed ST2L have also been detected on neutrophils (Alves-Filho et al., 2010). Interestingly, IL-33 treatment of basophils or neutrophils has been shown to significantly up-regulate ST2L mRNA and protein respectively, however ST2L expression in eosinophils ST2L is not induced by IL-33 (Alves-Filho et al., 2010; Suzukawa et al., 2008a; Suzukawa et al., 2008b). ST2L mRNA is also present in invariant natural killer (iNKT) cells, although surface expression was not detectable by FACS (Smithgall et al., 2008). Other cells types which express ST2L include B1 cells (Komai-Koma et al., 2011), macrophages (Espinassous et al., 2009), monocytes (Mun et al., 2010), epithelial cells (Zhao et al., 2012), endothelial cells (Zeyda et al., 2012), fibroblasts (Kurokawa et al., 2011), nuocytes (Neill et al., 2010), cardiomyocytes (Weinberg et al., 2002), astrocytes and microglia (Yasuoka et al., 2011). ST2L expressing cell types are shown in Figure 1.3.

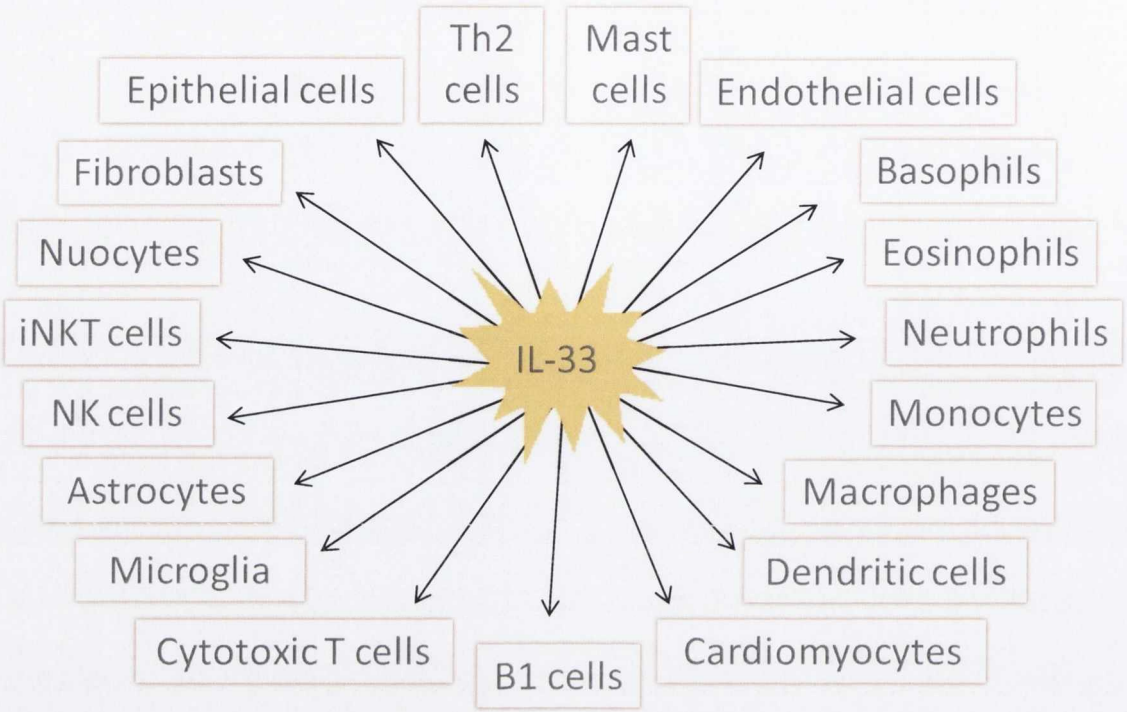


Figure 1.3 ST2L positive and IL-33 response cell types

While Th2 cells and mast cells express high levels of ST2L, the IL-33 receptor is also expressed by a wide range of other cell types. These include cells of the immune system such as basophils and eosinphils, as well as non-immune cells such as epithelial and endothelial cells.

1.9 ST2L ligand identification

Although ST2 was identified in 1989 (Tominaga, 1989), this receptor was classed as an orphan receptor until the identification of its ligand in 2005 (Schmitz et al., 2005). Its ligand, IL-33, was identified in a search for distant IL-1 and fibroblast growth factor (FGF)-like proteins in sequence databases. The authors described the human IL-33 cDNA sequence which encodes a 270 amino acid polypeptide and corresponds to a full-length protein with a calculated mass of 30 kDa. This 30 kDa form was thought to be the pro-form of the polypeptide, as incubation of in vitro translated IL-33 with caspase-1 led to the production of "mature" IL-33 with a mass of 18 kDa (Schmitz et al., 2005). However, multiple other groups have now demonstrated that caspase-1 does not cleave and activate IL-33 (Hong et al., 2011) and in fact the full length pro-form has been shown to be active by some groups (Hong et al., 2011; Luthi et al., 2009; Talabot-Ayer et al., 2009). In addition, the calcium dependent protease calpain, as well as neutrophil elastase and cathepsin G have been reported to cleave IL-33 (Hayakawa et al., 2009; Lefrancais et al., 2012) (Table 1.1). These caspase independent methods of IL-33 processing further enhance its biological activity and may serve to exacerbate the effects of the pro-form. An alternative splice variant of IL-33 has also been identified (Hong et al., 2011). This variant called spIL-33, was isolated from the Huh7 human hepatocarinoma cell line. It lacks the proposed caspase-1 cleavage site, but still contains the proposed caspase-3 and 7 cleavage sites, and was found to be capable of signalling via ST2L (Hong et al., 2011), although it is less active than mature IL-33 (amino acids 112-270).

As a member of the IL-1 family, IL-33 is most closely related to IL-18. Both lack classical secretory peptides and are found within the same branch of the IL-1 phylogenetic family tree, also shared with Il-1α and IL-1β. IL-33 adopts a β-trefoil fold

consisting of six β-strands which forms a barrel like structure, stabilised by large, internal hydrophobic residues, with another six β-strands forming a cap like structure (Figure 1.4A) (Murzin et al., 1992). IL-33 mRNA is expressed by numerous organs and cell types, in mice and human (Liew et al., 2010; Oboki et al., 2010). At the protein level, IL-33 is mainly expressed by structural and lining cells like fibroblasts, epithelial cells and endothelial cells and targets the cells mentioned in the previous section and shown in Figure 1.3.

IL-33 was actually firstly identified as a nuclear factor in high endothelial venules and thus became known as NF-HEV (Baekkevold et al., 2003). It appears to have an intracellular role where it is found in the nucleus in the absence of proinflammatory stimuli. Its N-terminal corresponds to a novel homeodomain-like Helix-Turn-Helix (HTH) DNA-binding domain and is thought to be responsible for its nuclear trafficking and chromatin binding ability (Baekkevold et al., 2003; Carriere et al., 2007). As yet, the function of IL-33 in the nucleus remains unclear, but it has been demonstrated to bind histone complexes and may be involved in transcriptional regulation (Roussel et al., 2008). IL-33 mediates the expression of intercellular adhesion molecule (ICAM)-1 and vascular cell adhesion molecule (VCAM)-1 in endothelial cells basally and in response to tumor necrosis factor-α (TNF-α) treatment via binding to the p65 promoter (Choi et al., 2012). Interestingly, full length IL-33 has also been shown to interact with the nulcear factor kappa B (NF-κB) subunits p65 and p50. Its interaction with the p65 subunit was enhanced following IL-1β stimulation, and resulted in the reduced ability of p65 to bind to its target DNA. Overexpressed IL-33 also resulted in reduced NF-κB activation following tumor necrosis factor alpha (TNF-α) stimulation. This may serve to reduce NF-κB triggered gene expression in order to dampen proinflammatory signalling (Ali et al., 2011). In addition, evidence suggests that IL-33 may act as a DAMP or alarmin,

getting released from necrotic cells (Luthi et al., 2009). While the role of nuclear IL-33 has not yet been fully elucidated, the role of IL-33 as an extracellular cytokine is better understood. Functioning as an extracellular cytokine, IL-33 can activate many different cell types via the ST2L receptor (Figure 1.3).

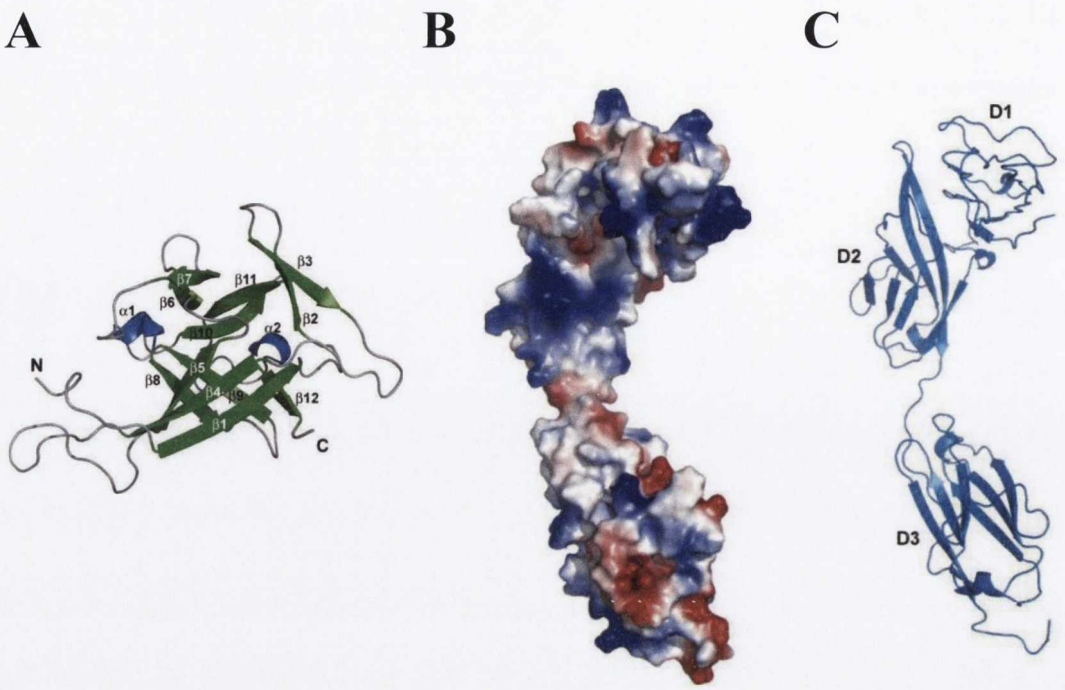


Figure 1.4 Structure of IL-33 and the extracellular domain of ST2L

(A) Ribbon representation of IL-33. Secondary structure elements are labelled. N: amino terminus, C: carboxyl terminus, α: alpha helix, β: beta strand. (B) Representation of the extracellular region of ST2L coloured by electrostatic potential. White, blue and red correspond to neutral, positive and negative electrostatic potential respectively. (C) A ribbon diagram is shown in the same orientation with the individual Ig domains labelled D1, D2 and D3 (Lingel et al., 2009).

1.10 The IL-33/ST2L signalling pathway

As mentioned earlier, the primary receptor for IL-33 is ST2L. However, association of ST2L with the coreceptor IL-1RAcP is also required for effective responsiveness to IL-33 (Chackerian et al., 2007; Palmer et al., 2008). Firstly, IL-33 binds ST2L with quite high affinity (26 pM K_D) (Palmer et al., 2008). The concave interaction surface of repeats D1-D2, which contains the first and second Ig domains of ST2L is positively charged. This complements a negatively charged residue cluster identified in IL-33. In contrast, D3 (containing the third Ig domain) is partly hydrophobic and partly electronegative, and therefore represents a complementary binding site for the second cluster region on IL-33 (Figure 1.4). The IL-33/ST2L complex in turn binds IL-1RAcP resulting in a 1:1:1 stoichiometry (Lingel et al., 2009). The presence of IL-1RAcP confers a measurable increase in the binding affinity of mIL-33 to ST2L (Palmer et al., 2008). The requirement for the TIR domain of IL-1RAcP was demonstrated with the use of a dominant negative form with a stop codon before the TIR domain, which inhibited IL-33 signalling (Chackerian et al., 2007).

Following the IL-33-induced formation of the ST2L-IL-1RAcP receptor complex, MyD88, IRAK4, IRAK1 and TRAF6 are all recruited to ST2L transiently and in a time dependent manner (Brint et al., 2004; Funakoshi-Tago et al., 2008; Schmitz et al., 2005). MyD88 is recruited to the complex via its TIR domain. IRAK4 and IRAK1 are also recruited via their death domains, and they phosphorylate components of the pathway with their kinase domains. Activation of this signalling pathway results in the phosphorylation of ERK1/2, p38 and JNK, as well as phosphorylation and degradation of IκBα (Brint et al., 2002; Funakoshi-Tago et al., 2008; Schmitz et al., 2005). Degradation of IκBα allows NF-κB proteins to enter the nucleus and induce gene expression. In the case of IL-33-induced signalling, the NF-κB complex involved consists of the p50 and

p65 subunits (Hayakawa et al., 2007). TRAF6 is needed for the p38, JNK and NF-κB activation, however IL-33-induced ERK activation was observed in the absence of TRAF6 (Funakoshi-Tago et al., 2008). It has been demonstrated that Lys-63-linked auto-ubiquitination of TRAF6 is a critical determinant in the activation of IκB kinase (IKK) (Lamothe et al., 2007) and indeed IL-33 can induce auto-ubiquitination of TRAF6 (Funakoshi-Tago et al., 2008). Similarly the involvement of Janus *kinase* 2 (JAK2) in this pathway has been elucidated. IL-33 activated the tyrosine kinase JAK2, which is required for NF-κB activation but is not needed for the activation of ERK, JNK and p38 (Funakoshi-Tago et al., 2011). It has been suggested that JAK2 regulates IKK activity, and thereby is by required only for IL-33 induced NF-κB activation. In addition, heterologous receptor ligation can synergise with the canonical IL-33 signalling pathway. IL-2R, IL-7R, thymic stomal lymphopoeitin receptor, c-kit and FcεR1-induced signalling have all been reported to synergise with IL-33 signalling (Andrade et al., 2011; Drube et al., 2010; Guo et al., 2009). These signalling pathways culminate in induction of the expression of various genes including IL-4, IL-5, IL-13, CXCL1, G-CSF, GM-CSF, IFN-γ, IL-1α, IL-1β, IL-6, IL-8, IL-10, IP-10, MCP-1, MCP-3, MIP-1α, MIP-2 and TNF-α (Drube et al., 2010; Funakoshi-Tago et al., 2008; Funakoshi-Tago et al., 2011; Hong et al., 2011; Moulin et al., 2007; Schmitz et al., 2005; Tare et al., 2010).

1.11 IL-33 and ST2L in host defence and disease

IL-33 is a potent activator of the immune system with roles in a variety of diseases. As a proinflammatory cytokine, IL-33 can play a dual role. It is associated with host-protection against infections and atherosclerosis but can also exacerbate inflammatory diseases, such as asthma (Alves-Filho et al., 2010; Miller et al., 2008; Smith, 2010). Therefore, the effects of IL-33 depend on the disease. Some of the diseases

in which IL-33 and ST2L have been implicated are shown in Table 1.2. While this is not inclusive of all conditions in which IL-33 and ST2L has been associated with, it gives an impression of the range of diseases which involve IL-33 and ST2L (Liew, 2012; Liew et al., 2010).

In the past two years, the discovery of novel subsets of IL-33 responsive innate immune cells has further increased the interest in this cytokine. IL-33 has been implicated in the function of these innate lymphoid cells that regulate protective responses in murine models of parasitic infection and allergic airway inflammation (Neill et al., 2010; Wilhelm et al., 2011). While as yet, it is unclear whether these different subsets are one single cell type at different stages of development or differentiation, or a number of distinct lineages, it is clear that these novel IL-33 responsive cell types play a vital role in type 2 immunity. The identification of these novel innate lymphoid cells has helped to clarify the role of IL-33 in some conditions such as allergy and anti-parasitic immunity (Mirchandani et al., 2012). As roles for IL-33 and ST2L continue to be defined in many conditions, the IL-33/ST2L signalling pathway may be worth considering for therapeutic targeting (Kakkar and Lee, 2008; Yuan et al., 2011). Therefore, a more complete understanding of the IL-33-induced signalling pathway would be of great benefit in coming to a deeper understanding of the many conditions with which it has been associated.

Disease	IL-33 involvement	Role	Reference
Infection			
Sepsis	- Sepsis attenuation following recombinant IL-33 treatment, as IL-33 increased neutrophil influx - Patients which circum to sepsis have elevated serum sST2 levels	IL-33 protective	(Alves-Filho et al., 2010)
Parasitic infection	- IL-33 upregulated during *Toxoplasma gondii* infection - IL-33 enhances parasite clearance	IL-33 protective	(Jones et al., 2010)
Cardiovascular disease			
Heart failure	- Serum ST2 levels increased in myocardial infarction and heart failure - Protective effect of IL-33 in experimental heart failure	IL-33 protective	(Miller, 2011; Sanada et al., 2007)
Atherosclerosis	- Attenuated in mice by IL-33 and exacerbated by soluble ST2	IL-33 protective	(Miller et al., 2008)
Allergy			
Asthma	- polymorphisms in the IL-33 and ST2 genes associated with susceptibility - patients have elevated IL-33 in their lungs - IL-33 exacerbates experimental asthma in mice - sST2 attenuates the disease in mice	IL-33 exacerbates	(Moffatt et al., 2010) (Kurowska-Stolarska et al., 2009) (Yin et al., 2012)
Autoimmune			
Arthritis	- Elevated IL-33 and sST2 in sera and synovial fluid of patients	IL-33 exacerbates	(Xu et al., 2008)
Inflammatory Bowel Disease	- IL-33 is upregulated in ulcerative colitis	IL-33 exacerbates	(Seidelin et al., 2010)
Nervous system			
Alzheimer's	- polymorphisms in IL-33 associated with susceptibility - IL-33 expression decreased in the brains of patients		(Chapuis et al., 2009)

Table 1.2 Examples of diseases in which IL-33 have been associated

1.12 Regulation of IL-33/ST2L signalling

The IL-1R/TLR-mediated inflammatory response is critical for innate immunity and host defence against infections, however uncontrolled inflammation can be detrimental to the host. Therefore, the ST2L signalling pathways must have regulatory mechanisms in place to modulate the host response.

Single immunoglobulin IL-1R-related protein (SIGIRR), also referred to as TIR8, has been identified as a negative regulator of the IL-33-induced signalling pathway (Bulek et al., 2009). Bulek *et al.* demonstrated a basal interaction between SIGIRR and ST2L, which was enhanced following stimulation with IL-33. The results presented suggest that both the extracellular Ig and intracellular TIR domain of SIGIRR are able to interact with ST2L but the Ig domain is more critical for the interaction with ST2L while the TIR domain is more important for inhibiting IL-33-induced signalling. SIGIRR can interact with MyD88, TRAF6 and IRAK following IL-1 treatment so it is possible that this also occurs following IL-33 stimulation (Qin et al., 2005). In the case of IL-1, SIGIRR inhibits heterodimerisation between IL-1R1 and IL-1RAcP, so it would be interesting to determine if it can also inhibit the heterodimerisation between ST2L and IL-1RAcP. SIGIRR is not only an inhibitor of the IL-1R family members, as inhibition of TLR4-induced responses has been demonstrated (Qin et al., 2005). In addition, TLR9 and TLR5 may also be targets of this inhibitory protein, although further evidence is needed in support of this (Qin et al., 2005; Wald et al., 2003).

The sST2 variant of the full length ST2 gene, generated by alternative splicing of pre-mRNA, is another regulator of IL-33/ST2L mediated signalling. It contains three Ig domains, but lacks the transmembrane and cytoplasmic domains contained within the structure of ST2L and includes a unique nine amino acid C terminal sequence (Gachter et al., 1996). As such, it can directly bind IL-33 and suppress NF-κB activation, and

abrogate expression of the Th2 associated cytokines IL-4, IL-5 and IL-13 (Hayakawa et al., 2007). It is likely to assert its effects by preventing IL-33 binding to functional ST2L.

The initial paper identifying IL-33 as the ST2L ligand, reported caspase-1 mediated cleavage of IL-33 in vitro, and this was proposed as a mechanism of activation of this cytokine, similar to IL-1β. More recent data found that caspase-1 does not cleave IL-33 at physiological concentrations. However, IL-33 was efficiently processed by caspase-3 and 7, which are selectively activated during apoptosis and this resulted in reduced activity of the cytokine, both in vitro and in vivo. As a result, caspase-dependent proteolysis of IL-33 during apoptosis may therefore represent a means of reducing the proinflammatory activity of this cytokine (Luthi et al., 2009).

Molecular regulation of ST2L expression following IL-33 stimulation is another way in which this pathway can be modulated and Zhao *et al.* have provided great insight the into mechanism by which this occurs. The authors demonstrate that following the association of IL-33 with ST2L, plasma membrane levels of the receptor are reduced as ST2L is internalised. ST2L is then phosphorylated on serine 442 by the glycogen synthase kinase GSK3β. In turn ST2L associates with F-box protein FBXL19, which is the substrate-recognition component of an E3 ubiquitin ligase complex. Subsequent to FBXL19 mediated polyubiquitination of ST2L, the receptor is degraded by the proteasome (Zhao et al., 2012). These regulatory events are also shown in Figure 1.5.

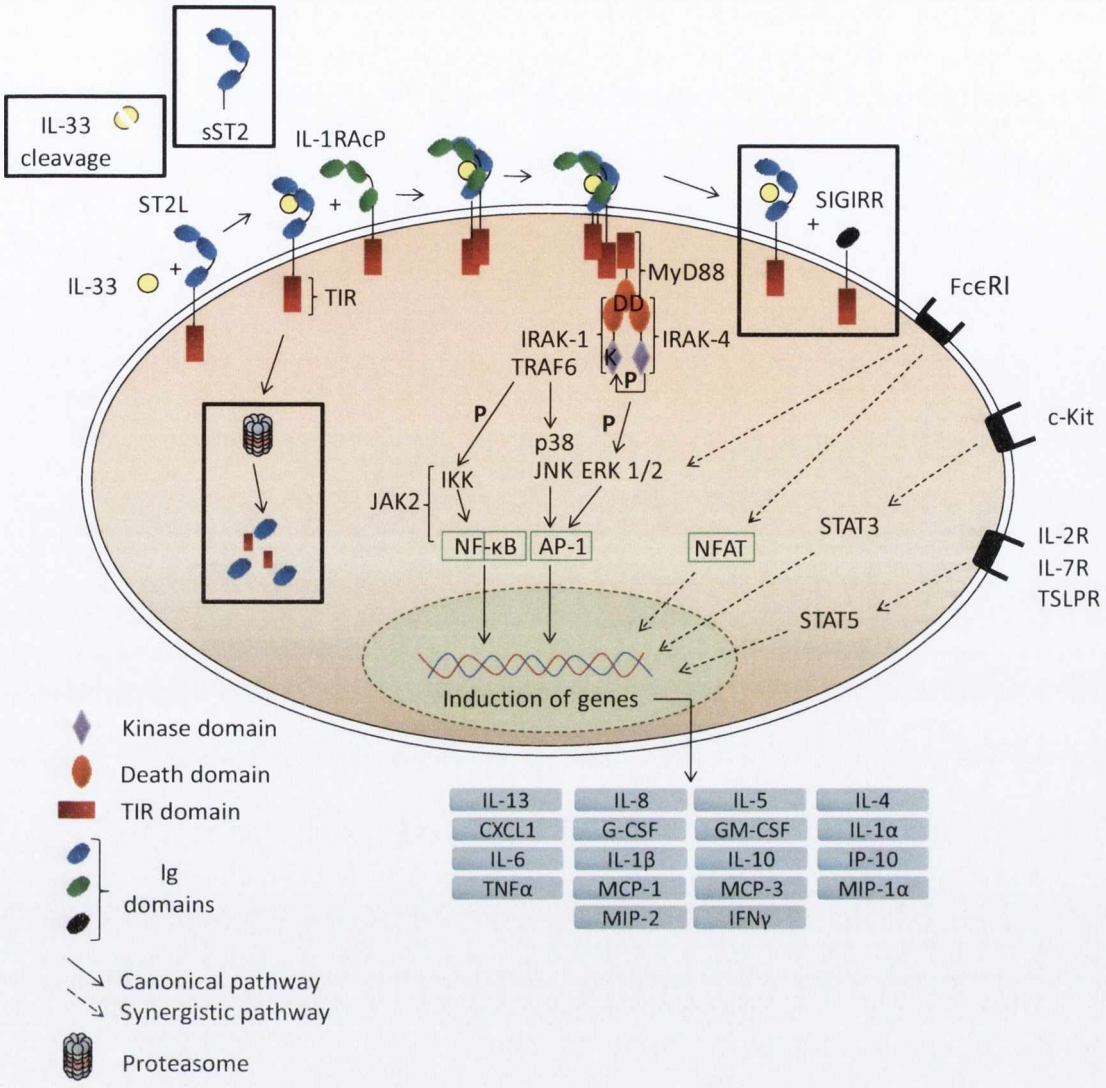


Figure 1.5 The IL-33/ST2L signalling pathway

IL-33 first associates with ST2L in a 1:1 stoichiometry, followed by the interaction with IL-1RAcP, resulting in the formation of an IL-33-ST2L-IL1-RAcP complex. MyD88, IRAK4 and IRAK1 are recruited to the complex resulting in the phosphorylation of ERK1/2, p38, JNK and degradation of IκBα. TRAF6 is required for IL-33 mediated p38, JNK and NF-κB activation but is not needed for the activation of ERK. JAK2 is required for NF-κB activation but is not needed for the activation of ERK, JNK and p38. Ultimately this results in increased expression of several genes. The boxed regions highlight known points of regulation for the pathway. sST2 is a soluble decoy receptor

which can bind IL-33. Cleavage of IL-33 by apoptotic associated caspases diminish its bioactivity, while IL-33 stimulation can induce SIGIRR binding to ST2L as well as proteasomal degradation of ST2L, both which also limit IL-33-induced pathway activation. Binding of other ligands to their receptors can also synergise with IL-33 signalling in a STAT or NFAT dependent manner. TIR, Toll-IL-1-receptor domain; DD, death domain; K, kinase domain; P, phosphorylation

1.13 Localisation and trafficking of the TLR and IL-1R superfamily members

A key aspect in achieving the optimum response when activating immune signalling pathways is the appropriate cellular location of the receptor. The localisation and trafficking of receptors is required to allow ligand detection, to allow the initiation of downstream signalling and is also required to limit the over-activation of signalling pathways.

Recent studies have demonstrated the important role that protein trafficking plays in TLR signalling pathways (McGettrick and O'Neill, 2010). The intracellular TLRs, TLR3, 7, 8 and 9 are localised to the endoplasmic reticulum (ER) in resting cells (Itoh et al., 2011; Johnsen et al., 2006; Latz et al., 2004). Following stimulation, these TLRs translocate to endosomes and initiation of the signalling pathways occurs from this location (Johnsen et al., 2006; Latz et al., 2004). The multi-transmembrane domain protein UNC93B1 has been implicated in the regulation of TLR3, 7 8 and 9. UNC93B1 interacts with the transmembrane domains of these TLRs (Brinkmann et al., 2007; Itoh et al., 2011). The requirement for UNC93B1 in the delivery of TLR3, 7, 8 and 9 to endosomes, where ligand will be encountered (Kim et al., 2008), was demonstrated by a single histidine-to-arginine substitution in UNC93B1. This mutation abolished its interaction with each of these TLRs, thus preventing their delivery to their correct intracellular location for ligand detection, thereby disrupting signalling (Itoh et al., 2011; Tabeta et al., 2006).

A protein associated with TLR4 (PRAT4A) has also been implicated in multiple TLR responses. Knockdown of this ER resident protein inhibited trafficking of TLR1 and TLR4 to the cell surface as well as ligand-induced trafficking of TLR9 (Takahashi et al., 2007). While PRAT4A acts as a positive regulator of TLR1 and TLR4 trafficking, PRAT4B positively regulates the trafficking of TLR4 (Konno et al., 2006) but negatively

regulates TLR1 trafficking (Hart and Tapping, 2012). Another chaperone, glycoprotein 96 (gp96) is required for TLR1, 2 and 4 transportation to the plasma membrane (Randow and Seed, 2001) and for the maturation and cleavage of TLR9 (Liu et al., 2010). A lack of gp96 renders cells unresponsive to bacterial stimuli, demonstrating the critical role this protein plays (Randow and Seed, 2001).

In addition to ensuring that these receptors localise to their correct cellular location in order to encounter ligand, protein trafficking after stimulation is another important point to consider. This trafficking can be required for the activation of additional branches of downstream signalling pathways or for the regulation or termination of signalling. The requirement of protein trafficking for both of these reasons can be demonstrated by LPS signalling via TLR4. LPS signalling via MyD88 occurs from the plasma membrane. The second phase of TLR4 signalling, the activation of the TRIF-TRAM pathway is initiated following internalisation of TLR4 into early endosomes (Kagan et al., 2008). Two splice variants of TRAM, named TRAM adaptor with GOLD domain (TAG), and transmembrane emp24 domain-containing protein 7 (TMED7), have been identified as negative regulators of the TRIF-TRAM pathway (Doyle et al., 2012; Palsson-McDermott et al., 2009). After LPS stimulation TLR4 and TRAM move from the plasma membrane to early endosomes, where they signal. They then move to late endosomes where they encounter TAG and TMED7. This disrupts the TRIF-TRAM interaction and results in reduced production of type I interferons (Doyle et al., 2012; Palsson-McDermott et al., 2009). TAG and TMED7 also promote TLR4 degradation at the late endosome.

While a substantial amount of research has been carried out regarding TLR trafficking, less is known about the trafficking of the IL-1R family members. The IL-1β dependent endocytosis and trafficking of the IL-1 receptor itself has been reported. The

IL-1 receptor has been suggested to be internalised through the endocytic caveosomes pathway and accumulates in the ER-Golgi and nucleus following IL-1β stimulation (Blanco et al., 2008). Another study, using mouse embryonic fibroblasts, reported that the IL-1 receptor translocates from the plasma membrane to late endosomes and subsequently on to lysosomes where it gets degraded (Brissoni et al., 2006). The internalisation of the IL-1R is thought to be dependent on the presence of IL-1RAcP (Korherr et al., 1997), and appears to be required for the complete activation of IL-1β induced signalling events (Li et al., 2006). While trafficking of the IL-1 receptor has been investigated to some extent, little is known about the trafficking of other IL-1 receptor family members.

1.14 Trafficking of the ST2L receptor

Under steady-state conditions, ST2L is known to be gradually internalised and degraded with a half-life of approximately five hours (Zhao et al., 2012) and although the internalisation of ST2L following IL-33 stimulation has previously been speculated (Choi et al., 2009), experimental evidence for this has now been established (Zhao et al., 2012). Following IL-33-induced internalisation of ST2L, the receptor is polyubiquitinated and degraded by the proteasome. While the internalisation of ST2L is known to be required for ST2L ligand-induced degradation, whether or not ST2L internalisation is also required for downstream signal activation remains to be investigated.

1.15 The p24 protein family

Gayle *et al.* have demonstrated a putative interaction between a member of the transmembrane emp24 domain-containing protein (TMED) family, TMED1 and ST2L. TMED1 is the major focus of this thesis and the p24 family to which it belongs will now be discussed in detail in the next section.

1.15.1 p24 Family Members

The p24 proteins constitute a family of transmembrane proteins of approximately 24 kDa in size. This family is conserved from yeast through to mammals, and can be divided into four subfamilies based on phylogenetic clustering called p24α, p24β, p24γ and p24δ (Dominguez et al., 1998). These can be further classified into two phylogenetically distinct groups; α-δ and β-γ (Carney and Bowen, 2004; Dominguez et al., 1998). Among species the exact composition and number of members in each of the subfamilies varies. The family consists of eight members in yeast (Marzioch et al., 1999), nine in *Drosophila* (Boltz et al., 2007), eleven in *Arabidopsis* (Carney and Bowen, 2004) and ten in mammals (Dominguez et al., 1998). Several nomenclatures for these proteins have been introduced and they are currently used in parallel. The *Drosophila* and yeast proteins, as well as various names for the ten vertebrates family members are summarised in Table 1.3 (Strating and Martens, 2009). In the protein database, most p24 proteins are annotated as ''TMED'' (transmembrane emp24 domain-containing protein) and this nomenclature will be used for the vertebrate proteins here.

The TMED proteins are trafficking proteins which operate mainly in the early secretory pathway (Figure 1.6) aiding protein transport between the ER and Golgi. Following protein synthesis at the ribosomes of the ER, correctly folded proteins undergo initial post-translational modification. They are then packaged onto coat protein complex

II (COPII) vesicles, leave the ER at ER exit sites (ERES) and are transported to organelles further along the pathway.

Following sorting through the early secretory pathway, proteins are transported further to their correct cellular location, such as endosomes or the plasma membrane. Proteins can also be secreted into the extracellular space via secretory vesicles. Forward transport in this direction is known as anterograde transport, while a retrograde transport system, involving COPI coated vesicles is also in place to retrieve resident ER proteins which have escaped (Strating and Martens, 2009). Many proteins have roles to play in the highly dynamic processes of protein sorting and trafficking but the TMED proteins are of particular interest here.

Vertebrates				*Drosophila*	Yeast
Subfamily	Systematic name	Database name	Additional names		
α	$p24\alpha_1$	TMED11	gp25L	Eclair	Erp1p
	$p24\alpha_2$	TMED9	p25,GMP25,gp25L2,p24d,p24D		Erp5p
	$p24\alpha_3$	TMED4	GMP25iso		Erp6p
β	p24β	TMED2	p24, p24a	CG3564	Emp24p
				CG9308	
γ	$p24\gamma_1$	TMED1	tp24, T1/ST2rbp	CG1967	Erp2p
	$p24\gamma_2$	TMED5	p28, T1/ST2iso	CG31787	Erp3p
	$p24\gamma_3$	TMED7	(g)p27	CG9053	Erp4p
	$p24\gamma_4$	TMED3	p26, p24b	Logjam	
	$p24\gamma_5$	TMED6			
δ	$p24\delta_1$	TMED10	p23, tmp21(l), p24c	Baiser	Erv25p
	$p24\delta_2$		p23iso		

Table 1.3 Nomenclature of the vertebrate, *Drosophila* and yeast TMED proteins

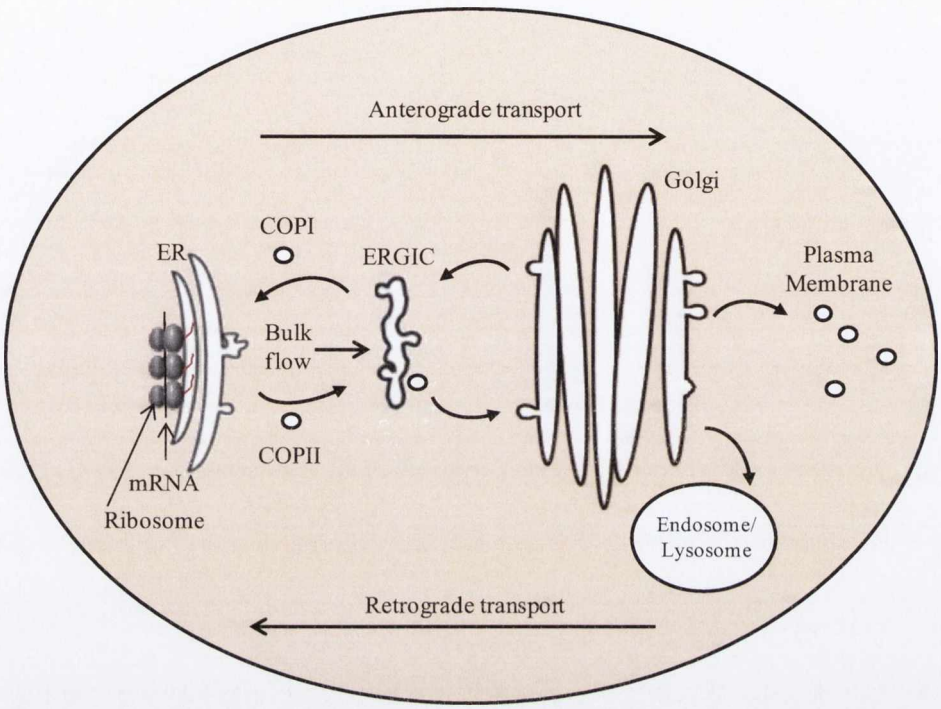


Figure 1.6 The early secretory pathway

Illustration of the anterograde and retrograde transport between the ER and the Golgi of the early secretory pathway. This dynamic process results in net anterograde transport of cargo in COPII (Coat protein complex II) vesicles, while COPI (Coat protein complex I) vesicles mediate retrograde transport of proteins which are normally maintained within the ER, ERGIC and Golgi. After sorting through the early secretory pathway, proteins can be further sorted to compartments such as endosomes, lysosomes or the plasma membrane where they can reside. Alternatively, proteins can be secreted in secretory vesicles.

1.15.2 The properties of TMED proteins

The TMED proteins are transmembrane proteins, consisting of a larger N-terminal region, followed by the transmembrane domain and a short C-terminal cytoplasmic tail of between 12 and 20 amino acids. The N-terminal region includes a GOLD (GOLgi Dynamics) domain. Secondary structure prediction for this domain suggests that it will adopt a β-fold structure with six to seven strands, forming a β-sandwich of two β sheets. It contains two cysteine residues which are well conserved throughout the family, and these are thought to form a disulfide bond within the GOLD domain (Anantharaman and Aravind, 2002). The cytoplasmic tail region contains highly conserved motifs, a double phenylalanine (FF) and a dibasic motif (KK, RR or RK) which are responsible for binding to coat complexes in COPI and COPII vesicles (Dominguez et al., 1998). The TMED proteins have been reported to exist as monomers, dimers, oligomers and hetero-oligomers (Barr et al., 2001; Blum and Lepier, 2008; Carney and Bowen, 2004; Jenne et al., 2002; Luo et al., 2007; Marzioch et al., 1999). One of these studies demonstrated that the occurrence of monomers or dimers depended on the organelle in question (Jenne et al., 2002). Their detection in various stoichiometries and oligomeric states is not surprising given that they are involved in highly dynamic cellular processes. Studies in yeast suggest that the expression levels of Erv25p, Emp24p, Erp1p, and Erp2p are interdependent. In addition, the knockdown or overexpression of a single TMED member has been shown by many groups in both yeast and mammals to affect the levels of other family members, which also attests to their interdependent roles (Hasegawa et al., 2010; Vetrivel et al., 2007; Zhang and Volchuk, 2010). There are also reports of retention of TMED proteins in the ER when a single family member is over-expressed alone (Emery et al., 2000).

Members of the family have been shown to span membranes belonging to the organelles of early secretory pathway, namely the ER, ERGIC and Golgi, and they shuttle between these compartments. Their involvement in the synthesis of COP vesicles which traffic between organelles of the early secretory pathway has been established in both yeast and mammalian systems (Aguilera-Romero et al., 2008; Dominguez et al., 1998). TMED9 and TMED11 are mainly localised at the ER (Dominguez et al., 1998). TMED7 (Fullekrug et al., 1999), TMED1 and TMED3 have been demonstrated to localise to the Golgi (Emery et al., 2000), while TMED2 can localise to the ERGIC (Zakariyah et al., 2012). TMED10, TMED2 and TMED11 have been identified in complexes with the Golgi matrix proteins GRASP55 and GRASP65. Binding was dependent on the presence of two valine residues at the extreme C-terminus of the TMED proteins as well as on the oligomeric state of the tail regions (Barr et al., 2001). The cytoplasmic domain of TMED10 also interacts with the small GTPase ARF-1, in its GDP state and is involved in the early stages of COPI coat assembly (Gommel et al., 2001).

Although TMED proteins are generally found in the ER, ERGIC and Golgi, some have been found in other post-Golgi locations. TMED1 and TMED10 have been found at the plasma membrane (Blum and Lepier, 2008; Chen et al., 2006; Gayle et al., 1996), TMED10 was un-expectedly isolated from the secretory granules of pancreatic β-cells (Hosaka et al., 2007) and TMED7 localises to early and late endosomes (Doyle et al., 2012). As well as having a functional role in secretory pathways, TMED proteins may also be important structural components of these organelles, as knockdown of TMED2 greatly disrupted the structural organisation of the Golgi (Luo et al., 2007).

1.15.3 Functions of TMED proteins

Members of the TMED family have been shown to act as receptors for the incorporation of specific cargo molecules into vesicles, using the luminal part of the protein. Recently several TMED binding partners or "cargo" have been identified. Protease-activated receptor-2 (PAR-2), a G protein coupled receptor has been identified as a binding partner for TMED2 (Luo et al., 2007). The TMED2-PAR-2 interaction was shown to occur at the Golgi, where PAR-2 is held until it is needed to repopulate the cell surface following stimulation. The GOLD domain and a small linker of TMED2 are required for this interaction. In addition, the authors mention that PAR-2 also strongly interacted with TMED10. TMED2 also interacts with the G-protein coupled receptors PAR-1, $P2Y_1R$, $P2Y_2R$, $P2Y_4R$, $P2Y_{11}R$ and the mu-opioid receptor 1B. In addition $P2Y_4R$ and mu-opioid receptor 1B have also been shown to interact with TMED10 (Luo et al., 2011). Also both TMED9 and TMED10 have been shown to interact with the protein tyrosine phosphatase TC48, and are required for targeting TC48 to its correct cellular location (Gupta and Swarup, 2006).

In yeast, TMED proteins are considered to act more as quality control factors of secretory pathways. Individual deletion mutants of each of the eight TMED proteins in yeast grow at rates equivalent to wild type (Marzioch et al., 1999) as does a strain of *Saccharomyes cerevisiae* which lacks all eight members (Springer et al., 2000). Nevertheless, deletion of Emp24, Erv25, Erp1, or Erp2 resulted in a selective transport defect of a GPI-anchored cell surface protein, Gas1p. These proteins appear to play a more prominent role in mice. A homozygous knock-out of a single family member (TMED10) in mice is actually embryonic lethal before blastocyst formation (Denzel et al., 2000), while those with a single point mutation which results in loss of TMED2 protein only survive until mid-gestation (Jerome-Majewska et al., 2010). In humans,

TMED2 is expressed in the trophoblast of placentas at all gestational stages, although the functional role of TMED2 during trophoblast differentiation in not yet known (Zakariyah et al., 2012).

TMED proteins may also modulate cellular stress pathways. Knockdown of TMED4 in mammals results in decreased sensitivity to oxidative stress, decreased apoptosis and an increase in heat shock protein 70 (HSP70) expression upon heat shock (Hwang et al., 2008). A role for TMED10 and potentially other family members has been identified in insulin secretion and proinsulin biosynthesis in pancreatic β-cells. Knock-down of TMED10 which also resulted in reduced endogenous TMED2 and TMED9 levels, reduced proinsulin biosynthesis and glucose-induced insulin secretion (Zhang and Volchuk, 2010). TMED6 has also been implicated in insulin secretion, as levels of secreted insulin are reduced following TMED6 knockdown, and TMED6 gene expression was lower in diabetic Goto-Kakizaki rats (Wang et al., 2012).

Interestingly, higher levels of TMED expression in certain cancers have been reported. TMED4 expression is significantly higher in invasive adenocarinoma mixed subtype bronchioloalveolar adenocarcinoma (BAC) than in BAC, however, the functional consequence of this is unclear (Ishiyama et al., 2007). TMED3 has been proposed as a potential novel drug target for Ets Related Gene oncogene positive tumors. TMED3 is highly expressed in prostate cancer compared to normal prostate or other normal tissues and its silencing produced anti-proliferative effects in cancer cell lines (Vainio et al., 2012).

1.16 Functions of TMED proteins in immune pathways

Although at an early point, there appears to be an emerging role for TMED proteins in diabetes and cancer biology. Simultaneously, a role for TMED proteins in immune signalling is coming to light. Evidence in the literature suggests that the TMED family may be an important family of immunoregulatory proteins, as other members of the family have been implicated in immune related functions. A TMED3 homologue in *Drosophila* known as logjam has been implicated in the negative regulation of a large number of immune-related genes, including targets of the Toll and Imd signalling pathways (Boltz and Carney, 2008). In vivo, LPS exposure upregulates TMED1 mRNA in Peyer's patch dendritic cells, however the functional consequence of this is not clear (Davies et al., 2010). In addition, TMED10 has been reported to bind to the Major Histocompatibility Complex (MHC) class I heavy chain (Jun and Ahn, 2011) and it is thought to protect free MHC class I heavy chains from ER-associated protein degradation. TMED7 is the most recent member to be implicated in immune signalling, as its role in MyD88-independent TLR4 signalling has been characterised. TMED7 inhibits TLR4, MyD88-indepedent signalling by working with TAG, the negative regulator of TRAM and mediating the disruption of the TRIF-TRAM complex at late endosomes (Doyle et al., 2012).

1.17 TMED1 (T1/ST2 receptor binding protein / p24γ_1 / tp24)

TMED1 was first isolated as a cell surface protein in the search for a T1/ST2 (ST2L) ligand (Gayle et al., 1996). As a result it was initially called T1/ST2 receptor binding protein, but now has several different names including p24γ_1, tp24 and TMED1. Here it will be referred to as TMED1. Gayle *et al.* found that its mRNA was widely expressed and the gene encoding the protein was mapped to chromosome 19p13.2. The

gene encodes a 227 amino acid protein, which results in a 25.2 kDa product. Its amino acid sequence and an illustration of its domain structure are shown in Figure 1.7. Although TMED1 was shown to bind ST2L, TMED1 was unable to initiate signal transduction via ST2L so was deemed not to be a ligand for the receptor.

Currently there is very limited literature available on TMED1. TMED1 is found in eukaryotes from yeast to humans. The human and mouse proteins are 96 % identical at the amino acid level and are both coded by four exons. It is widely expressed, as are most TMED proteins (Strating et al., 2009). Interestingly the zebra fish (Danio rerio) has two copies of this protein. It has been suggested that in zebra fish TMED1 is subject to alternative splicing (Rotter et al., 2002). However others propose that a duplication after a speciation event early in the teleost lineage resulted in two different TMED1 genes (Strating et al., 2009). In mammals, TMED1 has been shown to localise to the ER, ERGIC and Golgi (Jenne et al., 2002). In the Golgi it can co-localise with TMED10 (Emery et al., 2000).



Figure 1.7 Amino acid sequence and domain structure of TMED1

The amino acid sequence and domain structure of human TMED1 is shown. NCBI Reference Sequence NP_006849.1. Each of the domains is highlighted and the position of each region is indicated. SP-signal peptide, GOLD-Golgi dynamics domain, L-linker, CC-coiled-coiled, TM-transmembrane, C-cytoplasmic. The cysteine residues in red form a presumed disulfide bond within the GOLD domain.

1.18 Project aims and objectives

TMED1, a member of a GOLD domain containing family of trafficking proteins, was initially identified in a search for the ST2L ligand. Binding of TMED1 to ST2L was reported, although this did not initiate signal transduction, and as a result was not suspected to be a ligand for the receptor (Gayle et al., 1996). No further investigations were carried out to confirm or decipher a rationale for this interaction. Two GOLD domain containing proteins, TAG and TMED7 have been implicated in the regulation of TLR4 signalling (Doyle et al., 2012; Palsson-McDermott et al., 2009). In light of these observations the possible role for TMED1 in the ST2L signalling pathway was investigated.

The aims of this project are to:

- Further characterise TMED1 in terms of its subcellular location, the position of its transmembrane domain and the localisation of its GOLD domain
- Confirm the interaction between TMED1 and ST2L
- Investigate the cellular location of this interaction
- Determine the domains which mediate the interaction
- Investigate if TMED1 impacts on downstream ST2L signalling via IL-33

Overall the aim of this project is to further characterise the ST2L pathway and the role TMED1 plays in this pathway. I have uncovered a role for TMED1 in intracellular signalling by IL-33, specifically being involved in MAPK activation. A more complete understanding of the IL-33/ST2L pathway would be of great benefit in coming to a deeper understanding of the many conditions with which it has been associated and may help in the design of therapeutics in the future.

Chapter Two

Materials and Methods

2.1 Materials

Material/Reagent	Source
Tissue culture flasks (T25, T75 T175)	Fisher Scientific
6, 12, 24 and 96 well plates	Fisher Scientific
Dulbecco's Modified Eagle Medium (DMEM)	Gibco® Biosciences
Roswell Park Memorial Institute (RPMI) medium	Gibco® Biosciences
Iscove's Modified Dulbecco's Medium (IMDM)	Sigma®
Phosphate Buffered Saline (PBS)	Gibco® Biosciences
Fetal Calf Serum (FCS)	Biosera
Penicillin streptomycin (PS)	Sigma®
Trypsin-(Ethylenediaminetetraacetic acid) EDTA	Sigma®
α-thioglycerol	Sigma®
Trypan Blue	Sigma®
G418	Sigma®
HygroGold™	InvivoGen
Blasticidin	InvivoGen
Puromycin	Sigma®
Dimethyl sulfoxide (DMSO)	Sigma®
Dynasore	Sigma®

Table 2.1 Materials and reagents used for tissue culture

Cells	Source
HEK-293-hST2L	K. Bulek (Lerner Research Institute, Cleveland Clinic Foundation, OH, USA)
HMC 1.1	J. Butterfield (Mayo Clinic, Rochester, MN, USA)
HEK-293T	European Collection of Animal Cell Cultures
HEK-293-R1	A. Bowie (Trinity Biomedical Sciences Institute, TCD, Dublin, Ireland)
HEK-293-MD2-CD14-TLR4	InvivoGen
HEK-293-TLR3	European Collection of Animal Cell Cultures
THP-1	European Collection of Animal Cell Cultures

Table 2.2 Cell lines

Ligand	Source
IL-33	PeproTech®/Enzo® Life Sciences
IL-1	R&D Systems®
LPS	Enzo® Life Sciences
Poly I:C	InvivoGen
PMA	Merck
TNF-α	R&D Systems®

Table 2.3 Ligands used for cell stimulation

Reagent	Source
GeneJuice®	Novagen
Lipofectamine™ 2000	Invitrogen™
Lipofectamine™ RNAiMax	Invitrogen™
Amaxa Nucleofector™ Kits	Lonza
TMED1 siRNA	Qiagen and Dharmacon

Table 2.4 Reagents used for cell transfection

Plasmid	Source
TMED1-GFP	GeneCopoeia™
TMED1-myc	Origene
TMED2-GFP	R. Blum (Institute for Clinical Neurobiology, University Hospital Würzburg, Würzburg, Germany)
TMED3-GFP	R. Blum (Institute for Clinical Neurobiology, University Hospital Würzburg, Würzburg, Germany)
TMED7-GFP	GeneCopoeia™
ST2L	S. Martin (Institute of Genetics, TCD, Dublin, Ireland)
ER-CFP	Clontech
Golgi-CFP	H. Stenmark (Institute for Cancer Research, The Norwegian Radium Hospital, Oslo, Norway)
EEA1-CFP	H. Stenmark (Institute for Cancer Research, The Norwegian Radium Hospital, Oslo, Norway)
Rab11a-CFP	H. Husebye (Institute of Cancer Research and Molecular Medicine, NTNU, Trondheim, Norway)
Mal-HA	Generated in house (Fitzgerald et al., 2001)
MyD88-myc	M. Muzio (Mario Negri Institute, Milano, Italy)
TRAM-flag	K. Fitzgerald (University of Massachusetts, Boston, USA)
TRIF-HA	C. Basler (Mount Sinai School of Medicine, New York, USA)
p65-HA	K. Ray (GlaxoSmithKline, Stevenage, UK)
pcDNA 3.1	Stratagene
pGL3-NF-κB luciferase	R. Hofmeister (Universitat Regensburg, Regensburg, Germany)
pGL3-ISRE luciferase	Clontech
pAP-1luciferase	Stratagene
pRL-TK-Renilla luciferase	Promega

Table 2.5 Expression vectors

Reagent/Material	Source
DH5α™	Invitrogen™
EndoFree Plasmid Maxi Kit	Qiagen
Wizard® Plus SV Miniprep DNA Purification System kit	Promega
Site-Directed Mutagenesis Kit	Stratagene
RNeasy Mini Kit	Qiagen
Primers	Eurofins MWG
High Capacity cDNA Reverse Transcription Kit	Applied Biosystems
Platinum® SYBR® Green qPCR SuperMix	Invitrogen™
PCR microplate Thermo-Fast 96 well	Fisher Scientific
Taq DNA Polymerase with ThermoPol Buffer	New England Biolabs
dNTP mix	Promega
DNA markers	New England Biolabs

Table 2.6 Reagents used for DNA and RNA purification and amplification

Reagent	Source
Dithiothreitol (DTT)	Sigma®
N,N,N',N'-Tetramethylethylenediamine (TEMED)	Sigma®
Ammonium persulphate (APS)	Sigma®
30 % Acrylamide/Bis-acrylamide solution	National Diagnostics
Phenylmethanesulfonyl fluoride (PMSF)	Sigma®
Sodium orthovanadate	Sigma®
Leupeptin	Sigma®
Aprotinin	Sigma®
Digitonin	Merck
Trypsin	Sigma®
Triton X-100	Sigma®
Broad range pre-stained protein marker	New England Biolabs®
Polyvinylidene difloride (PVDF)	Millipore
Lumi-light western blotting substrate	Roche
20X LumiGLO® Reagent and 20X Peroxide	Cell Signalling
Supersignal®	Technology®
Re-Blot Plus Solution	Millipore
Photographic film	Fujifilm
Coelenterazine	Calbiochem
Passive Lysis Buffer	Promega
CytoTox 96® Non-Radioactive Cytotoxicity Assay	Promega

Table 2.7 Reagents used for protein isolation, protease protection assays and western blotting

Antibody	Source	Product Code
Anti-TMED1	Sigma®	HPA018507
Anti-ST2L	R&D Systems®	AF523
Anti-GFP	Santa-Cruz Biotechnology®	sc-9996
Anti-HA	Covance®	MSS-101R
Anti-β-actin	Sigma®	A5316
Anti-IκBα	Cell Signalling Technology®	4812S
Anti-pERK	Cell Signalling Technology®	9101S
Anti-pp38	Cell Signalling Technology®	9211S
Anti-pJNK	Cell Signalling Technology®	9251S
Anti-total ERK	Cell Signalling Technology®	4695S
Anti-EEA1	Abcam®	ab2900
Horse radish Peroxidase (HRP) conjugated antibodies	Jackson Immunoresearch	
Unconjugated IgG antibodies	Jackson Immunoresearch	

Table 2.8 Antibodies used for Western Blotting, co-immunoprecipitation and confocal analysis

Reagent	Source
Protein A/G-plus agarose beads	Santa-Cruz Biotechnology®
GFP-Trap®	ChromoTek

Table 2.9 Reagents used for co-immunoprecipitation assays

Reagent/Material	Source
Poly-L-lysine	Sigma®
Coverslips	Fisher Scientific
Slides	Sigma®
Glass bottomed confocal dishes	MatTek Corporation
Tx-100	Sigma®
Formaldehyde	Sigma®
Bovine Serum Albumin (BSA)	Sigma®
CellMask™ Plasma Membrane Stain	Invitrogen
Alexa Fluor® 647 Microscale Labelling Kit	Invitrogen

Table 2.10 Reagents used for confocal analysis

Reagent	Source
96 well microtitre plate	Fisher Scientific
DuoSet ELISA kits	R&D Systems®
Tween® 20	Sigma®
3,3',5,5'-tetramethyl-benzidine (TMB)	BD biosciences

Table 2.11 Reagents used for Enzyme-Linked ImmunoSorbent Assay

2.2 Bacterial transformation and plasmid purification

Competent cells (DH5α™) were thawed on ice. 2 µl of plasmid DNA was added to 25 µl competent cells and incubated on ice for 30 minutes. The cells were heat shocked for 45 seconds at 42 °C, and then placed on ice for 2 minutes. 1 ml sterile Luria-Bertani (LB) broth without antibiotic was then added to the cells and they were incubated at 37 °C for 1 hour at 200 rpm. After this incubation, samples were centrifuged at ~15,000 x g and most of the LB broth was removed. The remainder (containing the cells) was aseptically spread on sterile agar plates containing the appropriate antibiotic. The plates were incubated upside down at 37 °C overnight. A single colony was grown in 5 ml LB broth containing antibiotic for 6-8 hours at 37 °C. This was then transferred to 100 ml LB broth containing antibiotic and was incubated overnight at 37 °C at 200 rpm. The following day the bacteria were centrifuged and plasmids were purified using the EndoFree Plasmid Maxi Kit according to the manufacturer's instructions. To determine the yield, DNA concentration was measured using a NanoDrop ND-1000 (Thermo Scientific).

2.3 Cell culture

Cell lines were stored in liquid nitrogen in plastic cyrovials with FCS containing 10 % (v/v) DMSO. To thaw the cells they were removed from the liquid nitrogen and immediately warmed to 37 °C. They were then resuspended in warm media. The cells were centrifuged at 290 x g for 5 minutes and the pellet was resuspended in the appropriate media, which was transferred to a T25 culture flask and grown until confluent and then expanded.

The Human embryonic kidney (HEK)-293T, HEK-293-ILR1, HEK-293-hST2L, HEK-293-MD2-CD14-TLR4 and HEK-293-TLR3 cells were sub-cultured in DMEM supplemented with 10 % (v/v) FCS and 1 % (v/v) PS. Cells were grown at 37 °C with 5 % CO_2 and cultured when 80 % - 90 % confluent. Certain cells lines were also cultured with antibiotics to maintain expression of the receptor of interest. HEK-293-hST2L cells were cultured with 1 μg/ml puromycin, HEK-293-MD2-CD14-TLR4 with 10 mg/ml HygroGold™ and 1 mg/ml Blasticidin and HEK-293-TLR3 with 50 mg/ml G418. In order to sub-culture cells, they were washed with 5 ml PBS and incubated with 3 ml 0.25 % trypsin/EDTA until detachment occurred. Trypsinisation was terminated by the addition of 7 ml DMEM. Cells were centrifuged at 290 x g for 3 minutes. The pellet was resuspended with 1 ml fresh media and 10 μl was used to count cells using the following method: 40 μl DMEM, 10 μl trypan blue and 10 μl cells were mixed. 10 μl of the mixture was pipetted onto a haemocytometer, 15 boxes of the central grid were counted and this figure was divided by 3 to give the average number for 5 boxes. Then the following calculation was carried out which gave the number of cells present per ml:

Average of 5 boxes x 5 (will give number for all boxes on grid) x 6 (dilution factor) x 10,000 = no. of cells/ml

The Human mast cell (HMC) 1.1 cell line was cultured in IMDM supplemented with 10 % (v/v) FCS, 1 % (v/v) PS and 1.2 mM α-thioglycerol at 37 °C with 5 % CO_2 until media was cloudy. The media was centrifuged to pellet the suspension cells and they were sub-cultured. The THP-1 cell line was cultured in RPMI supplemented with 10 % (v/v) FCS, 1 % (v/v) PS at 37 °C with 5 % CO_2 until media was cloudy. Suspension cells were counted in the same way as the adherent cell lines for setting up experiments.

2.4 Transient transfection of HEK-293 cells with expression vectors

The GeneJuice® transfection reagent was used for transfection of these cell lines with plasmids encoding the proteins of interest. Cells were set up at 2 x 10^5 cells/ml and transfected 24 hours later. The appropriate amount of DNA was placed in an eppendorf. The GeneJuice®/serum free (SF)-media mix was then prepared, and incubated at room temperature for 5 minutes. The GeneJuice®/SF-media mix was added to the DNA and incubated at room temperature for a further 15 minutes. The DNA/GeneJuice®/SF-DMEM mix was added to the cells drop-wise. The following table shows the amount of DNA, GeneJuice® and SF-media used for various experimental formats.

Well format	Total amount of DNA	SF-media	GeneJuice®
96 well	220 ng	9.2 µl	0.8 µl
6 well	1 µg	100 µl	3 µl
10 cm dish	8 µg	235 µl	15 µl

Table 2.12 GeneJuice® quantities for transfection

2.5 Transient transfection of HEK-293 cells with siRNA and HMC 1.1 cells with expression vectors

The Lipofectamine™ 2000 or Lipofectamine™ RNAiMax transfection reagents were used for siRNA transfection of HEK-293 cells and the Lipofectamine™ 2000 reagent was used for the transfection of HMC 1.1 cells with plasmids encoding the protein of interest.

HEK-293 cells were set up at 0.75 or 1 x 10^5 cells/ml in 24 well plates in antibiotic free media. 24 hours later cells were transfected. Lipofectamine™ (3 µl per reaction) and serum free media (47 µl per reaction) mixes were prepared and incubated at

room temperature for 5 minutes. siRNA was also prepared in serum free media, to a total volume of 50 µl. siRNA and Lipofectamine™ mixes were combined and incubated at room temperature for 20 minutes. 100 µl of the siRNA- Lipofectamine™-SF media mix was then added drop-wise to each well of a 24 well plate and incubated for 48 hours before cell stimulation.

6 x 10^5 HMC 1.1 cells were used for each transfection, and set up in 500 µl antibiotic free media. For these transfections, 0.8 µg DNA prepared in SF media to a total volume of 50 µl and 4 µl Lipofectamine™ 2000 plus 46 µl SF media was prepared according to the protocol above.

2.6 Transient transfection of THP-1 cells with siRNA

THP-1 cells were transfected using the Amaxa® Cell Line Nucleofector® Kit *V*. Firstly, 1 ml pre-heated RPMI was placed in 24 well plates for each sample. Per transfection 1 x 10^6 cells were prepared in 100 µl Nucleofector® Solution V. The appropriate amount of siRNA was added to the cell suspension and transferred into the provided cuvette. The cuvette was inserted into the Nucleofector® Cuvette Holder and transfected using program V-001. Cells were then carefully removed using the supplied pipettes and added to the pre-heated media. Cells were allowed to rest for 48 hours before stimulation for ELISAs as in section 2.16.

2.7 Protease protection assay

HEK-293T cells were set up at 2 x 10^5 cells/ml. 24 hours later, if required, cells were transfected with TMED1-green fluorescent protein (GFP) as in section 2.4. A further 24 hours later, cells were trypsinised, washed twice in DMEM, and three times in Krebs-Henseleit buffer (110 mM potassium acetate, 20 mM HEPES (4-(2-hydroxyethyl)-1-piperazineethanesulfonic acid), 2 mM $MgCl_2$). Whole cell lysates were prepared from one quarter of the cells, and the remaining three quarters were transferred into three reaction tubes. Cells in the three tubes were permeabilised on ice for 10 minutes in Krebs-Henseleit buffer containing 20 µM digitonin. After permeabilisation, one tube was spun down at 100,000 x *g* at 4 °C for 30 minutes. The supernatant (cytosolic fraction) and the pellet (membrane fraction) were separated and boiled in sodium dodecyl sulphate (SDS)-Laemmli buffer. The other two tubes were incubated with 1 mM trypsin in the absence or presence of 1 % (v/v) Triton X-100 on ice for 30 min, and then ultracentrifuged. The pellets were boiled in 5 X SDS-Laemmli buffer, and analysed by SDS-PAGE (sodium dodecyl sulphate-polyacrylamide gel electrophoresis) and Western blot as in sections 2.10 and 2.11.

2.8 Co-immunoprecipitation assay

HEK-293T or HEK-293-hST2L cells were set up at 2 x 10^5 cells/ml in 10 cm dishes and transfected as described (Section 2.4). Between 1 x 10^7 and 3 x 10^7 HMC 1.1 cells were used for co-immunoprecipitations (Co-IPs). If required, cells were stimulated with IL-33, 50 ng/ml for the HEK-293-hST2L cells or 10 ng/ml for the HMC 1.1 cells, washed once in cold PBS and lysed in 800 µl lysis buffer (10 % (v/v) glycerol, 50 mM NaF, 20 mM Tris-Cl pH 8.0, 2 mM EDTA, 137 mM NaCl, 1 % (v/v) Nonidet P-40, 100 µg/ml PMSF, 1 mM sodium orthovanadate (Na_3VO_4), 1 µg/ml leupeptin, 6 µg/ml

aprotinin) and transferred to a microcentrifuge tube. If the Co-IPs were to be carried out at a later date, samples were snap frozen in liquid nitrogen and stored at -80 °C until needed and then one of the following protocols were followed.

For Co-IPs using antibody coupled A/G-plus beads, 1 µg of the antibody against the protein of interest was incubated with A/G-plus beads overnight at 4 °C. The following day the antibody coupled beads was pelleted by centrifuging at 2,200 x g for 3 minutes and washed three times in lysis buffer (centrifuged between each wash to pellet the antibody coupled beads). Meanwhile, the lysates were spun at maximum speed for 10 minutes to remove debris. 50 µl of each sample was removed at this point as the whole cell lysate. 12 µl 5 X SDS-Laemmli buffer was added to the lysate and they were boiled for 5 minutes. If required, supernatants were pre-cleared with 20 µl protein A/G-plus beads for 1 hour at 4 °C with rolling to remove any protein that stuck directly to the beads and not the antibody. The samples were then centrifuged at 2,200 x g to pellet the beads and the supernatants were transferred into microcentrifuge tubes containing the antibody coupled beads and rolled for 2/3 hours at 4 °C. Samples were then spun at 2,200 x g for 2 minutes to pellet the beads and they were washed in lysis buffer three times again. 50 µl SDS-Laemmli buffer was added and the samples were boiled for 5 minutes. The samples were then analysed by SDS-PAGE and Western blotting as described in sections 2.10 and 2.11.

For Co-IPs with GFP-Trap® beads, samples were lysed using lysis buffer (10 mM Tris/Cl pH 7.5, 150 mM NaCl, 0.5 mM EDTA, 0.5 % NP40, plus protease inhibitors). The beads were washed with wash buffer (10 mM Tris/Cl pH 7.5, 150 mM NaCl, 0.5 mM EDTA plus protease inhibitors) three times, spinning down at 2,700 x g following each wash. The samples were then incubated with beads for 1/2 hours at 4 °C with rolling and then washed three times. 50 µl 5 X SDS-Laemmli buffer was then

added, and the samples were boiled for 5 minutes. The samples were then analysed by SDS-PAGE and Western blotting as outlined in sections 2.10 and 2.11.

2.9 Site Directed Mutagenesis of TMED1 and ST2L constructs

Mutations and deletions were introduced into the TMED1 and ST2L sequences using the QuikChange™ site-directed mutagenesis kit according to manufacturer's instructions.

Six TMED1 mutants were generated; SS-TMED1 (two mutations: C45S and C106S), ΔTM-TMED1 (deletion of the transmembrane domain), ΔG-TMED1 (deletion of the GOLD domain), ΔGLCC-TMED1 (deletion of the GOLD, linker and coiled-coiled domains), ΔSP-TMED1 (deletion of the signal peptide) and ΔSPΔTM-TMED1 (deletion of the signal peptide and transmembrane domains). The primers used are listed in Table 2.13).

The site directed mutagenesis kit was also used to attach a C-terminal Haemagglutinin (HA) tag to the wild type ST2L protein. The primers which were used are listed in Table 2.14. Next, two ST2L deletion mutants were generated; the Ig domains were deleted in ΔIG-ST2L, while the TIR domain is removed from ΔTIR-ST2L.

Primer	Sequence
C45S forward	5'GGGGAGGAAGCAGTCTTTCTACCAGTCCG 3'
C45S reverse	5'CGGACTGGTAGAAAGACTGCTTGCTCCCC 3'
C106S forward	5'GGGGACTACAAGCTGTCCTTTGACAACTCCTTC 3'
C106S reverse	5'GAAGGAGTTGTCAAAGGACAGCTTGTAGTCCCC 3'
ΔTM-TMED1 forward	5'CTTGGAGCGGGTCACGCTCAAGCGC 3'
ΔTM-TMED1 reverse	5'GCGCTTGAGCGTGACCCGCTCCAAG 3'
ΔG-TMED1 forward	5'GTTCCTGTTGCCGGCGGGGAGGGACAGCCTCCAGGATG ACGAG 3'
ΔG-TMED1 reverse	5'CTCGTCATCCTGGAGGCTGTCCCTCCCCGCCGGCAACA GGAAC 3'
ΔGLCC-TMED1 forward	5'GTTCCTGTTGCCGGCGGGGAGGAACTTCTGGTCAGCTG TCAACGTG 3'
ΔGLCC-TMED1 reverse	5'CACGTTGACAGCTGACCAGAAGTTCCTCCCCGCCGGCA ACAGGAAC 3'
ΔSP-TMED1 forward	5' GGAGTTCGAACCATGGCGGGGCCCCCGCC 3'
ΔSP-TMED1 reverse	5' GGCGGGGGCCCCGCCATGGTTCGAACTCC 3'

Table 2.13 Primers used for mutagenesis of TMED1

Primer	Sequence
Insert HA forward	5'CAGAAGCAATACCCATACGACGTCCCAGACTACGCTTA GTGCCTGCTGTG 3'
Insert HA reverse	5'CACAGCAGGCACTAAGCGTAGTCTGGGACGTCGTATGG GTATTGCTTCTG 3'
ΔIG-ST2L forward	5'CAATTCTCATGTATTCCACAGCAGCAAGGAAAAATCCA ATTGATC 3'
ΔIG-ST2L reverse	5'GATCAATTGGATTTTTCCTTGCTGCTGTGGAATACATGA GAATTG 3'
ΔTIR-ST2L forward	5'CTAAACCTTACAAGACTAGGAATGATGGAAGCAAAATT CCCAGAAAGG 3'
ΔTIR-ST2L reverse	5'CCTTTCTGGGAATTTTGCTTCCATCATTCCTAGTCTTGTA AGGTTTAG 3'

Table 2.14 Primers used for tag attachment and mutagenesis of ST2L

Following site-directed mutagenesis, a single colony was selected for an overnight culture of each of the mutants. These were grown up and minipreps were carried out using the Wizard® Plus SV Miniprep DNA Purification System. Sequence analysis of the mutants was carried out by Geneservice. The plasmids were then re-transformed into DH5α™ cells as described in section 2.2, in order to have sufficient quantities for transfections.

2.10 SDS-PAGE (sodium dodecyl sulphate-polyacrylamide gel electrophoresis)

SDS-PAGE gels consist of a stacking gel and a resolving gel. Volumes for making up two resolving gels and two stacking gels are shown in Tables 2.15 and 2.16 respectively.

Resolving Gel

	6 %	8 %	10 %	12 %	15 %
30 % Acrylamide/Bis-acrylamide mix	3 ml	4 ml	5 ml	6 ml	7.5 ml
H_2O	7.9 ml	6.9 ml	5.9 ml	4.9 ml	3.4 ml
1.5 M Tris-HCL (pH 8.8)	3.8 ml	3.8 ml	3.8 ml	3.8 ml	3.8 ml
10 % SDS	150 µl	150 µl	150 µl	150 µl	150 µl
10 % APS*	150 µl	150 µl	150 µl	150 µl	150 µl
TEMED*	6 µl	6 µl	6 µl	6 µl	6 µl

Table 2.15

Stacking Gel

30 % Acrylamide/Bis-acrylamide mix	1 ml
H_2O	4.1 ml
1 M Tris-HCL (pH 6.8)	0.75 ml
10 % (w/v) SDS	60 µl
10 % (w/v) APS*	60 µl
TEMED*	6 µl

Table 2.16

*Ammonium persulphate (APS)

Tetramethylethylenediamine (TEMED)

Both APS and TEMED are added just before pouring of the gel.

The gels were run in a bio-rad gel box filled with 1 X SDS-running buffer (10 X = 25 mM Tris, 192 mM glycine, 0.1 % (w/v) SDS up to 1 L with ddH_20).

Protein samples were resolved on SDS polyacrylamide gels using a constant current of 25/30 mA per gel. Samples were first run through a stacking gel followed by a resolving gel. A pre-stained molecular marker was run alongside the proteins as molecular weight standards.

2.11 Western blotting

After the samples were electrophoresed on an SDS-gel they were transferred onto a PVDF membrane and treated with antibodies to allow detection of the protein of interest by enhanced chemiluminescence (ECL) using the method outlined below.

2.11.1 Transfer method

The resolved proteins were transferred onto PVDF using a semi-dry transfer system (Mason Technology). For the semi-dry system 3 buffers are needed: Anode buffer 1 (0.3 M Tris Base pH 10.4, 20 % methanol (MeOH)), Anode buffer 2 (0.025 M Tris Base pH 10.4, 20 % MeOH), Cathode buffer (0.025 M Tris Base pH 9.4, 0.04 M Caproic acid, 20 % MeOH). A sandwich was set up in the following order (Bottom to top); One piece of filter paper which had been immersed in Anode buffer 1, one piece which had been immersed in Anode buffer 2, a PVDF membrane which was activated by submerging it in MeOH for 2-3 seconds, followed by immersion in Anode buffer 2, next the gel was placed on top of this, followed by 2 pieces of filter paper which were immersed in Cathode buffer. Bubbles were carefully removed from the assembly, and the lid was securely placed on top. A constant voltage of 15 V was applied for 30 minutes.

2.11.2 Blocking the membrane

When the proteins had been transferred onto PVDF, the membrane was removed from the rig and incubated at room temperate for 1 hour in blocking buffer 5 % (w/v) Marvel in Tris buffered saline-Tween (TBST) (50 mM Tris-HCl pH 8.0, 150 mM NaCl, 0.05 % Tween-20).

2.11.3 Incubation with antibody

The membrane was transferred to a 50 ml tube containing 3 ml 5 % (w/v) Marvel in TBST plus the primary antibody of interest at 1:500 to 1:1000 dilutions, depending on the antibody. Incubation with the primary antibody was carried out with rolling at room temperature for 2 hours or at 4 °C overnight. The membrane was then washed three times in TBST, for at least 5 minutes per wash.

The membrane was then placed in a 50 ml tube containing 3 ml 5 % (w/v) Marvel in TBST plus a 1:2000 dilution of the appropriate horse radish peroxidise (HRP)-conjugated secondary antibody. The membrane was incubated with antibody with rolling for 45 minutes to 1 hour at room temperature. It was then washed three times in TBST for at least 5 minutes per wash and then developed by ECL using Fujifilm X-ray film and a Fuji RG II X Ray Film Processor.

2.11.4 Stripping and re-probing

The same membrane could be used more than once to examine other proteins if the membrane was stripped of the first set of antibodies and re-probed with a second

antibody of interest. The membrane was washed in 1 X TBST after ECL to remove excess chemiluminescent agent. The membrane was stripped for 15 minutes by placing it in 10 ml 1 X Re-blot solution with gentle shaking. The membrane was washed again briefly in 1 X TBST, blocked and probed with primary and secondary antibodies as described in the previous section.

2.12 Cytotoxicity Assay

For this assay, the CytoTox 96® Non-Radioactive Cytotoxicity Assay which measures lactate dehydrogenase (LDH) release was used as per the manufactures' instructions. HEK-293T cells were set up in 96 well plate format and transfected as in section 2.4. Additional triplicates were set up for spontaneous LDH release control and maximum LDH release control. 45 minutes prior to supernatant harvest, lysis solution (10 X) was added to maximum LDH release control wells. Then 50 µl of the supernatant from each well of the assay plate was then transferred to the corresponding well of a flat-bottom 96-well assay plate. 50 µl of a 1:5,000 dilution of LDH positive control was added to separate wells. 50 µl reconstituted substrate mix was then added to each well of the plate. The plate was covered, incubated at room temperature while protected from light for 30 minutes. Following this incubation, 50 µl stop solution was added to each well of the plate, and the absorbance was measured at 490 nm using a Tecan Sunrise™ 96 well Microplate Reader.

2.13 Reverse Transcriptase Polymerase Chain Reaction

RNA extractions were carried out using the RNeasy kit as per the manufactures' instructions. To determine the yield, RNA concentration was measured using a NanoDrop ND-1000 (Thermo Scientific). Next, cDNA was created using the High Capacity cDNA Reverse Transcription Kit. TMED1 and Glyceraldehyde 3-Phosphate Dehydrogenase (GAPDH) primers which were used for the Polymerase Chain Reaction (PCR) are listed below.

Primer	Sequence
TMED1 forward	5'ACTCCTTCAGCACCATCTCC 3'
TMED1 reverse	5' TTTGTCCCGTTCTTCCTTCC 3'
GAPDH forward	5'GAACGGGAAGCTTGTCATCAA 3'
GAPDH reverse	5'CTAAGCAGTTGGTGGTGCAG 3'

Table 2.17 Primers for PCR

The PCR reaction was set up as follows:

dNTP	1 µl
10 X Buffer	5 µl
Forward primer	1 µl
Reverse primer	1 µl
Taq polymerase	1 µl
DNA	1 µl
Nuclease Free H_2O	40 µl

PCR was carried out using either the Eppendorf Mastercycler Gradient or the Applied Biosystems Verti 96 well fast thermal cycler. The following PCR parameters were used:

95 °C	5 minutes	
95 °C	1 minute	x 30 cycles
55 °C	1 minute	
72 °C	1 minute	
72 °C	10 minutes	
4 °C	Hold	

2.14 Quantitative PCR

RNA extractions were carried out with the RNeasy kit and yield was determined using a NanoDrop ND-1000 (Thermo Scientific). The SuperScript® III First Strand Synthesis kit or the High Capacity cDNA Reverse Transcription Kit were used for synthesis of cDNA to be used for quantitative PCR. cDNA was prepared using a Eppendorf Mastercycler Gradient or Applied Biosystems Verti 96 well fast thermal cycler. Quantitative PCR was carried out with SYBR®-Green Real Time PCR kits using the 7900HT Fast Real-Time PCR System (Applied Biosystems). Primers used for the detection of TMED1 and GAPDH by quantitative PCR are listed in Table 2.18.

Primer	Sequence
TMED1 forward	5' TCCGAGAAGCTGGTGTTCTT 3'
TMED1 reverse	5' CAGTAGCGTGAGCATCTGGA 3'
GAPDH forward	5' GAACGGGAAGCTTGTCATCAA 3'
GAPDH reverse	5' CTAAGCAGTTGGTGGTGCAG 3'

Table 2.18 Primers used for quantitative PCR

2.15 Luciferase Assays

2.15.1 Luciferase Assays with TMED1 overexpression

Cells were set up in 96 well plate format at 2 x 10^5 cells/ml and allowed to rest for 24 hours. They were then transfected using GeneJuice® as shown in Table 2.12 with a total of 220 ng DNA consisting of 80 ng nulcear factor kappa B (NF-κB), *interferon*-stimulated response element (ISRE), or activator protein 1 (AP-1) luciferase reporter gene plasmids and 40 ng thymidine kinase (TK) Renilla reporter gene (for normalisation of the data) and TMED1-GFP and/or empty vector to make up the 220 ng DNA. Cells were allowed to rest for 24 hours and stimulated with the appropriate ligand for the required amount of time. Following stimulation media was removed and cells were lysed in 50 µl Passive Lysis Buffer with shaking for 15 minutes. 20 µl of the cellular lysates was used to assay Firefly Luciferase to determine the activity of NF-κB or ISRE and 20 µl was used to assay TK Renilla luciferase. 40 µl substrate was added per well; Luciferase Assay Mix (For 456 ml 2X solution: 20 mM Tricine, 2.67 mM $MgSO_4.7H_2O$, 0.1 mM EDTA, 33.3 mM DTT, 530 µM adenosine triphosphate (ATP), 270 µM Acetyl CoEnzyme A, 60 mg D-Luciferin made to 445.2 ml, add 1.14 ml 2 M NaOH and 2.42 ml 50 mM Magnesium Carbonate Hydroxide) for FireFly luciferase and *Coelenterazine* (diluted 1:1000 with PBS) for Renilla luciferase. The Firefly luciferase and TK Renilla luciferase values were then measured using a Mediators PhL™ Luminometer.

2.15.2 Luciferase Assays following endogenous TMED1 knockdown

Cells were set up in 24 well format at 0.75 x 10^5 cells/ml in antibiotic free media and allowed to rest for 24 hours. They were then transfected with 5 nM siRNA constructs using Lipofectamine™ RNAiMax as described in section 2.5 and allowed to rest for 24 hours. Cells were then transfected with the luciferase constructs using GeneJuice® as shown in section 2.4. A total of 770 ng DNA was used per transfection. This consisted of 280 ng NF-κB luciferase reporter, 140 ng TK Renilla reporter and empty vector (EV) pcDNA for the remainder. Cells were allowed to rest for 24 hours and stimulated with 50 ng/ml IL-33 for 6 hours if required. Following stimulation media was removed and cells were lysed in 100 µl Passive Lysis Buffer with shaking for 15 minutes. Lysates were assayed as described above in section 2.15.1.

2.16 Enzyme-Linked ImmunoSorbent Assay (ELISA)

2.16.1 Cell preparation and stimulation

HEK-293-hST2L cells were set up and transfected as described in section 2.4 or 2.5 in triplicate. THP-1 cells were set up and transfected as described in section 2.6. Cells were stimulated in triplicate at the required concentration and supernatants were collected 8 or 24 hours post stimulation for analysis by ELISA.

2.16.2 ELISA procedure

A 96-well microplate was coated with capture antibody (50 µl per well) diluted to a working concentration of 4 µg/ml in PBS, covered in Parafilm and incubated overnight

at room temperature. Wells were then aspirated and washed with Wash Buffer (0.05 % Tween 20 in PBS, pH 7.2-7.4) three times, and blotted on tissue paper to remove bubbles. Plates were blocked by adding 150 µl Reagent Diluent (1 % (w/v) BSA in PBS, pH 7.2-7.4) to each well and incubated at room temperature for a minimum of one hour. The reagent diluent was then removed and the aspiration-wash-blotting step was repeated three times. 50 µl of sample, or standard diluted in Reagent Diluent, was then added per well and incubated at room temperature for 2 hours or 4 °C overnight. The samples were then removed and the wash step was repeated three times. 50 µl Detection Antibody diluted to a working concentration of 20 ng/ml in Reagent Diluent was added to each well. The plate was covered with Parafilm and incubated at room temperature for at least 2 hours. The wash step was repeated three times as above. 50 µl Streptavidin-HRP (diluted 1:2 with Reagent Diluent) was added to each well and incubated at room temperature (in darkness) for 20 minutes. Wells were washed as before. 50 µl Substrate Solution was added per well and incubated at room temperature (in darkness) for 20 minutes. Wells were washed as before. 25 µl Stop Solution (2 N H_2SO_4) was added per well, the plate was tapped to ensure thorough mixing, and any bubbles present were removed. The absorbance measurements were read at 450 nm using a Tecan Sunrise™ 96 well Microplate Reader and concentrations were calculated using the known standards.

2.17 Labelling IL-33

Recombinant IL-33 was labelled using the Alexa Fluor® 647 Microscale Labelling Kit from Invitrogen according to the manufactures' instructions. Firstly, a 1 M sodium bicarbonate solution was prepared. 20 µl of a 1 mg/ml IL-33 solution was added to the reaction tube followed by 2 µl (a 1/10 volume) 1 M sodium bicarbonate and the

solutions were mixed my pipetting up and down several times. Next, the Alexa Fluor® 647 succinimidyl ester was reconstituted, and the appropriate amount was added to the reaction tube and mixed thoroughly. The reaction was incubated at room temperature for 15 minutes. The conjugated protein was separated from unreacted dye by purification using a spin column, the unreacted dye being retained in the column and labelled protein eluted and collected.

2.18 Confocal microscopy

HEK-293T or HEK-293-hST2L cells were set up at 0.5 x 10^5 cells/ml in glass bottom confocal dishes or on poly-L-lysine coated cover slips and incubated for 24 hours at 37 °C with 5 % CO_2. Cells were then transfected with 0.5 μg of plasmids encoding TMED1-GFP, ST2L-HA, Endoplamic reticulum-cyan fluorescent protein (ER-CFP), Golgi-CFP, early endosome antigen 1 (EEA1)-CFP, Rab11a-CFP or combinations of each as required. 24 hours later the media was changed and cells were allowed to rest for a further 24 hours.

For live cell imaging, cells were then viewed with an Olympics Fluoview FV1000 Imaging system. Dapi and CellMask™ Plasma Membrane Stain were used for nuclear and plasma membrane staining respectively.

The following protocol was followed for antibody staining. If cell stimulation was required, media was replaced and cells were allowed to recover for 30 minutes. Cells were then stimulated for the required time. If cells were stimulated with labelled ligand they were washed twice in media, prior to the addition of paraformaldehyde (PFA) to a final concentration of 2 % (v/v), which was incubated on ice for 15 minutes. PFA media was then removed and cells were permeabilised with PEM (80 mM

piperazinediethanesulfonate (PIPES), 5 mM ethylene glycol tetraacetic acid (EGTA), 1 mM $MgCl_2$)/0.15 % Triton X-100 on ice for 15 minutes. Free aldehyde groups were then quenched with 50 mM NH_4Cl/0.15 % Triton for 5 minutes at room temperature. Quenching buffer was then removed and cells were blocked for 1 hour at room temperature in 1 % BSA (w/v), 10 % FCS (v/v) and PBS. Primary antibody was added for 1 hour at room temperature or 4 °C overnight. Cells were washed gently in PBS/0.15 % Trition X-100 three times, and once in blocking buffer. Secondary antibody was then added for 45 minutes to one hour, followed by three more gentle washes in PBS/0.15 % Trition X-100. One drop of mounting solution was then added to the coverslips, and they were mounted cell-side down onto glass slides, and sealed with nail varnish. They were allowed to dry at room temperature and stored at 4 °C until they were viewed with the Olympics Fluoview FV1000 Imaging system.

2.19 Dynasore treatment

HEK-293-hST2L cells were set up at 2 x 10^5 cells/ml in 24 well plates. The following day, media was changed to serum free and cells were allowed to rest for approximately 1 hour. Next DMSO or dynsaore (to a final concentration of 80 μM) was added for 30 minutes. Cells were then stimulated with IL-33 (50 ng/ml) for the times required. Following the time course cells, were lysed in 5 X SDS-Laemmli buffer and analysed by Western blotting as in sections 2.10 and 2.11.

Chapter Three

Investigation into the characteristics of TMED1 and its putative interaction with ST2L

Chapter 3

3.1 Introduction

As mentioned in chapter 1, the information available on TMED1 in the literature is quite limited. TMED1 was first identified during a screen searching for possible ST2L binding proteins, and was deemed a member of the transmembrane emp24 domain-containing protein family (Gayle et al., 1996). TMED1 is believed to possess the same domain architecture as other members of the TMED protein family, having an N-terminal signal peptide, a GOLD domain, followed by a linker and coiled-coiled region, a transmembrane domain and a C-terminal tail. Subcellular fractionation and gel filtration analysis has revealed the presence of TMED1 in the ER, IC and Golgi in dimer form (Jenne et al., 2002). A second study using confocal microscopy reported that TMED1 can localise to the Golgi in Hela cells where it can co-localise with TMED10 (Emery et al., 2000).

Aside from these studies, TMED1 has not yet been characterised and studied. Therefore, in this study a further characterisation of TMED1 was carried out. Firstly, the localisation of TMED1 within the cell was investigated. The presence of TMED1 in the ER and Golgi was studied. TMED7, a related family member has recently been reported to limit TLR4 signalling, working in other cellular compartments such as early and late endosomes (Doyle et al., 2012). Therefore the presence of TMED1 in other cellular compartments was also investigated. In addition, results suggesting that TMED7 possess a second transmembrane domain and that its GOLD domain projects into the cytosol (Doyle et al., 2012) prompted an analysis of the position and localisation of the transmembrane and GOLD domains of TMED1.

As mentioned above, TMED1 was identified in a screen for possible ST2L binding proteins (Gayle et al., 1996). ST2L is a member of the IL-1R/TLR superfamily of receptors. For many years, ST2L was classed as an orphan receptor with no known ligand. Prior to the discovery of IL-33 (Schmitz et al., 2005), studies were undertaken to identify the ligand for ST2L. In one such study, cell lines were screened for their ability to bind a ST2L-Fc fusion protein and cDNA clones of putative binding proteins were then isolated using an expression cloning strategy (Gayle et al., 1996). Although this study was unsuccessful in identifying the ST2L ligand, it did lead to the discovery of the GOLD domain containing protein TMED1. However, this purported association was not confirmed by any other means and a functional consequence of the association was not described.

Following the implication of TAG, another GOLD domain containing protein in the regulation of MyD88-independent TLR4 signalling (Palsson-McDermott et al., 2009), interest in the putative TMED1 and ST2L association and the potential role for TMED1 in ST2L signalling was revived. This project aimed to confirm the putative interaction between TMED1 and the receptor protein ST2L utilising co-immunoprecipitation assays and confocal microscopy. In order to further characterise TMED1 an analysis of the transmembrane domains and topology of TMED1 was carried out using confocal imaging and protease protection assays. To determine which domains of TMED1 and ST2L were responsible for the interaction several mutation and deletion constructs were generated and used in co-immunoprecipitation assays.

3.2 Results

3.2.1 TMED1 localisation in resting cells

The localisation of TMED1 in the cell was investigated using a human mast cell line (HMC 1.1). They were transfected with a plasmid encoding TMED1 with a green fluorescent protein (GFP) tag. Cells were then viewed using the Olympics Fluoview FV1000 Imaging system. Figure 3.1 demonstrates that TMED1 had a reticular pattern of expression with some more focused regions adjacent to the nucleus (Figure 3.1, arrow).

Additional confocal microscopy was carried out in HEK-293T cells, as the transfection efficiency for the HMC 1.1 cell line was low. As Gayle *et al.* isolated TMED1 as a cell surface protein (Gayle et al., 1996), imaging was carried out to determine if TMED1 localised to the plasma membrane. Overexpressed TMED1-GFP was viewed in live cells and was not localised to the plasma membrane (Figure 3.2). Staining of the nucleus also demonstrated that TMED1-GFP did not localise to the nucleus (Figure 3.2).

Similar to the expression pattern of TMED1-GFP in HMC 1.1 cells, TMED1-GFP in HEK-293T cells seemed to have a reticular pattern of expression, with some regions of greater intensity in the peri-nuclear area (Figure 3.2). To further investigate this, TMED1-GFP was expressed together with the ER-retention sequence of calreticulin which is a marker for the endoplasmic reticulum (ER) fused to cyan fluorescent protein (CFP). Alternatively, TMED1-GFP was expressed together with the Golgi marker, β1,4-galactosyltransferase fused to CFP. As shown in Figure 3.3, TMED1-GFP can co-localise with ER-CFP. This reticular pattern is the predominant expression pattern which was observed for TMED1. TMED1 is also capable of Golgi localisation

(Figure 3.4, bottom panels). However, this is less frequent than its localisation at the ER, and does not occur in all cases (Figure 3.4, top panels).

TMED1-GFP co-expression with the early endosome marker, early endosome antigen 1 (EEA1) fused to CFP, was also examined. The top panels in Figure 3.5 demonstrate that TMED1-GFP can localise to the limiting membrane of early endosomes in resting cells. However, in other cases TMED1-GFP appeared to enclose the lumen of the early endosome (Figure 3.5, bottom panels, arrow). TMED1-GFP co-expression with the recycling endosomal marker Rab11a-CFP did not show any regions of co-localisation. However, TMED1-GFP did enclose Rab11a-CFP positive areas (Figure 3.6, top and bottom panels, arrows).

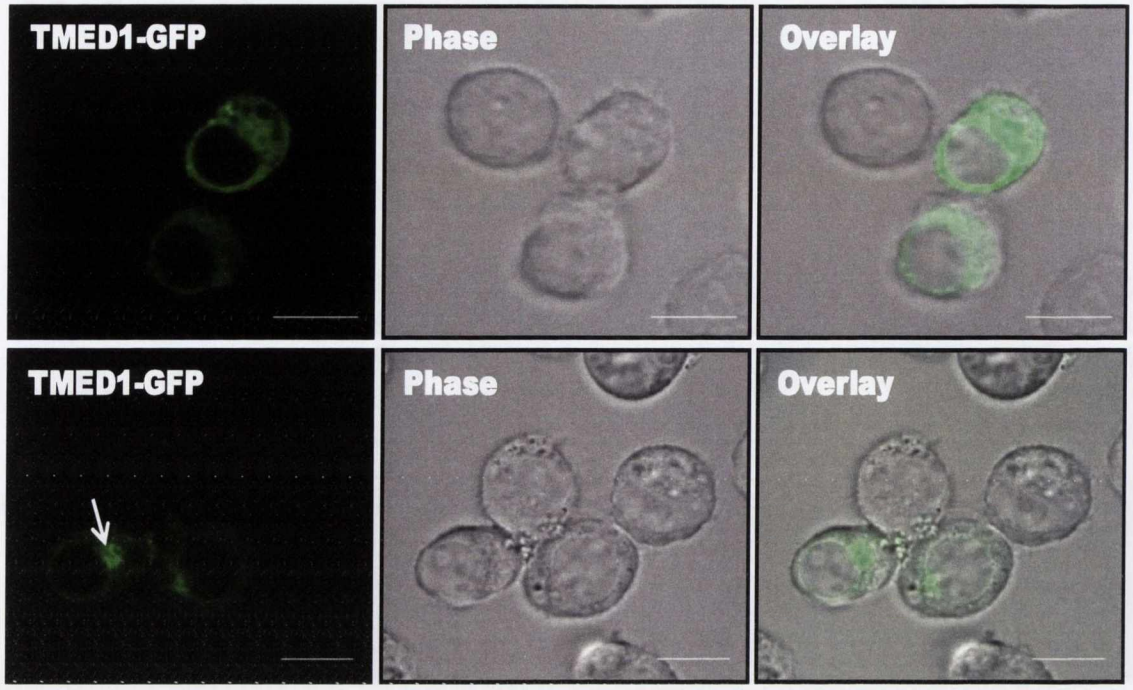


Figure 3.1 Localisation of TMED1 in HMC 1.1 cells

Confocal images of HMC 1.1 cells transfected with a plasmid encoding TMED1-GFP. Cells were viewed using the Olympics Fluoview FV1000 Imaging system. Data presented is representative of two experiments, in which a total of 24 cells were analysed. The top panels show the reticular like pattern of TMED1-GFP, which was evident in twenty two of the cells examined. The arrow in the bottom panel shows the region of greater intensity of TMED1-GFP, evident in 10 cells. Scale bars indicate 10 μM.

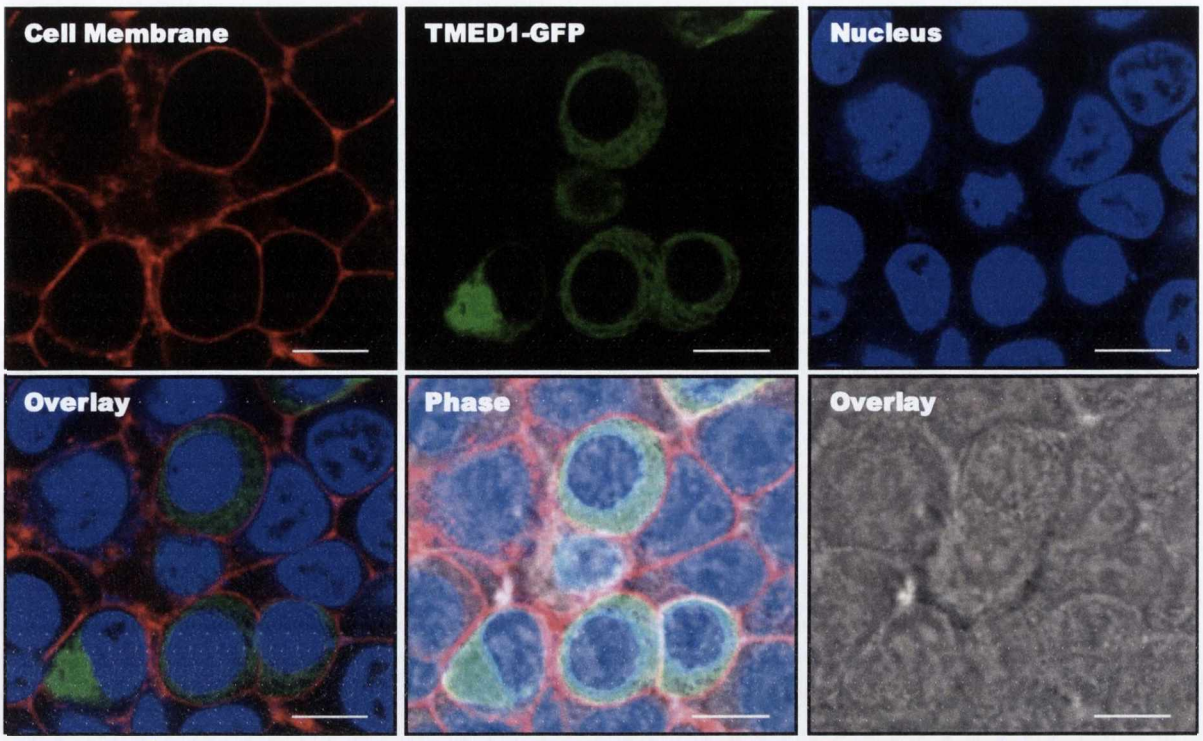


Figure 3.2 TMED1 is not localised to the plasma membrane or nucleus in HEK-293T cells

Confocal images of HEK-293T cells transfected with a plasmid encoding TMED1-GFP. Cells were stained with CellMask™ Plasma Membrane Stain to stain the plasma membrane and DAPI to stain the nuclei. Data demonstrating TMED1-GFP expression and staining of nuclei is representative of one experiment with 19 cells analysed. Data demonstrating TMED1-GFP expression and plasma membrane staining are representative of three independent experiments with a total of 70 cells analysed. Scale bars indicate 10 μM.

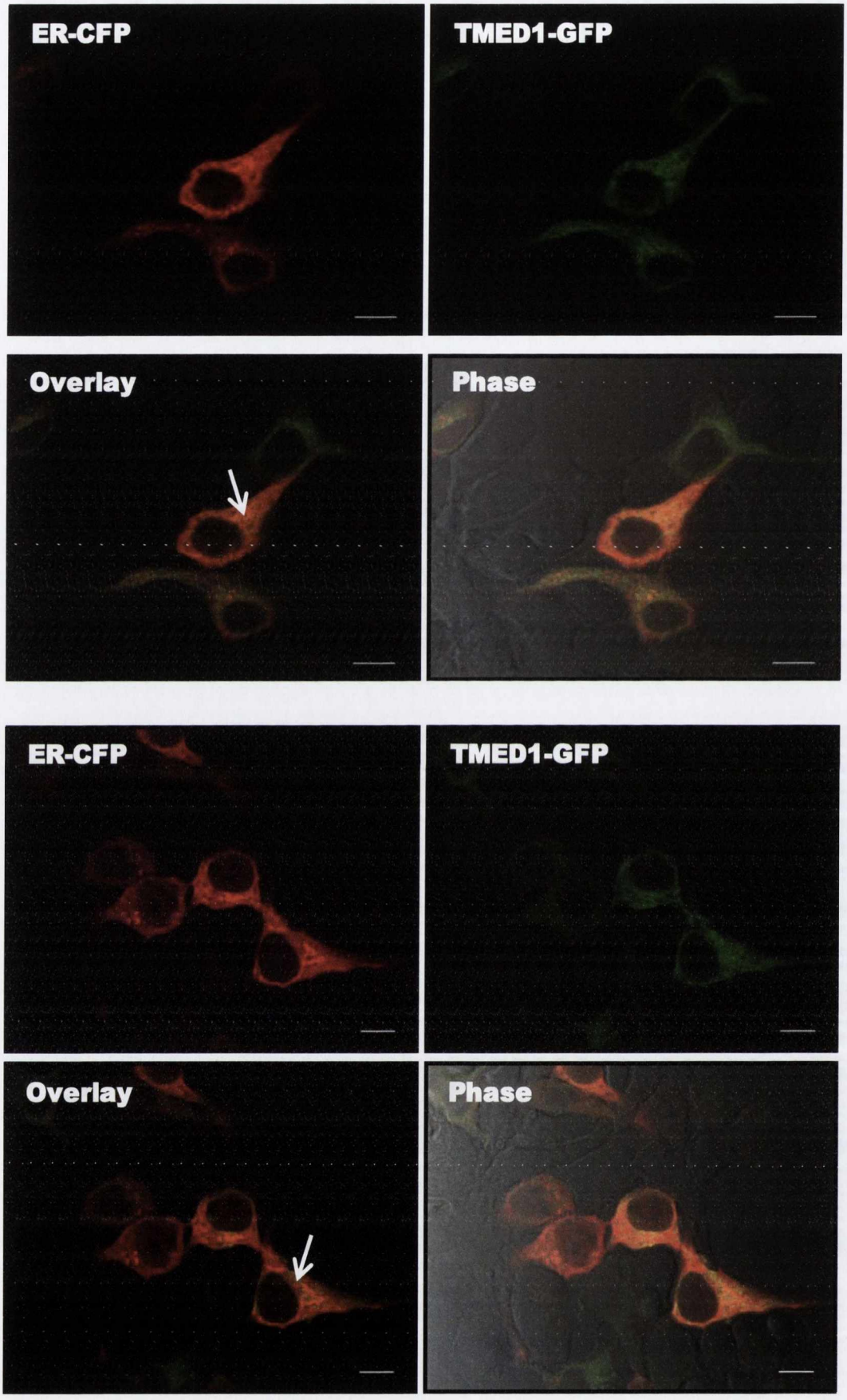


Figure 3.3 TMED1 co-expression with ER-CFP

Figure 3.3 TMED1 co-expression with ER-CFP

Confocal images of HEK-293T cells transfected with plasmids encoding TMED1-GFP and the ER-retention sequence of calreticulin fused to CFP (ER-CFP). The CFP channel was changed to red to allow for easier visualisation of the ER-CFP. Arrows show regions of co-localisation between TMED1-GFP and ER-CFP. Data is representative of 33 cells over a total of three experiments. Scale bars indicate 10 μM.

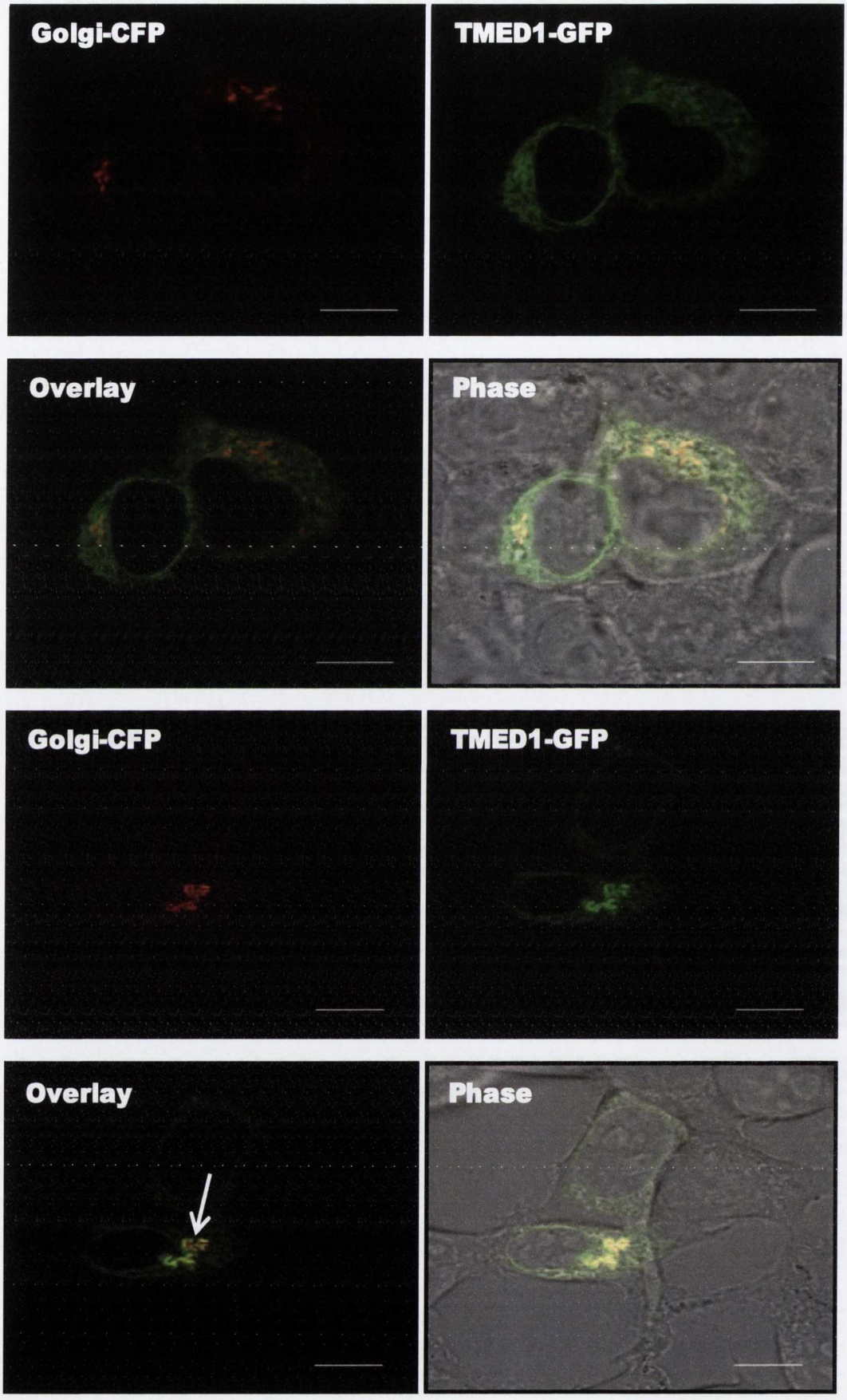


Figure 3.4 TMED1 co-expression with Golgi-CFP

Figure 3.4 TMED1 co-expression with Golgi-CFP

Confocal images of HEK-293T cells transfected with plasmids encoding TMED1-GFP and β1,4-galactosyltransferase-CFP (Golgi-CFP). The CFP channel was changed to red to allow for easier visualisation of the Golgi-CFP. Arrows show regions of co-localisation between TMED1-GFP and Golgi-CFP. Data in the bottom panel is representative of 10 cells from two experiments, in which a total of 28 cells were analysed. Scale bars indicate 10 μM.

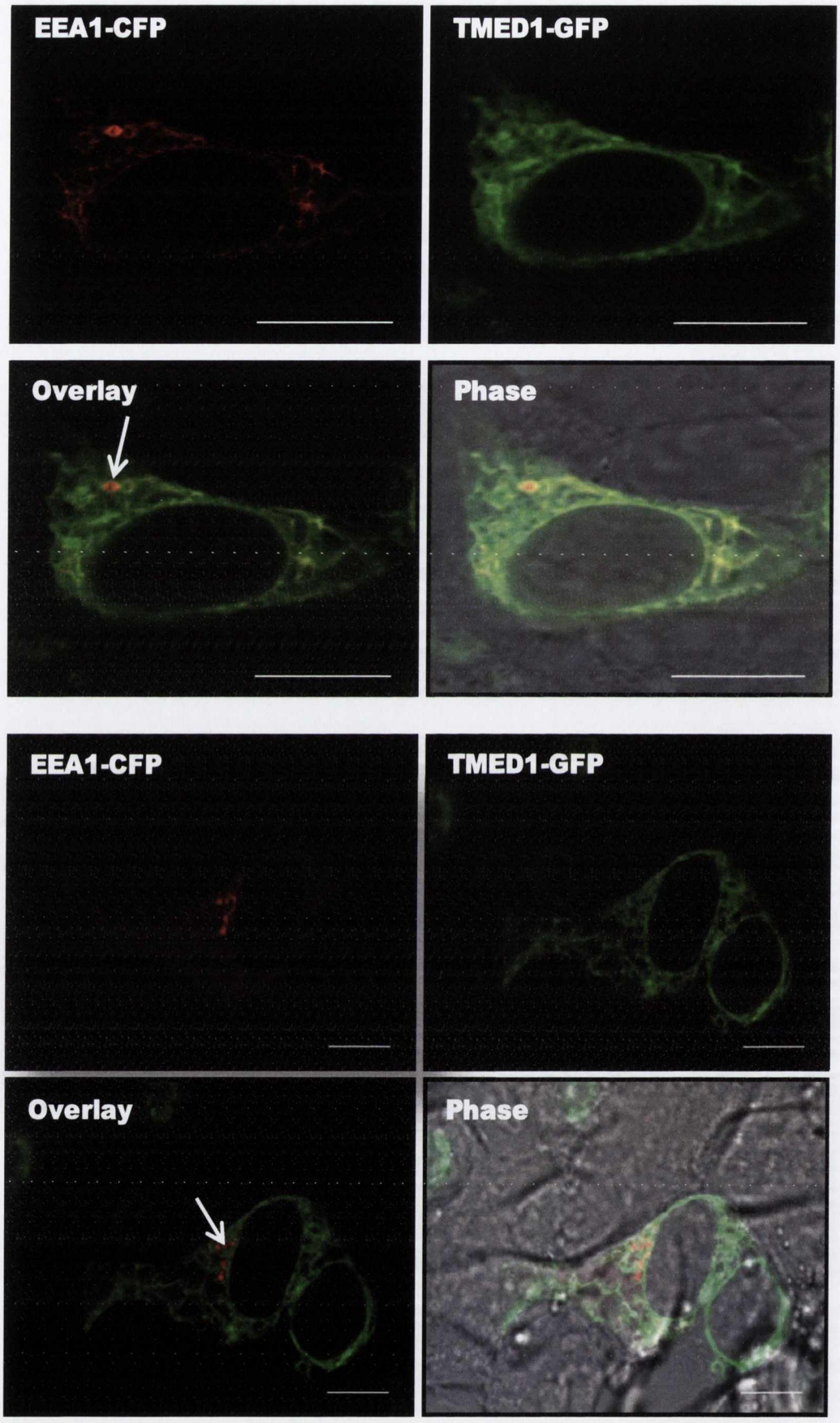


Figure 3.5 TMED1 co-expression with EEA1-CFP

Figure 3.5 TMED1 co-expression with EEA1-CFP

Confocal images of HEK-293T cells transfected with plasmids encoding TMED1-GFP and EEA1-CFP. The CFP channel was changed to red to allow for easier visualisation of EEA1-CFP. Data in the top panel is representative of 6 cells while data in the bottom panel is representative of 12 cells, in which a total of 18 cells were analysed in three experiments. Scale bars indicate 10 μM.

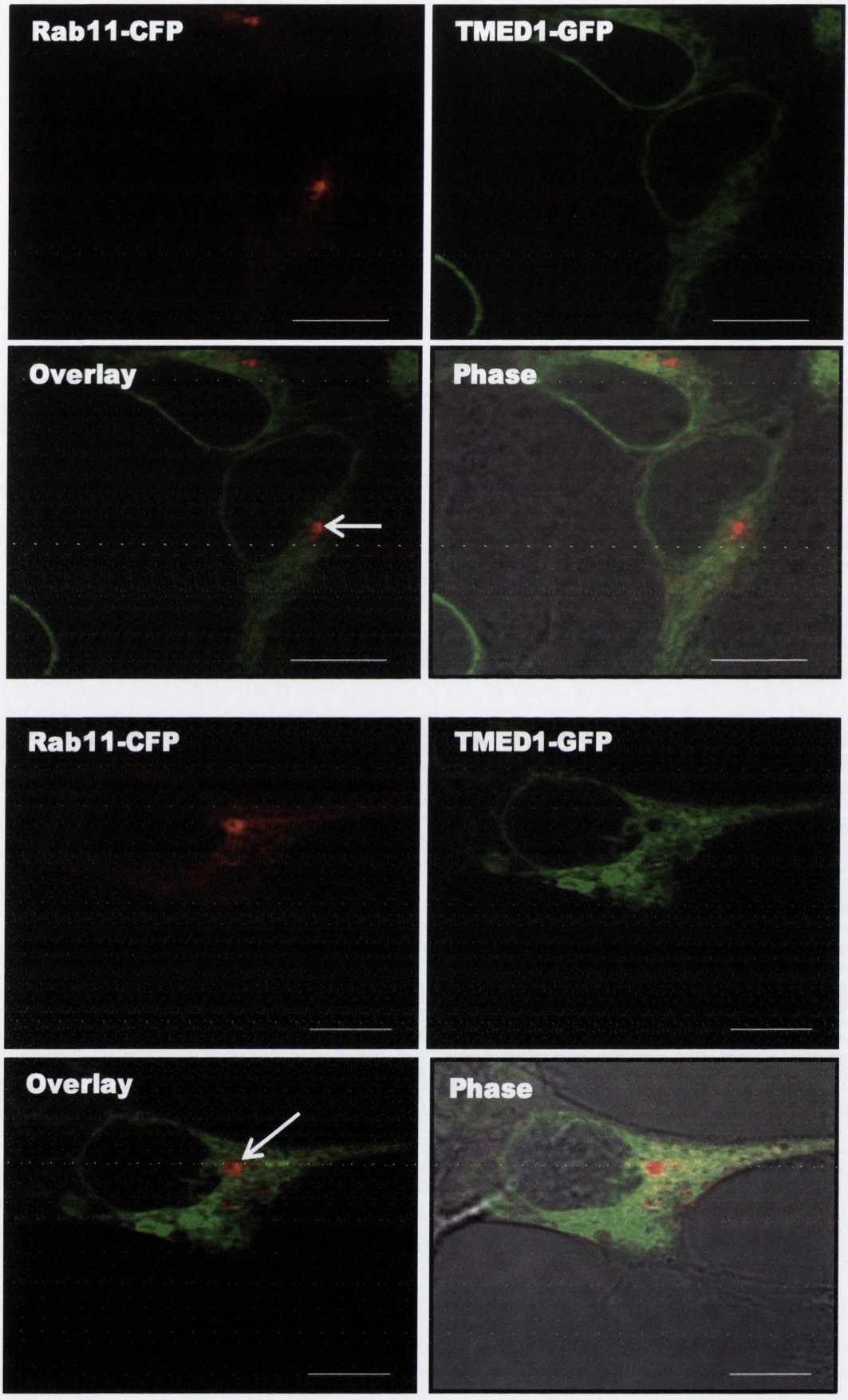


Figure 3.6 TMED1 co-expression with Rab11a-CFP

Figure 3.6 TMED1 co-expression with Rab11a-CFP

Confocal images of HEK-293T cells transfected with plasmids encoding TMED1-GFP and Rab11a-CFP. The CFP channel was changed to red to allow for easier visualisation of Rab11a-CFP. Arrows show regions of Rab11a-CFP expression. Data is representative of 29 cells from three experiments, in which a total of 29 cells were analysed. Scale bars indicate 10 μM.

3.2.2 Transmembrane domains of TMED1

Members of the TMED family were previously thought to contain an N-terminal signal peptide, a GOLD domain, followed by a linker and coil-coiled region, a transmembrane domain and a C-terminal tail. In the case of TMED1, the transmembrane domain is predicted to be at amino acids 193-213. However, recent investigations into the number of transmembrane domains in the related TMED family member, TMED7, have suggested that it has two potential transmembrane motifs, one near the C-terminus (amino acids 186-207) as well as an additional one near the N-terminus (amino acids 17-34) (Doyle et al., 2012).

Therefore, the TMED1 sequence was analysed for other potential transmembrane domains by a number of transmembrane prediction programmes. Table 3.1 lists the number of transmembrane domains predicted by each of the programmes and their position (Cserzo et al., 1997; Hirokawa et al., 1998; Jones, 2007; Kall et al., 2004; Krogh et al., 2001; Nugent and Jones, 2009; Tusnady and Simon, 1998). Each of these programmes identifies a transmembrane domain approximately in the region of amino acids 193-213. Some of these also identify a transmembrane domain at the N-terminus of the protein. The region incorporated by this potential transmembrane domain includes amino acids ranging from 1-26 depending on the programme. This corresponds to the signal sequence in TMED1 so is unlikely to be a transmembrane domain. None of these predict a transmembrane motif at positions 17-34, corresponding to the N-terminal transmembrane motif in TMED7 (Doyle et al., 2012).

To investigate this further, three additional TMED1-GFP constructs were generated. These were termed ΔTM-TMED1, ΔSP-TMED1 and ΔSPTM-TMED1 and lacked the transmembrane domain (TM), the signal peptide (SP) or both the signal

peptide and the transmembrane domain (SPTM) respectively. To investigate their localisation each of the constructs were viewed using confocal microscopy. In Figure 3.7 the reticular pattern of WT-TMED1 can be observed (top panels). Interestingly, the same reticular pattern can be observed for ΔTM-TMED1 (second panels from the top). However, removal of the signal peptide reveals a different expression pattern. ΔSP-TMED1 appears diffuse in the cytosol (third panels from the top). Removal of the signal peptide and the transmembrane domain completely disrupts TMED1 localisation, as it can be observed all over the cell (fourth panels), even in the nucleus and looks similar to EV-GFP which is not targeted to a particular organelle (fifth panels). MyD88-CFP was used as an additional control to demonstrate that cells have been allowed sufficient time to direct proteins to their correct cellular location beyond the early secretory pathway. MyD88 is expressed in cytoplasmic aggregates, an expression pattern which has been reported previously (Latz et al., 2002).

Transmembrane prediction for TMED1

Program	TM domain	No. of TMH	TM region
HMMTOP	Yes	1	193-210
TMHMM	Yes	1	193-215
Phobius	Yes	1	193-213
MEMSAT-SVM	Yes	1	193-216
MEMSAT3	Yes	2	3-26 196-215
TMPred	Yes	2	1-19/22 193/195-215
SOSUI	Yes	2	1-23 194-215
DAS	Yes	2	9-16 198-213

Table 3.1 Transmembrane domains of TMED1

Results from TMED1 sequence analysis using various transmembrane prediction programmes. TM: transmembrane, TMH: transmembrane helix.

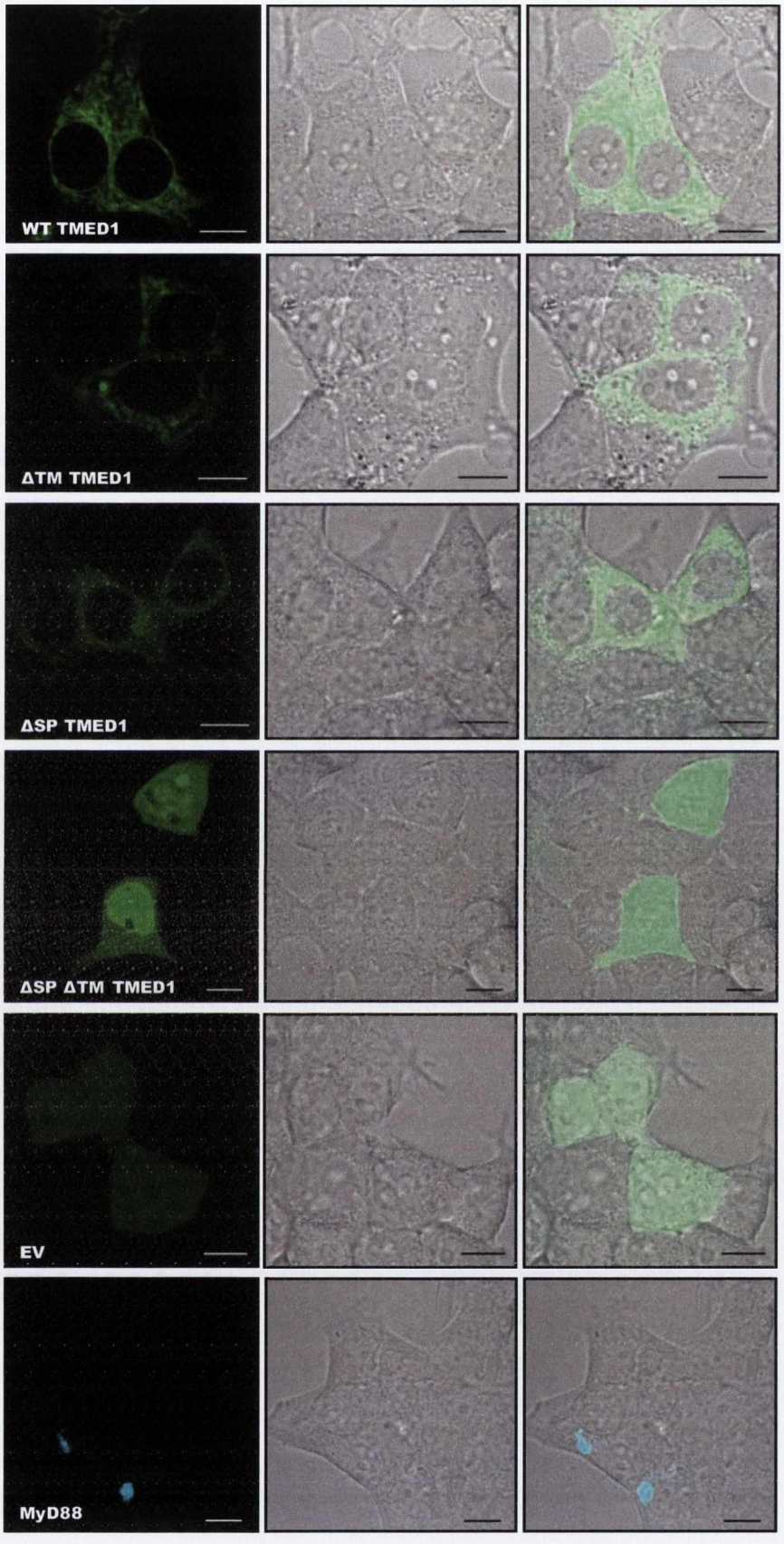


Figure 3.7 Localisation of TMED1 mutant constructs

Figure 3.7 Localisation of TMED1 mutant constructs

HEK-293T cells were transfected with plasmids encoding TMED1-GFP constructs (WT: wild type, ΔTM: transmembrane domain deleted, ΔSP: signal peptide deleted, ΔTMΔSP: transmembrane domain and signal peptide deleted) EV-GFP or MyD88-CFP. Cells were examined using an Olympus FV1000 Confocal Microscope. Data is representative of a minimum of 27 cells analysed for each construct over a total of three independent experiments. Scale bars indicate 10 μM.

3.2.3 Localisation of the GOLD domain of TMED1

The TMED family are thought to traverse the membrane and therefore the GOLD domain may project into the cytosol or lumen. The initial characterisation of TMED1 did not reveal if the GOLD domain projects into the cytosol or into the lumen of a vesicle.

To determine if the GOLD domain of TMED1 projects into the lumen of the organelle in which it is residing or if it projects into the cytosol a protease protection assay was carried out. This assay utilises two reagents to permeabilise particular cell membranes. The cholesterol binding drug digitonin is used to selectively permeabilise the plasma membrane. As the plasma membrane has the highest concentration of cholesterol, it is the prime target for digitonin intercalation. Other internal cell membranes are unaffected. Alternatively, the detergent Triton X-100 will permeabilise all membranes. When fractions which have been exposed to either digitonin alone or digitonin with Trition X-100 are incubated with trypsin, regions of the protein which are accessible will be sensitive to trypsin digestion. Consequently the assay can reveal which regions of a protein projects into the cytosol.

A protease protection assay was carried out on endogenous TMED1 in HEK-293T cells and samples were immunoblotted using a TMED1 antibody. This antibody was generated using the immunogen sequence from position 26 to 91 of TMED1, and therefore is directed against the first half of the GOLD domain. Figure 3.8 lane 1 shows TMED1 expression in whole cell lysates, lane 2 demonstrates that TMED1 is in the membrane fraction. No TMED1 is visible in the cytosolic fraction (lane 3). Permeabilisation of the plasma membrane alone with digitonin allowed trypsin to digest the GOLD domain of TMED1, as there is no band detected in lane 4. Permeabilisation of all membranes with Triton X-100 also allowed TMED1 to be digested (lane 5). These results demonstrate that the GOLD domain of TMED1 was sensitive to trypsin digestion

when the plasma membrane alone was permeabilised, suggesting it projects into the cytosol.

The protease protection assay was also carried out with overexpressed TMED1 with a C-terminal GFP tag to investigate whether the C-terminus of TMED1 is localised to the cytosol or a luminal compartment. This is shown in Figure 3.9. TMED1-GFP can be detected in the whole cell lysates in lane 1 between the 47 kDa and 62 kDa molecular weight markers. TMED1-GFP is detectable in the membrane fraction but not in the cytosolic fraction (compare lanes 2 and 3). When the plasma membrane is permeabilised with digitonin and TMED1-GFP is exposed to trypsin the intensity of this band is reduced and another band is detectable at approximately 25 kDa (lane 4). As anticipated both of these bands are cleaved by trypsin in the presence of Triton X-100 as internal membranes are also permeabilised. This suggests that the C-terminal tail of TMED1 is protected from trypsin digestion and is therefore localised inside a luminal compartment. A significant amount of the remainder of the protein appears to be in the cytosol, as this section is digested by trypsin in the presence of digitonin, leading to a reduction in the molecular weight of the GFP tagged fragment. These results suggest that the transmembrane domain is likely to be at position 193-213, with the first 192 amino acids in the cytosol and the last 14 amino acids in the lumen.

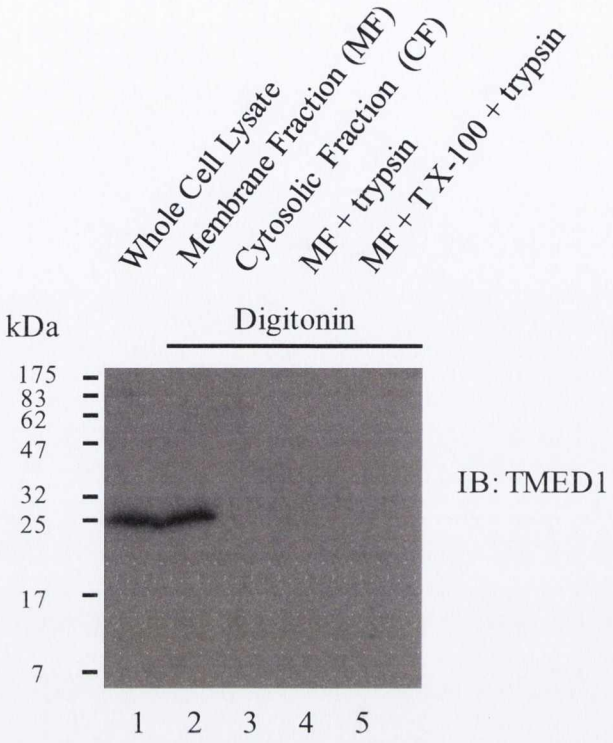


Figure 3.8 The GOLD domain of TMED1 projects into the cytosol

A protease protection assay was carried out on HEK-293T cells. Samples were analysed by Western blotting and probed with an anti-TMED1 antibody. Data is representative of three independent experiments. Molecular weight markers are shown on the left of the blot.

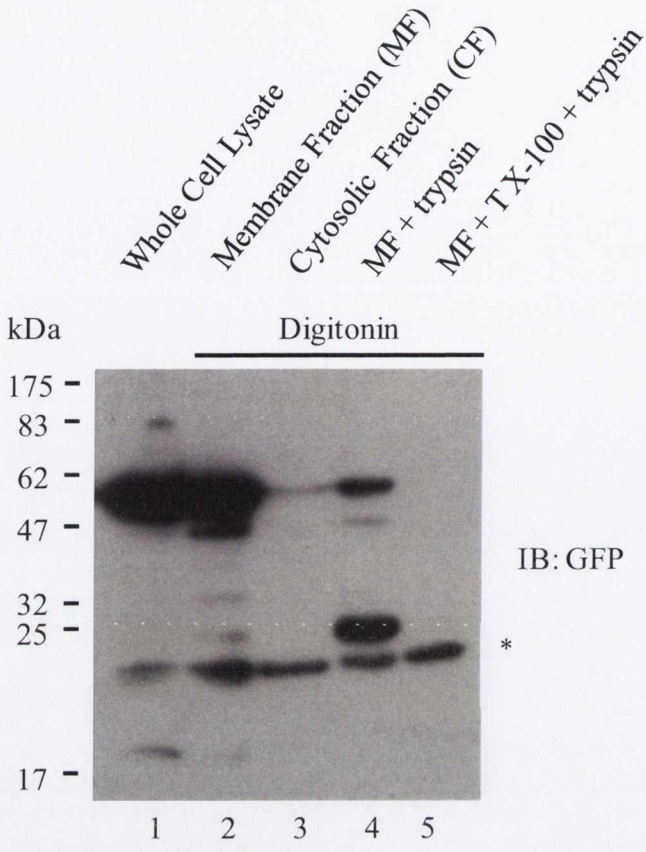


Figure 3.9 The C-terminus of TMED1 is located in the lumen

HEK-293T cells were transfected with a plasmid encoding TMED1-GFP and a protease protection assay was carried out. Samples were analysed by Western blotting and probed with an anti-GFP antibody. Results presented are representative of three independent experiments. Asterisks mark non-specific bands. Molecular weight markers are shown on the left of the blot.

3.2.4 TMED1 interacts with ST2L

Co-immunoprecipitation assays were carried out to investigate the interaction between TMED1 and ST2L. These were carried out in HEK-293T cells in which TMED1-GFP and ST2L-HA were both overexpressed (Figure 3.10). The interaction was detected in both directions, by immunoprecipitating TMED1-GFP and blotting for ST2L-HA (Figure 3.10, top panel, lane 4) and by immunoprecipitating ST2L-HA and blotting for TMED1-GFP (Figure 3.10, bottom panel, lane 3). The presence of immunoprecipitated TMED1-GFP and ST2L-HA in these samples was confirmed (Figure 3.10, bottom panel, lane 4 and top panel, lane 3 respectively). TMED1-GFP and ST2L-HA were also visible in the lysates as expected.

Next the interaction was confirmed using a cell line stably expressing human ST2L (HEK-293-hST2L). Figure 3.11 demonstrates that TMED1-GFP co-immunoprecipitates with stably overexpressed ST2L (top left panel, lane 2). Immunoprecipitated empty vector GFP (EV-GFP) does not co-immunoprecipitate with ST2L (Figure 3.11, top left panel, lane 1), demonstrating that the observed co-immunoprecipitation between TMED1-GFP and ST2L-HA is not due to the GFP tag. ST2L, EV-GFP and TMED1-GFP can be observed in the lysates as expected (Figure 3.11, right panels, top and bottom panels respectively).

To investigate the specificity of the interaction, the related family members TMED2, TMED3 and TMED7 were utilised. Figure 3.12 confirms previous results by demonstrating that TMED1-GFP co-immunoprecipitates with ST2L (top left panel, lane 1). However, TMED2-GFP, TMED3-GFP or TMED7-GFP do not co-immunoprecipitate with ST2L (Figure 3.12, top left panel, lanes 2, 3 and 4). This confirms the specificity of

the interaction between ST2L and TMED1. The whole cell lysates demonstrate that ST2L is present in each of the samples (top right panel).

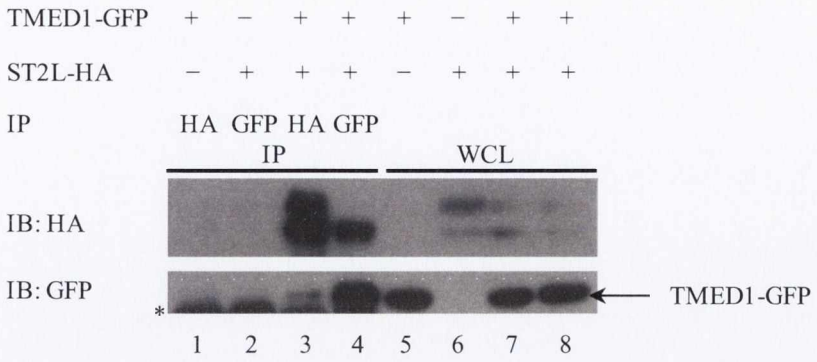


Figure 3.10 TMED1 co-immunoprecipitates with ST2L-HA in HEK-293T cells

HEK-293T cells were transfected with a plasmid encoding ST2L-HA, TMED1-GFP or both plasmids together. Samples were immunoprecipitated with either anti-HA or anti-GFP antibodies. Whole cell lysates (WCL) and immunoprecipitated samples were analysed by Western blot. The immunoblotting antibodies (IB) are listed beside the appropriate blot. Asterisks mark antibody heavy chain bands. Data are representative of eight independent experiments.

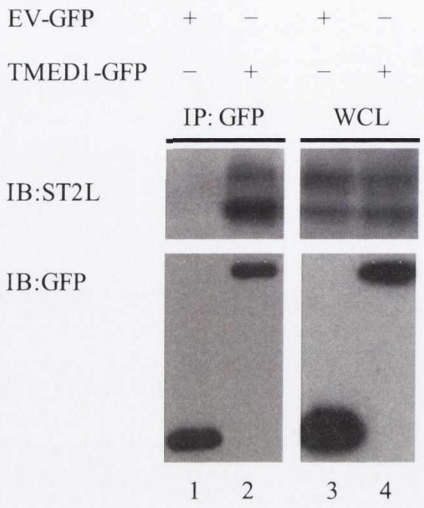


Figure 3.11 TMED1 co-immunoprecipitates with stably overexpressed ST2L in HEK-293-hST2L cells

HEK-293-hST2L cells were transfected with plasmids encoding empty vector GFP (EV-GFP) or TMED1-GFP. Samples were immunoprecipitated with anti-GFP Trap® beads. Whole cell lysates (WCL) and immunoprecipitated samples were analysed by Western blot. The immunoblotting antibodies (IB) are listed beside the appropriate blot. Data are representative of ten independent experiments.

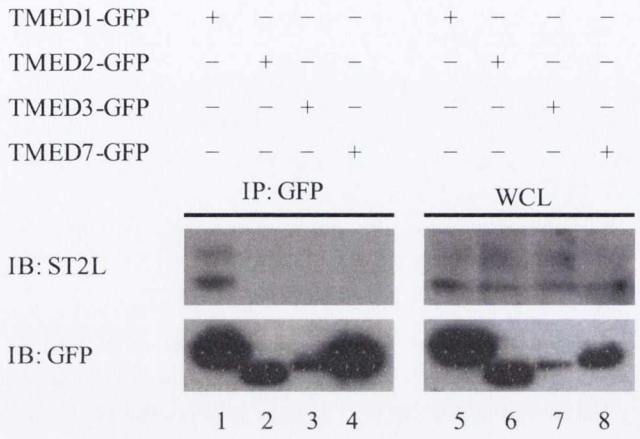


Figure 3.12 TMED2, TMED3 or TMED7 do not co-immunoprecipitate with stably overexpressed ST2L in HEK-293-hST2L cells

HEK-293-hST2L cells were transfected with empty vector GFP (EV-GFP), TMED1-GFP, TMED2-GFP, TMED3-GFP or TMED7-GFP. Samples were immunoprecipitated with anti-GFP Trap® beads. Whole cell lysates (WCL) and immunoprecipitated samples were analysed by Western blotting. The immunoblotting antibodies (IB) are listed beside the appropriate blot. Data is representative of two independent experiments.

3.2.5 TMED1 does not co-immunoprecipitate with MyD88

To further investigate the specificity of TMED1 for ST2L, the interaction of TMED1 with other TIR domain containing adaptor proteins was investigated. Like ST2L, MyD88, Mal and TRAM contain a TIR domain and are members of the IL-1R/TLR superfamily. To determine if TMED1 interacts with these adaptor proteins, co-immunoprecipitation assays were carried out. Figure 3.13A demonstrates that TMED1 and MyD88 do not interact (top panel lane 3, second panel lane 4). Although there is a band present in the experimental lane in Figure 3.13A (top panel, lane 3), there is also one present in the negative control (top panel, lane 1), as MyD88-myc is being pulled down by the anti-GFP antibody. Therefore the band present in the experimental lane (top panel, lane 3) is MyD88-myc being pulled down by the anti-GFP antibody, and not evidence of an interaction between TMED1 and MyD88. The IP using the anti-myc antibody was more straightforward, with no band in the negative control (second panel, lane 2) or experimental lane (second panel, lane 4). In the IPs blotted for GFP in both part A and B a lower band is visible. This band is likely to be the heavy chain band (~50kDa). These results highlight the specificity of TMED1 for the TIR domain of ST2L specifically. TMED1 also did not co-immunoprecipitate with other TIR domain containing adaptor proteins Mal and TRAM (Figure 3.13B and C, respectively).

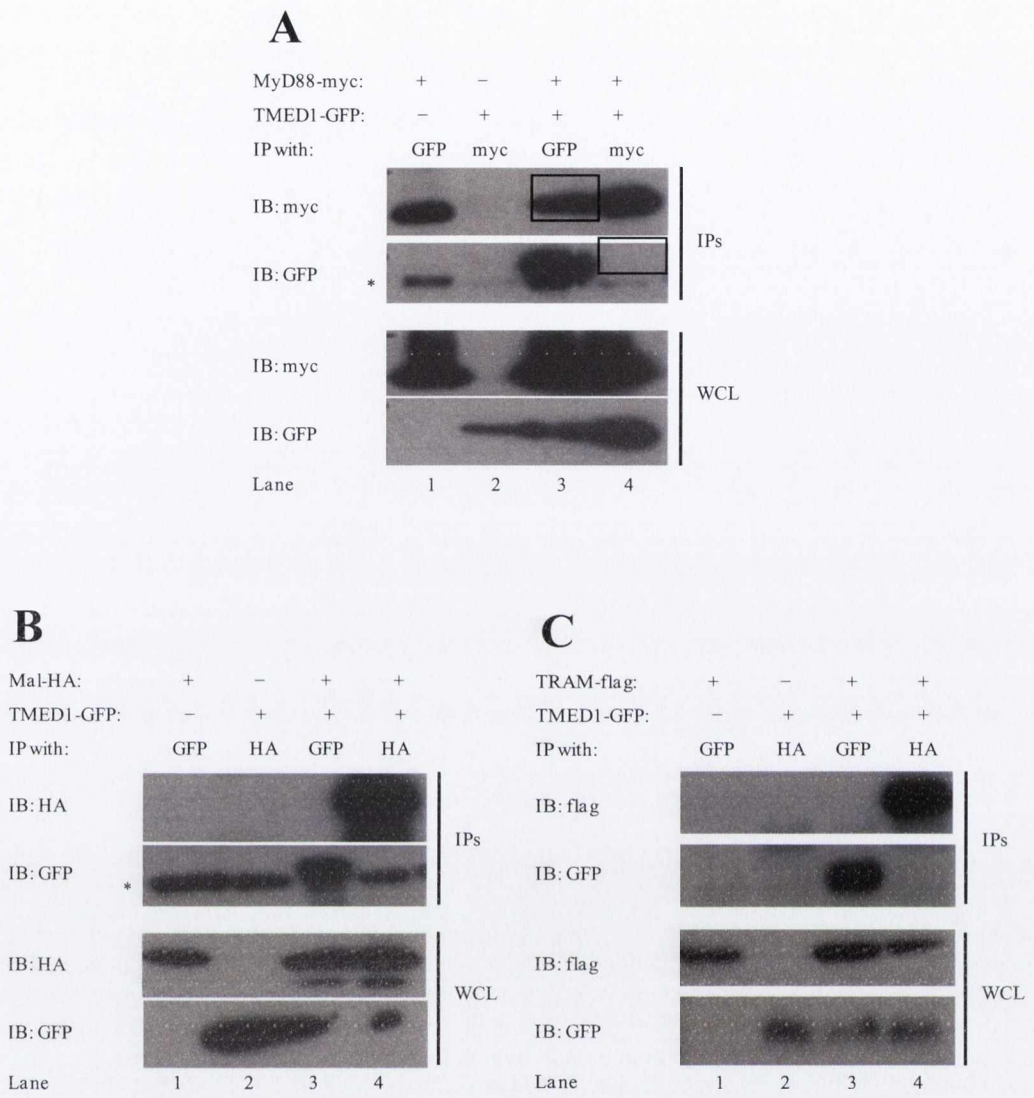


Figure 3.13 TMED1 does not co-immunoprecipitate with MyD88

HEK-293T cells were transfected with plasmids encoding TMED1-GFP and (A) MyD88-myc (B) Mal-HA or (C) TRAM-flag as shown. Samples were immunoprecipitated with anti-HA, anti-flag or anti-GFP coupled Protein A/G-plus agarose beads. Whole cell lysate (WCL) and immunoprecipitated samples were analysed by Western blot. Immunoblotting antibodies (IB) are listed beside the appropriate blot. Asterisks mark antibody heavy chains. Data is representative of two independent experiments.

3.2.6 TMED1 and ST2L interact endogenously

Having demonstrated the interaction using over-expressed TMED1, the next goal was to examine the interaction endogenously. ST2L is known to be highly expressed in mast cells, and its expression has been confirmed previously in the human mast cell (HMC) 1.1 cell line (Drube et al., 2010). However, the presence of TMED1 in this cell line has not been investigated. Figure 3.14A demonstrates that HMC 1.1 cells express TMED1 mRNA (lane 2). The expected size of the product is 389 base pairs. The presence of the TMED1 protein was demonstrated by immunoprecipitation using a TMED1 antibody. The anti-TMED1 antibody immunoprecipitated a protein of the correct size from HMC 1.1 cell lysates (Figure 3.14B, lane 9). To confirm the specificity of this band, lysates from HEK-293T cells in which TMED1 had been knocked down were run alongside the immunoprecipitated samples from HMC 1.1 cells. HEK-293T cells were used for the knockdown of TMED1 rather than HMC 1.1 cells as the HMC 1.1 cell line is difficult to transfect. TMED1 is visible in samples which received no siRNA or negative control siRNA (lanes 1, 2 and 5 respectively). The intensity of the TMED1 bands at this size was reduced in lanes 3, 4 and 7, as TMED1 was successfully knocked down using different siRNA in these samples. The corresponding size of the immunoprecipitated band in lane 9 confirms that TMED1 can be immunoprecipitated from the HMC 1.1 cell line.

Having demonstrated that it was possible to immunoprecipitate TMED1 in this cell line, the HMC 1.1 cells were chosen to examine the interaction endogenously. Figure 3.15 demonstrates the interaction between endogenous ST2L and endogenous TMED1. This is shown in lane 2. As the anti-TMED1 antibody was raised in rabbit, anti-rabbit IgG coupled Protein A/G-plus agarose beads were used as a control. The lack of a band in lane 1 of the top panel demonstrates that ST2L is specifically immunoprecipitated by

TMED1. Immunoblotting of the whole lysates demonstrates that both ST2L and TMED1 are present in all cases (Figure 3.15, third and fourth lanes).

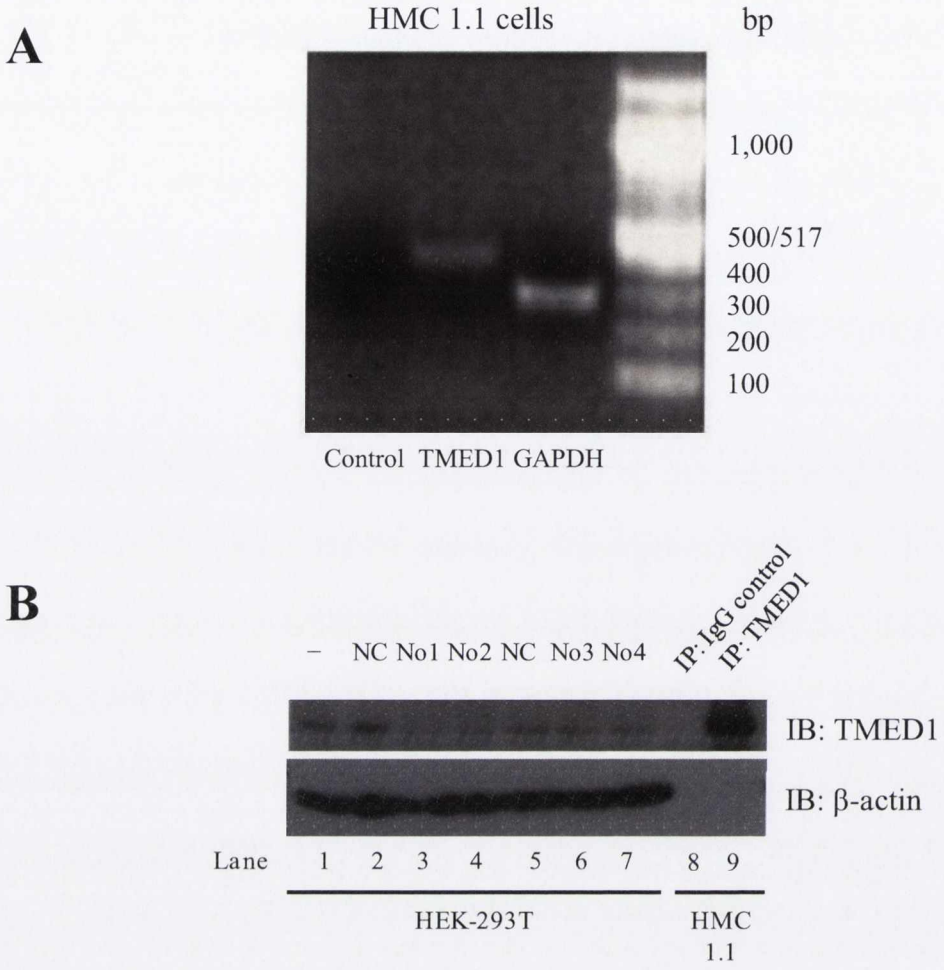


Figure 3.14 Detection of endogenous TMED1 in the HMC 1.1 cell line

(A) TMED1 and GAPDH cDNA generated from HMC 1.1 cells. The control reaction lacks primers. Expected TMED1 and GAPDH products are 389 and 284 base pairs (bp) respectively. (B) Immunoblot analysis of HEK-293T samples in which TMED1 was knocked down using several different siRNA (left, No1-No4) and non-silencing controls (NC) and HMC 1.1 samples in which TMED1 was immunoprecipitated (right). Immunoblotting (IB) antibodies are shown beside the appropriate blots.

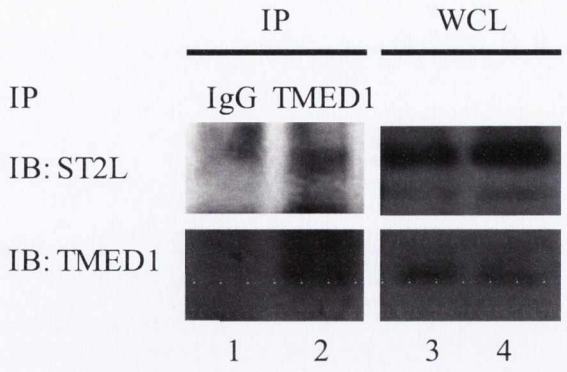


Figure 3.15 Endogenous TMED1 co-immunoprecipitates with endogenous ST2L

HMC 1.1 cell lysates were immunoprecipitated with anti-rabbit IgG or anti-TMED1 coupled Protein A/G-plus agarose beads. Whole cell lysates (WCL) and immunoprecipitated samples were then analysed by Western blotting. Immunoblotting antibodies (IB) are listed beside the appropriate blot. Results presented are representative of two experiments.

3.2.7 Defining the domains in TMED1 responsible for the TMED1-ST2L interaction

In order to decipher what domains of TMED1 are responsible for its interaction with ST2L, various mutants were generated and confirmed by sequence analysis. The four mutants, shown in Figure 3.16, were constructed using Stragene's Site Directed Mutagenesis Kit and the primers used are described in the Methods section. TMED1 contains a number of different regions; the signal peptide, a GOLD domain, a linker and coiled-coiled region, a transmembrane domain and finally a C-terminal tail. Within the GOLD domain there are two highly conserved cysteine residues which are thought to form a disulfide bond. In the SS-TMED1 mutant, these two cysteine residues of the GOLD domain were converted to serine residues. ΔG-TMED1 has the GOLD domain completely removed, ΔGLCC-TMED1 lacks the GOLD, linker and coiled-coiled domains, and ΔTM-TMED1 lacks the transmembrane domain. Sequence analysis confirmed that the correct base nucleotides had either been mutated or deleted.

The co-immunoprecipitation experiments with these TMED1 mutants were first carried out using the GFP Trap® beads. HEK-293-hST2L cells which stably express ST2L were used for these experiments. The WT TMED1-ST2L interaction can be observed (Figure 3.17, top left panel, lane 2). A considerately weaker band is observed with SS-TMED1-GFP and ΔG-TMED1-GFP in lane 3 and lane 5 respectively, while none is visible with ΔGLCC-TMED1-GFP and ΔTM-TMED1-GFP in lanes 4 and 6 (Figure 3.17). These co-immunoprecipitation experiments were also carried out using A/G-plus beads coupled to either anti-GFP or anti-ST2L. Similar results was also observed with TMED1-GFP and ST2L-HA constructs transiently overexpressed in HEK-293T cells (Figure 3.18).

Each of the changes made to TMED1 greatly reduce its ability to interact with ST2L. Mutation of the cysteine residues and deletion of the GOLD domain both

significantly disrupt the interaction to a similar degree. This demonstrates that correct folding of the GOLD domain is of critical importance. However, removal of the linker and coiled-coiled regions further disrupt the interaction. These results suggest that the interaction is primarily mediated by the GOLD domain, but that a region greater than the GOLD domain is also involved in the interaction. The transmembrane domain of TMED1 is also critical for the interaction to occur, as deletion of this domain also has a negative impact on the interaction.

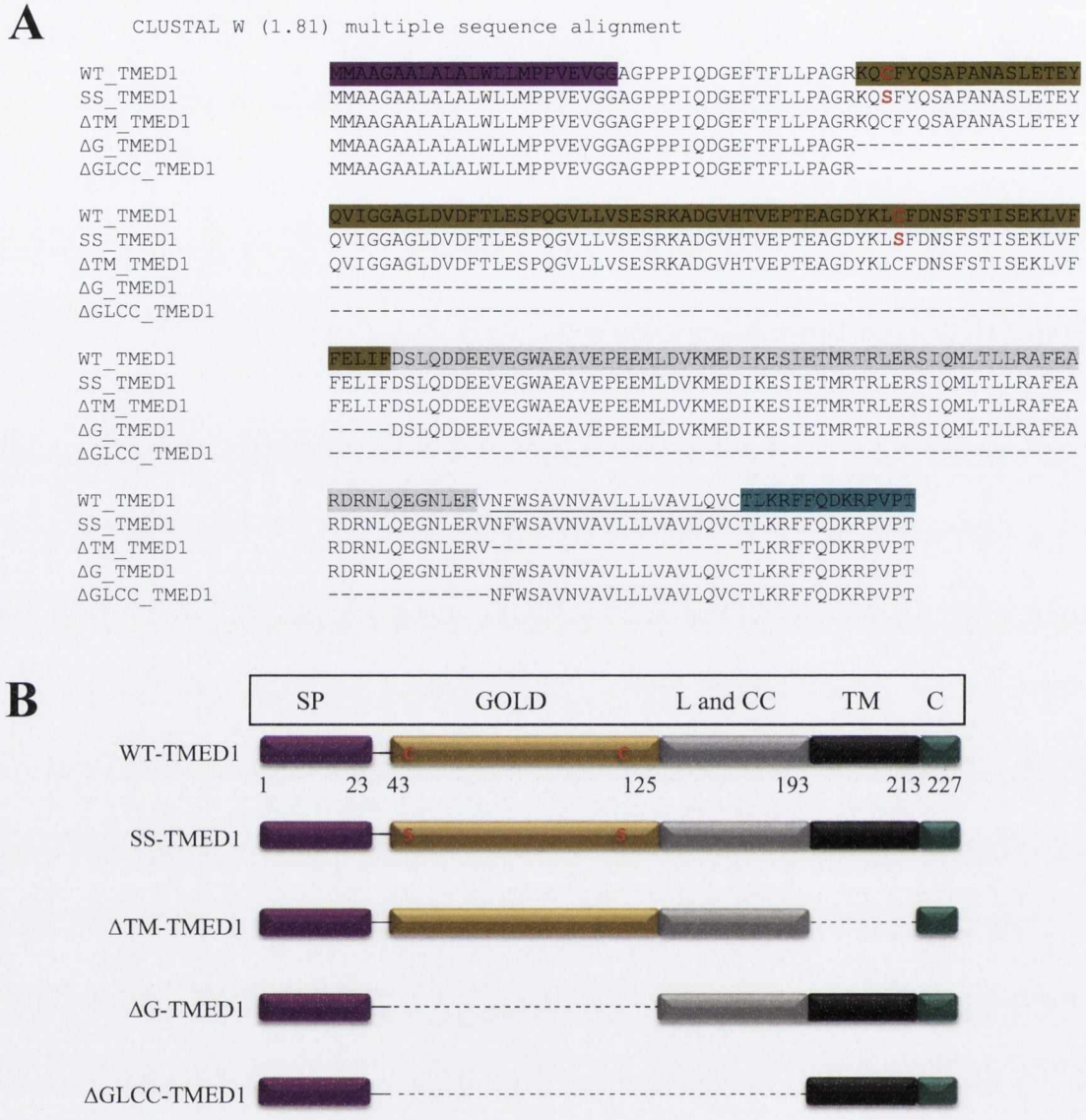


Figure 3.16 Sequence alignment and domain structure of wild type and mutant TMED1 constucts

The GOLD domain (highlighted in dark yellow) contains two cysteine residues (in red). These were both mutated to serine residues in the SS mutant. The underlined region in the WT-TMED1 sequence shown in part A, is a putative transmembrane domain which was deleted in the ΔTM mutant. ΔG has the GOLD domain removed, while ΔGLCC has the GOLD, linker and coiled-coiled domains removed. Each of the constructs are GFP tagged at the C-terminus.

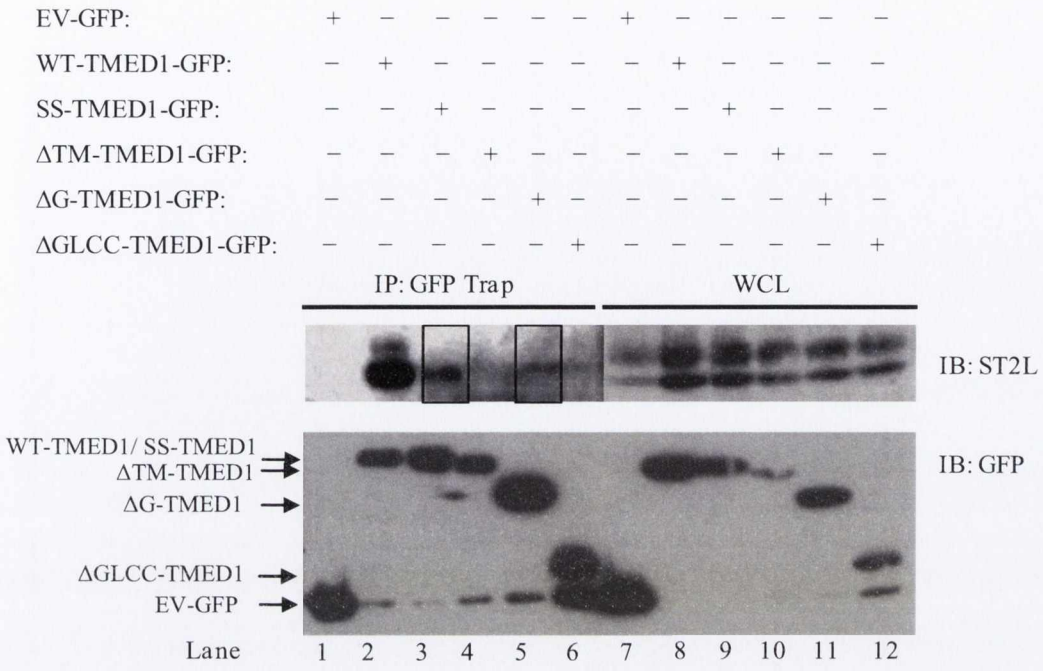


Figure 3.17 Mutations in TMED1 affect its ability to interact with ST2L: immunoprecipitation with GFP Trap® beads

HEK-293-hST2L cells were transiently transfected with a plasmid encoding EV-GFP or various TMED1 constructs as shown. (WT: wild type, SS: two cysteine residues converted to serine residues, ΔTM: transmembrane domain deleted, ΔG: GOLD domain deleted, ΔGLCC: GOLD, linker and coiled-coiled domains deleted). Samples were immunoprecipitated with anti-GFP Trap® beads. Whole cell lysates (WCL) and immunoprecipitated samples were analysed by Western blot. The immunoblotting antibodies (IB) are listed beside the appropriate blot. Data are representative of three independent experiments.

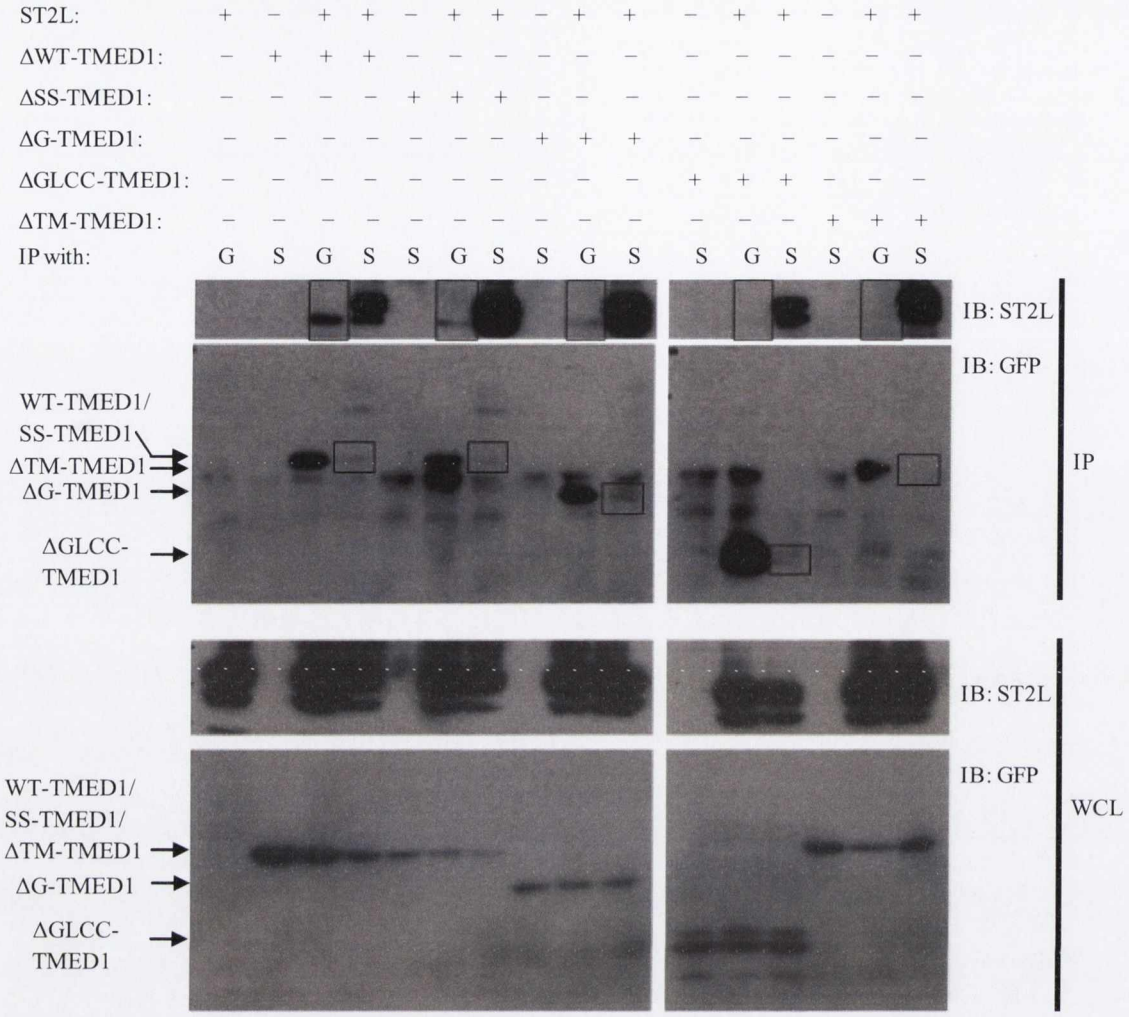


Figure 3.18 Mutations in TMED1 affect its ability to interact with ST2L: immunoprecipitation with antibody coupled A/G-plus beads

HEK-293T cells were transfected with plasmids encoding ST2L and GFP tagged TMED1 constructs (WT: wild type, SS: two cysteine residues converted to serine residues, ΔTM: transmembrane domain deleted, ΔG: GOLD domain deleted, ΔGLCC: GOLD, linker and coiled-coiled domains deleted). Samples were immunoprecipitated with A/G-plus beads precoupled to either anti-GFP (G) or anti-ST2L (S) antibodies. Immunoprecipitated samples and whole cell lysates (WCL) were analysed by Western blotting. Immunoblotting antibodies (IB) are listed beside the appropriate blot. Results presented are a representative of three experiments.

3.2.8 Defining the domains in ST2L responsible for the TMED1-ST2L interaction

In a similar manner to that described for generation of the TMED1 mutants, ST2L mutants were generated to determine what regions of ST2L are responsible for the interaction with TMED1. The polyclonal anti-ST2L antibody which was used in the prevoius IPs was generated against the extracellular part of ST2L. It recognises amino acids from position 19 to 328. As this antibody would not be able to detect ΔIG-ST2L, the ST2L-HA construct which has the HA tag at the C-terminus of the protein was used to create the deletion mutants. As shown in Figure 3.19, the three Ig domains of ST2L were removed resulting in the construct termed ΔIG-ST2L, while the TIR domain was removed in ΔTIR-ST2L. The new constucts were checked by sequence analysis to confirm the deletions and were then used in co-immunoprecipitation assays.

Figure 3.20 shows the results from the interaction analysis with these constructs. Lane 2 in the first and second panels of Figure 3.19 shows the interaction between ST2L and TMED1 as seen before. The Ig domains of ST2L are not required for the interaction (Figure 3.20, top panel, lane 3). However, although ΔTIR-ST2L is expressed better in lysates (Figure 3.20, fifth panel, lane 4 and 8) and immunoprecipitates itself to a greater degree than WT-ST2L (Figure 3.20, third panel, lane 4 and 8), its ability to interact with TMED1 is greatly impaired (first panel, lane 4). These results were confirmed by immunoprecipitating HA-tagged ST2L and blotting for GFP-TMED1 (Figure 3.20, second panel). The WT-TMED1-ST2L interaction was observed again (lane 2) and was also evident with the Ig domains deleted from ST2L (lane 3) as the ΔIG-ST2L construct still interacts with TMED1 strongly. Removal of the TIR domain however obliterated the interaction (lane 4).

A

```
CLUSTAL 2.0.12 multiple sequence alignment

WT_ST2L          MGFWILAILTILMYSTAAKFSKQSWGLENEALIVRCPRQGKPSYTVDWYYSQTNKSIPTQ 60
ΔIG_ST2L         MGFWILAILTILMYSTAA------------------------------------------ 60
ΔTIR_ST2L        MGFWILAILTILMYSTAAKFSKQSWGLENEALIVRCPRQGKPSYTVDWYYSQTNKSIPTQ 60

WT_ST2L          ERNRVFASGQLLKFLPAEVADSGIYTCIVRSPTFNRTGYANVTIYKKQSDCNVPDYLMYS 120
ΔIG_ST2L         ------------------------------------------------------------ 120
ΔTIR_ST2L        ERNRVFASGQLLKFLPAEVADSGIYTCIVRSPTFNRTGYANVTIYKKQSDCNVPDYLMYS 120

WT_ST2L          FVSGSEKNSKIYCPTIDLYNWTAPLEWFKNCQALQGSRYRAHKSFLVIDNVMTEDAGDYT 180
ΔIG_ST2L         ------------------------------------------------------------ 180
ΔTIR_ST2L        FVSGSEKNSKIYCPTIDLYNWTAPLEWFKNCQALQGSRYRAHKSFLVIDNVMTEDAGDYT 180

WT_ST2L          CKFIHNENGANYSVTATRSFTVKDEQGFSLFPVIGAPAQNEIKEVEIGKNANLTCSACFG 240
ΔIG_ST2L         ------------------------------------------------------------ 240
ΔTIR_ST2L        CKFIHNENGANYSVTATRSFTVKDEQGFSLFPVIGAPAQNEIKEVEIGKNANLTCSACFG 240

WT_ST2L          KGTQFLAAVLWQLNGTKITDFGEPRIQQEEGQNQSFSNGLACLDMVLRIADVKEEDLLLQ 300
ΔIG_ST2L         ------------------------------------------------------------ 300
ΔTIR_ST2L        KGTQFLAAVLWQLNGTKITDFGEPRIQQEEGQNQSFSNGLACLDMVLRIADVKEEDLLLQ 300

WT_ST2L          YDCLALNLHGLRRHTVRLSRKNPIDHHSIYCIIAVCSVFLMLINVLVIILKMFWIEATLL 360
ΔIG_ST2L         ------------------RKNPIDHHSIYCIIAVCSVFLMLINVLVIILKMFWIEATLL 360
ΔTIR_ST2L        YDCLALNLHGLRRHTVRLSRKNPIDHHSIYCIIAVCSVFLMLINVLVIILKMFWIEATLL 360

WT_ST2L          WRDIAKPYKTRNDGKLYDAYVVYPRNYKSSTDGASRVEHFVHQILPDVLENKCGYTLCIY 420
ΔIG_ST2L         WRDIAKPYKTRNDGKLYDAYVVYPRNYKSSTDGASRVEHFVHQILPDVLENKCGYTLCIY 420
ΔTIR_ST2L        WRDIAKPYKTRNDG-------------------------------------------- 420

WT_ST2L          GRDMLPGEDVVTTVETNIRKSRRHIFILTPQITHNKEFAYEQEVALHCALIQNDAKVILI 480
ΔIG_ST2L         GRDMLPGEDVVTTVETNIRKSRRHIFILTPQITHNKEFAYEQEVALHCALIQNDAKVILI 480
ΔTIR_ST2L        ------------------------------------------------------------ 480

WT_ST2L          EMEALSELDMLQAEALQDSLQHLMKVQGTIKWREDHIANKRSLNSKFWKHVRYQMPVPSK 540
ΔIG_ST2L         EMEALSELDMLQAEALQDSLQHLMKVQGTIKWREDHIANKRSLNSKFWKHVRYQMPVPSK 540
ΔTIR_ST2L        ----------------------------------------------------------SK 540

WT_ST2L          IPRKASSLTPLAAQKQ 556
ΔIG_ST2L         IPRKASSLTPLAAQKQ 556
ΔTIR_ST2L        IPRKASSLTPLAAQKQ 556
```

B

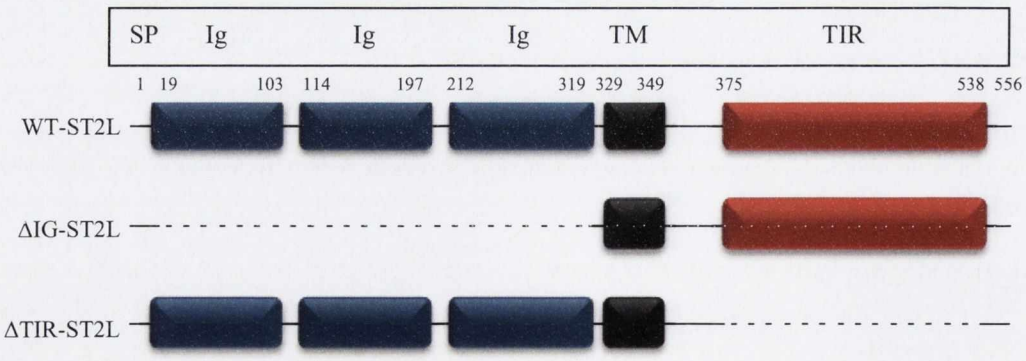


Figure 3.19 Wild type and mutant ST2L constucts

Figure 3.19 Wild type and mutant ST2L constucts

ST2L contains three Ig domains which are shown in blue. The transmembrane domain is underlined and the TIR domain is in red. In ΔIG-ST2L the Ig domains have all been removed, while in ΔTIR-ST2L the TIR domain is removed. A) Clustal alignment of WT-ST2L, ΔIG-ST2L and ΔTIR-ST2L and B) Representation of the domain structure of WT-ST2L, ΔIG-ST2L and ΔTIR-ST2L.

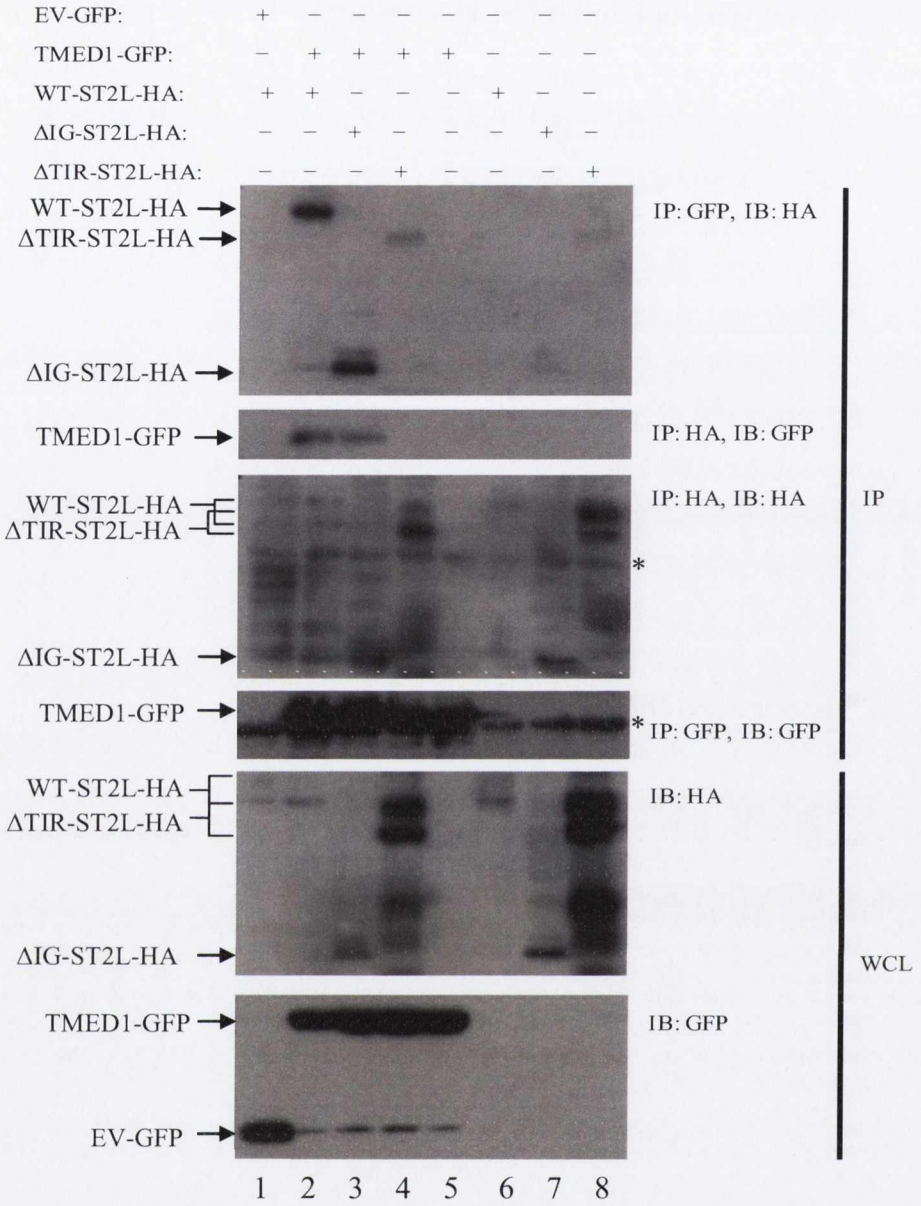


Figure 3.20 Mutations in ST2L affect its ability to interact with TMED1

HEK-293T cells were transfected with plasmids encoding EV-GFP, TMED1-GFP, or ST2L constructs (WT: wild type, ΔIG: Ig domains deleted, ΔTIR: TIR domains deleted). Samples were immunoprecipitated with anti-HA or anti-GFP coupled Protein A/G-plus agarose beads. Whole cell lysate (WCL) and immunoprecipitated samples were analysed by Western blot. Immunoblotting antibodies (IB) are listed beside the appropriate blot. Data are representative of three independent experiments. Asterisks mark antibody heavy chains. Results shown are representative of three experiments.

3.2.9 TMED1 and ST2L co-localise

Having demonstrated that TMED1 and ST2L interact, their co-localisation was investigated by confocal microscopy. For these experiments the TMED1-GFP and ST2L-HA constructs were expressed in HEK-293T cells. 48 hours later cells were fixed, permeabilised and stained with an anti-HA primary antibody followed by an Alexa-647 coupled secondary antibody for visualisation of ST2L. ST2L expression was visible throughout the cell, but a region of higher intensity in the peri-nuclear area was also noted. The co-localisation of TMED1 and ST2L was detected in most of the regions where both of these proteins were present, but in particular in the regions where there are higher levels of ST2L (Figure 3.21, arrows).

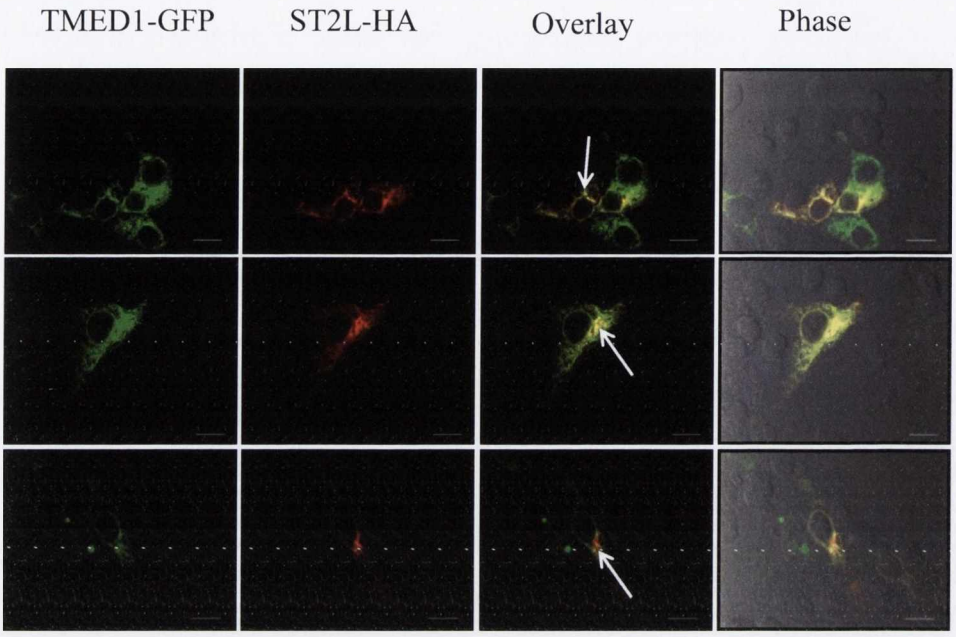


Figure 3.21 TMED1-GFP and ST2L-HA can co-localise in HEK-293T

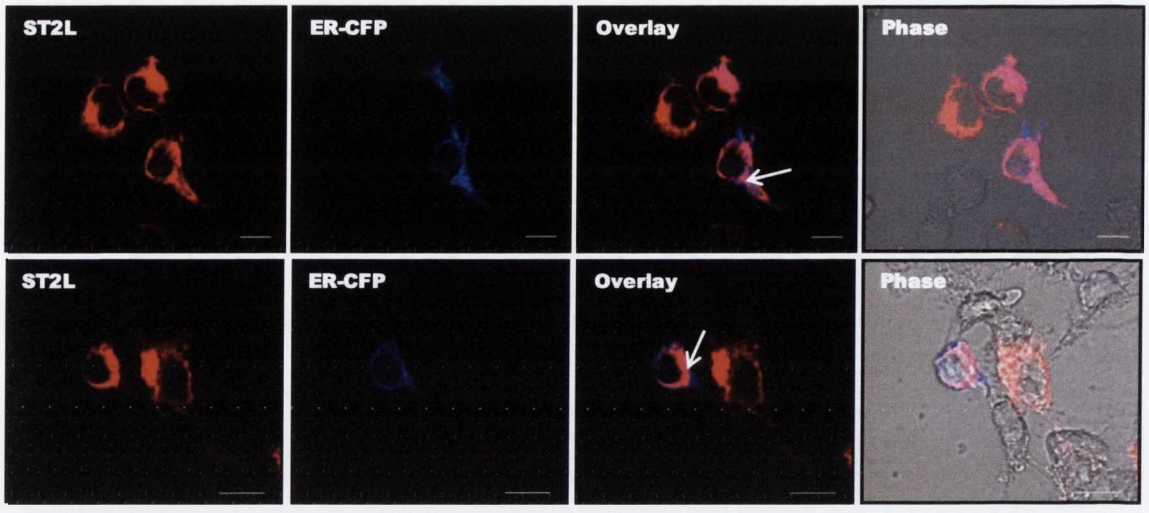
HEK-293T cells were transfected with a plasmid encoding TMED1-GFP and a plasmid encoding ST2L-HA. Cell were fixed, stained with primary anti-HA followed by secondary Alexa-647 antibodies and viewed using an Olympus FV1000 Confocal Microscope. Results presented are representative of 66 cells from three independent experiments.

3.2.10 Localisation of the TMED1 and ST2L interaction

The localisation of TMED1 had already been investigated earlier in this chapter, and it was found to mainly localise to the ER and Golgi. A similar approach was also undertaken to investigate the localisation of ST2L, as no studies investigating the intracellular localisation of ST2L by confocal microscopy have been carried out. Figure 3.22 demonstrates that ST2L can co-localise with ER-CFP (Part A, arrows). As an intense region of ST2L expression was often noted near the nucleus, co-transfection of ST2L and Golgi-CFP was carried out. These results demonstrate that the observed region of intense ST2L expression is indeed the Golgi, as the co-localisation of ST2L with Golgi-CFP can be detected (Figure 3.22B, arrows). The localisation of ST2L was also investigated in HMC 1.1 cells. Figure 3.23 shows that endogenous ST2L in HMC 1.1 cells displays a similar expression pattern to overexpressed ST2L in HEK-293T cells. ST2L can be seen at the plasma membrane in these cells, with some reticular staining and a notable area of higher expression in the perinuclear area, which is likely to be the Golgi.

Next, the co-localisation of TMED1 and ST2L was examined with ER and Golgi markers. HEK-293T cells were chosen as the HMC 1.1 cells had previously proved difficult to transfect. Results from these experiments are shown in Figure 3.24 and 3.25. TMED1-GFP and ST2L-HA co-localise as previously demonstrated in Figure 3.20. TMED1 and ST2L can also be detected co-localising with ER-CFP (Figure 3.24, panel number 7, arrow) and the Golgi marker Golgi-CFP (Figure 3.25, panel number 7, arrow). These results demonstrate that TMED1 and ST2L can associate at both the ER and Golgi.

A) Endoplasmic Reticulum



B) Golgi

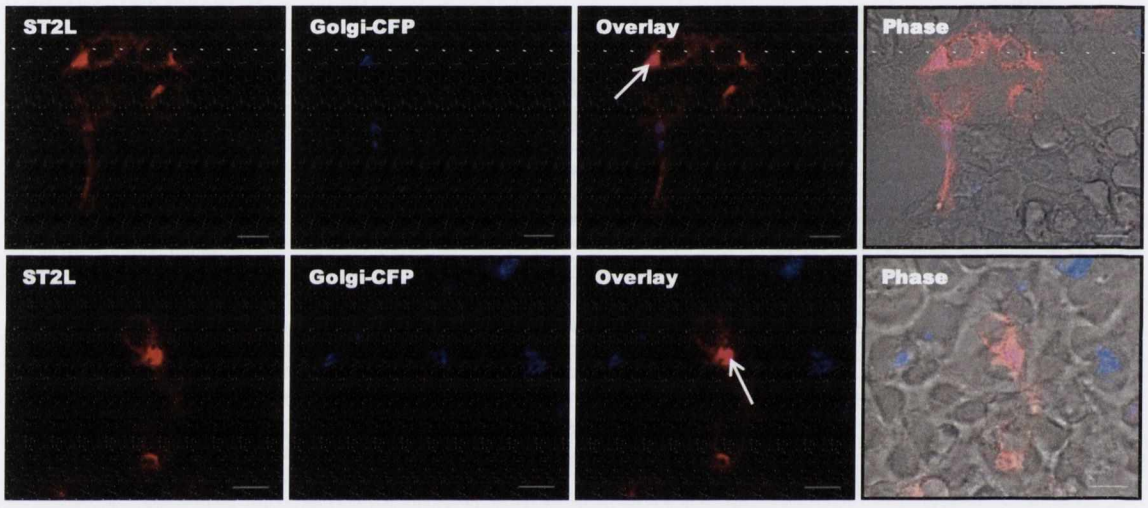


Figure 3.22 Localisation of ST2L in HEK-293T cells

HEK-293T cells were transfected with plasmids encoding ER-CFP and ST2L-HA (A) or Golgi-CFP and ST2L-HA (B). Cells were then fixed, stained with primary anti-HA antibody followed by a secondary Alexa-647 antibody and viewed using an Olympus FV1000 Confocal Microscope. Data shown is representative of two experiments. (A) 25 of the 32 cells analysed displayed co-localisation as represented here and (B) 30 of the 40 cells analysed display the co-localisation show here. Scale bars indicate 10 μM.

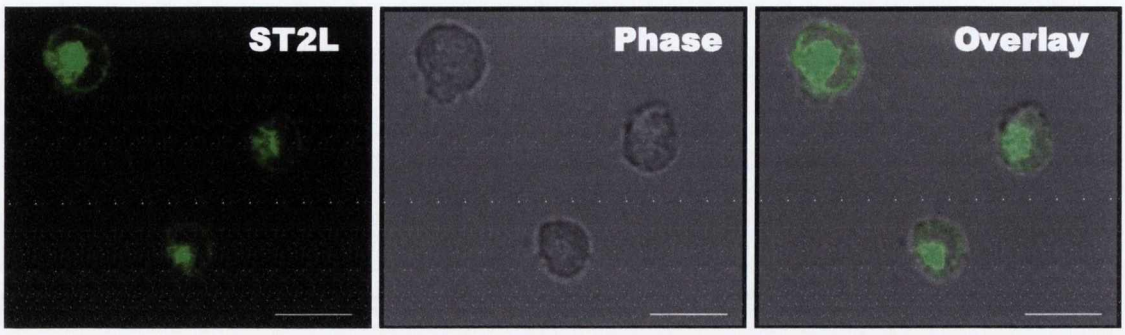


Figure 3.23 Localisation of endogenous ST2L in HMC 1.1 cells

Confocal images of ST2L in HMC 1.1 cells. Cells were fixed, stained with primary anti-ST2L followed by secondary Alexa-488 antibodies and viewed using the Olympics Fluoview FV1000 Imaging system. Data presented is representative of 25 cells. Scale bars indicate 10 μM.

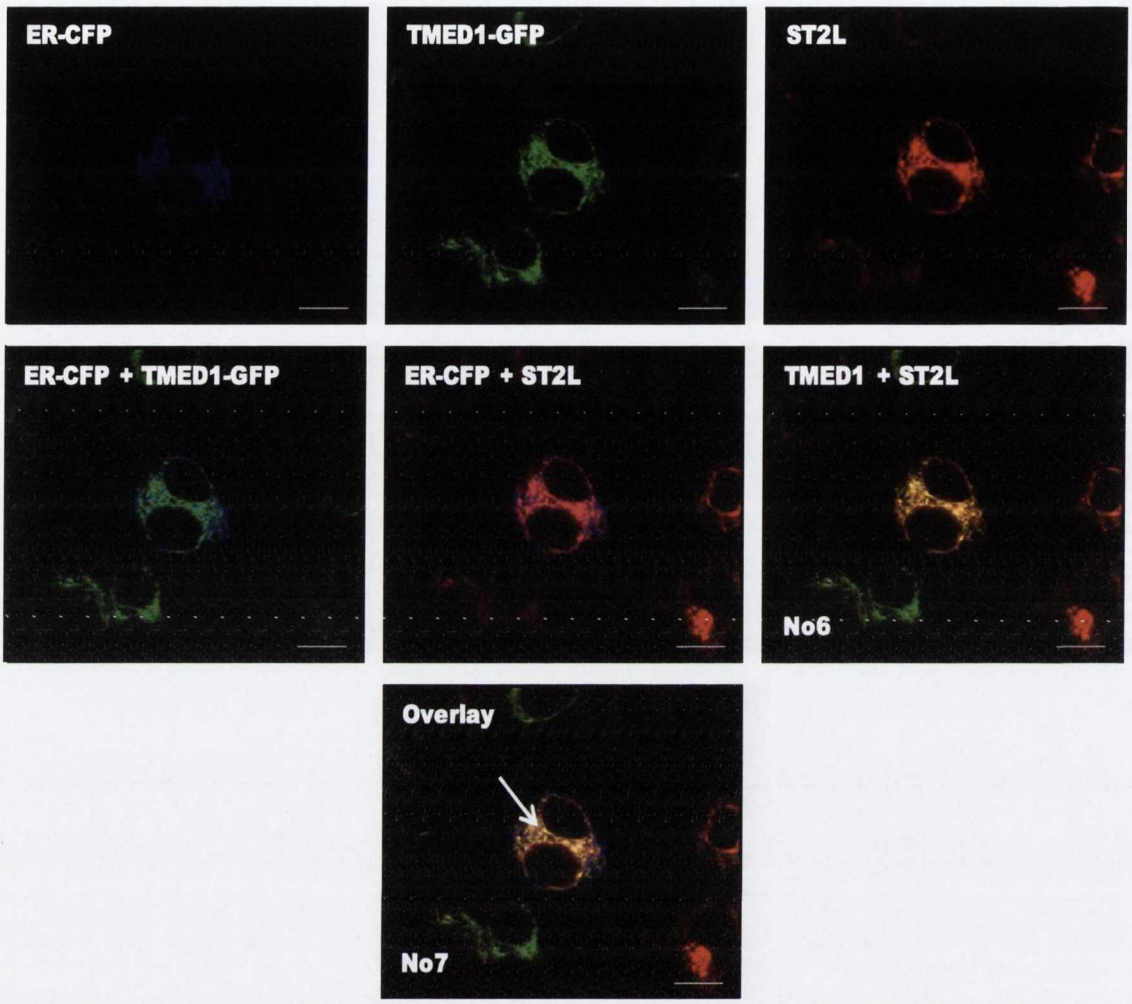


Figure 3.24 Co-localisation of TMED1 and ST2L at the ER

HEK-293T cells were transfected with plasmids encoding ER-CFP, TMED1-GFP and ST2L-HA. Cells were then fixed, stained with primary anti-HA followed by secondary Alexa-647 antibodies and viewed using an Olympus FV1000 Confocal Microscope. Data is representative of 14 cells. Scale bars indicate 10 μM.

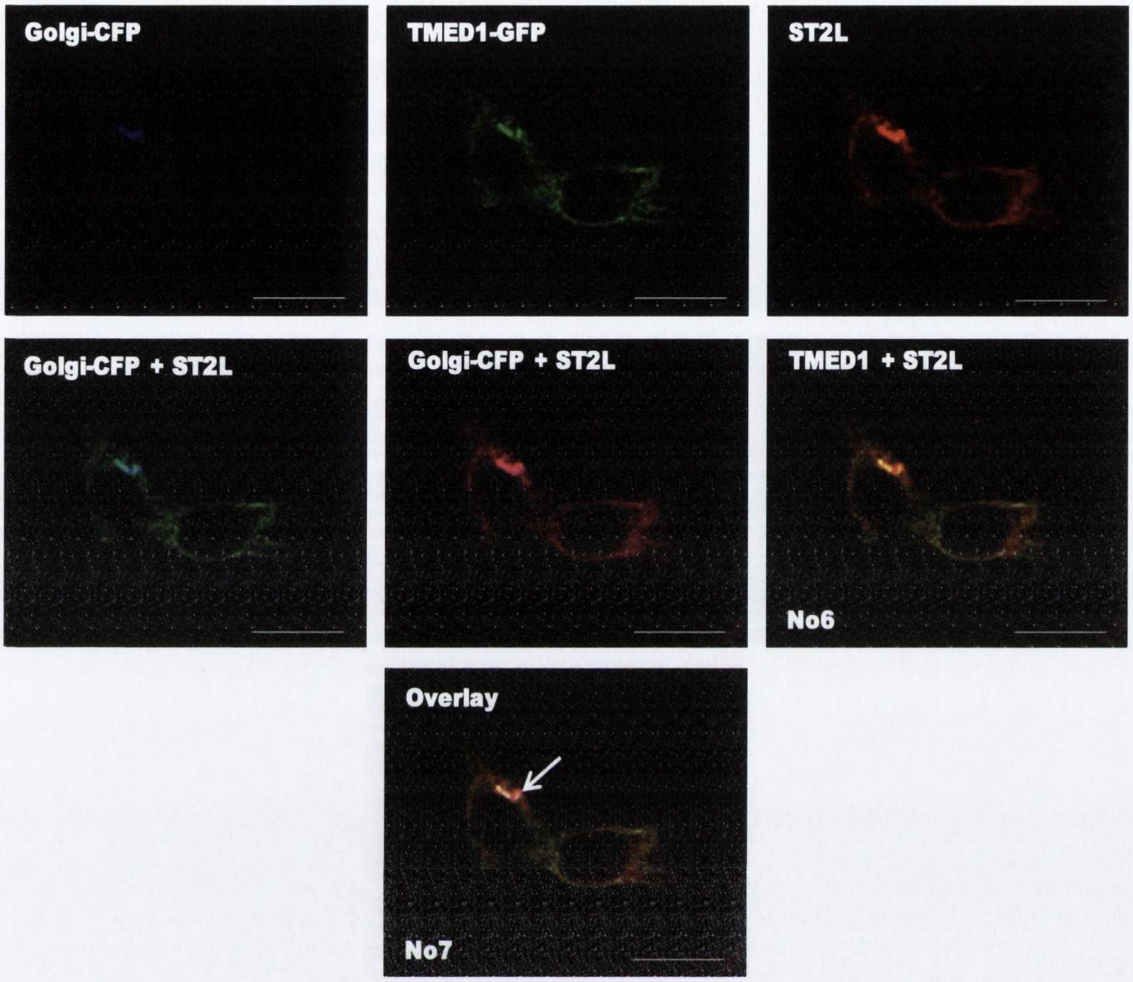


Figure 3.25 Co-localisation of TMED1 and ST2L at the Golgi

HEK-293T cells were transfected with plasmids encoding Golgi-CFP, TMED1-GFP and ST2L-HA. Cells were then fixed, stained with primary anti-HA followed by secondary Alexa-647 antibodies and viewed using an Olympus FV1000 Confocal Microscope. Data is representative of 10 cells. Scale bars indicate 10 μM.

3.3 Discussion

At the outset of this project a role for the TIR and GOLD domain containing protein TAG was emerging in the regulation of the MyD88-independent TLR4 signalling pathway (Palsson-McDermott et al., 2009). During these studies it was noted that TAG shared homology with the TMED family of proteins, as they also contain a GOLD domain. While there are ten members in the TMED family in mammals, TMED1 was of particular interest as it is a putative ST2 binding protein (Gayle et al., 1996). As both ST2L and TLR4 are members of the IL-1/TLR receptor superfamily the potential role for another GOLD domain containing protein was of great interest. TMED1 was isolated in a search for novel ST2L binding proteins (Gayle et al., 1996). To identify novel ST2L binding proteins, Gayle *et al.* first screened cell lines for their ability to bind a ST2L-Fc fusion protein and cDNA clones of putative binding proteins were then isolated. However, the putative interaction was not confirmed by any other means, and no other studies have been carried out regarding the association of TMED1 and ST2L. During the duration of this project, another TMED family member TMED7 has been shown to be required for TAG mediated regulation of TLR4 signalling (Doyle et al., 2012). This new information provides additional support to the concept that GOLD domain containing proteins are important players in immune signalling pathways.

As the current literature available on TMED1 is limited, a more in depth investigation into the characteristics of TMED1 was undertaken. The cellular location of TMED1 was examined by confocal microscopy and protease protection assays were carried out to investigate the topology of TMED1 and the localisation of its GOLD domain.

To learn more about the cellular localisation of TMED1, a GFP tagged construct was used for the visualisation of TMED1 by confocal microscopy. TMED1 was initially

isolated from a human glioblastoma cell line (A172) and thought to be a cell surface protein (Gayle et al., 1996). To determine if TMED1 resides at the plasma membrane, staining of the plasma membrane in TMED1-GFP expressing cells was carried out. TMED1 did not localise to the plasma membrane in these cells. Given the nature of protein trafficking it remains a possibility that TMED1 does localise to the plasma membrane but that this is a very transient event which may not have been revealed by the microscopy as images were taken of a number of individual cells, rather than one cell being monitored over time. Confocal microscopy also revealed that TMED1 can localise to the ER, Golgi and to early endosomes. The localisation of TMED1 in the ER and Golgi is consistent with previous reports on the localisation of both TMED1 as well as other TMED proteins (Dominguez et al., 1998; Emery et al., 2000; Jenne et al., 2002; Rojo et al., 1997). Members of the TMED family have also been reported to localise to compartments beyond the Golgi, such as early, recycling and late endosomes as well as secretory granules (Doyle et al., 2012; Hosaka et al., 2007). Work carried out on the localisation of TMED7 prompted experiments to determine if TMED1 could localise to other intracellular compartments. TMED7 has been shown to localise to the limiting membrane of early endosomes (Doyle et al., 2012), therefore co-localisation of TMED1 with the early endosomes marker EEA1 was investigated. While the majority of TMED1 resides at the ER, TMED1 is also capable of localising to the limiting membrane of early endosomes in resting cells. TMED7 has also been shown to co-localise with Rab11a (Doyle et al., 2012), the co-localisation of TMED1 with the recycling endosome marker Rab11a was investigated. However, no co-localisation of TMED1 with Rab11a was evident. Given that TMED7 has been demonstrated to traffic upon stimulation with LPS (Doyle et al., 2012), it is also possible that TMED1 moves in response to external stimuli. TMED1 may be recruited to certain compartments following stimulation and this may be

important in regulation of the signalling pathway. TMED1 trafficking may also result in the co-transport of other proteins. Similarly, this may affect downstream signalling.

There is some debate over the position of the transmembrane domain and localisation of the GOLD domain of the TMED proteins. TMED proteins were previously thought to be type I transmembrane proteins, with their transmembrane domain located near the C-terminus of the protein. They were also thought to be orientated with their N-terminus and GOLD domain localised in the lumen of the organelle in which they are residing, and their C-terminal tail projecting into the cytosol. However, TMED7 has been reported to have a transmembrane motif near the N-terminus of the protein and its GOLD domain projects into the cytosol (Doyle et al., 2012). Therefore an analysis of the position of the transmembrane domain of TMED1 and the compartment in which the GOLD domain is localised was carried out.

In order to investigate the number and position of transmembrane domains in TMED1, its amino acid sequence was analysed by a number of transmembrane prediction programmes. Each of these predicts a transmembrane domain near the C-terminus of the protein. This is the region which was initialling predicted to be a transmembrane domain in the original paper in which TMED1 was identified (Gayle et al., 1996). This region is also believed to be where the transmembrane domain is for other family members (Strating and Martens, 2009). Some other programmes predict an additional transmembrane domain near the N-terminus of the protein. However, an inherent problem in transmembrane protein prediction and signal peptide prediction is the high similarity between the hydrophobic regions of a transmembrane helix and that of a signal peptide. This leads to cross-reaction between the two types of predictions (Kall et al., 2004). Analyses of the TMED1 sequence with signal peptide prediction programmes all predict that that TMED1 possess a signal peptide at the N-terminus.

To determine if the transmembrane domain and signal peptide are required for the localisation of TMED1, constructs lacking each of these domains were generated and viewed by confocal microscopy. As mentioned previously, TMED1 displays a reticular staining pattern. Surprisingly, the TMED1 construct in which the transmembrane domain has been removed displays the same reticular patterning. As expected, removal of the signal peptide does disrupt the localisation of TMED1 as it is visible diffusely all over the cytosol with no distinct pattern. Removal of the C-terminal transmembrane domain in TMED7 also did not disrupt its ability to span the membrane, while removal of the predicted N-terminal transmembrane domain did (Doyle et al., 2012). This is similar to the results obtained here for TMED1. TMED7 may have a transmembrane domain at the N-terminus or may simply have a longer signal peptide than expected. TMED10 for example is predicted to have a longer signal peptide sequence than TMED1 (Rojo et al., 1997).

As yet, it is unclear why removal of the transmembrane domain does not affect the distribution of TMED1. While the maximum region predicted to span the membrane from all the prediction programmes is two amino acids longer than the segment which was removed, this is not likely to cause retention in the plasma membrane. One possibility is that the signal peptide of TMED1 is actually a signal anchor sequence. However, current information available on other TMED family members confirms that they have signal peptides, as N-terminal sequencing of TMED2, TMED9 and TMED10 does not initiate at the first Methionine (Blum et al., 1996; Dominguez et al., 1998).

As mentioned earlier, TMED proteins are thought to be orientated with their N-terminus and most of the protein in the lumen, with a short C-terminal cytosolic tail. This conclusion is based on protease protection assays which have been carried out on the family members TMED2, TMED9 and TMED10 (Blum and Lepier, 2008;

Dominguez et al., 1998; Rojo et al., 1997) which concludes that most of the proteins are located in the lumen, with a short cytoplasmic tail projecting into the cytosol. Post-translational modifications, such as glycosylation and disulfide bond formation which have been reported for the TMED proteins also suggest that the majority of the protein is in the lumen (Braakman and Bulleid, 2011). Two cysteine residues which are within the GOLD domain and are highly conserved throughout the TMED family are thought to form a disulfide bond (Anantharaman and Aravind, 2002). Although TMED7 and TMED9 have been reported to be glycosylated, this is not the case for all TMED proteins, as TMED2, TMED3 and TMED10 are not sensitive to Peptide-N-glycosidase F (PNGase) digestion (Fullekrug et al., 1999; Rojo et al., 1997).

To determine where the GOLD domain and C-terminus of TMED1 are situated, protease protection assays were carried out. Two independent experiments have suggested that the GOLD domain of TMED1 resides in the cytosol and the C-terminus projects into the lumen. This would suggest that the predicted transmembrane domain does span the membrane despite the fact that mutating this transmembrane domain does not affect the localisation of TMED1 when analysed using confocal microscopy. Mutating this transmembrane domain does however have a profound effect on the ability of TMED1 and ST2L to interact and this sequence does play a vital role in TMED1 function. Protease protection assays similar to those presented here have also been carried out for TMED7 (Doyle et al., 2012). These results revealed that like TMED1, the GOLD domain of TMED7 projects into the cytosol (Figure 3.25). However, unlike TMED1, the C-terminus of TMED7 projects into the cytosol. While it is more common for proteins to have their C-termini in the cytosolic compartment (Almen et al., 2009) there are two possible ways that homologous proteins can have oppositely oriented C-termini. There can be an extra transmembrane helix in one protein, or the two proteins

can be oppositely oriented in the membrane (von Heijne, 2006). As the GOLD domains of both proteins projects into in the cytosol opposite orientation of the C-termini of both proteins are likely to be due to an N-terminal transmembrane domain found in TMED7 that is not present in TMED1 (Figure 3.25). This data demonstrates that different members of the TMED family can be orientated differently, and previous assumptions that all TMED family members have the same orientation may have been over simplistic.

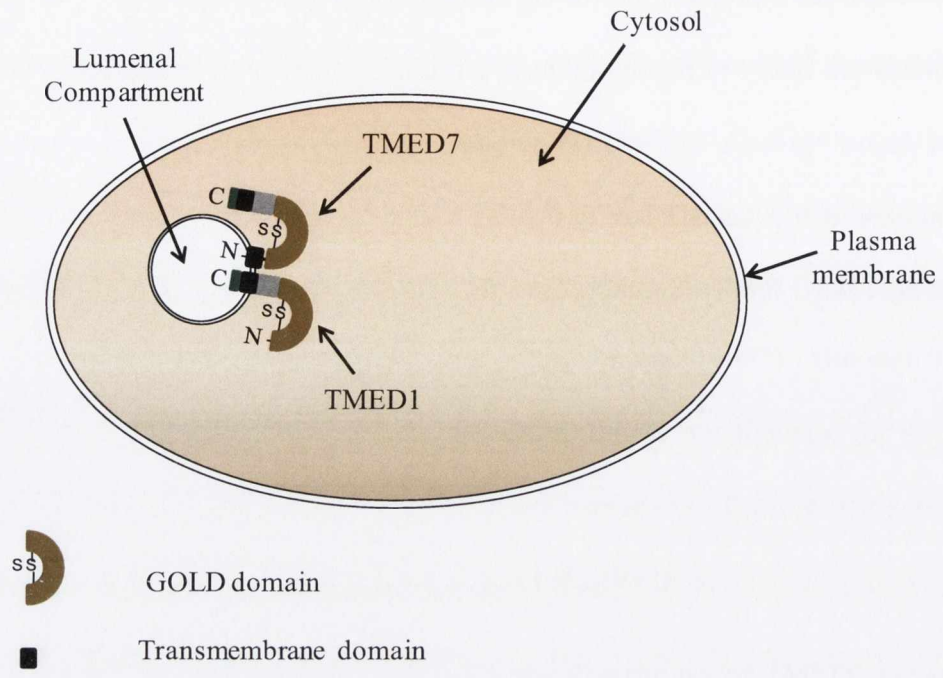


Figure 3.26 Orientation of TMED1 and TMED7

The GOLD domain of both TMED1 and TMED7 are localised in the cytosol. While the C-terminus of TMED1 is localised in the luminal compartment of organelles such as the ER and Golgi the C-terminus of TMED7 projects into the cytosol. This may be due to an N-terminal transmembrane domain present in TMED7 that is not present in TMED1.

Investigations into the putative association between TMED1 and ST2L have confirmed that these proteins do interact. The interaction between TMED1 and ST2L was confirmed by co-immunoprecipitation assays. This interaction was evident with both stably and transiently overexpressed ST2L and was extremely robust. The interaction was also observed in a more relevant endogenous system, the HMC 1.1 cell line.

Domain mapping analysis demonstrates that the GOLD domain of TMED1 primarily recognises ST2L, as mutation or removal of this domain greatly impairs the interaction. However, removal of the neighbouring linker and coiled-coiled regions completely abolishes the interaction. It may be that the linker or coiled-coiled regions are also involved in the interaction, particularly as the linker region is next to the GOLD domain. A small number of studies have established cargo for the TMED proteins. These studies have found that different regions are important depending on the cargo in question. The GOLD domain and a small linker region of TMED2 are most important for its interaction with PAR-2 (Luo et al., 2007). Interestingly, a construct containing the GOLD domain of TMED2 alone was only able to weakly interact with PAR-2. A construct containing both the GOLD domain and the linker region was needed to fully restore the interaction to a level comparable with full length TMED2. These results suggest that the linker domain of TMED2 is required, but not sufficient for the PAR-2 interaction. This could also be the case for TMED1. In other instances, C-terminal regions of TMED proteins are important. For example, the C-terminal region of TMED9 and TMED10 which encompasses the coiled-coiled, transmembrane and cytoplasmic domains are sufficient for their interaction with TC48 (Gupta and Swarup, 2006). Interestingly, TMED1 requires the transmembrane domain for its interaction with ST2L. Removal of the transmembrane domain may disrupt the localisation of the GOLD

domain, thereby disrupting the interaction, although the confocal data does not suggest a major disruption to its localisation upon removal of this transmembrane domain.

In addition, the domains of ST2L required for the TMED1 and ST2L interaction were also mapped. The ability of TMED1 to interact with a ST2L variant lacking all the Ig domains clearly demonstrates that this region is not required for the interaction. On the contrary the TIR domain of ST2L is required. Therefore the TMED1-ST2L interaction is primarily a GOLD domain-TIR domain mediated interaction. The GOLD domain of TMED1 has been shown to localise to the cytosol, facilitating the interaction between TMED1 and ST2L in this compartment.

This is the first interaction which has been shown to be mediated by these two domains. However, other proteins containing these domains have been shown to interact. TMED7 can interact with the TIR domain containing adaptor TRAM and its negative regulator TAG (Doyle et al., 2012). In addition, TRAM can interact with TAG (Palsson-McDermott et al., 2009). TRAM contains a TIR domain, TMED7 contains a GOLD domain and TAG contains both a TIR domain and a GOLD domain. The GOLD domains of both TMED7 and TAG are localised in the cytosol (Doyle et al., 2012). Although TRAM is membrane associated, its TIR domain is also localised in the cytosolic compartment (Rowe et al., 2006). Therefore it is possible that these interactions are also mediated by GOLD domain and TIR domain associations, as each of the domains are found in the same cellular compartment.

A portion of ST2L localises to the ER and Golgi and TMED1 and ST2L co-localised in these compartments. Other IL-1R/TLR superfamily members such as TLR2 and TLR4 have been shown to localise to the Golgi apparatus (Latz et al., 2003; Latz et al., 2002; Uronen-Hansson et al., 2004). Like the TLRs, members of the IL-1R

subgroup of the IL-1R/TLR superfamily have been shown to localise to regions other than the plasma membrane. The novel IL-1R family member DIGIRR has displayed subcellular distribution at the Golgi apparatus (Gu et al., 2011). The co-localisation of TMED proteins with their cargo proteins has been reported at both the ER and Golgi. TMED9 and TMED10 co-localise with the tyrosine phosphatase TC48 at the ER and Golgi (Gupta and Swarup, 2006). The PAR-2-TMED2 association has been shown to occur at the Golgi and is disrupted following PAR-2 stimulation to allow PAR-2 to replenish the plasma membrane (Luo et al., 2007). In a similar way, ST2L may localise to the ER and Golgi as presynthesised receptors, ready to repopulate the plasma membrane as the ligand bound receptor has been shown to be internalised and degraded following IL-33 binding (Zhao et al., 2012). In addition the IL-1R and IL-1RII have been reported to traffic following binding of their respective ligands (Blanco et al., 2008; Bourke et al., 2003; Brissoni et al., 2006; Korherr et al., 1997). Following ligand binding these trafficking events result in the distribution of these receptors to compartments such as the ER, Golgi, lysosomes and proteasomes and are involved in both signal activation and signal termination. TMED1 may be required for ST2L trafficking during the early secretory pathway or IL-33-induced signalling pathway.

This more in depth analysis of the properties of TMED1 has revealed new information on the localisation of TMED1. It also demonstrates that the GOLD domain of TMED1 is found in the cytosol, while its C-terminus is not. Is it hoped that this analysis will aid in the elucidation of the function of TMED1. Results have also confirmed that TMED1 and ST2L interact. It appears that this interaction occurs at least in part at the ER and Golgi and it is possible to conclude that the interaction is mediated primiraly by the GOLD domain of TMED1 and the TIR domain of ST2L. Given that ST2L is the receptor required for the detection of IL-33 and is responsible for subsequent

induction of downstream signalling, the possible role for TMED1 in ST2L mediated signalling was investigated next.

Chapter Four

Investigation into the involvement of TMED1 in the ST2L signalling pathway

Chapter 4

4.1 Introduction

As an interaction between TMED1 and ST2L has been established the next step was to determine the purpose of this association. Therefore, an investigation into the functional consequence of the TMED1-ST2L interaction was carried out. The investigation into the implications of the TMED1-ST2L association was further warranted given that a role for other TMED family members have been established in the regulation of receptor mediated processes. TMED7 has been shown to be involved in the regulation of MyD88-independent TLR4 signalling, where it inhibits LPS-induced IRF3 activation by facilitating the disruption of the TRIF-TRAM complex and the degradation of TLR4 (Doyle et al., 2012). TMED2 binds the PAR-2 receptor and is involved in the regulation of receptor re-sensitization to the plasma membrane after its activation (Luo et al., 2007). TMED2 and TMED10 have also been shown to bind to other GPCRs and may function in a similar manner to that of TMED2 with regard to PAR-2, by controlling receptor trafficking in the biosynthetic pathway and thereby regulating signalling (Luo et al., 2011).

As mentioned previously, the ligand for the ST2L receptor is IL-33 (Schmitz et al., 2005). Many of the proteins involved in the IL-33/ST2L signalling pathway have now been identified. However, as our understanding of immune signalling pathways continues to develop, details of the ST2L signalling pathway and related processes continue to be elucidated. For example, as described in chapter 1, the mechanism by which ST2L protein expression is regulated following ligand binding has recently been revealed (Zhao et al., 2012). This has shed light on a previously unknown element of the ST2L signalling pathway, which is important for the limitation of the signalling pathway after IL-33 ligation. Given that TMED1 interacts with ST2L, this protein may be another

component of the ST2L signalling pathway and could be required for pathway activation or could be involved in the negative regulation of the pathway.

IL-33 has a wide range of target cells, and the ST2L signalling pathway has been implicated in numerous conditions including infection, allergic autoimmune and cardiovascular disease (Liew et al., 2010; Oboki et al., 2010). Therefore, a deeper understanding of this pathway will ultimately contribute to our understanding of the range of disorders in which IL-33 and ST2L have been implicated. Additionally, a fuller understanding of the ST2L pathway may also aid in the identification of molecular targets that mediate proinflammatory signalling by IL-33.

4.2 Results

4.2.1 The effect of IL-33 stimulation on the TMED1-ST2L interaction

As signalling pathways are extremely dynamic processes, some protein interactions which are involved in signalling pathways change with stimulation. For example, TMED7 and TRAM interact basally but LPS stimulation can enhance this interaction (Doyle et al., 2012). On the contrary, TMED2 and TMED10 dissociates from PAR-2 after stimulation with PAR-2 agonists (Luo et al., 2007, 2011). To investigate the effect of IL-33 on the TMED1-ST2L interaction, co-immunoprecipitation experiments were carried out in HEK-293-hST2L cells which had been stimulated with IL-33 for various lengths of time.

Figure 4.1 (top panel, lane 2) demonstrates that the TMED1-ST2L interaction can be observed before IL-33 stimulation. Following stimulation for various time points of up to 2 hours the interaction continues to be observed (Figure 4.1, top panel, lanes 3-8). Interestingly the interaction appears more intense at 30 and 45 minutes following IL-33 stimulation. In this experiment the level of co-immunoprecipitated TMED1 and ST2L is lower following 60 minutes IL-33 stimulation (Figure 4.1, top panel, lane 7), which may be as a result of the lower levels of ST2L detectable in the corresponding whole cell lysate (third panel, lane 7). Lysates were also immunoblotted for IκBα to confirm the responsiveness of these cells and β-actin as a loading control.

Experiments to co-immunoprecipitate endogenous ST2L and TMED1 following IL-33 stimulation were technically very challenging so a conclusive result in these cells proved difficult. Two co-immunoprecipitation assays are shown in Figure 4.2A and 4.2B. The responsiveness of the cells at the time of each experiment was confirmed by probing whole cell lysates for either IκBα or phosphorylated p38 (data not shown). The

TMED1-ST2L interaction is evident in unstimulated cells (Figure 4.2A, lane 2 of the first panel and Figure 4.2B, lane 2 of the first panel). The interaction is also evident after IL-33 stimulation for various lengths of time (Figure 4.2A, top panel lanes 3-5). While the levels of co-immunoprecipitated TMED1 and ST2L were greater following stimulation in the experiment shown in Figure 4.2A (top panel), the same trend was not noted in the experiment shown in Figure 4.2B (top two panels). For this reason, it is difficult to conclude if the endogenous interaction between TMED1 and ST2L is affected by IL-33 stimulation.

Overall these co-immunoprecipitation experiments demonstrate that the TMED1-ST2L interaction is still evident following IL-33 stimulation. While some experiments suggest that the interaction is enhanced after stimulation, it was not possible to conclude that this is definitely the case.

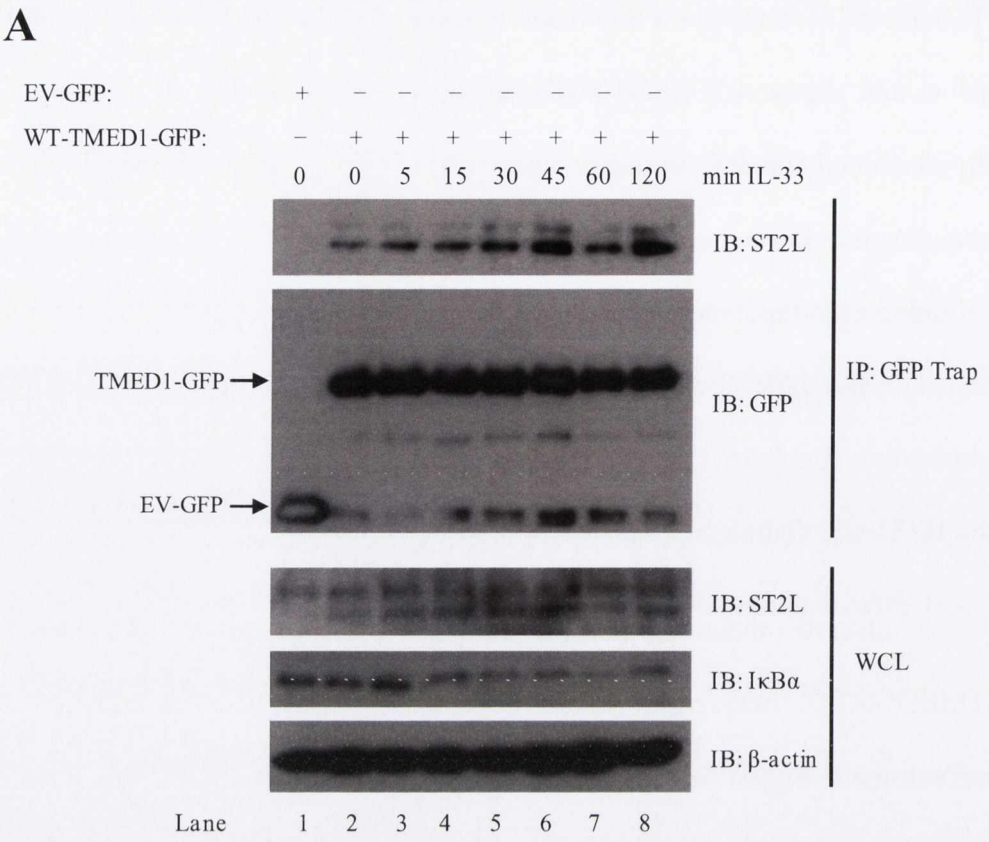


Figure 4.1 The TMED1-ST2L interaction is evident after stimulation with IL-33

HEK-293-hST2L cells were transfected with plasmids encoding EV-GFP or TMED1-GFP. Cells were stimulated with 50 ng/ml IL-33 for the times indicated and samples were immunoprecipitated with anti-GFP Trap® beads. Whole cell lysates (WCL) and immunoprecipitated samples were analysed by Western blot. The immunoblotting antibodies (IB) are listed beside the appropriate blots. Data is representative of three experiments from a total of four independent experiments.

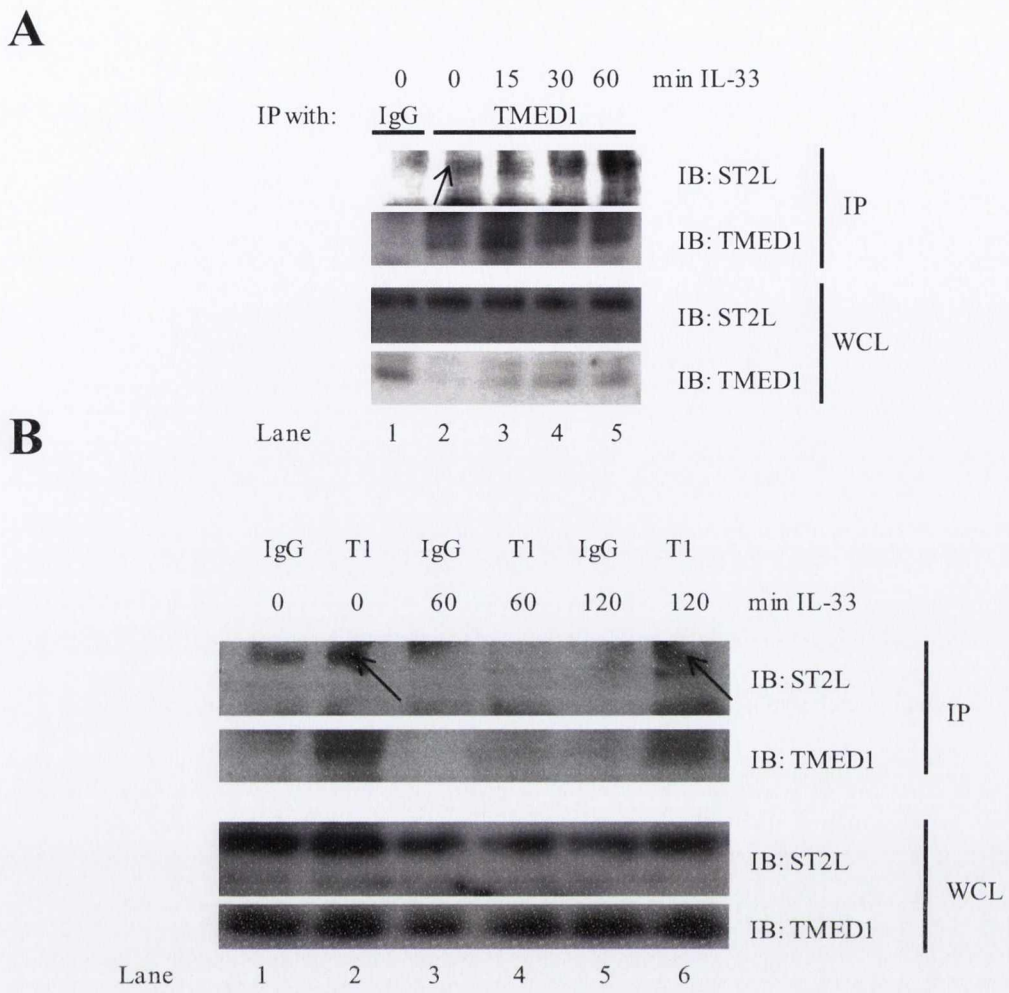


Figure 4.2 The endogenous TMED1-ST2L interaction is evident after stimulation with IL-33

(A) and (B) HMC 1.1 cells were stimulated with 10 ng/ml IL-33 for the times indicated. Cells were lysed, a sample was taken as whole cell lysate and the remainder was immunoprecipitated with anti-rabbit IgG or anti-TMED1 coupled Protein A/G-plus agarose beads. Whole cell lysate (WCL) and immunoprecipitated samples were analysed by Western blot. Immunoblotting antibodies (IB) are shown beside the appropriate blots.

4.2.2 TMED1-GFP dose dependent overexpression in HEK-293T cells

The involvement of TMED1 in IL-33-induced signalling was next investigated. In order to do this, the effect of increasing amounts of TMED1-GFP on IL-33-induced signalling was investigated. To ensure increasing amounts of TMED1-GFP would express in HEK-293T cells, these cells were transfected with increasing amounts of a plasmid encoding TMED1-GFP. As shown in Figure 4.3A, the expression of increasing amounts of TMED1 was confirmed by Western blot using an anti-GFP antibody. Given that the molecular weights of TMED1 and GFP are 25.2 and 27 kDa respectively the bands observed are of the expected combined molecular weight.

A Cytotoxicity Assay was carried out to determine if the overexpression of these amounts of TMED1-GFP was toxic to cells. This assay measures lactate dehydrogenase (LDH), a stable cytoplasmic enzyme which is released following the disruption of membrane integrity. As shown in Figure 4.3B the overexpression of TMED1-GFP did not affect cellular LDH release, and therefore does not induce cell death.

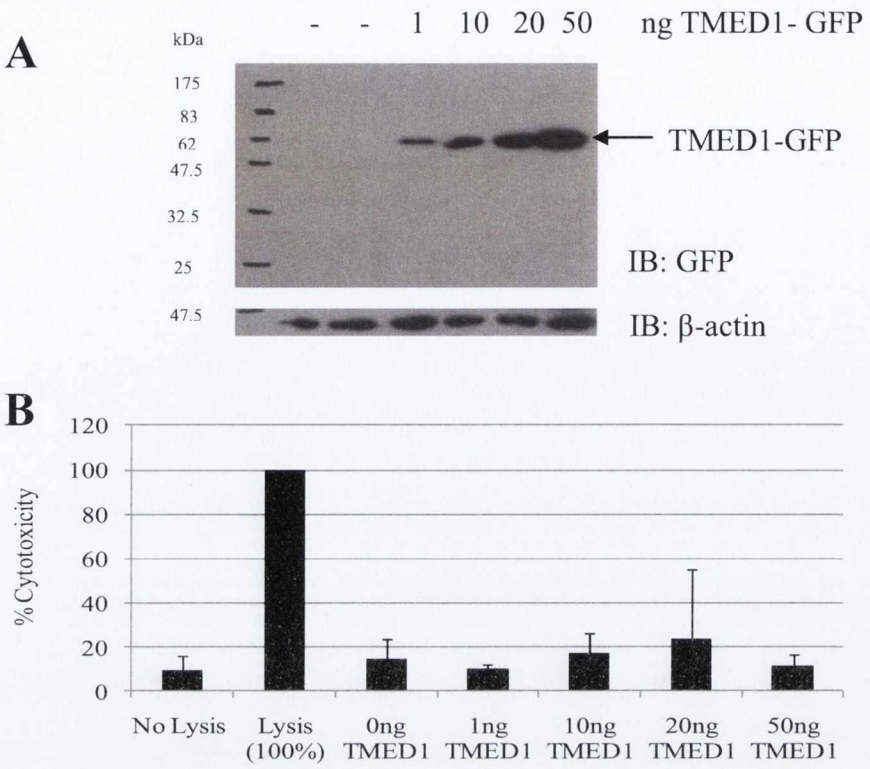


Figure 4.3 TMED1 dose dependent expression in HEK-293T cells can be detected by Western blot analysis and is not cytotoxic to cells

HEK-293T cells were transiently transfected with various amounts of a plasmid encoding TMED1-GFP as shown. With the addition of empty vector (pcDNA) the total amount of DNA per transfection was 220 ng in all cases. (A) Cells were lysed in sample buffer and analysed by Western blotting with anti-GFP and anti-β-actin antibodies. (B) 30 hours after transfection, supernatants were collected and assayed for lactate dehydrogenase. As a representative of maximum cytotoxicity a sample of untransfected cells were lysed, and this group is set as 100 %. Data shown are the mean ± spread of two separate experiments, each one carried out in triplicate.

4.2.3 TMED1 does not affect basal NF-κB, AP-1 or ISRE activity

Prior to the investigation into the effect of TMED1 on the IL-33-induced signalling pathway, the effect of TMED1 on the basal levels of transcription factor activity was assessed. NF-κB and AP-1 activity was assessed as the activation of these transcription factors occurs downstream of IL-33. As TMED7 is involved in the ISRE pathway (Doyle et al., 2012), the effect of TMED1 on its activation was also investigated. TMED1 overexpression did not have any effect on the basal level of NF-κB, AP-1 or ISRE activity. This is in agreement with the observations that TMED7 overexpression does not affect basal NF-κB or ISRE activity (Doyle et al., 2012).

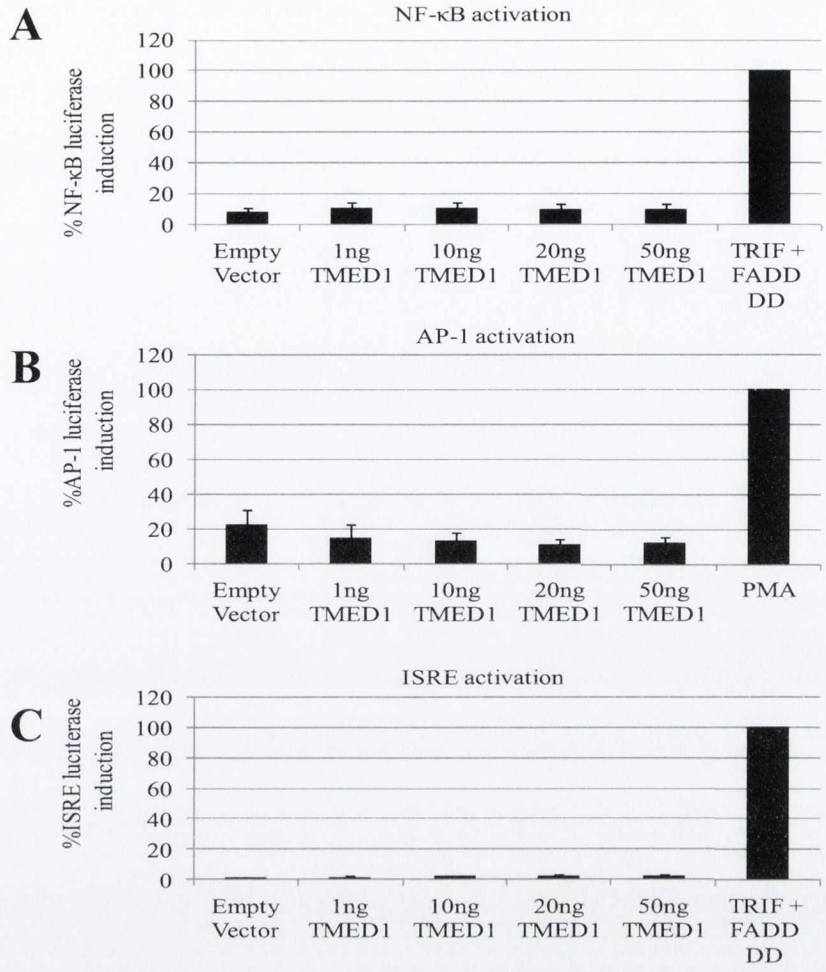


Figure 4.4 TMED1 overexpression does not affect basal NF-κB, AP-1 or ISRE activity

HEK-293T cells were transfected with plasmids encoding 40 ng TK Renilla luciferase and 80 ng NF-κB luciferase (A), 80 ng AP-1 luciferase (B) or 80 ng ISRE luciferase (C) along with increasing amounts of a plasmids encoding TMED1-GFP. For positive controls cells in (A) and (C) were transfected with 5 ng of a plasmid encoding TRIF and 5 ng of a plasmid encoding FADD and cells in (B) were stimluated with 50 ng/ml PMA overnight. The total amount of DNA per transfection was 220 ng in each case with the addition of empty vector (pcDNA). Results are normalised to Renilla luciferase and expressed as percent luciferase induction, representing the mean ± S.E.M of results for five independent experiments, each carried out in triplicate.

4.2.4 Effect of TMED1 on induced luciferase activity

As mentioned previously, IL-33 stimulation leads to the activation of NF-κB and AP-1, therefore experiments were carried out to investigate if the presence of TMED1 had any effect on the activation of these transcription factors following IL-33 stimulation. IL-33 did not induce AP-1 luciferase activity in HEK-293-hST2L cells. However, the AP-1 construct was functional as it was responsive to phorbol 12-myristate 13-acetate (PMA). Therefore it was only possible to examine the effect of TMED1 on IL-33-induced NF-κB luciferase activity. As shown in Figure 4.5A, IL-33-induced NF-κB luciferase activity and the expression of increasing amounts of TMED1 inhibited this activity in a dose dependent manner. In Figure 4.5B, a cell line stably expressing the IL-1 receptor (HEK-293-IL1R1) was used. The overexpression of TMED1 also inhibited IL-1β-induced NF-κB luciferase activity. Similar experiments were also carried out with other cell lines available in the lab, namely HEK-293-MD2-CD14-TLR4, HEK-293-TLR3 and HEK-293T cells, which express the receptors for lipopolysaccharide (LPS), polyinosinic-polycytidylic acid (PolyI:C) and tumor necrosis factor alpha (TNF-α) respectively. Results with these cells lines are shown in Figure 4.6. The overexpression of TMED1 resulted in an inhibition of luciferase activity with each of the ligands tested.

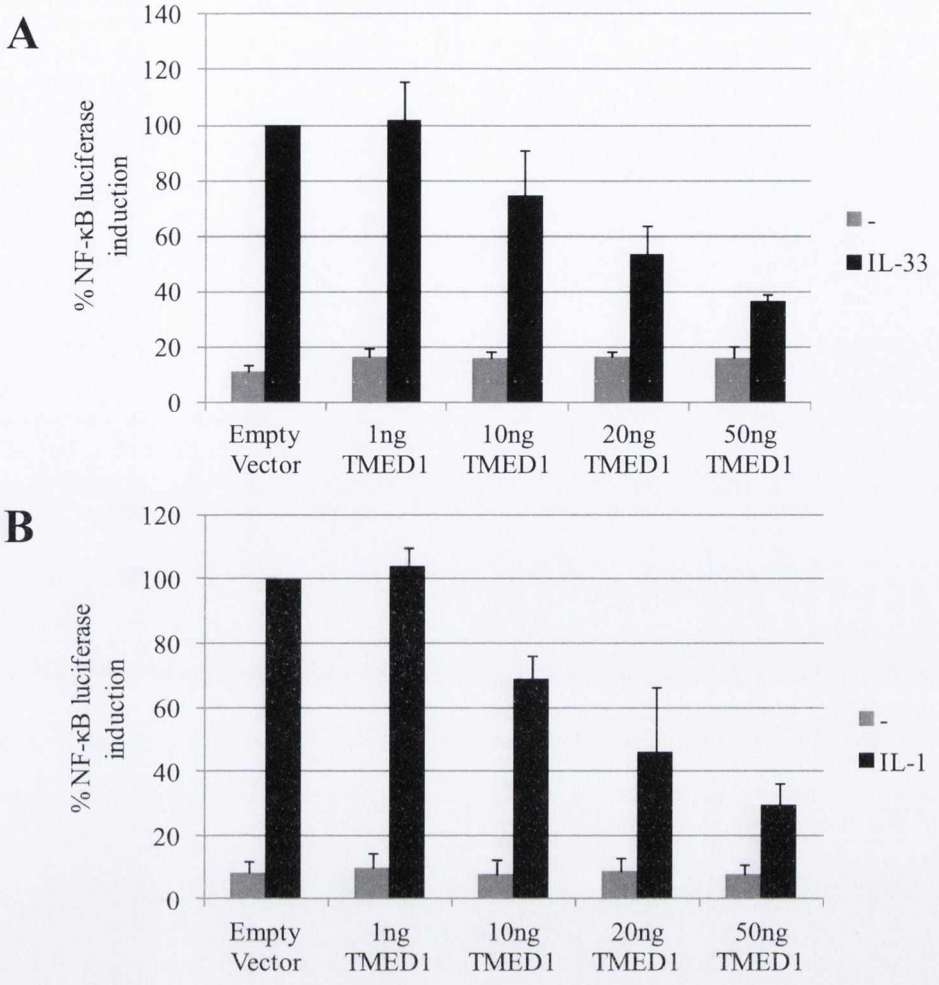


Figure 4.5 TMED1 overexpression inhibits IL-33 and IL-1-induced NF-κB luciferase

HEK-293-hST2L cells (A) or HEK-293-IL1R1 cells (B) were transfected with plasmids encoding 80 ng NF-κB luciferase and 40 ng TK Renilla luciferase along with increasing amounts of a plasmid encoding TMED1-GFP as shown. With the addition of empty vector (pcDNA) the total amount of DNA per transfection was 220 ng. 24 hours following transfection cells were stimulated with 50 ng/ml IL-33 (A) or 100 ng/ml IL-1β (B) for 6 hours. Lysates were then assayed for luciferase activity. Results are normalised to Renilla luciferase and expressed as percent NF-κB luciferase induction, representing the mean ± S.E.M of results for five independent experiments (A) or three independent experiments (B), each carried out in triplicate..

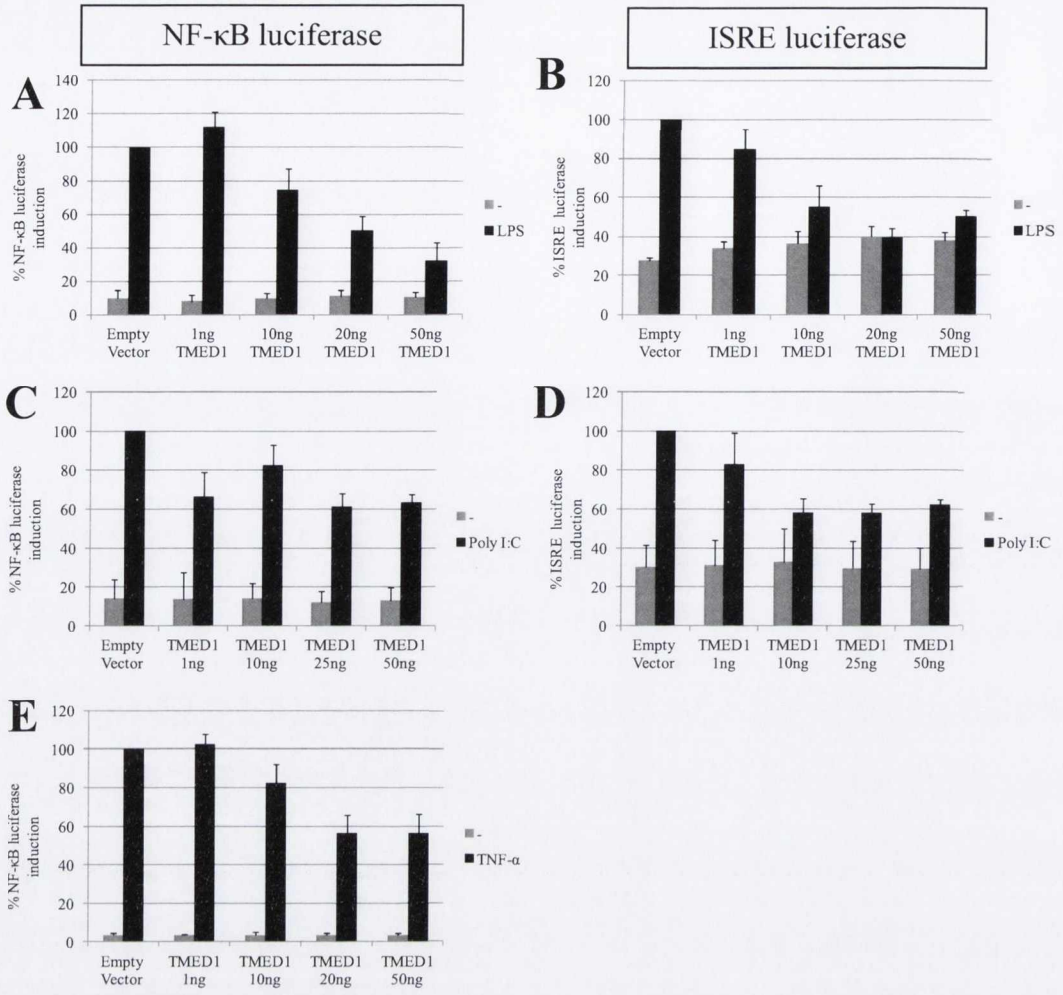


Figure 4.6 TMED1 overexpression inhibits LPS, PolyI:C and TNF-α-induced NF-κB luciferase as well as LPS and Poly I:C-induced ISRE luciferase

HEK-293-MD2-CD14-TLR4 cells (A and B), HEK-293-TLR3 cells (C and D) or HEK-293T (E) cells were transfected with plasmids encoding 80 ng NF-κB luciferase (A, C and E) or 80 ng ISRE luciferase (B, D), 40 ng TK Renilla luciferase and increasing amounts of a plasmid encoding TMED1-GFP as shown. With the addition of empty vector (pcDNA) the total amount of DNA per transfection was 220 ng. Cells were stimulated with LPS at 1 μg/ml overnight (A and B), Poly I:C at 25 μg/ml overnight (C and D) or TNF-α at 100 ng/ml for 6 hours (E). Lysates were then assayed for luciferase activity. Results are normalised to Renilla luciferase and expressed as percent luciferase induction, representing the mean ± S.E.M of results for three independent experiments, each carried out in triplicate.

4.2.5 The effect of TMED1 on p65-induced luciferase activity

Next, NF-κB luciferase activity was induced by p65 overexpression. p65 is a downstream component of the NF-κB pathway and part of the NF-κB transcription complex. Figure 4.7A shows that TMED1-GFP was also capable of inhibiting p65-induced luciferase activity. Considering TMED1-GFP was able to inhibit luciferase activity from each of the ligands examined as well as p65-induced NF-κB luciferase activity it suggested a possible non-specific effect. Since TMED1 was tagged to GFP, the effect could be due to this tag. To investigate if this was the case, a myc tagged TMED1 construct was also used to see if this inhibits NF-κB-induced luciferase activity. Figure 4.7B demonstrates that TMED1-myc can also inhibit p65-induced NF-κB luciferase activity. This demonstrates that the observed inhibitory effect of overexpressed TMED1 is not due to either the GFP or myc tags as both constructs were able to inhibit p65-induced NF-κB luciferase activity to a similar extent.

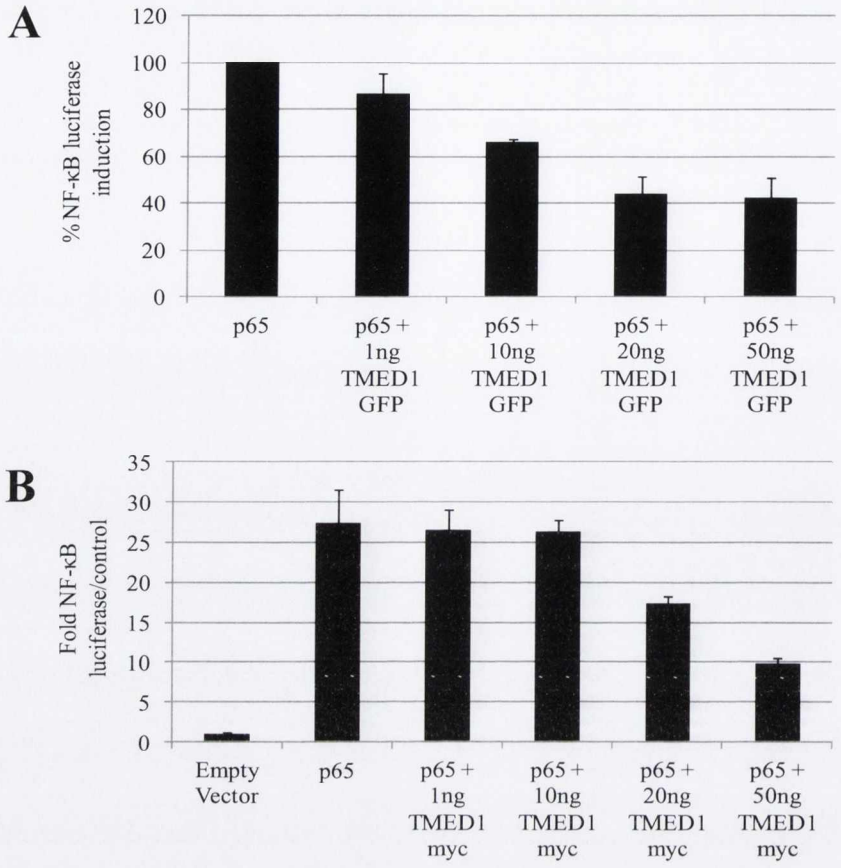


Figure 4.7 The observed inhibition of TMED1 in luciferase experiments is not a result of the GFP tag

HEK-293T cells were transfected with plasmids encoding 80 ng NF-κB luciferase, 40 ng TK Renilla luciferase and 10 ng p65 along with increasing amounts of a plasmid encoding TMED1-GFP (A) or TMED1-myc (B). With the addition of empty vector (pcDNA) the total amount of DNA per transfection was 220 ng. 24 hours following transfection cell lysates were assayed for luciferase activity. Results in (A) are normalised to Renilla luciferase and expressed as percent luciferase induction, representing the mean ± S.E.M of results for three independent experiments, each carried out in triplicate. Results in (B) are normalised to Renilla luciferase and presented relative to the activity in unstimulated empty vector transfected cells, which is set as 1.

4.2.6 The effect of TMED1 overexpression on IL-33-induced IL-8 production

The effect of TMED1 overexpression on IL-33-induced IL-8 production was also investigated. This is a means to further investigate the observed inhibitory effect of TMED1 noted in the luciferase assays. The IL-8 promoter contains NF-κB binding sites and stimulation results in the recruitment of NF-κB subunits to the IL-8 promoter (Hoffmann et al., 2002). Therefore, if TMED1 is truly inhibiting NF-κB activity following IL-33 stimulation, a reduction in IL-33-induced IL-8 production would be observed in the presence of TMED1. Figure 4.8A shows that a dose dependent increase in TMED1-GFP levels did not inhibit IL-8 production. Whole cell lysates were blotted for TMED1-GFP to confirm that TMED1 has been expressed in a dose dependent manner. As shown in Figure 4.8B, TMED1-GFP can be detected in the lysates as expected.

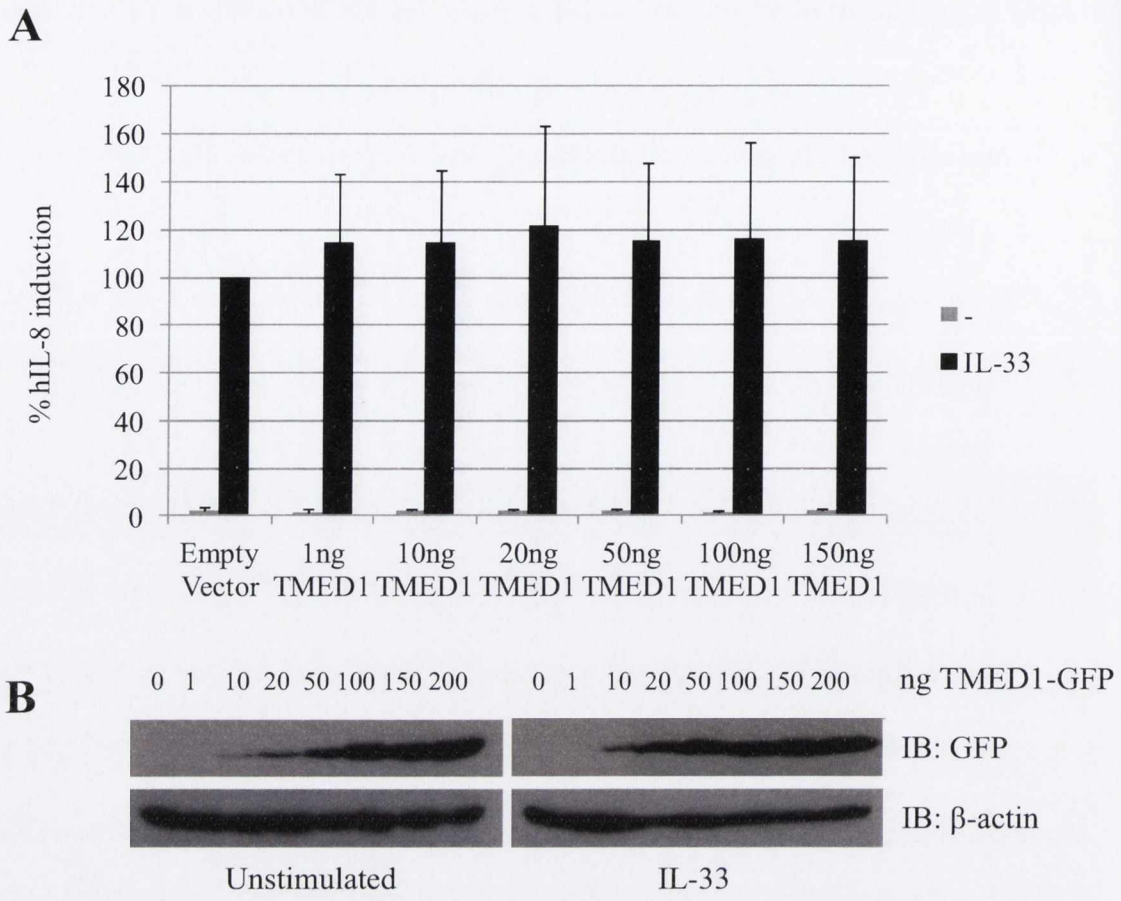


Figure 4.8 TMED1 overexpression does not affect IL-8 production in response to IL-33 in HEK-293-hST2L cells

HEK-293-hST2L were transfected in triplicate with increasing amounts of a plasmid encoding TMED1-GFP as shown. In all cases the total amount of DNA per transfection was 200 ng with the addition of empty vector pcDNA. 24 hours following transfection, cells were stimulated with 50 ng/ml IL-33 for 24 hours. (A) Supernatants were then collected and analysed for IL-8 levels by ELISA. Results are represented as percent IL-8 induction and represent the mean ± S.E.M of results for three independent experiments, each one carried out in triplicate. (B) Expression levels of TMED1-GFP were analysed by western blotting and a representative blot is shown.

4.2.7 Luciferase assays following knockdown of TMED1

To further investigate the inhibitory effect of overexpressed TMED1 in luciferase assays, additional luciferase experiments were carried out. In these luciferase assays, TMED1 was knocked down. PCR was firstly carried out to confirm that the HEK-293-hST2L cell line expressed endogenous TMED1 (Figure 4.9). Next, optimisation of TMED1 knockdown by siRNA was carried out. A knockdown time of 48 hours was selected when the siRNA optimisation experiments were carried out. 5 nM, 10 nM or 50 nM siRNA all resulted in similar TMED1 knockdown, as determined using RT-PCR (Figure 4.10) and a final concentration of 5 nM siRNA was selected for use in further experiments. For the luciferase experiments cells were set up at 7.5 x 10^4 cells/ml and transfected with siRNA oligos 24 hours later. 24 hours later cells were transfected with luciferase constructs and allowed to rest for a further 24 hours, before a 6 hour stimulation with IL-33. The luciferases carried out with siRNA No1 and No2 (Figure 4.11 top panel) are a representative of 5 experiments. With siRNA construct No1, a marginal boost in luciferase activity was observed each time. However, knockdown with siRNA oligo No2 generally inhibited the luciferase activity (4 out of 5 times), but again this was not statistically significant. Experiments carried out with siRNA oligos No3 and No4 (Figure 4.11 bottom panel) are a representative of 2 experiments. In the experiment shown above knockdown of TMED1 did not result in an effect on NF-κB luciferase activity. The second time these oligos were used, a boost in luciferase activity was observed with only one of the oligos while no change was noted in the other case, even though the resulting level of knockdown was very similar in both cases. In conclusion, the measurement of NF-κB luciferase activity was not a good readout for determining the role of TMED1 in IL-33 signalling, with TMED1 overexpression somehow inhibiting luciferase.

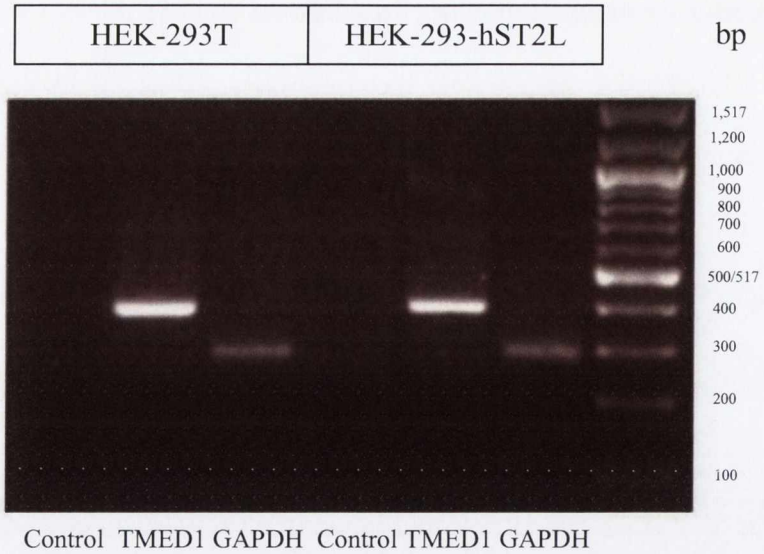


Figure 4.9 TMED1 mRNA can be detected in HEK-293T and HEK-293-hST2L cell lines

RNA was extracted from HEK-293T, HEK-293-hST2L and cDNA was generated. PCR reactions were carried out using primers for human TMED1. GAPDH primers were used as a positive control while the control reaction lacked primers. The expected TMED1 and GAPDH products are 389 and 284 base pairs (bp) respectively.

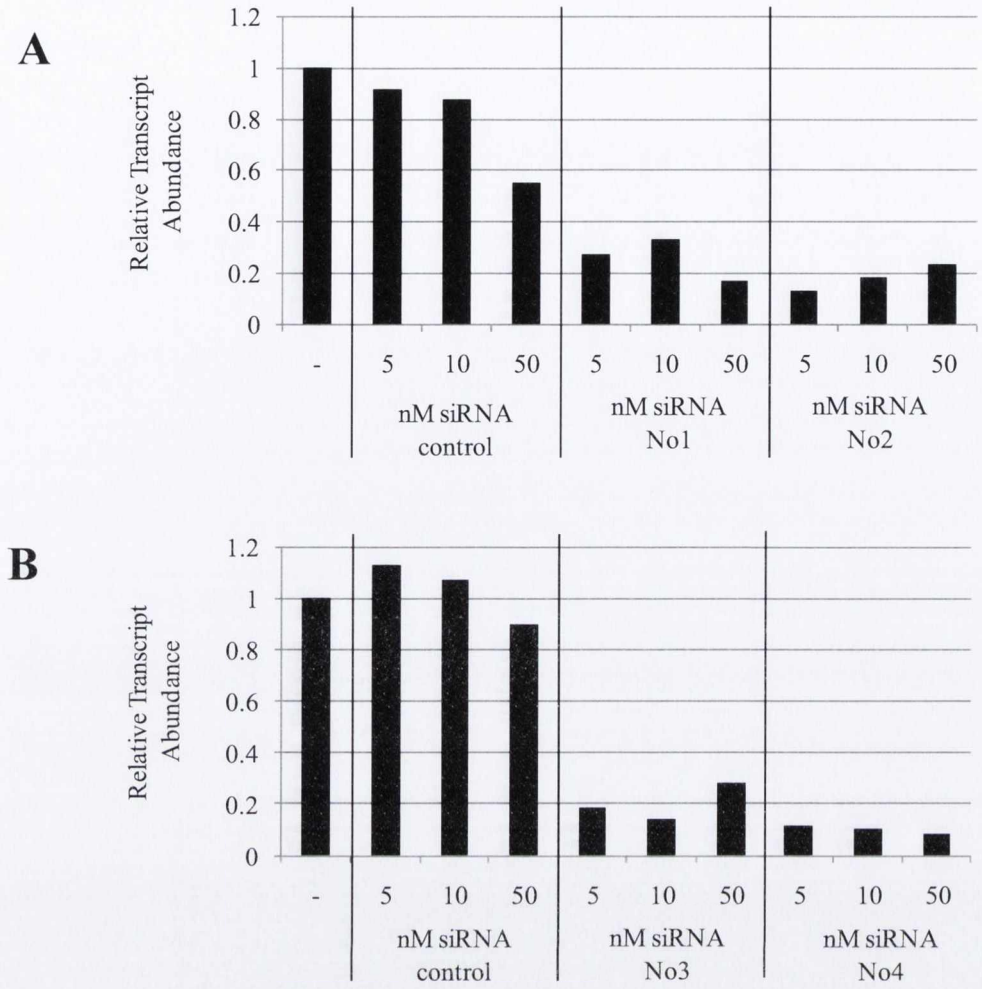


Figure 4.10 Optimisation of TMED1 knockdown in HEK-293-hST2L cells

HEK-293-hST2L cells were transfected with siRNA from Qiagen (A) or Dharmacon (B) to final concentrations of 5 nM, 10 nM or 50 nM as indicated. 48 hours later RT-PCR was carried out to determine the level of knockdown. TMED1 expression is normalised to GAPDH and is presented relative to that of samples which did not include any siRNA, set as 1.

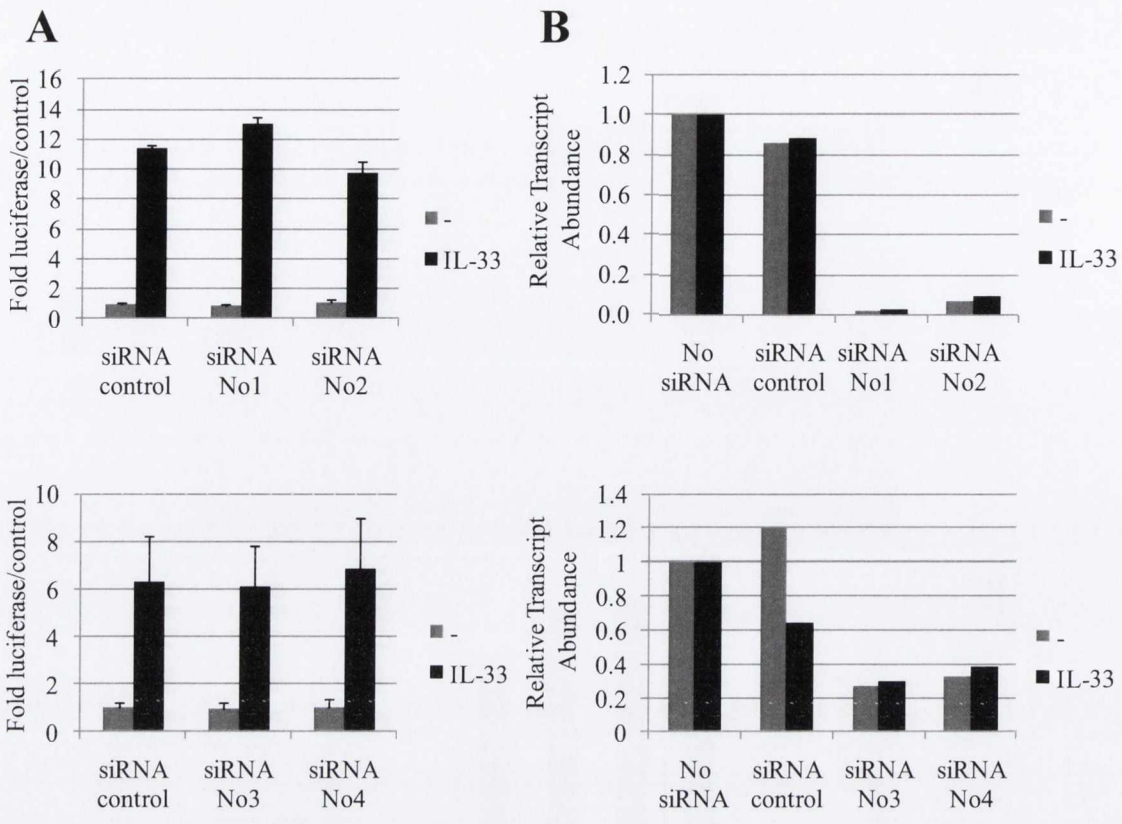


Figure 4.11 TMED1 knockdown does not affect IL-33-induced NF-κB luciferase

(A) HEK-293-hST2L cells were transfected with TMED1 siRNA to a final concentration of 5 nM. 24 hours later they were transfected with 280 ng of a plasmid encoding NF-κB luciferase and 140 ng of a plasmid encoding TK Renilla luciferase. A further 24 hours later, cells were stimulated with 50 ng/ml IL-33 for 6 hours. Lysates were then assayed for NF-κB luciferase activity (left panel). Results are normalised to Renilla luciferase and presented relative to the activity in siRNA control transfected cells, which is set as 1. Error bars represent standard deviation. Luciferases carried out with siRNA No1 and No2 are a representative of 5 experiments, while those carried out with siRNA No3 and No4 are a representative of 2 experiments. (B) Additional samples were analysed by RT-PCR for knockdown. Expression is normalised to GAPDH and is presented relative to that of samples which did not include any siRNA, set as 1.

4.2.8 TMED1 knockdown impairs IL-33-induced responses

As luciferase assays were proving somewhat inconsistent IL-33-induced responses were also analysed by Western blotting analysis. TMED1 protein levels were reduced in HEK-293-hST2L cells by siRNA mediated mRNA knockdown. These cells were then stimulated with IL-33 for time courses of up to two hours. Western blotting confirms that both siRNA No1 and siRNA No2 knockdown TMED1 at the protein level efficiently (Figure 4.12, lanes 7-12 and 19-24). In agreement with the results shown in Figure 4.11, knockdown of TMED1 does not affect IL-33-induced NF-κB activation, as the degradation of IκBα occurs to a similar extent in cells which received Negative control siRNA or TMED1 targeted siRNA (Figure 4.12, compare panel one lanes 1-6 with 7-12 and lanes 13-18 with 19-24). However, the knockdown of TMED1 does impair IL-33-induced phosphorylation of pERK and p38 (Figure 4.12, second and third panels). This effect is particularly evident when knocking down TMED1 using siRNA No2. The phosphorylation of JNK was also assessed in these experiments; however a consistent difference between pJNK in Negative control siRNA and TMED1 siRNA treated samples was not evident.

IL-33-induced IL-8 levels were also examined following TMED1 knockdown in HEK-293-hST2L cells. Following TMED1 knockdown, cells were stimulated with IL-33 at 20 or 40 ng/ml for 8 or 24 hours. Figure 4.13 shows that knockdown of TMED1 results in reduced levels of IL-8 production following IL-33 stimulation for either 8 or 24 hours for both of these concentrations. While the difference in IL-33-induced IL-8 production is significant in each case between the Negative control siRNA and TMED1 siRNA No2, the reduction in IL-33-induced IL-8 was also evident, albeit to a lesser degree with TMED1 siRNA No1. Stimulations were also carried out with IL-33 at a

concentration of 50 ng/ml, however reduced IL-8 production was not consistently observed at this dose. Higher doses of IL-33 are likely to drive pathway activation to a greater extent, perhaps overcoming or masking the need for TMED1 for IL-8 production.

To determine if the effect of TMED1 knockdown was specific for the IL-33/ST2L pathway, TMED1 was knocked down in THP-1 cells. Figure 4.14 demonstrates that TMED1 targeted siRNA at both 50 nM and 100 nM results in reduced levels of TMED1 protein in THP-1 cell lysates. Following TMED1 knock down, THP-1 cells were stimulated with LPS for 24 hours and IL-8 supernatant levels were assessed. Figure 4.14 demonstrates that reduction of TMED1 levels does not impair LPS-induced IL-8 production, suggesting specificity for the IL-33/ST2L signalling pathway.

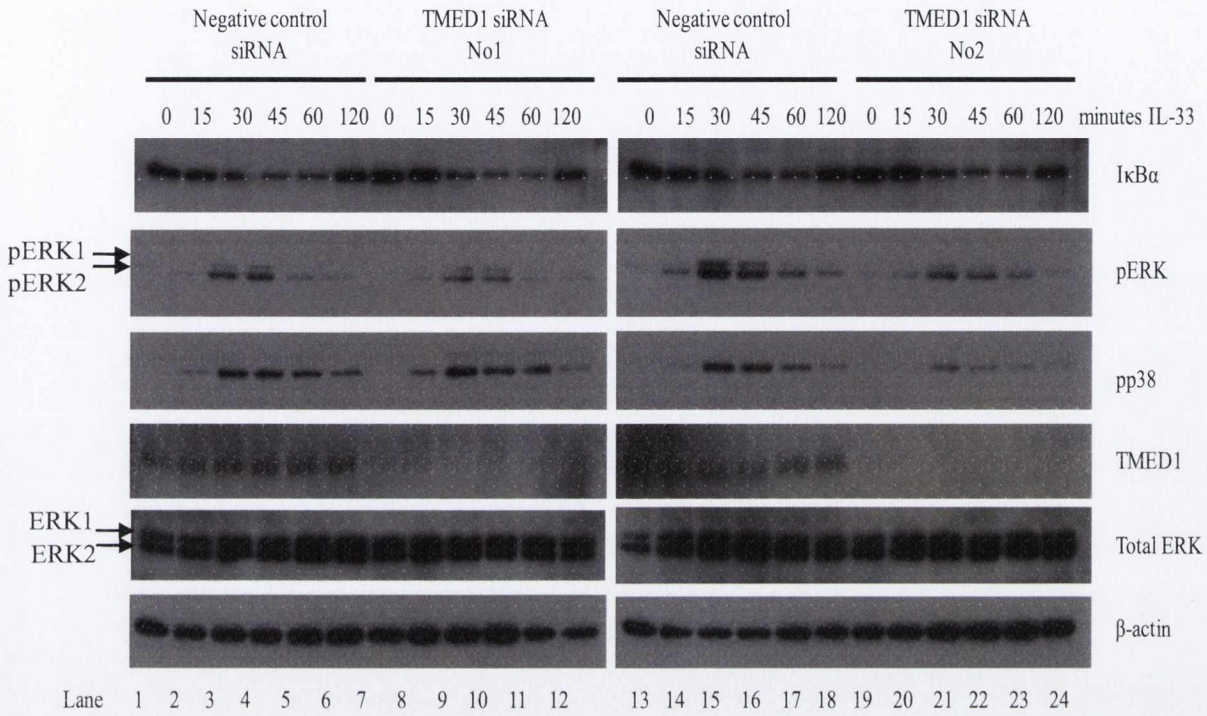


Figure 4.12 TMED1 is needed for optimal IL-33-induced responses

HEK-293-hST2L cells were transfected with control siRNA or TMED1 targeted siRNA (No1 and No2). 48 hours following transfection, cells were stimulated with IL-33 (50 ng/ml) for the times shown and samples were analysed by Western blotting. Immunoblotting (IB) antibodies are shown beside the appropriate blot. Data is representative of three independent experiments.

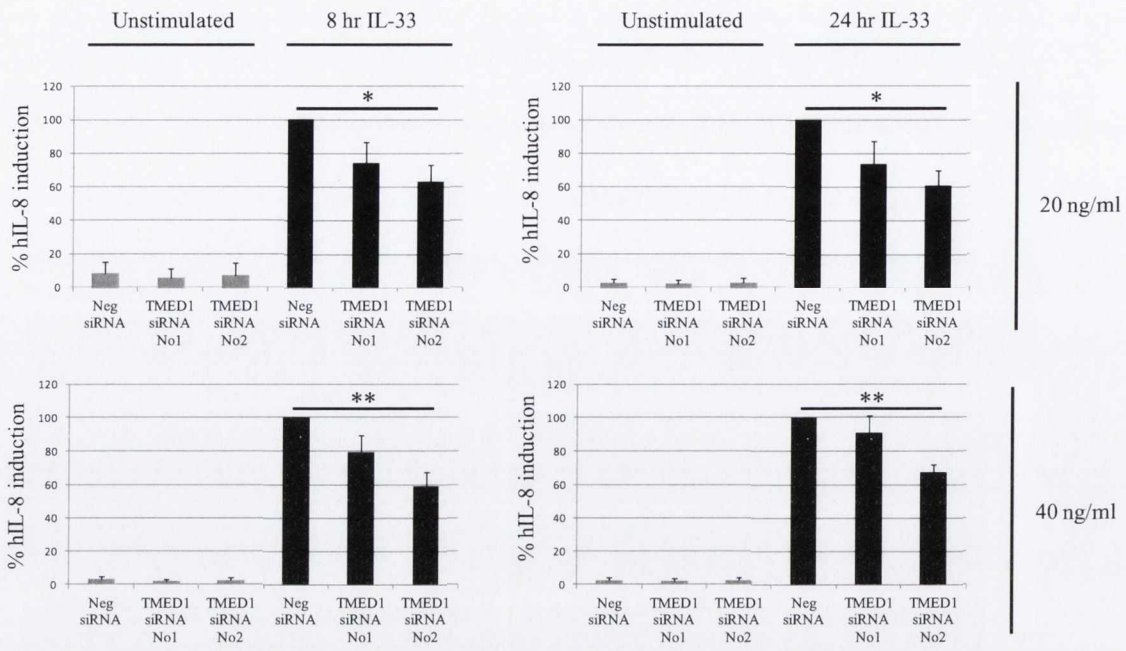


Figure 4.13 TMED1 is required for optimal IL-33-induced IL-8 production

HEK-293-hST2L cells were transfected with negative control siRNA, TMED1 siRNA No1 or TMED1 siRNA No2 to a final concentration of 5 nM. 48 hours following transfection cells were stimulated with 20 or 40 ng/ml IL-33 for 8 or 24 hours as shown. Supernatants were then analysed for IL-8 levels by ELISA. Results are expressed as percent IL-8 induction and represent the mean ± S.E.M of results for three independent experiments, each carried out in triplicate. *, $p < 0.05$ **, $p < 0.01$.

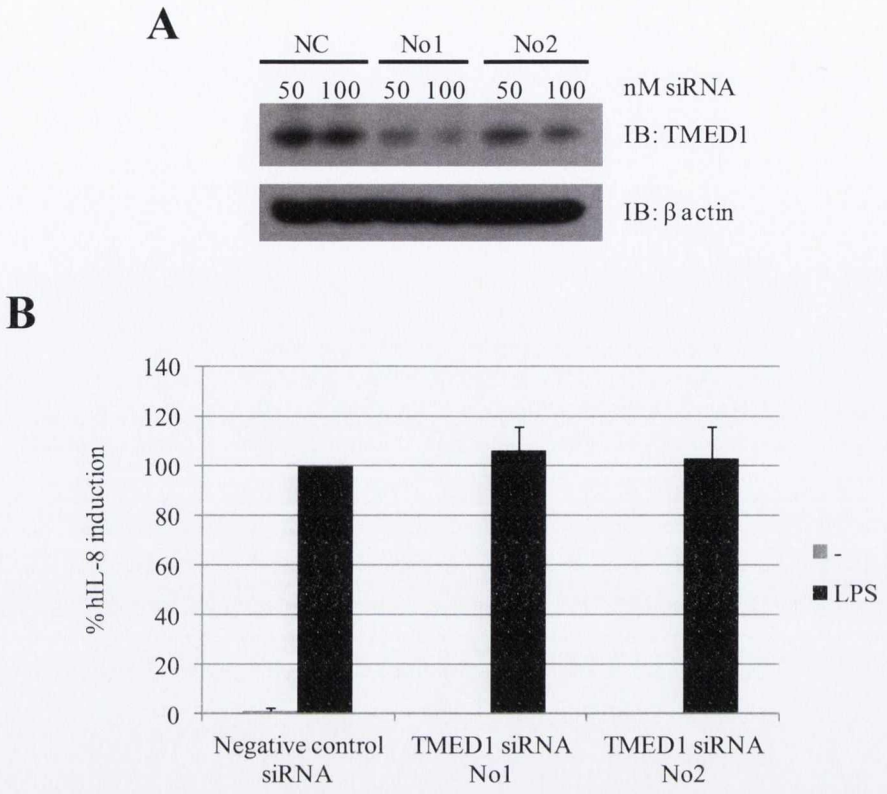


Figure 4.14 TMED1 knockdown in THP-1 cells

(A) THP-1 cells were transfected with 50 or 100 nM Negative Control siRNA (NC) or TMED1 targeted siRNA (No1 and No2). Cell lysates were analysed by Western blotting. Immunoblotting (IB) antibodies are shown beside the appropriate blot. (B) THP-1 cells were transfected with negative control siRNA or TMED1 targeted siRNA (No1 and No2). Cells were unstimulated or stimulated with LPS (100 ng/ml) for 24 hours. Supernatants were analysed for IL-8 levels by ELISA. Results are expressed as percent IL-8 induction and represent the mean ± S.E.M of results for three independent experiments, each carried out in triplicate.

4.2.9 IL-33 is internalised in a time dependent manner

IL-1β and its receptor IL-1R are known to get internalised following the association of ligand and receptor. To determine if IL-33 gets internalised this ligand was labelled with a dye which fluoresces at 647 nm so that its localisation could be monitored by confocal microscopy. Labelling of IL-33 was carried out using a protein labelling kit from Invitrogen™. Figure 4.15A demonstrates that HEK-293-hST2L cells do not bind fluorescent dye alone, while binding of labelled IL-33 to cells at both 10 and 30 minutes post stimulation was observed. To confirm that the reactivity of IL-33 was not affected by the bound fluorescent dye, cells were stimulated with unlabelled or labelled IL-33 for various time points and samples were analysed by Western blotting. Figure 4.15B demonstrates that HEK-293-hST2L cells respond similarly to both unlabelled and labelled IL-33, as the phosphorylation of p38 and degradation of IκBα occur to the same extent and at the same time points regardless of the absence or presence of the attached fluorescent dye. This demonstrates that the activity of the ligand is not affected by the presence of the dye.

Next, HEK-293-hST2L cells were stimulated with IL-33-647 for varying lengths of time. Live cells were viewed using an Olympus FV1000 Confocal Microscope. Figure 4.16 demonstrates that 5 minutes post stimulation IL-33 can bind to the plasma membrane (white arrows). Plasma membrane bound IL-33-647 continues to be observed at later time points. However, an increasing amount of IL-33-647 becomes internalised over time (Figure 4.16, orange arrows).

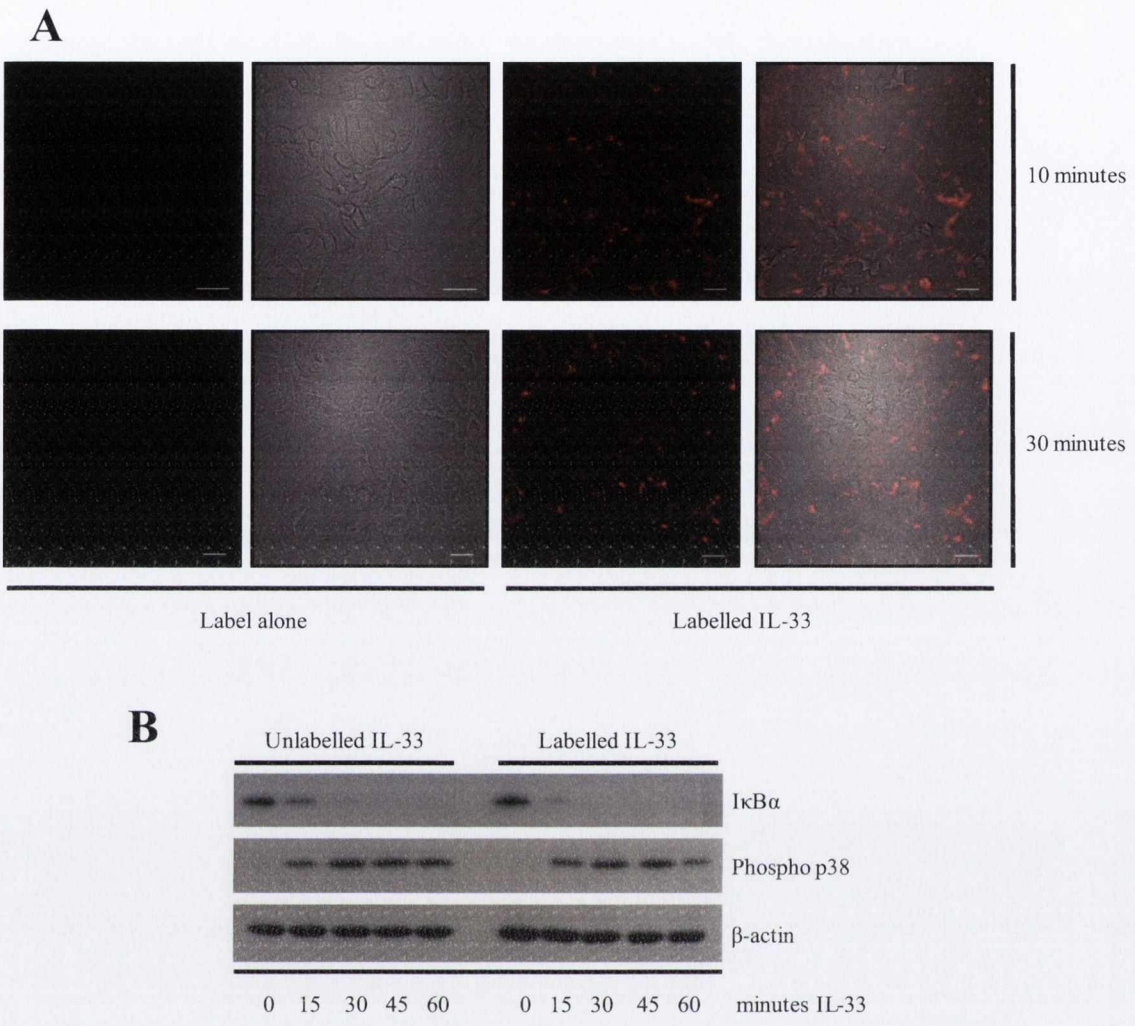


Figure 4.15 HEK-293-hST2L cells bind labelled IL-33 and the response to labelled IL-33 is comparable to unlabelled IL-33

(A) HEK-293-hST2L cells were set up on Poly-L-Lysine coated slides. Three days later they were stimulated with Alexa-647 label alone or Alexa-647 labelled IL-33 for 10 or 30 minutes. Cells were fixed, mounted onto coverslides and viewed using an Olympus FV1000 Confocal Microscope. Results are representative of at least five different images for each condition. Scale bars represent 10 μM. (B) HEK-293-hST2L cells were stimulated with 50 ng/ml unlabelled or labelled IL-33 for the times shown. Samples were analysed by Western blotting. Immunoblotting antibodies are shown beside the appropriate blot.

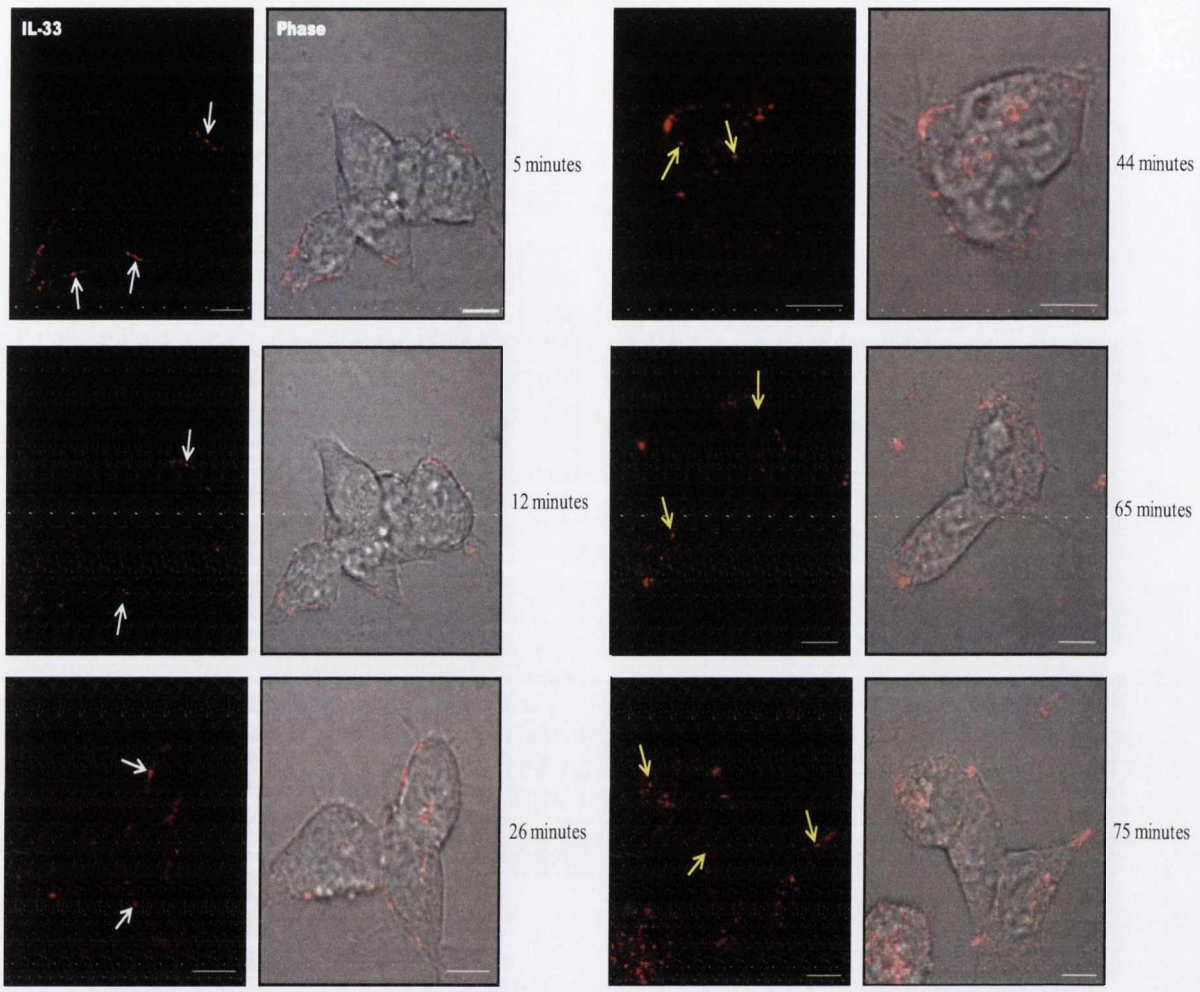


Figure 4.16 IL-33 gets internalised in a time dependent manner

Live HEK-293-hST2L cells were stimulated with fluorescently labelled IL-33 for the times indicated and cells were viewed with an Olympus FV1000 Confocal Microscope. White arrows show plasma membrane associated IL-33. Orange arrows show internalised IL-33. Results are representative of three experiments, in which a minimum of 13 cells were analysed over the duration of each time course. Scale bars represent 10 μM.

4.2.10 IL-33 is internalised into compartments surrounded by TMED1

As mentioned previously, the related TMED family member, TMED7 has been investigated with regard to LPS signalling. Following LPS stimulation TMED7 traffics from the Golgi into maturing endosomes (Doyle et al., 2012). The effect of IL-33 on the localisation of TMED1 was investigated. IL-33-647 was also used for these experiments. Figure 4.17 again demonstrates that IL-33 is internalised in a time dependent manner. Figure 4.17 shows IL-33 along the plasma membrane (second panel, white arrows). 30 minutes post stimulation, IL-33 can still be seen along the plasma membrane (Figure 4.17, white arrows), however a portion of IL-33 has been internalised (orange arrows). Interestingly, IL-33 is internalised into vesicles surrounded by TMED1 (Figure 4.17, third panels, orange arrows). Internalised IL-33 in TMED1 surrounding vesicles is still evident 60 minutes post simulation (Figure 4.17, fourth panels, orange arrows).

With stimulation the pattern of TMED1 localisation appears to change. Prior to IL-33 stimulation, TMED1 has a reticular pattern which is also apparent 10 minutes post stimulation (Figure 4.17, first and second panels). Following IL-33 stimulation, TMED1 localisation shows a gradual change to a more vesicular like patterning (Figure 4.17, third and fourth panels). The compartments which TMED surrounds are possibly maturing endosomes generated following IL-33 stimulation, similar to those which TMED7 moves to after LPS treatment (Doyle et al., 2012).

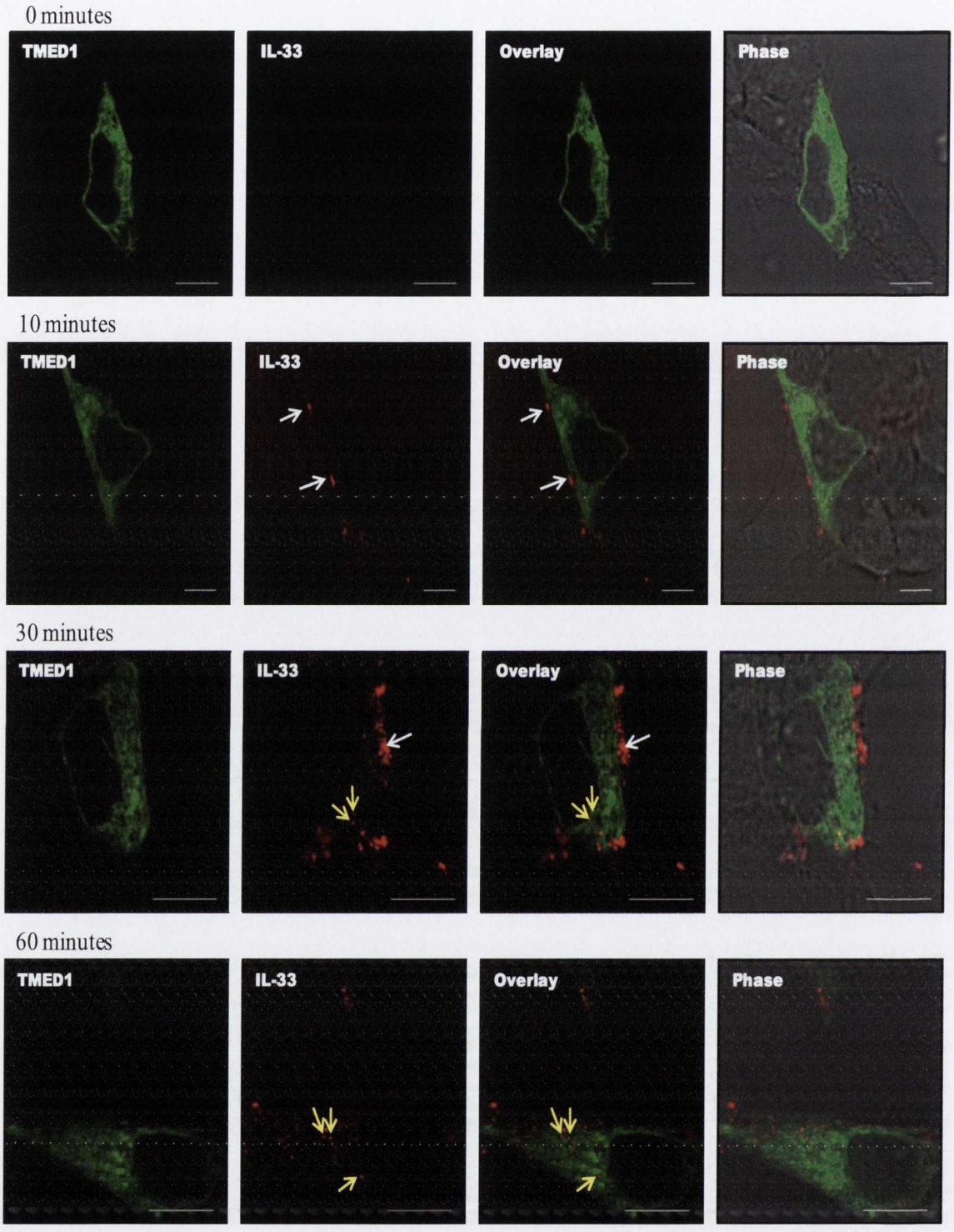


Figure 4.17 IL-33 gets internalised in a time dependent manner to compartments surrounded by TMED1

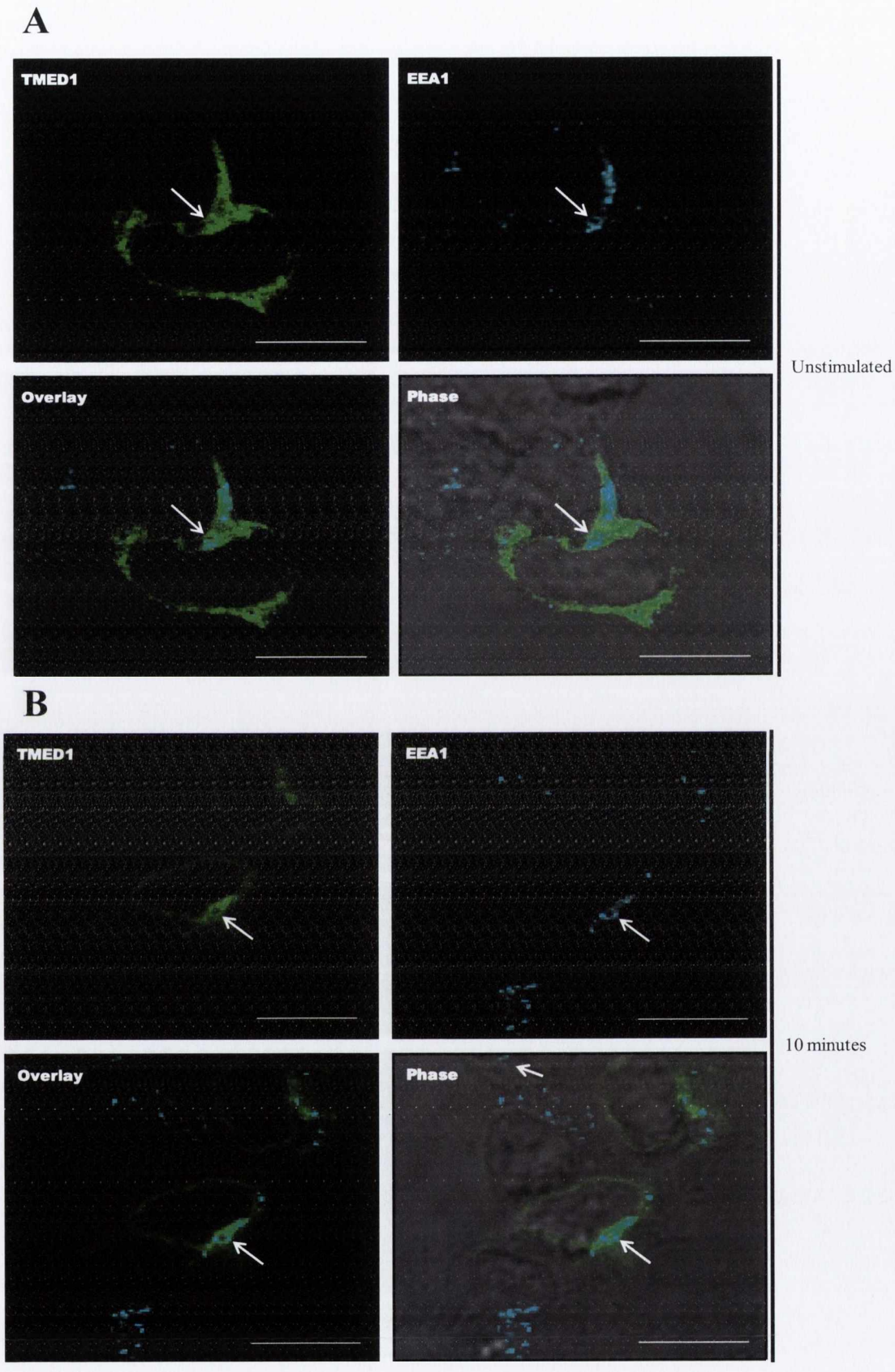
Figure 4.17 IL-33 gets internalised in a time dependent manner to compartments surrounded by TMED1

HEK-293-hST2L cells transfected with TMED1-GFP were stimulated with IL-33-647 (150 ng/ml) for the times shown. Following stimulation cells were fixed and viewed using an Olympus FV1000 Confocal Microscope. Data is representative of three independent experiments in which a total of 67 cells were analysed, with a minimum of 12 cells per time point. TMED1-GFP and IL-33-647 are shown in green and red respectively. White arrows show plasma membrane associated IL-33. Orange arrows show internalised IL-33. Scale bars inducate 10 μM.

4.2.11 Enhanced localisation of TMED1 at endosomes after IL-33 stimulation

The pattern of TMED1 appeared to alter with IL-33 stimulation, changing from a more reticular pattern to a pattern in which a greater amount of the protein surrounded vesicles. TMED1 has been shown to localise to early endosomes (Figure 3.5). Therefore, the effect of IL-33 on the co-localisation of TMED1 and EEA1 was investigated. Figure 4.18 (panel A) shows that TMED1 and EEA1 co-localise in the absence of ligand. Interestingly, with stimulation of IL-33, the co-localisation of TMED1 and EEA1 is more evident (Figure 4.18, panel B, C and D), particularly at 30 minutes post stimulation (Panel C).

The effect of IL-33 stimulation on the association between TMED1 and EEA1 was also investigated using co-immunoprecipitation assays. Figure 4.19 demonstrates that following IL-33 stimulation the interaction between EEA1 and TMED1 is enhanced. While an interaction is evident prior to stimulation (Figure 4.19, lane 2), the intensity of the band is increased in lane 3, following 5 minutes IL-33 treatment. The interaction appears to be enhanced transiently and reduced at later time points. Other experiments which were carried out also showed an enhanced interaction between TMED1 and EEA1 following IL-33 stimulation, at 5, 15 and 30 minutes IL-33 stimulation. Overall, these results validate those obtained by confocal analysis, demonstrating an enhanced transient association between TMED1 and EEA1 after IL-33 stimulation.


A
TMED1
EEA1
Overlay
Phase
Unstimulated
B
TMED1
EEA1
Overlay
Phase
10 minutes

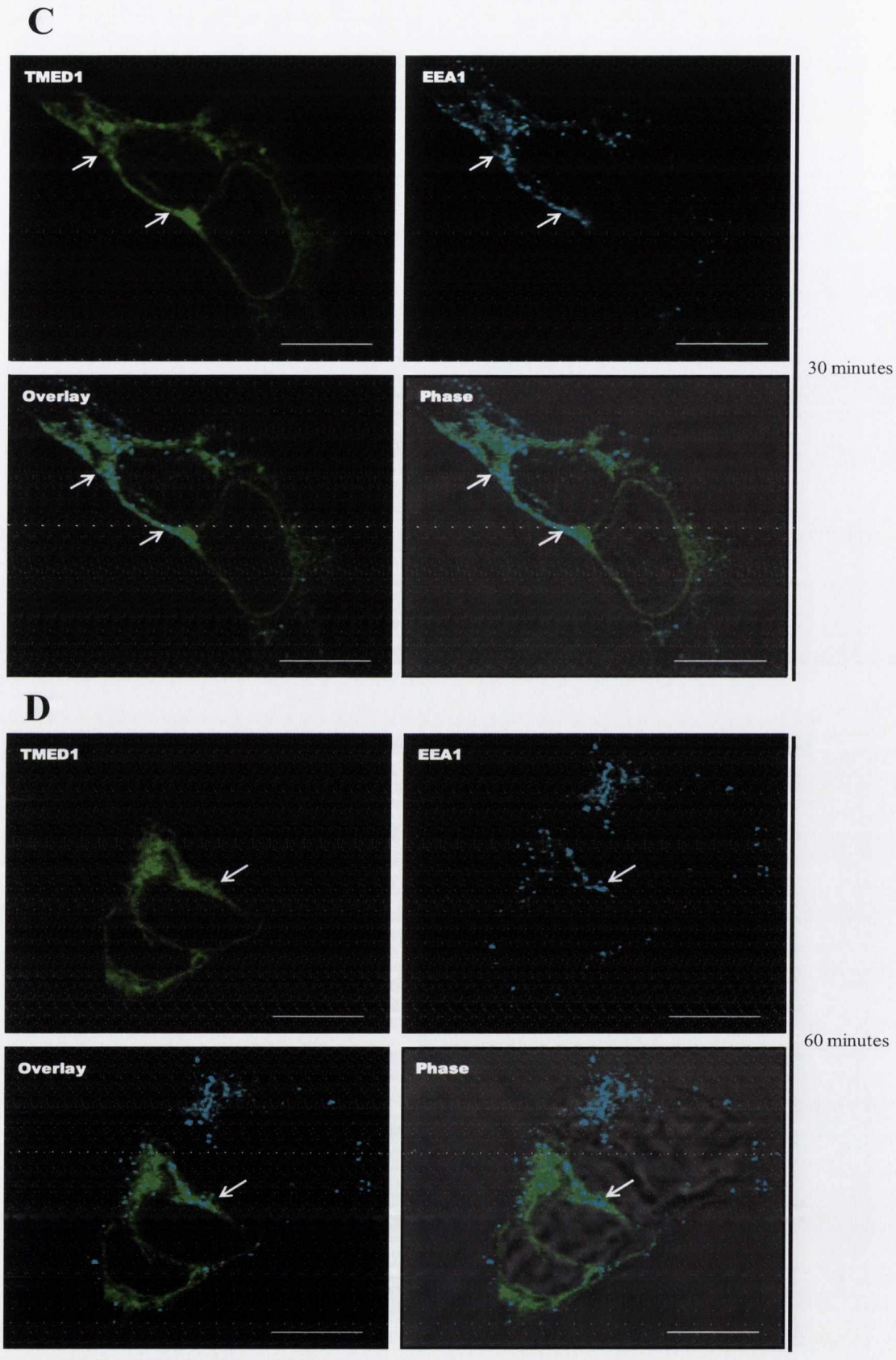
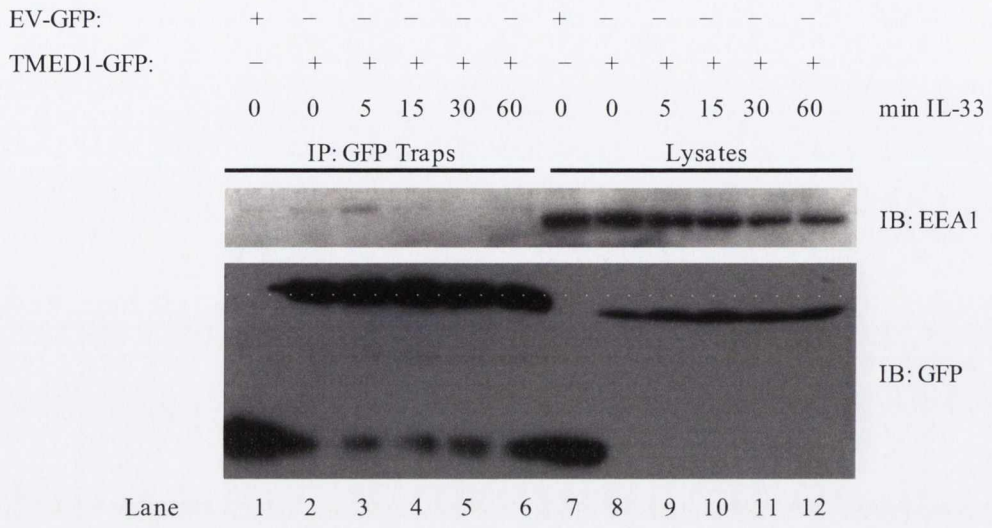


Figure 4.18 Enhanced co-localisation of TMED1 and EEA1 after IL-33 stimulation

Figure 4.18 Enhanced co-localisation of TMED1 and EEA1 after IL-33 stimulation

TMED1-GFP transfected HEK-293-hST2L cells seeded on poly-L-lysine coverslides were stimulated with IL-33 for 10, 30 or 60 minutes, fixed and stained with an anti-EEA1 antibody followed by an anti-rabbit Alexa-546 coupled secondary antibody. The 546 channel has been changed to cyan to allow for easier visualisation of the EEA1-546. Data is representative of results from three independent experiments in which a total of 95 cells were analysed with a minimum of 15 cells per time point. Scale bars indicate 10 μM.



4.19 Enhanced co-immunoprecipitation of TMED1 with EEA1 after IL-33 stimulation

HEK-293-hST2L cells were transfected with plasmids encoding EV-GFP or TMED1-GFP. Cells were stimulated with 50 ng/ml IL-33 for the times indicated and samples were immunoprecipitated with anti-GFP Trap® beads. Whole cell lysates (WCL) and immunoprecipitated samples were analysed by Western blot. The immunoblotting antibodies (IB) are listed beside the appropriate blots. Data are representative of five independent experiments.

4.2.12 IL-33 signalling requires endocytosis

My experiments have suggested that TMED1 is required for the phosphorylation of MAPKs such as ERK and p38 but not for the activation of NF-κB. TMED1 is also shown to surround IL-33 containing endosomes upon IL-33 stimulation. Although functional studies have been carried out on ST2L, the subcellular sites of ST2L-induced signal transduction remain unknown. While IL-33-induced ST2L internalisation ultimately results in the elimination of ST2L via the proteasome (Zhao et al., 2012), ST2L internalisation could also be a requisite step in certain ST2L signalling pathways. To determine the functional consequence of disrupting the IL-33-induced internalisation of ST2L, a highly specific, cell-permeable small molecule inhibitor of dynamin, termed dynasore, was used (Macia et al., 2006). Dynamin GTPases regulate endocytosis by controlling the 'pinching off' of plasma membrane invaginations, which creates early endosomes (Doherty and McMahon, 2009).

In Figure 4.20, a time course which was carried out in Dimethyl sulfoxide (DMSO) or dynasore treated, IL-33 stimulated HEK-293-hST2L cells, is shown. DMSO was used as the control, as dynasore is dissolved in DMSO. Inhibition of endocytosis by dynasore has a significant effect on the phosphorylation of ERK and JNK (Figure 4.20, second and fourth panel) and a partial effect on the phosphorylation of p38 (Figure 4.20, third panel).While there is slightly less degradation of IkBα in dynasore treated cells 15 minutes post stimulation, the levels of IkBα are comparable at 30 and 45 minutes after IL-33 treatment (Figure 4.20, second panel). These data indicate that blocking dynamin dependent endocytosis following IL-33 stimulation has a significantly greater effect on MAPK activation compared to IκBα activation, suggesting that IL-33-induced signalling may occur from two different locations, NF-κB activation being initiated from the plasma

membrane and MAPK activation getting initiated from a compartment formed as a result of endocytosis, such as early endosomes.

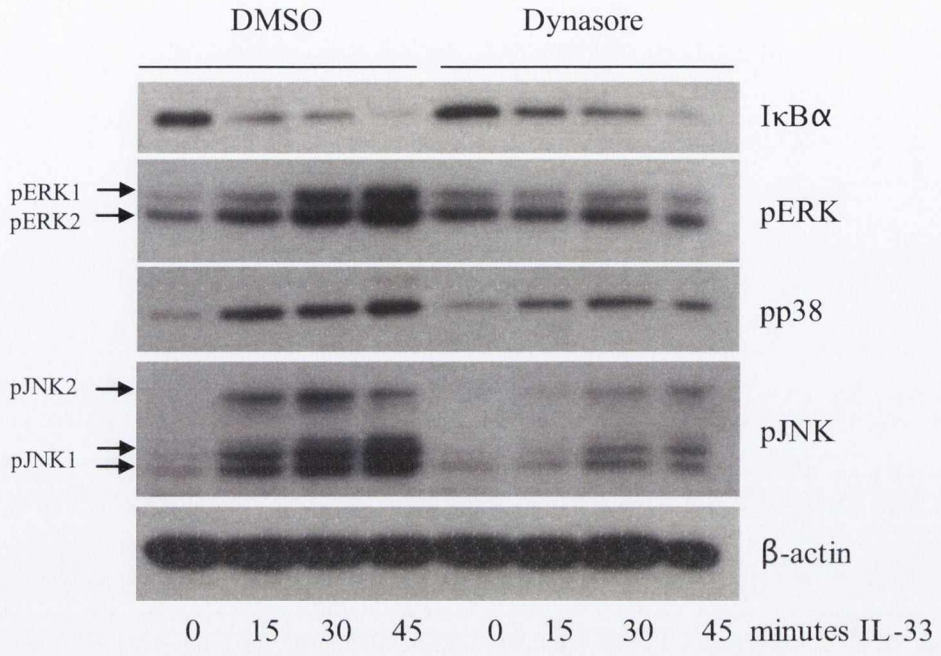


Figure 4.20 IL-33 signalling requires endocytosis

HEK-293-hST2L were treated with DMSO or dynasore (80 μM) for 30 minutes prior to stimulation with IL-33 (50 ng/ml) for the times shown. Cells were lysed and analysed by Western blotting. Immunoblotting (IB) antibodies are shown beside the appropriate blots. Data is representative of four independent experiments.

4.3 Discussion

Having confirmed an interaction between TMED1 and ST2L, next the functional consequence of this association was investigated. Firstly, the effect of IL-33 on the interaction between TMED1 and ST2L was examined. Co-immunoprecipitation experiments suggest that the interaction between transiently overexpressed TMED1 and stably overexpressed ST2L is gradually enhanced following IL-33 stimulation. While further experiments are needed to clarify if IL-33 has the same effect on the interaction between endogenous TMED1 and endogenous ST2L, it is intriguing to speculate why the interaction might be enhanced following ligand treatment. One possibility is that following IL-33 stimulation increased trafficking of ST2L through the early secretory pathway is needed to replenish the plasma membrane after ligand bound ST2L is internalised and degraded. Therefore the enhanced interaction may be as a result of increased trafficking of ST2L by TMED1 through the ER and Golgi. Additionally, the interaction between TMED1 and ST2L may be enhanced following IL-33 stimulation as TMED1 may have a role to play in IL-33 mediated signalling pathways. This would also likely result in a transient enhanced association between the two proteins. It would be interesting to determine the effect of IL-33 on the interaction between TMED1 and ST2L at later time points. Over time the interaction may return to a level similar to that observed prior to stimulation.

As TMED7 has been shown to be involved in TLR4 dependent signalling (Doyle et al., 2012), the possible involvement of TMED1 in the ST2L signalling pathway was investigated. Initial experiments carried out to address this aimed to determine if the overexpression of TMED1 affected ligand induced NF-κB and ISRE luciferase activity. TMED1 overexpression appeared to dose dependently inhibit IL-33-induced NF-κB luciferase activity. This observation was very interesting and in order to test specificity,

various other HEK-293 cell lines stably expressing other receptors were used in NF-κB and ISRE luciferase experiments. These included HEK-293-IL1R1 cells which respond to IL-1, HEK-293-MD2-CD14-TLR4 which respond to LPS, HEK-293-TLR3 which respond to Poly I:C and HEK-293T which respond to TNF-α. TMED1 overexpression dose dependently inhibited the luciferase activity induced by each of the ligands tested. The IL-33 and IL-1-induced signalling pathways are remarkably similar and several of the proteins involved are also components of the LPS and Poly I:C signalling pathways, but only a small number are also shared by the TNF-α pathway. As very few proteins are common to each of the signalling pathways considered here, there are consequently only a limited number of points at which TMED1 could be causing the observed inhibitory effect. TMED1 also inhibited NF-κB luciferase activity induced by the transient overexpression of a much further downstream pathway component, p65, which is a subunit of NF-κB transcription complex. As TMED1 can inhibit luciferase activity induced by a wide range of ligands, as well as the much further downstream component p65, it is possible that the inhibitory effect of TMED1 overexpression is non-specific and acting on luciferase itself. It was therefore necessary to utilise other techniques to determine if TMED1 is involved in IL-33-induced signalling.

In an attempt to clarify this and to investigate if endogenous TMED1 does play a role in IL-33/ST2L signalling, TMED1 was knocked down using siRNA and further luciferase experiments were carried out. Knockdown of endogenous TMED1 (confirmed by quantitative PCR) did not consistently affect IL-33-induced NF-κB luciferase activity, suggesting that the possible inhibitory effect revealed by the initial luciferase experiments is actually an experimental artifact.

Activation of the IL-33-induced signalling pathway was also monitored by blotting for IκBα, pp38, pERK and pJNK following TMED1 knockdown. These results

reveal that knockdown of TMED1 negatively impacted on the IL-33-induced signalling pathway. In particular, pp38 and pERK signal activation was impaired in the absence of TMED1, while there was no difference in the level of activation of NF-κB. These results are in agreement with those discussed above demonstrating that TMED1 knockdown had no effect on IL-33-induced NF-κB luciferase activity. Additional experiments to examine the effect of TMED1 knockdown on IL-33-induced AP-1 luciferase activity would be another means by which to examine the effect on MAPK activation. However, this was not possible as IL-33 could not induce AP-1 luciferase activity in the cell line used in this study.

Given that the knockdown of TMED1 impacted MAPK activation, IL-8 production in response to IL-33 was also measured following TMED1 knockdown. While IL-8 is an NF-κB dependent gene, IL-33-induced IL-8 is also known to be dependent on p38 and ERK activity (Yagami et al., 2010). Overexpression of TMED1 had no effect on IL-8 production following IL-33 stimulation. Interestingly, a reduction in the levels of IL-8 produced after IL-33 stimulation following TMED1 knockdown was evident. The results suggest that TMED1 is in abundance in the cell and adding more TMED1 to the system has no effect on signalling while removal of TMED1 reveals a role for TMED1 in IL-33 signalling.

It was noted during the analysis of time courses monitoring IL-33-induced pathway activation and IL-8 production, that one TMED1 targeted siRNA consistently blocked pathway activation to a greater extent. While the same trend was evident using both TMED1 targeted siRNAs, use of a third would help to clarify the extent of the effect of knocking down TMED1 on the IL-33/ST2L signalling pathway. This would establish if the observed effect was more prominent, similar to the effect noted when using siRNA No2, or less so, similar to that noted when using siRNA No1.

In recent years, it has become increasingly apparent that the localisation and trafficking of IL-1R/TLR superfamily members is an important mechanism modulating the overall cellular response to ligands, by regulating signal activation as well as signal termination (McGettrick and O'Neill, 2010). Ligand induced activation of some receptors such as TLR3 and TLR9 occurs in intracellular compartments (Johnsen et al., 2006; Latz et al., 2004). On the other hand, the initial activation of TLR4 and IL-1R occurs at the plasma membrane. However, ligand induced internalisation of these receptors is required for full activation of downstream signalling pathways (Kagan et al., 2008; Li et al., 2006; Oakley et al., 2009) and their subsequent trafficking to lysosomes for degradation ultimately limits signalling (Brissoni et al., 2006; Husebye et al., 2006). While a considerable amount of research has been carried out on the localisation and trafficking of TLRs, less is known about the IL-1R related superfamily members. The mechanism by which ST2L is regulated following ligand binding has recently been partially elucidated. Following IL-33 binding, ST2L is internalised and finally degraded by the proteasome (Zhao et al., 2012). Results presented herein demonstrate that IL-33 is internalised in a time dependent manner which concurs with data published by Zhao *et al.* IL-33 is internalised into vesicles surrounded by TMED1. Furthermore, confocal and co-immunoprecipitation data demonstrate that following IL-33 treatment, TMED1 is recruited to early endosomes. This suggets that the role of TMED1 in IL-33 signalling occurs in the early endosomes. The use of a fluorescently tagged ST2L along with TMED1-GFP in confocal experiments could also be carried out to determine if these TMED1 and EEA1 positive endosomes also contain ST2L on their membranes. Staining for endogenous ST2L in the HEK-293-hST2L cells was attempted during the course of this study, however due to difficulties arising from the non-specific binding of certain secondary antibodies to these cells it was not possible to stain for ST2L. Alternatively,

enriched endomembrane fractions could be examined for the presence of ST2L before and after IL-33 treatment to determine if ST2L also travels to endosomes after IL-33 stimulation. Like other members of the IL-1R/TLR superfamily the translocation of ST2L to an intracellular compartment appears to be a requisite step in the effective propagation of signal transduction, as blocking dynamin dependent endocytosis negatively impacted downstream signal activation after IL-33 treatment. The inhibition of endocytosis particularly inhibited activation of the MAPKs ERK, p38 and JNK, with only a minor effect on NF-κB activation. While the inhibitoin of endoctyosis has not previously been studied with regard to IL-33 signalling, the effect of inhibition of dynamin, lipid raft and clathrin mediated endocytosis on IL-1-induced NF-κB activation has been assessed (Hornef et al., 2003; Li et al., 2006; Oakley et al., 2009). These studies demonstrate that the inhibition of dynamin or lipid raft mediated endocytosis inhibts IL-1-induced NF-κB luciferase activity, however inhibition of clathrin mediated endocytosis had no effect, albeit though the levels of IL-1-induced NF-κB in the abence of inhibitor were also low. To allow sufficent time for luciferase expression following IL-1 treatment, these experiments require that cells are stimulated for at least two hours. Time courses presented herein assess pathway activation at 15, 30 and 45 minutes post stimulation for both NF-κB and MAPK activity. Hansen *et al.* have recently used a similar approch to investigate the effect of blocking endocytosis on IL-1-induced MAPK and NF-κB activation. In contrast to the results presented herein, which suggest that endocytosis is required for IL-33 induced MAPK activation, the inhibition of endocytosis in shorter time courses does not impair IL-1-induced MAPK (or NF-κB) activation (Hansen et al., 2012). This emphasises the importance of investigating each pathway individually, and is a reminder that although both the IL-1R and ST2L are members of the same family, this does not necessarily mean that generalisations can be applied to

downstream signalling pathways from all family members. A lack of involvement of TMED1 in the IL-1R signalling pathway may explain the observed difference between both of these pathways. This is the first time that the importance of internalistion on IL-33-induced signalling has been assessed, and these results suggest that internalisation is particularly important for IL-33-induced MAPK activation. It is also worth noting that the activation of MAPK cascades by receptor tyrosine kinases (RTK) and G protein-coupled receptors (GPCR) has also been proposed to occur from endosomes (Sorkin and Von Zastrow, 2002).

Figure 4.21 illustrates how TMED1 may be involved in the IL-33 signalling pathway. IL-33 firstly binds its primary receptor ST2L, followed by the co-receptor IL-1RAcP (Chackerian et al., 2007; Palmer et al., 2008). MyD88 is then recruited, followed by IRAK-4, IRAK-1 and TRAF6 (Funakoshi-Tago et al., 2008; Schmitz et al., 2005). Activation of this pathway results in the phosphorylation of ERK1/2, p38 and JNK, as well as phosphorylation and degradation of inhibitor of kappa B alpha (IκBα) (Funakoshi-Tago et al., 2008; Schmitz et al., 2005). This in turn allows NF-κB and AP-1 to enter the nucleus and induce expression of genes such as IL-8. TMED1 positively regulates IL-33-induced signal activation, particularly those which require receptor internalisation for activation. No studies have examined the localisation of ST2L when downstream pathway components are recruited. However, in the case of the IL-1R, MyD88 has been shown to be recruited to the TIR domain of the IL-1R prior to receptor internalisation and TRAF6 is engaged by the receptor complex when it translocates to endosomes (Li et al., 2006). As alluded to earlier, this does not necessarily mean that the same is true for recruitment to ST2L, however is it a reminder that signalling is not all initiated from the plasma membrane. It is also raises the question as to at what point MyD88, the IRAKs and TRAF6 are engaged by ST2L. As TMED1 is recruited to early

endosomes following IL-33 stimulation, it is plausible that this is where it carries out its role in the IL-33 signalling pathway. It is also possible that the contribution of endosomal signalling is proportional to the residence time of the ST2L complex at the endosome, and TMED1 may be required for ST2L maintenance at endosome to allow for sufficient MAPK activation.

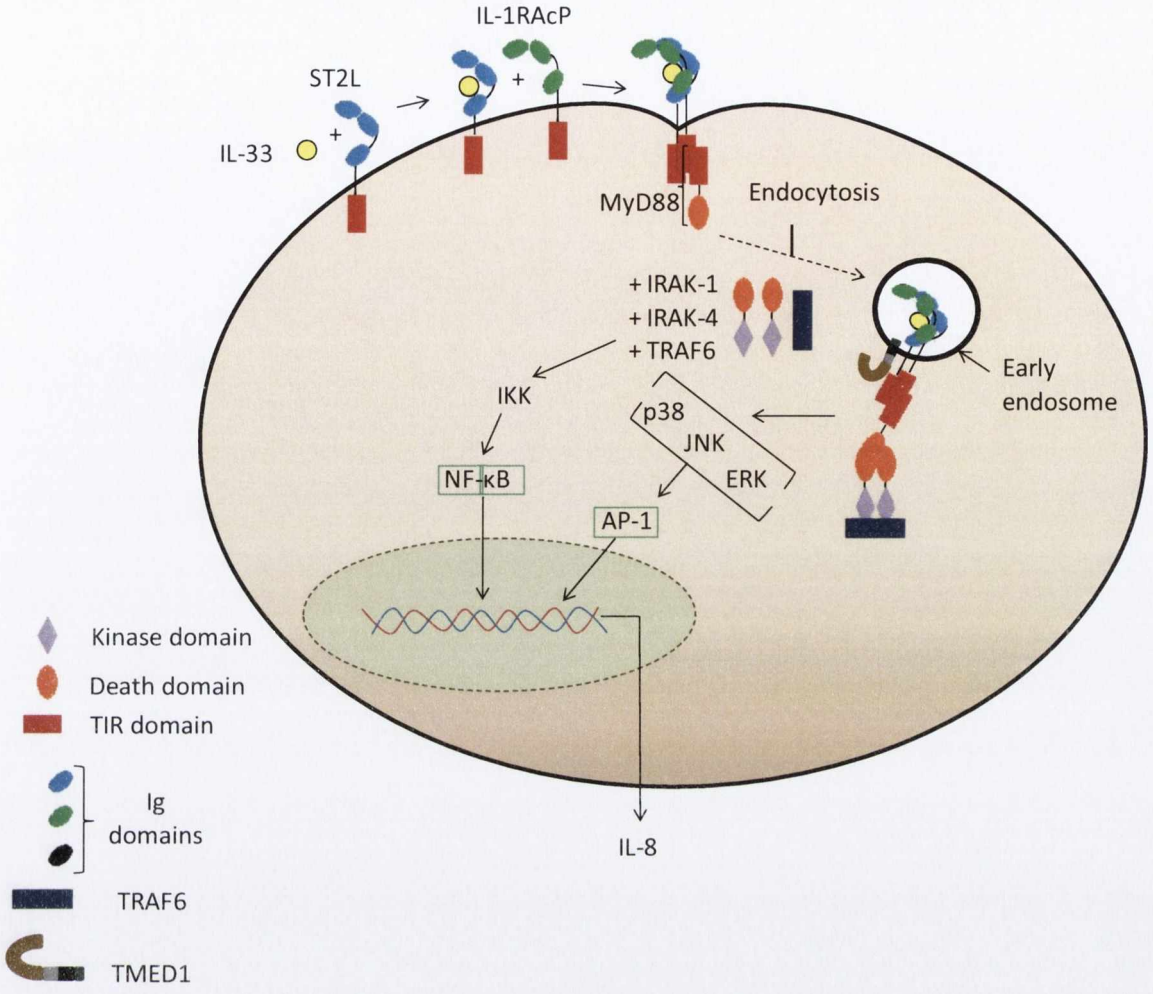


Figure 4.21 Schemeatic for the involvement of TMED1 in IL-33/ST2L signalling

The recruitment of TMED1 to early endosomes is enhanced following IL-33 stimulation and this is likely to be where TMED1 carries out its role in the IL-33 signalling pathway. TMED1 is particularly involved in MAPK activation. As ST2L internalisation appears to be particularly important for MAPK activation and an enhanced association between TMED1 and ST2L occurs following IL-33 stimulation, this may allow TMED1 and ST2L to accomplish MAPK activation from an intercellular compartment such as the early endosome.

Chapter Five

Final discussion and future perspectives

5.1 Final discussion and future perspectives

This thesis set out to further characterise the GOLD domain containing protein, TMED1 and to investigate its relationship with the IL-33 receptor, ST2L. Members of the TMED family possess a GOLD domain, which is a β-strand rich domain found in several proteins involved in Golgi dynamics and intracellular protein trafficking (Anantharaman and Aravind, 2002). This project confirmed the interaction between ST2L and TMED1 and demonstrated that the GOLD domain of TMED1 and the TIR domain of ST2L are essential for this association. This study also revealed a role for TMED1 in the IL-33/ST2L signalling pathway by demonstrating that TMED1 positively modulates IL-33-induced downstream signalling. In particular, TMED1 appears to be required for the activation of ERK and p38 and IL-33-induced IL-8 production. The study also revealed that the localisation of TMED1 changes following IL-33 stimulation, with TMED1 becoming more concentrated at early endosomes. The final goal of the project was to further characterise TMED1 and these studies revealed that TMED1 localises to the ER, Golgi and early endosomes. For the first time the membrane orientation of TMED1 was investigated using protease protection assays. These results have demonstrated that the GOLD domain of TMED1 projects into the cytosol.

The IL-33/ST2L pathway is an important immune signalling pathway which can influence a number of cell types. Perhaps as a result of the range of cells targeted by IL-33, both it and ST2L have been implicated in numerous conditions. These include infection, allergic autoimmune and cardiovascular diseases (Liew et al., 2010; Oboki et al., 2010). As this pathway may be one considered for therapeutic targeting in the future, it is critical that it is understood in as much detail as possible. While the general sequence of events and signalling molecules involved in the ST2L signalling pathway are known, the pathway may be more complex and contain more intermediates than previously

considered. Other signalling pathways such as those downstream of the IL-1R or TLRs have been known for many years, but novel accessory molecules, adaptor proteins, trafficking proteins and negative regulators still continue to be defined for these pathways. These proteins all work together and cooperate to illicit downstream signal activation in the correct manner, allowing sufficient signal activation while preventing pathway over-activation. Signalling pathways by their nature are multi-protein, multistep processes and therefore knowledge of all components of the pathway affords us a complete understanding of how the pathway operates. Ultimately, if further clarity is obtained regarding the nature and means by which IL-33 modulates NF-κB and AP-1 activation this may highlight points along the signalling cascade that are amenable to manipulation. While certain proteins, such as MyD88, are involved in multiple pathways, certain proteins are unique to one particular signalling pathway. For example, TMED7 and TAG specifically target the TLR4 MyD88-independent signalling pathway.

The work presented herein has demonstrated that TMED1 is required for optimal IL-33-induced downstream signal activation. This work suggests that the interaction between TMED1 and ST2L is specific as TMED1 does not interact with other TIR domain containing adaptor proteins, and does not appear to be required for LPS-induced signalling. The specificity of TMED1 for ST2L could be advantageous if considering TMED1 as a protein which could be targeted in the IL-33/ST2L signalling pathway. Future work should confirm the specificity of the TMED1-ST2L interaction by addressing if TMED1 interacts with other receptors of the IL-1R family. If TMED1 does not interact with other IL-1R family members and moreover, is not involved in signalling pathways mediated by other IL-1 family ligands, this raises the possibility that TMED1 may be a suitable therapeutic target, targeting the ST2L signalling pathway while allowing the remaining TLR/IL-1R superfamily to function as normal. Results from this

study suggest that TMED1 may be a target specific for the manipulation of IL-33-induced AP-1 activation.

Based on the evidence demonstrating roles for TMED1 and TMED7 in downstream signalling from receptors of the IL-1R/TLR superfamily it is interesting to speculate that TMED proteins may be important immunoregulators. These two members of the TMED family have important, yet distinct roles in the regulation of the IL-1R/TLR superfamily. TMED1 positively regulates the IL-33/ST2L pathway, while TMED7 negatively regulates the MyD88-indepedent TLR4 pathway. It is common for different members of the same family to have different roles in immune signalling pathways. For example, some TIR domain containing adaptors, such as MyD88 and TRAM act as positive mediators in TLR signalling pathways while others such as SARM and BCAP can negatively regulate TLR signalling pathways (Carty et al., 2006; O'Neill et al., 2003; Troutman et al., 2012). Central to the roles of TMED1 and TMED7 in the IL-1R/TLR signalling pathways are their ability to interact with TIR domain containing proteins. This study has demonstrated that the interaction between ST2L and TMED1 is mediated by their TIR and GOLD domains respectively. These domains may also mediate the TMED7-TRAM, TMED7-TAG, and TRAM-TAG interactions (Doyle et al., 2012; Palsson-McDermott et al., 2009). There is also some evidence to suggest that TMED7 may interact with TLR4, which also could be mediated by GOLD and TIR domains. A structural model of the association between these domains may be beneficial in determining the interface which mediates the TIR-GOLD associations and may reveal particular amino acids of the TIR and GOLD domains which are important. More broadly speaking, there is also the possibility that other TMED proteins interact with other members of the IL-1R/TLR superfamily via the association of their GOLD and TIR

domains. Future research in this area may find novel roles for other TMED proteins in the regulation of the IL-1R/TLR superfamily.

In addition, the TMED family may have a more general role to play in immunoregulation. While the publication from Doyle *et al.* was the first to characterise in detail the role of a TMED family member in an immune pathway, there is also some literature suggesting a role for other TMED proteins in immune regulatory roles in *Drosophila*, mice and human systems (Boltz and Carney, 2008; Davies et al., 2010; Doyle et al., 2012; Jun and Ahn, 2011), suggesting that their immunoregulatory functions may be conserved across species. In addition, the involvement of TMED proteins has also been demonstrated with a role for TMED10 in MHC class I molecule expression (Jun and Ahn, 2011).

In addition to their emerging role in immune related functions, there is some evidence implicating TMEDs in insulin biosynthesis and secretion, and cancer (Zhang and Volchuk, 2010). TMED3, TMED4 and TMED7 have all been shown to be upregulated in cancer cell lines (Ishiyama et al., 2007; Vainio et al., 2012; Yang et al., 2005). Although the reasons for their upregulation are not currently known, roles for modulating certain TMED proteins in anti-tumour immunity may be worth exploring in the future. As our knowledge for the involvement of TMED proteins in a wider range of cellular processes continues to grow, our basic understanding of the TMED proteins themselves must also increase.

Much of this work has been carried out using the HEK-293-hST2L cell line. The HEK-293T cell line and variants expressing receptors of interest are widely used and are an extremely useful tool to investigate signalling pathways. However, a subsequent step in the progression of this project would be to demonstrate the requirement for TMED1 in another experimental system. A cell line which expresses endogenous ST2L and can be

transfected with siRNA would be ideal. Alternatively, the generation of other cell lines in which TMED1 is completely knocked out or stably knocked down would also be useful in verifying the involvement of TMED1 in the IL-33/ST2L pathway. During the course of this project shRNA mediated stable knockdown of TMED1 was attempted, however, while TMED1 targeted shRNAs were successfully expressed, none were successful in knocking down TMED1. If TMED1 was knocked down using alternative shRNAs, the restoration of IL-33-induced MAPK activation and IL-8 production following the reintroduction of TMED1 into these cells would further strengthen the current evidence for the involvement of TMED1 in the IL-33/ST2L signalling pathway. Even better, would be the use of primary human cells to validate the results obtained from the HEK-293-hST2L cells. It would then be possible to examine the involvement of TMED1 in the IL-33-induced signalling pathway by using other readouts such as IL-6.

While the knockdown of TMED1 has a significant effect on IL-33-induced signalling events, it is quite subtle. It may also be benefical to verify that TMED1 knockdown does not effect the levels of other TMED proteins. As TMED proteins are known to be interdependent, perhaps another TMED family member can compensate for the reduced level of TMED1. As TMED2, TMED3 and TMED7 do not interact with ST2L, it is unlikely that any of these fulfill this role, but it is not possible to completely rule out other family members.

A subsequent issue to address, would be to unravel the mechansim whereby TMED1 exerts its positive modulatory effects on the IL-33/ST2L pathway. In particular deciphering the mechanism whereby TMED1 differentially regulates NF-κB and AP-1 activation would be of interest. While the observations suggest that TMED1 functions at the early endosome to mediate positive regulatory events, the exact mechanism of how it does so is not known. It is now well established that in many cases signalling continues

or is initiated after receptor internalisation from endosomal compartments. Perhaps TMED1 is recruited to the early endosomes following IL-33 stimulation to interact with ST2L at this location and maintains it there for a sufficient length of time to allow downstream signalling to occur from this location. Alternatively, TMED1 may acts as an intergrator of trafficking and signalling events, interacting with ST2L following its internalisation, trafficking it to the early endosomes and thereby allowing downstream signal activation from this compartment. Evidence demonstrating that both the TMED1-ST2L association and TMED1 levels at the early endosomes is enhanced following IL-33 stimulation would support this hypothesis. However, additional experiments to demonstrate that both of these events are linked could be carried out. For example, the recruitment of TMED1 to early endosomes and the enhanced interaction between TMED1 and ST2L following IL-33 stimulation could be investigated in conditions in which endocytosis is blocked. Alternatively, inhibitors of clathrin-dependent endocytosis such as mono-dansylcadaverine or Pitstop2, could also be used as IL-1R internalisation has also been shown to be both dynamin and clathrin dependent. If, in these cases, the TMED1-ST2L interaction is not enhanced and TMED1 is not recruited to early endosomes after IL-33 stimulation, this would demonstrate that both events are dependent on endocytosis.

The importance of intracellular trafficking in TLR signalling has been revealed by the involvement of other families of trafficking proteins. One such example is the Ras related in brain (Rab) family of guanosine triphosphatases (GTPases). Alongside their function in membrane trafficking, Rabs are also involved in signal transduction by regulating the trafficking of cell surface receptors. Members of this family have been implicated in both the positive and negative regulation of TLR signalling pathways. Rab10 acts as a positive regulator of TLR4 signalling, by promoting transport of TLR4

from the Golgi to the plasma membrane (Wang et al., 2010), while Rab7b acts as a negative regulator of TLR4 signalling, promoting TLR4 movement to late endosomes for degradation (Wang et al., 2007). Rab11a is also an important regulator of TLR4 and TRAM transport from the endocytic recycling compartment (ERC) to *Escherichia coli*-containing phagosomes (Husebye et al., 2010). Evidence from this thesis, alongside the work carried out on TMED7 (Doyle et al., 2012), adds to the emerging evidence implicating the TMED family as important regulators in the control of innate immune signalling, and may place the TMED family, alongside the Rab family as important regulators of these processes.

In conclusion, this study demonstrates that TMED1 is a component of the IL-33/ST2L inflammatory signalling pathway. TMED1 interacts with the IL-33 receptor ST2L and positively modulates IL-33-induced phosphorylation of p38 and ERK, and IL-8 production. It is likely that TMED1 carries out its positive regulatory role at the early endosome although the exact mechanism whereby this occurs remains to be determined. This study provides additional support to the concept that the TMED family are important players in the complex process of innate immune regulation. Further investigation into the role of TMED proteins in the regulation of innate immunity, in particular with regard to IL-1R/TLR signalling is likely to provide exciting new insights into the control of innate immunity and may establish a conserved role for the TMED family in the innate immune system.

References

Afonina, I.S., Tynan, G.A., Logue, S.E., Cullen, S.P., Bots, M., Luthi, A.U., Reeves, E.P., McElvaney, N.G., Medema, J.P., Lavelle, E.C., and Martin, S.J. (2011). Granzyme B-dependent proteolysis acts as a switch to enhance the proinflammatory activity of IL-1alpha. Mol Cell *44*, 265-278.

Aguilera-Romero, A., Kaminska, J., Spang, A., Riezman, H., and Muniz, M. (2008). The yeast p24 complex is required for the formation of COPI retrograde transport vesicles from the Golgi apparatus. J Cell Biol *180*, 713-720.

Akita, K., Ohtsuki, T., Nukada, Y., Tanimoto, T., Namba, M., Okura, T., Takakura-Yamamoto, R., Torigoe, K., Gu, Y., Su, M.S., *et al.* (1997). Involvement of caspase-1 and caspase-3 in the production and processing of mature human interleukin 18 in monocytic THP.1 cells. J Biol Chem *272*, 26595-26603.

Alexopoulou, L., Holt, A.C., Medzhitov, R., and Flavell, R.A. (2001). Recognition of double-stranded RNA and activation of NF-kappaB by Toll-like receptor 3. Nature *413*, 732-738.

Ali, S., Mohs, A., Thomas, M., Klare, J., Ross, R., Schmitz, M.L., and Martin, M.U. (2011). The dual function cytokine IL-33 interacts with the transcription factor NF-kappaB to dampen NF-kappaB-stimulated gene transcription. J Immunol *187*, 1609-1616.

Allakhverdi, Z., Smith, D.E., Comeau, M.R., and Delespesse, G. (2007). Cutting edge: The ST2 ligand IL-33 potently activates and drives maturation of human mast cells. J Immunol *179*, 2051-2054.

Almen, M.S., Nordstrom, K.J., Fredriksson, R., and Schioth, H.B. (2009). Mapping the human membrane proteome: a majority of the human membrane proteins can be classified according to function and evolutionary origin. BMC Biol *7*, 50.

Alves-Filho, J.C., Sonego, F., Souto, F.O., Freitas, A., Verri, W.A., Jr., Auxiliadora-Martins, M., Basile-Filho, A., McKenzie, A.N., Xu, D., Cunha, F.Q., and Liew, F.Y. (2010). Interleukin-33 attenuates sepsis by enhancing neutrophil influx to the site of infection. Nat Med *16*, 708-712.

Anantharaman, V., and Aravind, L. (2002). The GOLD domain, a novel protein module involved in Golgi function and secretion. Genome Biol *3*, research0023.

Andrade, M.V., Iwaki, S., Ropert, C., Gazzinelli, R.T., Cunha-Melo, J.R., and Beaven, M.A. (2011). Amplification of cytokine production through synergistic activation of NFAT and AP-1 following stimulation of mast cells with antigen and IL-33. Eur J Immunol *41*, 760-772.

Baekkevold, E.S., Roussigne, M., Yamanaka, T., Johansen, F.E., Jahnsen, F.L., Amalric, F., Brandtzaeg, P., Erard, M., Haraldsen, G., and Girard, J.P. (2003). Molecular characterization of NF-HEV, a nuclear factor preferentially expressed in human high endothelial venules. Am J Pathol *163*, 69-79.

Barr, F.A., Preisinger, C., Kopajtich, R., and Korner, R. (2001). Golgi matrix proteins interact with p24 cargo receptors and aid their efficient retention in the Golgi apparatus. J Cell Biol *155*, 885-891.

Bianchi, M.E. (2007). DAMPs, PAMPs and alarmins: all we need to know about danger. J Leukoc Biol *81*, 1-5.

Blanco, A.M., Perez-Arago, A., Fernandez-Lizarbe, S., and Guerri, C. (2008). Ethanol mimics ligand-mediated activation and endocytosis of IL-1RI/TLR4 receptors via lipid rafts caveolae in astroglial cells. J Neurochem *106*, 625-639.

Blum, R., Feick, P., Puype, M., Vandekerckhove, J., Klengel, R., Nastainczyk, W., and Schulz, I. (1996). Tmp21 and p24A, two type I proteins enriched in pancreatic microsomal membranes, are members of a protein family involved in vesicular trafficking. J Biol Chem *271*, 17183-17189.

Blum, R., and Lepier, A. (2008). The luminal domain of p23 (Tmp21) plays a critical role in p23 cell surface trafficking. Traffic *9*, 1530-1550.

Boltz, K.A., and Carney, G.E. (2008). Loss of p24 function in Drosophila melanogaster causes a stress response and increased levels of NF-kappaB-regulated gene products. BMC Genomics *9*, 212.

Boltz, K.A., Ellis, L.L., and Carney, G.E. (2007). Drosophila melanogaster p24 genes have developmental, tissue-specific, and sex-specific expression patterns and functions. Dev Dyn *236*, 544-555.

Born, T.L., Smith, D.E., Garka, K.E., Renshaw, B.R., Bertles, J.S., and Sims, J.E. (2000). Identification and characterization of two members of a novel class of the interleukin-1 receptor (IL-1R) family. Delineation Of a new class of IL-1R-related proteins based on signaling. J Biol Chem *275*, 41528.

Bourke, E., Cassetti, A., Villa, A., Fadlon, E., Colotta, F., and Mantovani, A. (2003). IL-1 beta scavenging by the type II IL-1 decoy receptor in human neutrophils. J Immunol *170*, 5999-6005.

Bowie, A., and O'Neill, L.A. (2000). The interleukin-1 receptor/Toll-like receptor superfamily: signal generators for pro-inflammatory interleukins and microbial products. J Leukoc Biol *67*, 508-514.

Braakman, I., and Bulleid, N.J. (2011). Protein folding and modification in the mammalian endoplasmic reticulum. Annu Rev Biochem *80*, 71-99.

Brinkmann, M.M., Spooner, E., Hoebe, K., Beutler, B., Ploegh, H.L., and Kim, Y.M. (2007). The interaction between the ER membrane protein UNC93B and TLR3, 7, and 9 is crucial for TLR signaling. J Cell Biol *177*, 265-275.

Brint, E.K., Fitzgerald, K.A., Smith, P., Coyle, A.J., Gutierrez-Ramos, J.C., Fallon, P.G., and O'Neill, L.A. (2002). Characterization of signaling pathways activated by the interleukin 1 (IL-1) receptor homologue T1/ST2. A role for Jun N-terminal kinase in IL-4 induction. J Biol Chem *277*, 49205-49211.

Brint, E.K., Xu, D., Liu, H., Dunne, A., McKenzie, A.N., O'Neill, L.A., and Liew, F.Y. (2004). ST2 is an inhibitor of interleukin 1 receptor and Toll-like receptor 4 signaling and maintains endotoxin tolerance. Nat Immunol *5*, 373-379.

Brissoni, B., Agostini, L., Kropf, M., Martinon, F., Swoboda, V., Lippens, S., Everett, H., Aebi, N., Janssens, S., Meylan, E., *et al.* (2006). Intracellular trafficking of interleukin-1 receptor I requires Tollip. Curr Biol *16*, 2265-2270.

Bulek, K., Swaidani, S., Qin, J., Lu, Y., Gulen, M.F., Herjan, T., Min, B., Kastelein, R.A., Aronica, M., Kosz-Vnenchak, M., and Li, X. (2009). The essential role of single Ig IL-1 receptor-related molecule/Toll IL-1R8 in regulation of Th2 immune response. J Immunol *182*, 2601-2609.

Burns, K., Martinon, F., Esslinger, C., Pahl, H., Schneider, P., Bodmer, J.L., Di Marco, F., French, L., and Tschopp, J. (1998). MyD88, an adapter protein involved in interleukin-1 signaling. J Biol Chem *273*, 12203-12209.

Carney, G.E., and Bowen, N.J. (2004). p24 proteins, intracellular trafficking, and behavior: Drosophila melanogaster provides insights and opportunities. Biol Cell *96*, 271-278.

Carrie, A., Jun, L., Bienvenu, T., Vinet, M.C., McDonell, N., Couvert, P., Zemni, R., Cardona, A., Van Buggenhout, G., Frints, S., *et al.* (1999). A new member of the IL-1 receptor family highly expressed in hippocampus and involved in X-linked mental retardation. Nat Genet *23*, 25-31.

Carriere, V., Roussel, L., Ortega, N., Lacorre, D.A., Americh, L., Aguilar, L., Bouche, G., and Girard, J.P. (2007). IL-33, the IL-1-like cytokine ligand for ST2 receptor, is a chromatin-associated nuclear factor in vivo. Proc Natl Acad Sci U S A *104*, 282-287.

Carty, M., Goodbody, R., Schroder, M., Stack, J., Moynagh, P.N., and Bowie, A.G. (2006). The human adaptor SARM negatively regulates adaptor protein TRIF-dependent Toll-like receptor signaling. Nat Immunol *7*, 1074-1081.

Chackerian, A.A., Oldham, E.R., Murphy, E.E., Schmitz, J., Pflanz, S., and Kastelein, R.A. (2007). IL-1 receptor accessory protein and ST2 comprise the IL-33 receptor complex. J Immunol *179*, 2551-2555.

Chapuis, J., Hot, D., Hansmannel, F., Kerdraon, O., Ferreira, S., Hubans, C., Maurage, C.A., Huot, L., Bensemain, F., Laumet, G., *et al.* (2009). Transcriptomic and genetic studies identify IL-33 as a candidate gene for Alzheimer's disease. Mol Psychiatry *14*, 1004-1016.

Chen, F., Hasegawa, H., Schmitt-Ulms, G., Kawarai, T., Bohm, C., Katayama, T., Gu, Y., Sanjo, N., Glista, M., Rogaeva, E., *et al.* (2006). TMP21 is a presenilin complex component that modulates gamma-secretase but not epsilon-secretase activity. Nature *440*, 1208-1212.

Cheung, H., Chen, N.J., Cao, Z., Ono, N., Ohashi, P.S., and Yeh, W.C. (2005). Accessory protein-like is essential for IL-18-mediated signaling. J Immunol *174*, 5351-5357.

Choi, Y.S., Choi, H.J., Min, J.K., Pyun, B.J., Maeng, Y.S., Park, H., Kim, J., Kim, Y.M., and Kwon, Y.G. (2009). Interleukin-33 induces angiogenesis and vascular permeability through ST2/TRAF6-mediated endothelial nitric oxide production. Blood *114*, 3117-3126.

Choi, Y.S., Park, J.A., Kim, J., Rho, S.S., Park, H., Kim, Y.M., and Kwon, Y.G. (2012). Nuclear IL-33 is a transcriptional regulator of NF-kappaB p65 and induces endothelial cell activation. Biochem Biophys Res Commun *421*, 305-311.

Cserzo, M., Wallin, E., Simon, I., von Heijne, G., and Elofsson, A. (1997). Prediction of transmembrane alpha-helices in prokaryotic membrane proteins: the dense alignment surface method. Protein Eng *10*, 673-676.

Davies, J.M., MacSharry, J., and Shanahan, F. (2010). Differential regulation of Toll-like receptor signalling in spleen and Peyer's patch dendritic cells. Immunology *131*, 438-448.

Denzel, A., Otto, F., Girod, A., Pepperkok, R., Watson, R., Rosewell, I., Bergeron, J.J., Solari, R.C., and Owen, M.J. (2000). The p24 family member p23 is required for early embryonic development. Curr Biol *10*, 55-58.

Dinarello, C., Arend, W., Sims, J., Smith, D., Blumberg, H., O'Neill, L., Goldbach-Mansky, R., Pizarro, T., Hoffman, H., Bufler, P., *et al.* (2010). IL-1 family nomenclature. Nat Immunol *11*, 973.

Doherty, G.J., and McMahon, H.T. (2009). Mechanisms of endocytosis. Annu Rev Biochem *78*, 857-902.

Dominguez, M., Dejgaard, K., Fullekrug, J., Dahan, S., Fazel, A., Paccaud, J.P., Thomas, D.Y., Bergeron, J.J., and Nilsson, T. (1998). gp25L/emp24/p24 protein family members of the cis-Golgi network bind both COP I and II coatomer. J Cell Biol *140*, 751-765.

Doyle, S.L., Husebye, H., Connolly, D.J., Espevik, T., O'Neill, L.A., and McGettrick, A.F. (2012). The GOLD domain-containing protein TMED7 inhibits TLR4 signalling from the endosome upon LPS stimulation. Nat Commun *3*, 707.

Drube, S., Heink, S., Walter, S., Lohn, T., Grusser, M., Gerbaulet, A., Berod, L., Schons, J., Dudeck, A., Freitag, J., *et al.* (2010). The receptor tyrosine kinase c-Kit controls IL-33 receptor signaling in mast cells. Blood *115*, 3899-3906.

Eisenberg, S.P., Brewer, M.T., Verderber, E., Heimdal, P., Brandhuber, B.J., and Thompson, R.C. (1991). Interleukin 1 receptor antagonist is a member of the interleukin 1 gene family: evolution of a cytokine control mechanism. Proc Natl Acad Sci U S A *88*, 5232-5236.

Emery, G., Rojo, M., and Gruenberg, J. (2000). Coupled transport of p24 family members. J Cell Sci *113 (Pt 13)*, 2507-2516.

Espinassous, Q., Garcia-de-Paco, E., Garcia-Verdugo, I., Synguelakis, M., von Aulock, S., Sallenave, J.M., McKenzie, A.N., and Kanellopoulos, J. (2009). IL-33 enhances lipopolysaccharide-induced inflammatory cytokine production from mouse macrophages by regulating lipopolysaccharide receptor complex. J Immunol *183*, 1446-1455.

Fitzgerald, K.A., Palsson-McDermott, E.M., Bowie, A.G., Jefferies, C.A., Mansell, A.S., Brady, G., Brint, E., Dunne, A., Gray, P., Harte, M.T., *et al.* (2001). Mal (MyD88-adapter-like) is required for Toll-like receptor-4 signal transduction. Nature *413*, 78-83.

Fullekrug, J., Suganuma, T., Tang, B.L., Hong, W., Storrie, B., and Nilsson, T. (1999). Localization and recycling of gp27 (hp24gamma3): complex formation with other p24 family members. Mol Biol Cell *10*, 1939-1955.

Funakoshi-Tago, M., Tago, K., Hayakawa, M., Tominaga, S., Ohshio, T., Sonoda, Y., and Kasahara, T. (2008). TRAF6 is a critical signal transducer in IL-33 signaling pathway. Cell Signal *20*, 1679-1686.

Funakoshi-Tago, M., Tago, K., Sato, Y., Tominaga, S., and Kasahara, T. (2011). JAK2 is an important signal transducer in IL-33-induced NF-kappaB activation. Cell Signal *23*, 363-370.

Gachter, T., Werenskiold, A.K., and Klemenz, R. (1996). Transcription of the interleukin-1 receptor-related T1 gene is initiated at different promoters in mast cells and fibroblasts. J Biol Chem *271*, 124-129.

Gay, N.J., and Keith, F.J. (1991). Drosophila Toll and IL-1 receptor. Nature *351*, 355-356.

Gayle, M.A., Slack, J.L., Bonnert, T.P., Renshaw, B.R., Sonoda, G., Taguchi, T., Testa, J.R., Dower, S.K., and Sims, J.E. (1996). Cloning of a putative ligand for the T1/ST2 receptor. J Biol Chem *271*, 5784-5789.

Gommel, D.U., Memon, A.R., Heiss, A., Lottspeich, F., Pfannstiel, J., Lechner, J., Reinhard, C., Helms, J.B., Nickel, W., and Wieland, F.T. (2001). Recruitment to Golgi membranes of ADP-ribosylation factor 1 is mediated by the cytoplasmic domain of p23. EMBO J *20*, 6751-6760.

Greenfeder, S.A., Nunes, P., Kwee, L., Labow, M., Chizzonite, R.A., and Ju, G. (1995). Molecular cloning and characterization of a second subunit of the interleukin 1 receptor complex. J Biol Chem *270*, 13757-13765.

Gu, Y.F., Fang, Y., Jin, Y., Dong, W.R., Xiang, L.X., and Shao, J.Z. (2011). Discovery of the DIGIRR gene from teleost fish: a novel Toll-IL-1 receptor family member serving as a negative regulator of IL-1 signaling. J Immunol *187*, 2514-2530.

Guo, L., Wei, G., Zhu, J., Liao, W., Leonard, W.J., Zhao, K., and Paul, W. (2009). IL-1 family members and STAT activators induce cytokine production by Th2, Th17, and Th1 cells. Proc Natl Acad Sci U S A *106*, 13463-13468.

Gupta, V., and Swarup, G. (2006). Evidence for a role of transmembrane protein p25 in localization of protein tyrosine phosphatase TC48 to the ER. J Cell Sci *119*, 1703-1714.

Hansen, B., Dittrich-Breiholz, O., Kracht, M., and Windheim, M. (2012). Regulation of NF-kappaB-dependent gene expression by ligand-induced endocytosis of the interleukin-1 receptor. Cell Signal.

Hart, B.E., and Tapping, R.I. (2012). Cell surface trafficking of TLR1 is differentially regulated by the chaperones PRAT4A and PRAT4B. J Biol Chem *287*, 16550-16562.

Hasan, U., Chaffois, C., Gaillard, C., Saulnier, V., Merck, E., Tancredi, S., Guiet, C., Briere, F., Vlach, J., Lebecque, S., *et al.* (2005). Human TLR10 is a functional receptor,

expressed by B cells and plasmacytoid dendritic cells, which activates gene transcription through MyD88. J Immunol *174*, 2942-2950.

Hasegawa, H., Liu, L., and Nishimura, M. (2010). Dilysine retrieval signal-containing p24 proteins collaborate in inhibiting gamma-cleavage of amyloid precursor protein. J Neurochem *115*, 771-781.

Hayakawa, H., Hayakawa, M., Kume, A., and Tominaga, S. (2007). Soluble ST2 blocks interleukin-33 signaling in allergic airway inflammation. J Biol Chem *282*, 26369-26380.

Hayakawa, M., Hayakawa, H., Matsuyama, Y., Tamemoto, H., Okazaki, H., and Tominaga, S. (2009). Mature interleukin-33 is produced by calpain-mediated cleavage in vivo. Biochem Biophys Res Commun *387*, 218-222.

Hirokawa, T., Boon-Chieng, S., and Mitaku, S. (1998). SOSUI: classification and secondary structure prediction system for membrane proteins. Bioinformatics *14*, 378-379.

Hoffmann, E., Dittrich-Breiholz, O., Holtmann, H., and Kracht, M. (2002). Multiple control of interleukin-8 gene expression. J Leukoc Biol *72*, 847-855.

Hong, J., Bae, S., Jhun, H., Lee, S., Choi, J., Kang, T., Kwak, A., Hong, K., Kim, E., Jo, S., and Kim, S. (2011). Identification of constitutively active IL-33 splice variant. J Biol Chem.

Hornef, M.W., Normark, B.H., Vandewalle, A., and Normark, S. (2003). Intracellular recognition of lipopolysaccharide by toll-like receptor 4 in intestinal epithelial cells. J Exp Med *198*, 1225-1235.

Hosaka, M., Watanabe, T., Yamauchi, Y., Sakai, Y., Suda, M., Mizutani, S., Takeuchi, T., Isobe, T., and Izumi, T. (2007). A subset of p23 localized on secretory granules in pancreatic beta-cells. J Histochem Cytochem *55*, 235-245.

Husebye, H., Aune, M.H., Stenvik, J., Samstad, E., Skjeldal, F., Halaas, O., Nilsen, N.J., Stenmark, H., Latz, E., Lien, E., *et al.* (2010). The Rab11a GTPase controls Toll-like receptor 4-induced activation of interferon regulatory factor-3 on phagosomes. Immunity *33*, 583-596.

Husebye, H., Halaas, O., Stenmark, H., Tunheim, G., Sandanger, O., Bogen, B., Brech, A., Latz, E., and Espevik, T. (2006). Endocytic pathways regulate Toll-like receptor 4 signaling and link innate and adaptive immunity. EMBO J *25*, 683-692.

Hwang, S.O., Boswell, S.A., Seo, J.S., and Lee, S.W. (2008). Novel oxidative stress-responsive gene ERS25 functions as a regulator of the heat-shock and cell death response. J Biol Chem *283*, 13063-13069.

Irmler, M., Hertig, S., MacDonald, H.R., Sadoul, R., Becherer, J.D., Proudfoot, A., Solari, R., and Tschopp, J. (1995). Granzyme A is an interleukin 1 beta-converting enzyme. J Exp Med *181*, 1917-1922.

Ishiyama, T., Kano, J., Anami, Y., Onuki, T., Iijima, T., Morisita, Y., Yokota, J., and Noguchi, M. (2007). OCIA domain containing 2 is highly expressed in adenocarcinoma mixed subtype with bronchioloalveolar carcinoma component and is associated with better prognosis. Cancer Sci *98*, 50-57.

Itoh, H., Tatematsu, M., Watanabe, A., Iwano, K., Funami, K., Seya, T., and Matsumoto, M. (2011). UNC93B1 physically associates with human TLR8 and regulates TLR8-mediated signaling. PLoS One *6*, e28500.

Iwahana, H., Hayakawa, M., Kuroiwa, K., Tago, K., Yanagisawa, K., Noji, S., and Tominaga, S. (2004). Molecular cloning of the chicken ST2 gene and a novel variant form of the ST2 gene product, ST2LV. Biochim Biophys Acta *1681*, 1-14.

Iwahana, H., Yanagisawa, K., Ito-Kosaka, A., Kuroiwa, K., Tago, K., Komatsu, N., Katashima, R., Itakura, M., and Tominaga, S. (1999). Different promoter usage and multiple transcription initiation sites of the interleukin-1 receptor-related human ST2 gene in UT-7 and TM12 cells. Eur J Biochem *264*, 397-406.

Janeway, C.A., Jr. (1989). Approaching the asymptote? Evolution and revolution in immunology. Cold Spring Harb Symp Quant Biol *54 Pt 1*, 1-13.

Janeway, C.A., Jr. (1992). The immune system evolved to discriminate infectious nonself from noninfectious self. Immunol Today *13*, 11-16.

Janeway, C.A., Jr. (1993). How the immune system recognizes invaders. Sci Am *269*, 72-79.

Janeway, C.A., Jr. (2001). How the immune system protects the host from infection. Microbes Infect *3*, 1167-1171.

Janeway, C.A., Jr., and Medzhitov, R. (2002). Innate immune recognition. Annu Rev Immunol *20*, 197-216.

Jenne, N., Frey, K., Brugger, B., and Wieland, F.T. (2002). Oligomeric state and stoichiometry of p24 proteins in the early secretory pathway. J Biol Chem *277*, 46504-46511.

Jerome-Majewska, L.A., Achkar, T., Luo, L., Lupu, F., and Lacy, E. (2010). The trafficking protein Tmed2/p24beta(1) is required for morphogenesis of the mouse embryo and placenta. Dev Biol *341*, 154-166.

Johnsen, I.B., Nguyen, T.T., Ringdal, M., Tryggestad, A.M., Bakke, O., Lien, E., Espevik, T., and Anthonsen, M.W. (2006). Toll-like receptor 3 associates with c-Src tyrosine kinase on endosomes to initiate antiviral signaling. EMBO J *25*, 3335-3346.

Jones, D.T. (2007). Improving the accuracy of transmembrane protein topology prediction using evolutionary information. Bioinformatics *23*, 538-544.

Jones, L.A., Roberts, F., Nickdel, M.B., Brombacher, F., McKenzie, A.N., Henriquez, F.L., Alexander, J., and Roberts, C.W. (2010). IL-33 receptor (T1/ST2) signalling is necessary to prevent the development of encephalitis in mice infected with Toxoplasma gondii. Eur J Immunol *40*, 426-436.

Jun, Y., and Ahn, K. (2011). Tmp21, a novel MHC-I interacting protein, preferentially binds to Beta(2)-microglobulin-free MHC-I heavy chains. BMB Rep *44*, 369-374.

Kagan, J.C., Su, T., Horng, T., Chow, A., Akira, S., and Medzhitov, R. (2008). TRAM couples endocytosis of Toll-like receptor 4 to the induction of interferon-beta. Nat Immunol *9*, 361-368.

Kakkar, R., and Lee, R.T. (2008). The IL-33/ST2 pathway: therapeutic target and novel biomarker. Nat Rev Drug Discov *7*, 827-840.

Kall, L., Krogh, A., and Sonnhammer, E.L. (2004). A combined transmembrane topology and signal peptide prediction method. J Mol Biol *338*, 1027-1036.

Kavita, U., and Mizel, S.B. (1995). Differential sensitivity of interleukin-1 alpha and -beta precursor proteins to cleavage by calpain, a calcium-dependent protease. J Biol Chem *270*, 27758-27765.

Kawai, T., and Akira, S. (2010). The role of pattern-recognition receptors in innate immunity: update on Toll-like receptors. Nat Immunol *11*, 373-384.

Khan, J.A., Brint, E.K., O'Neill, L.A., and Tong, L. (2004). Crystal structure of the Toll/interleukin-1 receptor domain of human IL-1RAPL. J Biol Chem *279*, 31664-31670.

Kim, Y.M., Brinkmann, M.M., Paquet, M.E., and Ploegh, H.L. (2008). UNC93B1 delivers nucleotide-sensing toll-like receptors to endolysosomes. Nature *452*, 234-238.

Klemenz, R., Hoffmann, S., and Werenskiold, A.K. (1989). Serum- and oncoprotein-mediated induction of a gene with sequence similarity to the gene encoding carcinoembryonic antigen. Proc Natl Acad Sci U S A *86*, 5708-5712.

Kollewe, C., Mackensen, A.C., Neumann, D., Knop, J., Cao, P., Li, S., Wesche, H., and Martin, M.U. (2004). Sequential autophosphorylation steps in the interleukin-1 receptor-associated kinase-1 regulate its availability as an adapter in interleukin-1 signaling. J Biol Chem *279*, 5227-5236.

Komai-Koma, M., Gilchrist, D.S., McKenzie, A.N., Goodyear, C.S., Xu, D., and Liew, F.Y. (2011). IL-33 activates B1 cells and exacerbates contact sensitivity. J Immunol *186*, 2584-2591.

Konno, K., Wakabayashi, Y., Akashi-Takamura, S., Ishii, T., Kobayashi, M., Takahashi, K., Kusumoto, Y., Saitoh, S., Yoshizawa, Y., and Miyake, K. (2006). A molecule that is associated with Toll-like receptor 4 and regulates its cell surface expression. Biochem Biophys Res Commun *339*, 1076-1082.

Korherr, C., Hofmeister, R., Wesche, H., and Falk, W. (1997). A critical role for interleukin-1 receptor accessory protein in interleukin-1 signaling. Eur J Immunol *27*, 262-267.

Krogh, A., Larsson, B., von Heijne, G., and Sonnhammer, E.L. (2001). Predicting transmembrane protein topology with a hidden Markov model: application to complete genomes. J Mol Biol *305*, 567-580.

Kumar, S., Hanning, C.R., Brigham-Burke, M.R., Rieman, D.J., Lehr, R., Khandekar, S., Kirkpatrick, R.B., Scott, G.F., Lee, J.C., Lynch, F.J., *et al.* (2002). Interleukin-1F7B (IL-1H4/IL-1F7) is processed by caspase-1 and mature IL-1F7B binds to the IL-18 receptor but does not induce IFN-gamma production. Cytokine *18*, 61-71.

Kurokawa, M., Matsukura, S., Kawaguchi, M., Ieki, K., Suzuki, S., Odaka, M., Watanabe, S., Homma, T., Sato, M., Yamaguchi, M., *et al.* (2011). Expression and effects of IL-33 and ST2 in allergic bronchial asthma: IL-33 induces eotaxin production in lung fibroblasts. Int Arch Allergy Immunol *155 Suppl 1*, 12-20.

Kurowska-Stolarska, M., Stolarski, B., Kewin, P., Murphy, G., Corrigan, C.J., Ying, S., Pitman, N., Mirchandani, A., Rana, B., van Rooijen, N., *et al.* (2009). IL-33 amplifies the polarization of alternatively activated macrophages that contribute to airway inflammation. J Immunol *183*, 6469-6477.

Lamothe, B., Besse, A., Campos, A.D., Webster, W.K., Wu, H., and Darnay, B.G. (2007). Site-specific Lys-63-linked tumor necrosis factor receptor-associated factor 6

auto-ubiquitination is a critical determinant of I kappa B kinase activation. J Biol Chem *282*, 4102-4112.

Latz, E., Schoenemeyer, A., Visintin, A., Fitzgerald, K.A., Monks, B.G., Knetter, C.F., Lien, E., Nilsen, N.J., Espevik, T., and Golenbock, D.T. (2004). TLR9 signals after translocating from the ER to CpG DNA in the lysosome. Nat Immunol *5*, 190-198.

Latz, E., Visintin, A., Lien, E., Fitzgerald, K.A., Espevik, T., and Golenbock, D.T. (2003). The LPS receptor generates inflammatory signals from the cell surface. J Endotoxin Res *9*, 375-380.

Latz, E., Visintin, A., Lien, E., Fitzgerald, K.A., Monks, B.G., Kurt-Jones, E.A., Golenbock, D.T., and Espevik, T. (2002). Lipopolysaccharide rapidly traffics to and from the Golgi apparatus with the toll-like receptor 4-MD-2-CD14 complex in a process that is distinct from the initiation of signal transduction. J Biol Chem *277*, 47834-47843.

Lecart, S., Lecointe, N., Subramaniam, A., Alkan, S., Ni, D., Chen, R., Boulay, V., Pene, J., Kuroiwa, K., Tominaga, S., and Yssel, H. (2002). Activated, but not resting human Th2 cells, in contrast to Th1 and T regulatory cells, produce soluble ST2 and express low levels of ST2L at the cell surface. Eur J Immunol *32*, 2979-2987.

Lefrancais, E., Roga, S., Gautier, V., Gonzalez-de-Peredo, A., Monsarrat, B., Girard, J.P., and Cayrol, C. (2012). IL-33 is processed into mature bioactive forms by neutrophil elastase and cathepsin G. Proc Natl Acad Sci U S A *109*, 1673-1678.

Lemaitre, B., Nicolas, E., Michaut, L., Reichhart, J.M., and Hoffmann, J.A. (1996). The dorsoventral regulatory gene cassette spatzle/Toll/cactus controls the potent antifungal response in Drosophila adults. Cell *86*, 973-983.

Li, Q., Harraz, M.M., Zhou, W., Zhang, L.N., Ding, W., Zhang, Y., Eggleston, T., Yeaman, C., Banfi, B., and Engelhardt, J.F. (2006). Nox2 and Rac1 regulate H2O2-dependent recruitment of TRAF6 to endosomal interleukin-1 receptor complexes. Mol Cell Biol *26*, 140-154.

Li, S., Strelow, A., Fontana, E.J., and Wesche, H. (2002). IRAK-4: a novel member of the IRAK family with the properties of an IRAK-kinase. Proc Natl Acad Sci U S A *99*, 5567-5572.

Liew, F.Y. (2012). IL-33: a Janus cytokine. Ann Rheum Dis *71 Suppl 2*, i101-104.
Liew, F.Y., Pitman, N.I., and McInnes, I.B. (2010). Disease-associated functions of IL-33: the new kid in the IL-1 family. Nat Rev Immunol *10*, 103-110.

Lingel, A., Weiss, T.M., Niebuhr, M., Pan, B., Appleton, B.A., Wiesmann, C., Bazan, J.F., and Fairbrother, W.J. (2009). Structure of IL-33 and its interaction with the ST2 and

IL-1RAcP receptors--insight into heterotrimeric IL-1 signaling complexes. Structure *17*, 1398-1410.

Liu, B., Yang, Y., Qiu, Z., Staron, M., Hong, F., Li, Y., Wu, S., Hao, B., Bona, R., Han, D., and Li, Z. (2010). Folding of Toll-like receptors by the HSP90 paralogue gp96 requires a substrate-specific cochaperone. Nat Commun *1*, 79.

Luo, W., Wang, Y., and Reiser, G. (2007). p24A, a type I transmembrane protein, controls ARF1-dependent resensitization of protease-activated receptor-2 by influence on receptor trafficking. J Biol Chem *282*, 30246-30255.

Luo, W., Wang, Y., and Reiser, G. (2011). Proteinase-activated receptors, nucleotide P2Y receptors, and mu-opioid receptor-1B are under the control of the type I transmembrane proteins p23 and p24A in post-Golgi trafficking. J Neurochem *117*, 71-81.

Luthi, A.U., Cullen, S.P., McNeela, E.A., Duriez, P.J., Afonina, I.S., Sheridan, C., Brumatti, G., Taylor, R.C., Kersse, K., Vandenabeele, P., *et al.* (2009). Suppression of interleukin-33 bioactivity through proteolysis by apoptotic caspases. Immunity *31*, 84-98.

Macia, E., Ehrlich, M., Massol, R., Boucrot, E., Brunner, C., and Kirchhausen, T. (2006). Dynasore, a cell-permeable inhibitor of dynamin. Dev Cell *10*, 839-850.

Marzioch, M., Henthorn, D.C., Herrmann, J.M., Wilson, R., Thomas, D.Y., Bergeron, J.J., Solari, R.C., and Rowley, A. (1999). Erp1p and Erp2p, partners for Emp24p and Erv25p in a yeast p24 complex. Mol Biol Cell *10*, 1923-1938.

Matsushima, N., Tanaka, T., Enkhbayar, P., Mikami, T., Taga, M., Yamada, K., and Kuroki, Y. (2007). Comparative sequence analysis of leucine-rich repeats (LRRs) within vertebrate toll-like receptors. BMC Genomics *8*, 124.

McGettrick, A.F., and O'Neill, L.A. (2010). Localisation and trafficking of Toll-like receptors: an important mode of regulation. Curr Opin Immunol *22*, 20-27.

Medzhitov, R., and Janeway, C., Jr. (2000). Innate immunity. N Engl J Med *343*, 338-344.

Medzhitov, R., Preston-Hurlburt, P., and Janeway, C.A., Jr. (1997). A human homologue of the Drosophila Toll protein signals activation of adaptive immunity. Nature *388*, 394-397.

Miller, A.M. (2011). Role of IL-33 in inflammation and disease. J Inflamm (Lond) *8*, 22.

Miller, A.M., Xu, D., Asquith, D.L., Denby, L., Li, Y., Sattar, N., Baker, A.H., McInnes, I.B., and Liew, F.Y. (2008). IL-33 reduces the development of atherosclerosis. J Exp Med *205*, 339-346.

Mirchandani, A.S., Salmond, R.J., and Liew, F.Y. (2012). Interleukin-33 and the function of innate lymphoid cells. Trends Immunol.

Mizutani, H., Schechter, N., Lazarus, G., Black, R.A., and Kupper, T.S. (1991). Rapid and specific conversion of precursor interleukin 1 beta (IL-1 beta) to an active IL-1 species by human mast cell chymase. J Exp Med *174*, 821-825.

Moffatt, M.F., Gut, I.G., Demenais, F., Strachan, D.P., Bouzigon, E., Heath, S., von Mutius, E., Farrall, M., Lathrop, M., and Cookson, W.O. (2010). A large-scale, consortium-based genomewide association study of asthma. N Engl J Med *363*, 1211-1221.

Morr, M., Takeuchi, O., Akira, S., Simon, M.M., and Muhlradt, P.F. (2002). Differential recognition of structural details of bacterial lipopeptides by toll-like receptors. Eur J Immunol *32*, 3337-3347.

Moulin, D., Donze, O., Talabot-Ayer, D., Mezin, F., Palmer, G., and Gabay, C. (2007). Interleukin (IL)-33 induces the release of pro-inflammatory mediators by mast cells. Cytokine *40*, 216-225.

Mun, S.H., Ko, N.Y., Kim, H.S., Kim, J.W., Kim do, K., Kim, A.R., Lee, S.H., Kim, Y.G., Lee, C.K., Kim, B.K., *et al.* (2010). Interleukin-33 stimulates formation of functional osteoclasts from human CD14(+) monocytes. Cell Mol Life Sci *67*, 3883-3892.

Murzin, A.G., Lesk, A.M., and Chothia, C. (1992). beta-Trefoil fold. Patterns of structure and sequence in the Kunitz inhibitors interleukins-1 beta and 1 alpha and fibroblast growth factors. J Mol Biol *223*, 531-543.

Nakae, S., Iwakura, Y., Suto, H., and Galli, S.J. (2007). Phenotypic differences between Th1 and Th17 cells and negative regulation of Th1 cell differentiation by IL-17. J Leukoc Biol *81*, 1258-1268.

Neill, D.R., Wong, S.H., Bellosi, A., Flynn, R.J., Daly, M., Langford, T.K., Bucks, C., Kane, C.M., Fallon, P.G., Pannell, R., *et al.* (2010). Nuocytes represent a new innate effector leukocyte that mediates type-2 immunity. Nature *464*, 1367-1370.

Netea, M.G., Simon, A., van de Veerdonk, F., Kullberg, B.J., Van der Meer, J.W., and Joosten, L.A. (2010). IL-1beta processing in host defense: beyond the inflammasomes. PLoS Pathog *6*, e1000661.

Neumann, D., Kollewe, C., Pich, A., Cao, P., Resch, K., and Martin, M.U. (2008). Threonine 66 in the death domain of IRAK-1 is critical for interaction with signaling molecules but is not a target site for autophosphorylation. J Leukoc Biol *84*, 807-813.

Ninomiya-Tsuji, J., Kishimoto, K., Hiyama, A., Inoue, J., Cao, Z., and Matsumoto, K. (1999). The kinase TAK1 can activate the NIK-I kappaB as well as the MAP kinase cascade in the IL-1 signalling pathway. Nature *398*, 252-256.

Novick, D., Kim, S.H., Fantuzzi, G., Reznikov, L.L., Dinarello, C.A., and Rubinstein, M. (1999). Interleukin-18 binding protein: a novel modulator of the Th1 cytokine response. Immunity *10*, 127-136.

Nugent, T., and Jones, D.T. (2009). Transmembrane protein topology prediction using support vector machines. BMC Bioinformatics *10*, 159.

O'Neill, L.A. (2008). The interleukin-1 receptor/Toll-like receptor superfamily: 10 years of progress. Immunol Rev *226*, 10-18.

O'Neill, L.A., Fitzgerald, K.A., and Bowie, A.G. (2003). The Toll-IL-1 receptor adaptor family grows to five members. Trends Immunol *24*, 286-290.

Oakley, F.D., Smith, R.L., and Engelhardt, J.F. (2009). Lipid rafts and caveolin-1 coordinate interleukin-1beta (IL-1beta)-dependent activation of NFkappaB by controlling endocytosis of Nox2 and IL-1beta receptor 1 from the plasma membrane. J Biol Chem *284*, 33255-33264.

Oboki, K., Ohno, T., Kajiwara, N., Saito, H., and Nakae, S. (2010). IL-33 and IL-33 receptors in host defense and diseases. Allergol Int *59*, 143-160.

Ozinsky, A., Underhill, D.M., Fontenot, J.D., Hajjar, A.M., Smith, K.D., Wilson, C.B., Schroeder, L., and Aderem, A. (2000). The repertoire for pattern recognition of pathogens by the innate immune system is defined by cooperation between toll-like receptors. Proc Natl Acad Sci U S A *97*, 13766-13771.

Palmer, G., Lipsky, B.P., Smithgall, M.D., Meininger, D., Siu, S., Talabot-Ayer, D., Gabay, C., and Smith, D.E. (2008). The IL-1 receptor accessory protein (AcP) is required for IL-33 signaling and soluble AcP enhances the ability of soluble ST2 to inhibit IL-33. Cytokine *42*, 358-364.

Palsson-McDermott, E.M., Doyle, S.L., McGettrick, A.F., Hardy, M., Husebye, H., Banahan, K., Gong, M., Golenbock, D., Espevik, T., and O'Neill, L.A. (2009). TAG, a splice variant of the adaptor TRAM, negatively regulates the adaptor MyD88-independent TLR4 pathway. Nat Immunol *10*, 579-586.

Poltorak, A., He, X., Smirnova, I., Liu, M.Y., Van Huffel, C., Du, X., Birdwell, D., Alejos, E., Silva, M., Galanos, C., *et al.* (1998). Defective LPS signaling in C3H/HeJ and C57BL/10ScCr mice: mutations in Tlr4 gene. Science *282*, 2085-2088.

Qin, J., Qian, Y., Yao, J., Grace, C., and Li, X. (2005). SIGIRR inhibits interleukin-1 receptor- and toll-like receptor 4-mediated signaling through different mechanisms. J Biol Chem *280*, 25233-25241.

Randow, F., and Seed, B. (2001). Endoplasmic reticulum chaperone gp96 is required for innate immunity but not cell viability. Nat Cell Biol *3*, 891-896.

Rank, M.A., Kobayashi, T., Kozaki, H., Bartemes, K.R., Squillace, D.L., and Kita, H. (2009). IL-33-activated dendritic cells induce an atypical TH2-type response. J Allergy Clin Immunol *123*, 1047-1054.

Rojo, M., Pepperkok, R., Emery, G., Kellner, R., Stang, E., Parton, R.G., and Gruenberg, J. (1997). Involvement of the transmembrane protein p23 in biosynthetic protein transport. J Cell Biol *139*, 1119-1135.

Rotter, J., Kuiper, R.P., Bouw, G., and Martens, G.J. (2002). Cell-type-specific and selectively induced expression of members of the p24 family of putative cargo receptors. J Cell Sci *115*, 1049-1058.

Roussel, L., Erard, M., Cayrol, C., and Girard, J.P. (2008). Molecular mimicry between IL-33 and KSHV for attachment to chromatin through the H2A-H2B acidic pocket. EMBO Rep *9*, 1006-1012.

Rowe, D.C., McGettrick, A.F., Latz, E., Monks, B.G., Gay, N.J., Yamamoto, M., Akira, S., O'Neill, L.A., Fitzgerald, K.A., and Golenbock, D.T. (2006). The myristoylation of TRIF-related adaptor molecule is essential for Toll-like receptor 4 signal transduction. Proc Natl Acad Sci U S A *103*, 6299-6304.

Sanada, S., Hakuno, D., Higgins, L.J., Schreiter, E.R., McKenzie, A.N., and Lee, R.T. (2007). IL-33 and ST2 comprise a critical biomechanically induced and cardioprotective signaling system. J Clin Invest *117*, 1538-1549.

Schmitz, J., Owyang, A., Oldham, E., Song, Y., Murphy, E., McClanahan, T.K., Zurawski, G., Moshrefi, M., Qin, J., Li, X., *et al.* (2005). IL-33, an interleukin-1-like cytokine that signals via the IL-1 receptor-related protein ST2 and induces T helper type 2-associated cytokines. Immunity *23*, 479-490.

Seidelin, J.B., Bjerrum, J.T., Coskun, M., Widjaya, B., Vainer, B., and Nielsen, O.H. (2010). IL-33 is upregulated in colonocytes of ulcerative colitis. Immunol Lett *128*, 80-85.

Seong, S.Y., and Matzinger, P. (2004). Hydrophobicity: an ancient damage-associated molecular pattern that initiates innate immune responses. Nat Rev Immunol *4*, 469-478.

Sims, J.E., March, C.J., Cosman, D., Widmer, M.B., MacDonald, H.R., McMahan, C.J., Grubin, C.E., Wignall, J.M., Jackson, J.L., Call, S.M., and et al. (1988). cDNA expression cloning of the IL-1 receptor, a member of the immunoglobulin superfamily. Science *241*, 585-589.

Sims, J.E., Nicklin, M.J., Bazan, J.F., Barton, J.L., Busfield, S.J., Ford, J.E., Kastelein, R.A., Kumar, S., Lin, H., Mulero, J.J., *et al.* (2001). A new nomenclature for IL-1-family genes. Trends Immunol *22*, 536-537.

Smith, D.E. (2010). IL-33: a tissue derived cytokine pathway involved in allergic inflammation and asthma. Clin Exp Allergy *40*, 200-208.

Smithgall, M.D., Comeau, M.R., Yoon, B.R., Kaufman, D., Armitage, R., and Smith, D.E. (2008). IL-33 amplifies both Th1- and Th2-type responses through its activity on human basophils, allergen-reactive Th2 cells, iNKT and NK cells. Int Immunol *20*, 1019-1030.

Sorkin, A., and Von Zastrow, M. (2002). Signal transduction and endocytosis: close encounters of many kinds. Nat Rev Mol Cell Biol *3*, 600-614.

Springer, S., Chen, E., Duden, R., Marzioch, M., Rowley, A., Hamamoto, S., Merchant, S., and Schekman, R. (2000). The p24 proteins are not essential for vesicular transport in Saccharomyces cerevisiae. Proc Natl Acad Sci U S A *97*, 4034-4039.

Strating, J.R., and Martens, G.J. (2009). The p24 family and selective transport processes at the ER-Golgi interface. Biol Cell *101*, 495-509.

Strating, J.R., van Bakel, N.H., Leunissen, J.A., and Martens, G.J. (2009). A comprehensive overview of the vertebrate p24 family: identification of a novel tissue-specifically expressed member. Mol Biol Evol *26*, 1707-1714.

Suzukawa, M., Iikura, M., Koketsu, R., Nagase, H., Tamura, C., Komiya, A., Nakae, S., Matsushima, K., Ohta, K., Yamamoto, K., and Yamaguchi, M. (2008a). An IL-1 cytokine member, IL-33, induces human basophil activation via its ST2 receptor. J Immunol *181*, 5981-5989.

Suzukawa, M., Koketsu, R., Iikura, M., Nakae, S., Matsumoto, K., Nagase, H., Saito, H., Matsushima, K., Ohta, K., Yamamoto, K., and Yamaguchi, M. (2008b). Interleukin-33 enhances adhesion, CD11b expression and survival in human eosinophils. Lab Invest *88*, 1245-1253.

Tabeta, K., Hoebe, K., Janssen, E.M., Du, X., Georgel, P., Crozat, K., Mudd, S., Mann, N., Sovath, S., Goode, J., *et al.* (2006). The Unc93b1 mutation 3d disrupts exogenous antigen presentation and signaling via Toll-like receptors 3, 7 and 9. Nat Immunol *7*, 156-164.

Takahashi, K., Shibata, T., Akashi-Takamura, S., Kiyokawa, T., Wakabayashi, Y., Tanimura, N., Kobayashi, T., Matsumoto, F., Fukui, R., Kouro, T., *et al.* (2007). A protein associated with Toll-like receptor (TLR) 4 (PRAT4A) is required for TLR-dependent immune responses. J Exp Med *204*, 2963-2976.

Talabot-Ayer, D., Lamacchia, C., Gabay, C., and Palmer, G. (2009). Interleukin-33 is biologically active independently of caspase-1 cleavage. J Biol Chem *284*, 19420-19426.

Tare, N., Li, H., Morschauser, A., Cote-Sierra, J., Ju, G., Renzetti, L., and Lin, T.A. (2010). KU812 cells provide a novel in vitro model of the human IL-33/ST2L axis: functional responses and identification of signaling pathways. Exp Cell Res *316*, 2527-2537.

Thomassen, E., Renshaw, B.R., and Sims, J.E. (1999). Identification and characterization of SIGIRR, a molecule representing a novel subtype of the IL-1R superfamily. Cytokine *11*, 389-399.

Thornberry, N.A., Bull, H.G., Calaycay, J.R., Chapman, K.T., Howard, A.D., Kostura, M.J., Miller, D.K., Molineaux, S.M., Weidner, J.R., Aunins, J., and et al. (1992). A novel heterodimeric cysteine protease is required for interleukin-1 beta processing in monocytes. Nature *356*, 768-774.

Tominaga, S. (1989). A putative protein of a growth specific cDNA from BALB/c-3T3 cells is highly similar to the extracellular portion of mouse interleukin 1 receptor. FEBS Lett *258*, 301-304.

Tominaga, S., Kuroiwa, K., Tago, K., Iwahana, H., Yanagisawa, K., and Komatsu, N. (1999). Presence and expression of a novel variant form of ST2 gene product in human leukemic cell line UT-7/GM. Biochem Biophys Res Commun *264*, 14-18.

Towne, J.E., Renshaw, B.R., Douangpanya, J., Lipsky, B.P., Shen, M., Gabel, C.A., and Sims, J.E. (2011). Interleukin-36 (IL-36) ligands require processing for full agonist (IL-36alpha, IL-36beta, and IL-36gamma) or antagonist (IL-36Ra) activity. J Biol Chem *286*, 42594-42602.

Troutman, T.D., Hu, W., Fulenchek, S., Yamazaki, T., Kurosaki, T., Bazan, J.F., and Pasare, C. (2012). Role for B-cell adapter for PI3K (BCAP) as a signaling adapter linking Toll-like receptors (TLRs) to serine/threonine kinases PI3K/Akt. Proc Natl Acad Sci U S A *109*, 273-278.

Tusnady, G.E., and Simon, I. (1998). Principles governing amino acid composition of integral membrane proteins: application to topology prediction. J Mol Biol *283*, 489-506.

Uronen-Hansson, H., Allen, J., Osman, M., Squires, G., Klein, N., and Callard, R.E. (2004). Toll-like receptor 2 (TLR2) and TLR4 are present inside human dendritic cells, associated with microtubules and the Golgi apparatus but are not detectable on the cell surface: integrity of microtubules is required for interleukin-12 production in response to internalized bacteria. Immunology *111*, 173-178.

Vainio, P., Mpindi, J.P., Kohonen, P., Fey, V., Mirtti, T., Alanen, K.A., Perala, M., Kallioniemi, O., and Iljin, K. (2012). High-throughput transcriptomic and RNAi analysis identifies AIM1, ERGIC1, TMED3 and TPX2 as potential drug targets in prostate cancer. PLoS One *7*, e39801.

Vetrivel, K.S., Gong, P., Bowen, J.W., Cheng, H., Chen, Y., Carter, M., Nguyen, P.D., Placanica, L., Wieland, F.T., Li, Y.M., *et al.* (2007). Dual roles of the transmembrane protein p23/TMP21 in the modulation of amyloid precursor protein metabolism. Mol Neurodegener *2*, 4.

von Heijne, G. (2006). Membrane-protein topology. Nat Rev Mol Cell Biol *7*, 909-918.
Wald, D., Qin, J., Zhao, Z., Qian, Y., Naramura, M., Tian, L., Towne, J., Sims, J.E., Stark, G.R., and Li, X. (2003). SIGIRR, a negative regulator of Toll-like receptor-interleukin 1 receptor signaling. Nat Immunol *4*, 920-927.

Wang, C., Deng, L., Hong, M., Akkaraju, G.R., Inoue, J., and Chen, Z.J. (2001). TAK1 is a ubiquitin-dependent kinase of MKK and IKK. Nature *412*, 346-351.

Wang, D., Lou, J., Ouyang, C., Chen, W., Liu, Y., Liu, X., Cao, X., Wang, J., and Lu, L. (2010). Ras-related protein Rab10 facilitates TLR4 signaling by promoting replenishment of TLR4 onto the plasma membrane. Proc Natl Acad Sci U S A *107*, 13806-13811.

Wang, X., Yang, R., Jadhao, S.B., Yu, D., Hu, H., Glynn-Cunningham, N., Sztalryd, C., Silver, K.D., and Gong, D.W. (2012). Transmembrane emp24 protein transport domain 6 is selectively expressed in pancreatic islets and implicated in insulin secretion and diabetes. Pancreas *41*, 10-14.

Wang, Y., Chen, T., Han, C., He, D., Liu, H., An, H., Cai, Z., and Cao, X. (2007). Lysosome-associated small Rab GTPase Rab7b negatively regulates TLR4 signaling in macrophages by promoting lysosomal degradation of TLR4. Blood *110*, 962-971.

Weinberg, E.O., Shimpo, M., De Keulenaer, G.W., MacGillivray, C., Tominaga, S., Solomon, S.D., Rouleau, J.L., and Lee, R.T. (2002). Expression and regulation of ST2, an interleukin-1 receptor family member, in cardiomyocytes and myocardial infarction. Circulation *106*, 2961-2966.

Werenskiold, A.K., Hoffmann, S., and Klemenz, R. (1989). Induction of a mitogen-responsive gene after expression of the Ha-ras oncogene in NIH 3T3 fibroblasts. Mol Cell Biol *9*, 5207-5214.

Wilhelm, C., Hirota, K., Stieglitz, B., Van Snick, J., Tolaini, M., Lahl, K., Sparwasser, T., Helmby, H., and Stockinger, B. (2011). An IL-9 fate reporter demonstrates the induction of an innate IL-9 response in lung inflammation. Nat Immunol *12*, 1071-1077.

Xu, D., Chan, W.L., Leung, B.P., Huang, F., Wheeler, R., Piedrafita, D., Robinson, J.H., and Liew, F.Y. (1998). Selective expression of a stable cell surface molecule on type 2 but not type 1 helper T cells. J Exp Med *187*, 787-794.

Xu, D., Jiang, H.R., Kewin, P., Li, Y., Mu, R., Fraser, A.R., Pitman, N., Kurowska-Stolarska, M., McKenzie, A.N., McInnes, I.B., and Liew, F.Y. (2008). IL-33 exacerbates antigen-induced arthritis by activating mast cells. Proc Natl Acad Sci U S A *105*, 10913-10918.

Yagami, A., Orihara, K., Morita, H., Futamura, K., Hashimoto, N., Matsumoto, K., Saito, H., and Matsuda, A. (2010). IL-33 mediates inflammatory responses in human lung tissue cells. J Immunol *185*, 5743-5750.

Yanagisawa, K., Takagi, T., Tsukamoto, T., Tetsuka, T., and Tominaga, S. (1993). Presence of a novel primary response gene ST2L, encoding a product highly similar to the interleukin 1 receptor type 1. FEBS Lett *318*, 83-87.

Yang, X.Y., Ren, C.P., Wang, L., Li, H., Jiang, C.J., Zhang, H.B., Zhao, M., and Yao, K.T. (2005). Identification of differentially expressed genes in metastatic and non-metastatic nasopharyngeal carcinoma cells by suppression subtractive hybridization. Cell Oncol *27*, 215-223.

Yasuoka, S., Kawanokuchi, J., Parajuli, B., Jin, S., Doi, Y., Noda, M., Sonobe, Y., Takeuchi, H., Mizuno, T., and Suzumura, A. (2011). Production and functions of IL-33 in the central nervous system. Brain Res *1385*, 8-17.

Yin, H., Li, X.Y., Liu, T., Yuan, B.H., Zhang, B.B., Hu, S.L., Gu, H.B., Jin, X.B., and Zhu, J.Y. (2012). Adenovirus-mediated delivery of soluble ST2 attenuates ovalbumin-induced allergic asthma in mice. Clin Exp Immunol *170*, 1-9.

Yuan, F.L., Li, X., Lu, W.G., Li, C.W., Xu, R.S., and Dong, J. (2011). IL-33: a promising therapeutic target for rheumatoid arthritis? Expert Opin Ther Targets *15*, 529-534.

Zakariyah, A., Hou, W., Slim, R., and Jerome-Majewska, L. (2012). TMED2/p24beta1 is expressed in all gestational stages of human placentas and in choriocarcinoma cell lines. Placenta *33*, 214-219.

Zeyda, M., Wernly, B., Demyanets, S., Kaun, C., Hammerle, M., Hantusch, B., Schranz, M., Neuhofer, A., Itariu, B.K., Keck, M., *et al.* (2012). Severe obesity increases adipose tissue expression of interleukin-33 and its receptor ST2, both predominantly detectable in endothelial cells of human adipose tissue. Int J Obes (Lond).

Zhang, C., Wu, X., Zhao, Y., Deng, Z., and Qian, G. (2011). SIGIRR inhibits toll-like receptor 4, 5, 9-mediated immune responses in human airway epithelial cells. Mol Biol Rep *38*, 601-609.

Zhang, L., and Volchuk, A. (2010). p24 family type 1 transmembrane proteins are required for insulin biosynthesis and secretion in pancreatic beta-cells. FEBS Lett *584*, 2298-2304.

Zhao, J., Wei, J., Mialki, R.K., Mallampalli, D.F., Chen, B.B., Coon, T., Zou, C., Mallampalli, R.K., and Zhao, Y. (2012). F-box protein FBXL19-mediated ubiquitination and degradation of the receptor for IL-33 limits pulmonary inflammation. Nat Immunol *13*, 651-658.

Appendices

Record of publications

Doyle, S.L., Husebye, H., Connolly, D.J., Espevik, T., O'Neill, L.A., and McGettrick, A.F. (2012). The GOLD domain-containing protein TMED7 inhibits TLR4 signalling from the endosome upon LPS stimulation. Nat Commun *3*, 707.

Connolly, D.J., and O'Neill, L.A. (2012). New developments in Toll-like receptor targeted therapeutics. Curr Opin Pharmacol *12*, 510-518.

Connolly, D.J., O'Neill L.A., McGettrick, A.F. The GOLD domain-containing protein TMED1 is required for IL-33 signalling. The Journal of Biological Chemistry. (Accepted subject to minor revisions)